THE UNIVERSITY OF OKLAHOMA

GRADUATE COLLEGE

THE PILOTED IGNITION OF WOOD BY RADIANT HEAT

A DISSERTATION

SUBMITTED TO THE GRADUATE FACULTY

in partial fulfillment of the requirements for the degree of

DOCTOR OF ENGINEERING

BY

HAROLD ROBINSON WESSON

Norman, Oklahoma

1970

THE PILOTED IGNITION OF WOOD

BY RADIANT HEAT

APPROVED BY

C M Sliepcevich

K E Starling

William N. Hugh

Jerry L. Russell

DISSERTATION COMMITTEE

ACKNOWLEDGMENTS

Without the assistance of a number of people this research could not have been successfully completed. Among those who have contributed to this work I would like to express my sincere gratitude to the following persons:

Dr. C. M. Sliepcevich, George Lynn Cross Research Professor of Engineering, for his direction and support.

Dr. J. R. Welker, Associate Director of the Flame Dynamics Laboratory, for his assistance and constructive criticism throughout the entire program.

Dr. William Huff, Professor of Mathematics; Dr. Tom J. Love, Jr., Director of the School of Aerospace and Mechanical Engineering; Dr. John Francis, Associate Professor of the School of Aerospace and Mechanical Engineering; for their advise and service on my graduate committee. Dr. Jerry L. Purswell, Associate Professor of the School of Industrial Engineering; Dr. Kenneth Starling, Associate Professor of the School of Chemical Engineering and Material Science; for their service on my dissertation examination committee.

Mr. John Hallman and Mr. Dwight Pfenning, my fellow graduate students, for their assistance in obtaining monochromatic reflectance measurements on numerous wood specimens.

I am most grateful to University Engineers, Inc. of Norman for providing financial assistance and to the University of Oklahoma Research Institute for part-time employment. I also appreciate the efforts of Mrs. Joyce Meyer, Mrs. Connie Kirk and Miss Ann Haynes in the preparation of the manuscript.

Finally, I wish to thank my wife and children for waiting patiently and encouraging me to complete this study.

Harold R. Wesson

THE PILOTED IGNITION OF WOOD BY RADIANT HEAT

ABSTRACT

Several investigators have studied the ignition of wood and wood products by radiant energy. In general, their results have differed due to different specimens and different experimental techniques. The work reported here was undertaken in order to investigate the important variables involved in wood ignition in such a way that ignition times could be predicted for all types of wood materials.

The ignition experiments were performed in a specially-designed ignition cabinet. The cabinet provided for radiation from open diffusion flames and high-temperature tungsten filament lamps. Thus the ignition response of wood specimens could be studied using radiation of two different spectral qualities. Irradiances up to 3 cal/cm^2-sec could be obtained from benzene flames and up to 3.5 cal/cm^2-sec from the tungsten lamps. The irradiance was quite uniform over the surface of the 10-cm square samples. A heated coil of wire was placed above the sample as a pilot light.

The coil was large enough to prevent its location from being an important parameter in ignition time measurements.

More than a dozen different wood samples and one wood derivative were subjected to the piloted ignition tests. Their densities ranged from less than 0.1 gm/cm^3 to more than 1.0 gm/cm^3 and samples from less than 2.5 mm to more than 25 mm thick were tested. All samples were oven-dried for at least 24 hours prior to testing.

The ignition time of the samples depended primarily on the incident irradiance. However, the sample density, thickness, and spectral absorptance were all important parameters in determining ignition time. The heat conduction equation for an inert, opaque, infinite slab was used as the basis for correlating the ignition time. It showed that the ignition time could be expressed as a combination of the incident irradiance, the sample density, the average absorptance for the incident radiation, and the sample thickness.

The analysis of the ignition time data yielded the following conclusions:

1. The ignition time for dry wood is inversely proportional to the third power of the incident irradiance.

2. The ignition time also depends strongly on the spectral distribution of the incident radiation. In general, wood reflects radiation from about 0.6 microns to 2 microns quite efficiently, but absorbs the longer wavelengths. The average absorptance for flame radiation is about 0.76, and for tungsten lamps at 2500°K the average absorptance is about 0.48. As a result ignition of wood takes 4 times as long for tungsten lamps as for flames at the same incident irradiance.
3. Ignition time is directly proportional to wood density over the range studied.
4. The effect of sample thickness can be accounted for by the error function of the Fourier number.
5. Ignition data for all wood species using different thicknesses, densities, and radiation sources fit a single correlation when all important ignition parameters are accounted for.

TABLE OF CONTENTS

TABLE OF CONTENTS (CONTINUED)

TABLE OF CONTENTS (Continued)

TABLE OF CONTENTS (Continued)

LIST OF TABLES

LIST OF TABLES (Continued)

LIST OF TABLES (Continued)

LIST OF ILLUSTRATIONS

LIST OF ILLUSTRATIONS (Continued)

LIST OF ILLUSTRATIONS (Continued)

LIST OF ILLUSTRATIONS (Continued)

LIST OF ILLUSTRATIONS (Continued)

LIST OF ILLUSTRATIONS (Continued)

LIST OF ILLUSTRATIONS (Continued)

LIST OF ILLUSTRATIONS (Continued)

THE PILOT IGNITION OF WOOD BY RADIANT HEAT

CHAPTER I

INTRODUCTION

When combustible solids are exposed to radiant energies part of the incident energy will be reflected, part may be transmitted through the solid, and part will be absorbed by the material under consideration. Of that portion of the incident energy that is initially absorbed part will be reradiated, part will be removed by convective cooling effects, and the remainder will be retained within the material being irradiated. Some of the energy which is retained by the irradiated material will also be utilized to produce and/or sustain internal chemical reactions. The magnitude of the absorbed energy depends primarily on the absorptance characteristics of the material surface and the spectral distribution of the incident energy. The amount of the initially absorbed energy that is retained by the material is also affected by the thermal properties and physical thickness of the irradiated material.

Aside from the possibility that a portion of the incident energy that is absorbed, particularly that in the ultraviolet region of the spectrum, may be consumed in initiating chemical reactions within the material, practically all of the retained energy is converted directly into heat. As a consequence the temperature of the absorbing material rises and thermal damage may result depending on the magnitude of the absorbed energy and the time factor. The thermal properties and the thickness of the material (up to some finite physical limit) will affect the internal heat energy distribution, i.e., define the rate of heat conduction away from the radiant energy absorbing region. However, when the temperature of a given material reaches certain limits, thermal decomposition is initiated. This process is called pyrolysis. If the rate of energy absorption is relatively slow, the material may continue to decompose into gaseous products and char material. At higher energy absorption rates, the gaseous products resulting from pyrolysis may be ignited after a given time period by a small pilot flame, a spark or a hot wire. This form of ignition is generally termed pilot ignition and is of great practical significance since it is the most common method of fire spread. At even higher energy absorption rates the gaseous products resulting

from pyrolysis evolve at a sufficient rate and concentration that upon free mixing with the surrounding air they can ignite spontaneously in the absence of an external ignition source. This type of ignition is generally termed spontaneous ignition.

Ignition behavior studies have been carried out by many different investigators under widely different experimental conditions for the past several decades. However, despite that massive experimental effort, attempts to define ignition criteria in terms of a single or limited usable number of significant practical parameters, such as surface temperature or rate of volatile gas production, have been uniformly unsuccessful. It is also important to note that attempts to determine a usable correlation of different investigative results on similar materials have also been unsuccessful. The predominate reasons for this gross diversity of experimental results appear to be the use of different types of radiation sources, the use of different experimental techniques, and widely divergent physical test configurations.

Since the vast majority of the total heat transfer from fully developed fires and atomic explosions toward external targets is by thermal radiation, the bulk of recent experimental programs have utilized thermal radiation

sources such as gas-fired panels, tungsten filament lamps, carbon arcs, and solar furnaces. Although the literature is voluminous, the bulk of the work reported is concerned with the ignition behavior of combustible solids by high intensity thermal radiation simulating nuclear devices. Some of the recent work is concerned with the use of carbon arcs at relatively low incident irradiance levels to evaluate the ignition behavior of fabrics. One investigator has reported on thermal radiation studies on wood samples using a sheet of flames from a pool of liquid hydrocarbon as a source of irradiance. This latter work is the first reported using actual flames as an irradiating source and the reported data clearly demonstrates that conventional criteria such as sample weight loss rates or surface temperatures in themselves are not adequate for prediction of the ignition characteristics of woods exposed to thermal radiation emanating from fully developed fires.

This latter investigative effort using flame radiation also provides the first experimental indication of the very significant effects of the incident energy spectral distribution and sample surface monochromatic absorptance properties on ignition behavior. It has been recognized for some time that these effects were present, but in general they have been assumed to be negligible. The work

reported indicates that differences in similar wood ignition times of a factor of 3 to 5 will result from using conventional test apparatus as compared to flames, i.e., flames radiation will produce ignition 3 to 5 times faster than will shorter wavelength energy sources at the same sample incident irradiance level. However, due to different experimental techniques, lack of spectral distribution data for other radiation sources used in prior investigations, and a lack of spectral absorptance data for the sample specimens, a direct comparison of these first flame radiation results cannot be made with the results from prior investigations using other types of radiation sources.

In the investigations reported herein an improved method for the study of the ignition behavior of woods has been devised. The experimental apparatus has different and unique features from those reported in the literature. The experimental method reported herein differs from others in the ability to supply incident radiation from two different sources, flames from different liquid fuels and tungsten filament lamps operating at about 2500°K, without appreciably changing the physical test configuration. Other aspects of this method include consideration of the spectral distribution of the different incident radiation as well as experimental evaluation of sample surface reflectances.

The sample reflectances are discussed in Appendix A. Briefly, this test method includes a determination of the effects of radiation source spectral distribution combined with sample absorptance properties on sample ignition behavior. Simultaneously it eliminates effects introduced by different experimental techniques and physical test configurations for each radiation source by utilizing a separate determination of the absorbed energy levels for completing the description of ignition behavior.

Approximately 500 ignition tests were made using flames and tungsten lamp radiation on twelve different types of woods. Additional tests were also made with the different radiation sources on three of these woods with varying thicknesses. The resulting data are tabulated in Appendix B and are discussed in Chapter IV.

In Chapter II the reader is cautioned to be aware of the diversity in terminology and definitions used by the previous investigators cited. To a large extent these differences reflect the individual investigator's taste in words and the experimental method. A standardized terminology which is consistent with the discussions of this chapter and later discussions on the present work is given in a separate section entitled "Terminology" in

Chapter II. The nomenclature used in the subsequent mathematical treatments is consistent throughout this thesis. A comprehensive listing of nomenclature is given in Appendix D.

CHAPTER II

REVIEW OF PREVIOUS WORK

Numerous concepts of the ignition process and many proposed methods for establishing ignition criteria have been presented in the literature. The following discussions define the generally accepted sequence of events that apparently results in the ignition phenomena and reviews the more important aspects of this ignition process. The results of prior investigations, the proposed criteria of ignition and the reasons (s) that these criteria do not adequately define the ignition behavior of cellulosic materials are also reviewed. Comparisons of typical examples of the reported data are also presented. The effects of different types of incident radiation, sample surface reflectance properties, pilot flame position and size, and air flow across the sample surfaces are noted. The potential effects of sample density and thickness are discussed and the published data on these factors are reviewed.

Ignition Process

From a comprehensive survey of the literature Brown (3) concluded that if a combustible solid is heated gradually in the presence of sufficient air, a certain sequence of events must take place as the material being heated absorbs energy. At low temperatures a very slow reaction between the material and the oxygen in the surrounding air occurs and becomes appreciable at higher temperatures. This combustion reaction produces heat which tends to raise the temperature of the absorbing material and thus increases the rate of the reaction. Opposing this tendency toward rising internal temperatures is the energy loss to the immediate surroundings by radiation, conduction and convection mechanisms. However, at a certain temperature level, the rate of reaction between the combustible material and the oxygen is sufficiently rapid such that the resulting rate of heat production exceeds that of the heat loss, and the temperature of the material rises faster than it would due to external heating effects alone. Thus, the reaction accelerates itself and very rapid heating follows. Provided favorable conditions still exist, this heating process continues until visible indications of ignition occur, such as glowing or flaming.

Brown (3) also makes the point that ignition is a process requiring time rather than being an event in time. In other words, ignition does not imply a discontinuity between the rate of the reaction and temperature. He also emphasizes that ignition cannot be considered synonymous with the appearance of glowing or flaming, as sometimes held, since these processes cannot occur unless the ignition process is first carried out.

The process of ignition of cellulosic materials is probably best understood from the following discussion which is based on the work of Martin (28), Brown (3), Schaffer (37), and Lipska (22) on the pyrolysis of cellulosic and synthetic materials. They concluded that with the exception of charcoal and some punky materials, solid fuels do not burn directly. The combustion of solids involves two separate and distinct processes; the decomposition of the solid into simple volatile products, followed by a gas phase oxidation of these products usually at some finite distance from the surface of the solid. Unless the sum of the heat contributed to the solid by the gas phase reaction, exothermic pyrolysis of the solid, and energy absorption from outside heating is at least as great as the heat consumed in the endothermic pyrolysis of the solid plus heat loss to the surroundings, the solid will not continue to burn.

When an organic solid is heated above certain temperature limits, the molecules begin to shed molecular fragments, and the remaining solid rearranges and condenses into a form which is more stable at that temperature range. These molecular fragments escape the solid in their original form, or in combination with one another, and mix with the surrounding air. If this process continues at a sufficiently high rate glowing and/or flaming ignition occurs. However, it should be noted that the mechanism of thermal decomposition and the composition of the products are different for the two extreme cases of very low and very high thermal radiation. For very slow heating the specimen may eventually be completely charred without flaming. The rate of evolution of gases is so low that upon mixing with surrounding air the mixture concentration is below the flammable limits. Simms (38) reports that below a certain incident irradiance, flaming ignition of the volatiles did not occur although specimens were observed to glow.

Martin and Ramstad (28) discuss the results of other investigations. They state that contrary to normal processes which precede and accompany the ignition resulting from slow heating, intensely irradiated cellulose undergoes no discernible charring up to about the time of ignition. It subsequently decomposes rapidly, and almost completely,

to volatile substances, leaving only a trace of solid residue. This type of rapid thermal decomposition has been termed "flash pyrolysis".

The experimental work of Lincoln (21) deals with the analysis of the products of flash pyrolysis of solid fuels exposed to pulses of high intensity radiation for periods of the order of one millisecond or less. The analysis was carried out in vacuo or in an inert atmosphere by means of gas chromatography and mass spectrometry. Lincoln confirmed the dependence of the product composition on the rate of heating. For example, he found that 2-mil sheets of black cellulose were almost completely vaporized by a total radiant heat exposure as low as 2 cal/cm^2 incident on both surfaces. The irradiance used by Lincoln in these experiments was on the order of 3000 cal/cm^2-sec (peak value) over a period of 1/2 millisecond.

To summarize, the results of the discussion of this section demonstrate that:

1. Ignition of flammable solids involves two separate and distinct processes: (a) the thermal decomposition of a solid phase into volatile products and a residue and, (b) gas phase

oxidation reactions of volatiles near the surface.

2. Flaming ignition is identified as visible phenomena in the gas phase near the surface of the solid. Glowing ignition is identified as visible phenomena at the surface of the solid which is the result of direct oxidation.
3. The pyrolysis product composition is dependent on the rate of external heating.
4. Minimum incident irradiance levels are required to produce either glowing or flaming ignition.

Terminology

Unfortunately, the terminology used in the literature on ignition is not standardized. Koohyar (14) made a comprehensive survey of the literature and cited several examples of these terminology inconsistencies. Koohyar, in the first experimental study on ignition of wood samples by flame radiation, proposed terminology standards. For the sake of consistency--at least in the flame radiation sphere of interest--the terminology proposed by Koohyar will also be utilized in this effort. As defined below,

Glowing Ignition

In this type of ignition no flaming is observed and the solid starts glowing.

Pilot Ignition

At a certain temperature the volatiles evolved from the solids form a mixture with the surrounding air which can be ignited by a pilot flame or spark placed in the volatile gas stream. This temperature has been called the condition of potential ignitibility.

Pilot Ignition Temperature

The surface temperature of the solid sample at the moment when flaming ignition by a pilot occurs is called the pilot ignition temperature. In the present work, the pilot consists of a nichrome wire heater element located above and along the sample surface (see Figure III-11).

Spontaneous Ignition

At a sufficiently high heating rate, the temperature of the solid reaches a point such that a sufficient amount of volatiles are evolved and the mixture of these volatiles and the surrounding air is ignited without the presence of a pilot source. This condition is also referred to as spontaneous flaming ignition or as self-ignition. The occurrence of spontaneous ignition has been said to be

independent of material thickness (6); however, this contention may be open to question.

Spontaneous Ignition Temperature

The surface temperature of the solid sample at the moment when spontaneous ignition occurs is called the spontaneous ignition temperature.

Sustained Flaming Ignition

If the solid material continues to burn completely after removal of the external heating source, sustained flaming ignition or sustained ignition is said to have occurred. This condition must necessarily be preceded by either pilot or spontaneous ignition. Whether a material under a given heating condition, which normally causes either pilot or spontaneous ignition, undergoes sustained flaming ignition or not depends on the thickness of the material sample. In addition to a high surface temperature, a high equilibrium temperature within the material is required for sustained flaming ignition. This condition is also referred to as sustained, persistent or continued burning or flaming. The condition in which the flaming is not sustained is referred to as transient flaming.

Surface Ignition

Surface ignition is similar to pilot ignition except that the pilot is placed in contact with the surface of the solid instead of in the volatile gas stream.

Criteria for Ignition

In order to define an acceptable criterion for ignition, it is necessary to review briefly the experimental and mathematical studies made by some of the previous investigators. Each of the mathematical treatments of the ignition process has been made with several different simplifying assumptions. For this reason, as illustrated in depth by Koohyar (14), a general case and its assumptions will be presented first so that the reader can better evaluate the effect of the further simplifcations made by varicus investigators. Because of the complexity of the problem all of the treatments have been confined to one-dimensional models.

The preliminary assumptions made for deriving a reasonably general equation defining the process of thermal damage to cellulosic material are:

1. The solid material is porous and the transfer of heat and vclatile products is one-dimensional.
2. The gaseous products escape with neglibible pressure drop.

3. The vapor temperature at any depth can be approximated as the solid temperature at that depth.
4. The process is diffusion controlled. In other words, it is controlled by diffusion of heat and not by rate of reaction.
5. An overall first order reaction with a constant heat of reaction for the weight loss is applicable.
6. The material is isotropic and its properties are independent of temperature.
7. The incident irradiance is constant and uniform over the entire surface boundaries.
8. Average constant values can be used for optical properties of the sample.
9. Lambert's law for semi-transparent material is applicable.
10. Some modified physical properties can be used to offset the effect of moisture content.
11. The dimensions of the solid remain constant.

Assumption 1 is valid for materials manufactured from cellulose. However, it has been noticed that the volatile products resulting from the decomposition of irradiated natural wood samples normally evolve from one or several

cracks which are not uniformly distributed over the surface. The assumption of one-dimensional mass transfer in these models may therefore be questionable. The amount of energy transfer by gaseous products is relatively small and therefore Assumptions 2 and 3 are considered to be fair. Experimental results show that Assumption 4 may be considered valid. Assumption 5, as discussed later in a section concerning the reaction kinetics, has been shown to be acceptable by experimental work. Assumption 6, especially in the case of wood, is open to debate. The properties of wood across the grain are different from those along the grain. The properties of wood and charcoal are also different. However, the thermal diffusivity of wood and charcoal are approximately the same (35). In the case of the one-dimensional model the properties along the heat transfer path are reasonably constant provided that the sample is free from checks, knots, and cross grain structures. Without Assumption 6 analysis of ignition problems is extremely difficult; with it, simplified models can be used. Assumption 7 depends on the experimental conditions, and Assumption 8 introduces errors of the order of several magnitudes when different types of irradiance are considered. Assumptions 9 and 10 may be considered valid if some suitable values for the optical and physical properties are used.

Assumption 11 is usually valid prior to ignition, but expansion and/or shrinkage are common during pyrolysis and following ignition.

On the basis of these assumptions the energy balance for a one-dimensional, diathermanous, porous solid undergoing thermal decomposition is

$$K \frac{\partial^2 T}{\partial x^2} + \gamma H e^{-\gamma x} - \frac{C_g \, \partial (m \Delta T)}{\partial x} = \rho c \frac{\partial T}{\partial t} + Q \frac{\partial \omega}{\partial t} \qquad \text{(II-1)}$$

$$- \frac{\partial \omega}{\partial t} = f\omega \, e^{-E/RT} \qquad \text{(II-2)}$$

where

K = thermal conductivity

γ = Lambert's law attenuation factor

H = incident flux at the surface (surface absorptance assumed to be unity)

m = the rate of weight loss per unit volume

C_g = average heat capacity of volatile products

ρ = density

c = heat capacity of solid

Q = overall heat of decomposition reaction per unit volume

ω = the weight loss per unit volume

E = activation energy

R = gas constant

T = absolute temperature

t = time

The nomenclature used above is consistent with this study. New variables are defined as they appear later. A comprehensive listing of nomenclature is given in Appendix F.

Consideration of every aspect of the ignition process greatly complicates the analytical treatment of the problem. Even after all the above simplifying assumptions are made, Equations II-1 and II-2 are too complicated to be solved analytically. Several investigators have attempted to discuss the ignition process of combustible solids mathematically with further simplifications. In this section some of the most important mathematical and experimental approaches made to formulate the criteria of ignition and thermal damage to organic solids will be reviewed briefly.

Brown (3) took the ignition point to be the point of inflection on the temperature-time curve. He also listed certain requirements that must be met in order for ignition to occur. They are:

1. A combustible must be present.
2. A source of oxygen, such as air, must be available within certain concentrations relative to the combustible.

3. Heat must be evolved as the net result of the reaction or reactions, producing active combustion.
4. The reaction must proceed more or less rapidly over a certain temperature range.
5. The reaction must be accelerated by a rise in temperature.
6. A supply of energy, sufficient to raise the temperature of the reacting substances to the point where the reaction becomes autogeneous, is necessary.

Lawrence (17) reviewed the above conditions critically. Condition 6 does not seem to be general and would be required only for the cases of spontaneous ignition. Statement 4 is vague and misleading. Probably by the word rapid, Brown meant rapid enough that the rate of heat gain from external sources and chemical reactions exceeds all heat losses. The heating of the samples in Brown's experimental apparatus was accomplished by convection. Under this condition there was very little possibility of heat dissipation except by radiation.

By the term reaction Brown refers to the heterogeneous combustion reaction of solid and oxygen. The criterion of a temperature inflection point is not acceptable as

a general definition of an ignition point because that is the point at which the self-heating from exothermic pyrolysis plus the external heat balances the cooling effects of endothermic pyrolysis and the heat loss to the surroundings. If the source of energy is removed immediately after the inflection point, pyrolysis may not continue. It is also noticed that Brown's concept of ignition is not based on gas phase reactions. However, the other conditions listed are, in general, correct.

In his experiments, Brown exposed the sample to a continuously rising temperature environment in a muffle furnace. The ignition temperature was assumed to be the central temperature of the sample at an inflection point in the temperature-time curve. These temperatures were listed for different materials. They ranged from 172°C for hay and tobacco to 314°C for cellulose acetate. For wood, Brown's ignition temperatures range from 192°C for western red cedar to 220°C for longleaf pine.

In his review of the literature, Martin (26) gave general qualitative statements for the necessary and sufficient conditions for the spontaneous ignition of the fuel gas and air mixtures which apply to gas phase reactions in ignition processes. These conditions were stated as: (a) the gaseous fuel must have a high chemical potential by

virtue of its chemical composition and/or its kinetic energy and, (b) the relative concentration of fuel and oxygen must lie between the two flammability limits. Each of these conditions commonly exists at different levels above the decomposing solid, but until they occur simultaneously at the same location, ignition will not occur. If the oxygen concentration is less than the lower flammable limit, the generated heat dissipates faster than it is released and the reactive species decay via collision. If the concentration of oxygen is greater than the upper flammable limits the temperature can rise high enough so that the mixture ignites.

Although the above conditions have to be fulfilled for the ignition of a solid to occur, they do not quantitatively give the desired answer to the problem of finding the criteria of ignition. For example, it might be more practical to ascribe the flammable limits to a certain rate of evolution of volatiles from the material.

Bamford et al. (2) simplified their one-dimensional slab model to the case of an opaque solid and neglected the energy transfer due to mass transfer through the sample. Since heating of the slab was accomplished by contacting luminous gas flames on both sides, the system was symmetrical and only half of the slab need be considered.

However, in order to obtain solutions for their one-dimensional slab model equations a finite difference method and assigned numerical values for all constants had to be utilized. From interpretation of their calculated results for weight loss, they reported that a minimum rate of evolution of gases of 2.5×10^{-4} gm/cm^2 - sec^1 is necessary for a sample to burn with flames. It was also calculated that the temperature of the pyrolysis zone ranged from 300 to 450°C. The suggested criterion of the rate of evolution of gases from the surface as stated by Bamford *et al.* (2) was only calculated for sustained flaming under conditions where the heating source contacted the sample. The required rate of evolution of gases prior to ignition for different cases of piloted and spontaneous ignition are not known.

Subsequently, Lawrence (17), in his study of spontaneous ignition of woods and plastics, stated the necessary conditions for ignition to occur as: (a) the rate of evolution of combustible gases during the thermal decomposition should exceed a certain minimum value and (b) the kindling (ignition) temperature of the combustible gas should be reached or exceeded. Lawrence made two basic assumptions. He assumed the rate of evolution to be 5.0×10^{-4} gm/cm^2-sec^1, twice the figure reported by Bamford *et al.* (2). He also assumed a constant surface ignition temperature of

500°C. Based on his assumptions and computations, Lawrence concluded that the rate of production of volatiles reported by Bamford et al. (2) was never a critical factor. Lawrence also found that the effect of exothermic decomposition was negligible for an activation energy of 35,000 cal/gm mole. However, a reduction from 35,000 to 25,000 cal/gm mole caused the thermal effect of decomposition to become important.

Since it is generally concluded that the rate of decomposition reactions of organic materials depends directly upon the rate of absorbed energy and the resultant temperature of the material, several investigators have tried to express ignition criteria in terms of the required energy or surface temperature. Fons (11) solved the equation of heat conduction in an inert cylinder, of radius R_1 and initial temperature T_o, for several different atmospheres of constant temperature T_a ranging from 450 to 700°C. The equation used was

$$K \left[\frac{\partial^2 T}{\partial r^2} + \frac{1}{r} \frac{\partial T}{\partial r} \right] = \rho c \frac{\partial T}{\partial t} \qquad \text{(II-3)}$$

where r is the radial distance from the center of the cylinder. The boundary conditions were:

$$@\ t > 0;\ r = R;\ \frac{\partial T}{\partial r} = \frac{h}{K} (T_a - T) \qquad \text{(II-4)}$$

$$t \rightarrow \infty;\ 0 \leq r \leq R;\ T = T_a \qquad \text{(II-5)}$$

From the analytical solution of the above equations he tabulated the values of dimensionless temperature for certain ranges of other dimensionless parameters. By measuring the temperature at two different depths in the wood sample at the time of flaming ignition and by using his table, he estimated the surface temperature at the ignition point. With this method he found the ignition point of ponderosa pine to be around 340°C. From the results of experiments he mentioned that the material may spontaneously ignite if parts of it are at 425°C or higher. If part of the wood has been reduced to charcoal he stated that it can glow at about 230°C.

Lawson and Simms (18) studied the heating rates required for ignition of wood and noticed that lowering the intensity of radiation increases the ignition time. They also determined that there existed a minimum rate of heating that would result in flaming ignition. They correlated the radiation heat flux and time for the two cases of pilot and spontaneous ignition as follows:

$$(H - H_p)\ t^{2/3} = 0.025 \times 10^6\ (K\rho c + 68 \times 10^{-6}) \qquad \text{(II-6)}$$

$$(H - H_s)\ t^{4/5} = 0.05 \times 10^6\ (K\rho c + 35 \times 10^{-6}) \qquad \text{(II-7)}$$

where H = incident radiation flux, $cal/cm^2 sec$

H_p, H_s = critical irradiance of pilot and spontaneous ignition respectively, $cal/cm^2 sec$

K = thermal conductivity, $cal/cm^2 sec\ °C/cm$

ρ = density, gm/cm^3

c = specific heat, $cal/gm\ °C$.

Values of H_p and H_s correspond to ignition at infinite exposure time. Based on their experiments, Lawson and Simms assigned values of 0.35 and 0.6 cal/cm^2 sec, respectively. Koohyar (14) in studying wood ignition from exposure to flame irradiances determined values of approximately 0.32 cal/cm^2 sec for one-sided piloted heating and about 0.15 cal/cm^2 sec for two-sided piloted heating. For two-sided spontaneous heating a value of 0.33 cal/cm^2 sec was determined by Koohyar. He did not draw any conclusions regarding one-sided spontaneous ignition critical irradiances although he reported data.

Buschman (5) using the same method of correlation as Lawson and Simms for pilot ignition conditions, determined that the constants of Equation II-6 are not the same for all materials. Therefore, Equations II-6 and II-7 cannot be generalized.

Lawson and Simms (18), in continuation of their earlier studies, suggested that wood ignites when the

surface reaches a fixed temperature rather than when it has received a fixed quantity of energy. They estimated the spontaneous ignition temperature to be 350-450°C for different species of wood and 600°C for fiber insulating board. The level of irradiance for their experiments was between 0.5 and 2.0 cal/cm^2 sec.

Koohyar (14) noted that Simms (38, 39, 40, 41, 42) later did a semi-quantative analysis by considering Equations II-1 and II-2 and compared the outcome with the experimental results. He neglected the effect of mass convection through the solid and included the general case of a radiation pulse which has a peak flux of H_p' at the time t_p so that

$$H = \lambda \, H_p' \, (t/t_p) \qquad \text{(II-8)}$$

where λ is a shape function which is unity for a constant intensity. Equation II-1 and II-2 are combined to yield

$$K \frac{\partial^2 T}{\partial x^2} + \gamma \, H_p' \, \lambda \, (t/t_p) e^{-\gamma x} = \rho c \frac{\partial T}{\partial t} - Qf\omega e^{-E/RT} \qquad \text{(II-9)}$$

The initial condition is given as $T = T_o$ and $\omega = \omega_o$ and the boundary conditions are described by Newtonian cooling, $h(T - T_o)$. By introducing the following dimensionless groups,

$\zeta = x/L$; dimensionless distance

$\tau = ft$; dimensionless time

$\Phi = TR/E$; dimensionless temperature

Equation (II-9) becomes

$$\frac{\alpha}{fL^2}\ \frac{\partial^2\Phi}{\partial\zeta^2} + \lambda\left(\frac{\tau}{ft_p}\right)\ \left(\frac{\gamma H_p{}'R}{E\rho cf}\right)e^{-\gamma L\zeta} = \frac{\partial\Phi}{\partial\tau} + \frac{QR\omega_o}{E\rho c}\ \frac{\partial(\omega/\omega_o)}{\partial\tau} \qquad \text{(II-10)}$$

where
$$\frac{\partial(\omega/\omega_o)}{\partial\tau} = \left(\frac{\omega}{\omega_o}\right)\ e^{-1/\Phi} \qquad \text{(II-11)}$$

The initial conditions for all ζ then become $\Phi = \Phi_o = RT_o/E$ and $\omega/\omega_o = 1$. The boundary conditions become

$$@\ \tau > 0;\ \zeta = 0 \text{ or } 1;\ \pm\frac{\partial\Phi}{\partial\zeta} = \frac{hL}{K}\ (\Phi - \Phi_o) \qquad \text{(II-12)}$$

From these equations it follows that the solution will be in the form

$$\frac{RT}{E} = \mathcal{F}\left[\frac{RT_o}{E},\ \gamma L,\ \frac{hL}{K},\ \frac{\alpha}{fL^2},\ \frac{x}{L},\ ft,\ \frac{QR\omega_o}{E\rho c},\ \frac{\gamma H_p{}'R}{E\rho cf},\ ft_p\right] \qquad \text{(II-13)}$$

$$\frac{\omega}{\omega_o} = \mathcal{F}\left[\frac{RT}{E},\ ft\right] \qquad \text{(II-14)}$$

Useful simplifications are made by neglecting one or more terms. For example, if the effect of diathermancy is

neglected, the terms containing γ are omitted from the above equations. However, any groups that can be formed out of the excluded terms which do not contain γ must be retained. The same result would be obtained by reverting to and modifying the original differential equation and boundary conditions. In the following paragraphs some important cases as well as the significance of some of the dimensionless groups are discussed.

In the case of <u>opaque</u> materials the terms γL and $\gamma H_p' R/E\rho cf$ are excluded, but $H_p'R/E\rho cfL$, their ratio, is retained. Combining this ratio with the group ft_p the energy modulus $H_p't_pR/E\rho cL$ is formed and Equation II-13 reduces to:

$$\frac{RT}{E} = \mathcal{F}\left[\frac{RT_o}{E}, \frac{hL}{K}, \frac{\alpha}{fL^2}, \frac{x}{L}, ft, \frac{QR\omega_o}{E\rho c}, \frac{H_p't_pR}{E\rho cL}, ft_p\right] \tag{II-15}$$

If the material is inert, all terms containing Q, E, R, and f must be deleted from Equation II-13, and it is the temperature rise, $(T - T_o)$, not the absolute value of T, which is the relevant parameter. The result for the case of an <u>inert</u>, <u>diathermanous</u> material in terms of the energy modulus $H_p't_p/\rho cL(T - T_o)$, becomes

$$\frac{H_p' t_p}{\rho cL(T - T_o)} = \mathcal{F}\left[\frac{hL}{K}, \frac{x}{L}, \frac{\alpha t}{L^2}, \frac{\gamma K}{h}, \frac{\alpha t_p}{L^2}\right] \tag{II-16}$$

For an opaque, inert material it becomes

$$\frac{H_p' \, t_p}{\rho c L (T - T_o)} = \int \left[\frac{hL}{K}, \frac{x}{L}, \frac{\alpha t}{L^2}, \frac{\alpha t_p}{L^2} \right] \qquad \text{(II-17)}$$

Equation II-17 may be further simplified by referring to two cases of thick and thin materials. All dimensionless groups may be regarded as the ratio of two terms, each of which usually has a physical meaning attached to it. The two important groups considered here are $\alpha t/L^2$, the Fourier number (F) or dimensionless time variable, and h L/K, the Biot number. The Fourier number may be written as

$$\frac{(K/L)\Delta T \; t}{\rho c L \Delta T} = \frac{\text{rate of conduction of heat away from surface}}{\text{rate of heat retention}}$$

The Fourier number is a measure of the age of the process. When $\alpha t/L^2$ is small, the conducted heat will not have penetrated very far into the material, and the material can be considered as infinite in depth. When $\alpha t/L^2$ is large, the rate retention is relatively small and the material is approaching conditions where conductivity is no longer a relevant factor since the material is effectively thin.

The Biot number, hL/K, may be considered to be the ratio of surface to internal resistance to heat flow. For the case of the semi-infinite solid, the thickness of the

specimen is not a factor in heat-transfer modeling. Eliminating L from the Fourier and Biot numbers by combining the two yields the parameter $h^2t/K\rho c$. Therefore, the solution of Equation II-13 for the case of a semi-infinite, opaque and inert solid becomes

$$\frac{H_p' t_p}{\rho c (\alpha t_p)^{1/2} (T - T_o)} = \mathcal{F}\left[\frac{hx}{K}, \frac{t}{t_p}, \frac{h^2 t}{K\rho c}\right] \quad \text{(II-18)}$$

For a constant pulse of radiation, t/t_p is unity, and may be neglected. The surface condition ($x = 0$) for this case is expressed by

$$\frac{Ht}{\rho c (\alpha t)^{1/2} \Delta T_s} = \mathcal{F}\left[\frac{h^2 t}{K\rho c}\right] \quad \text{(II-19)}$$

The analytical solution of Equation II-10 corresponding to the case of Equation II-19 was given by Simms (38) as

$$\frac{Ht}{\rho c (\alpha t)^{1/2} \Delta T_s} = \frac{\beta}{1 - \exp\beta^2 \cdot \operatorname{erfc}\beta} \quad \text{(II-20)}$$

where $\beta = [h^2 t/K\rho c]^{1/2}$. β is called the cooling modulus and Δt_s is the surface temperature rise. If β^2 is small, the surface heat losses may also be neglected. The energy modulus therefore would be constant.

When the Fourier number is large enough for a quasi-steady state to exist, thermal conductivity must not appear in the groups containing time. By eliminating K from the

product of the Fourier number and the Biot number, the resulting parameter becomes $ht/\rho cL$ and the solution to the case of an <u>infinite slab of opaque and inert solid</u> for a constant flux becomes

$$\frac{Ht}{\rho cL\ \Delta Tm} = \mathcal{S}\left[\frac{ht}{\rho cL}\right] \qquad \text{(II-21)}$$

where ΔTm is the mean temperature rise of the slab. If the effect of cooling is negligible, the cooling modulus ($ht/\rho cL$) is also omitted. The analytical solution of Equation II-10 was given by Simms (38) as

$$\frac{Ht}{\rho cL\ \Delta Tm} = \frac{2ht/\rho cL}{1 - \exp(-2ht/\rho cL)} \qquad \text{(II-22)}$$

Simms (38, 41) then plotted the energy modulus against the cooling modulus, $h\sqrt{t}/\sqrt{K\rho c}$, and applied a <u>constant ignition temperature</u> such that the theoretical curve gave the best fit through the experimental data (within 30 percent). The characteristic ignition temperature or surface temperature rise at ignition was found to be $\Delta T_s = 525°C$ for the case of spontaneous ignition of thick or mathematically semi-infinite samples of wood. Simms then concluded that a fixed surface temperature is a reasonable criterion for the attainment of spontaneous ignition. He applied the same procedure to the case of piloted ignition (42).

Buschman (5), using his data and the solution of the conduction equation for opaque, inert solids, calculated the pilot ignition temperature. The tabulated results show a relatively constant value for surface temperature of each species of wood at ignition. The reported ignition temperatures varied for different kinds of wood ranging from 298°C for tempered hard board to 391°C for Balsa.

Butler et al. (6), cross plotting from Gardon (12), noticed that dimensionless groups plotted as energy versus time with depth of char as a parameter show an essentially isothermal profile for $\sqrt{F} > 3.0$, F = Fourier number, if the thermal properties and the irradiance are constant. Butler noted that the surface temperature rise for an infinite slab of thickness L, considering the case of a one-dimensional, inert, opaque solid, could be expressed as

$$\frac{\Delta T_s \sqrt{K\rho c}}{H\sqrt{t}} = \sqrt{F} + \frac{1}{\sqrt{F}} \left[\frac{1}{3} - \frac{2}{\pi^2} \sum_{n=1}^{\infty} \frac{1}{n^2} e^{-n^2 \pi^2 F} \right] \qquad \text{(II-23)}$$

where the left side of the equation is the dimensionless temperature rise. Plots of Equation II-23 and the surface temperature rise of semi-infinite solids show that for $\sqrt{F} \leq 0.6$, F = Fourier number, a slab heated on one side can be considered a semi-infinite solid. Based on Equation

II-23 for $\sqrt{F} < 0.6$, Butler et al. (6) estimated the surface temperature of cellulosic materials for the case of spontaneous ignition to be in the range of 700 to 800°C.

Williams (50) neglected the chemical reaction term and derived the one-dimensional heat conduction equation for diathermanous solids as

$$K \frac{\partial^2 T}{\partial x^2} + \gamma H e^{-\gamma x} = c\rho \frac{\partial T}{\partial t} \qquad \text{(II-24)}$$

He then considered the following three cases:

Case I - Heat flow in a semi-infinite solid with no heat losses from the irradiated surface.

Case II - Surface temperature in semi-infinite solids allowing for first power losses from the irradiated surface.

Case III - Heat flow in semi-infinite diathermanous solids allowing for linear decrease in the reflectivity of the irradiated surface with time.

The solution to Case I showed that the temperature behavior approached that of opaque solids (i.e., γx or $\gamma\sqrt{\alpha t}$ equal to ∞) with increasing γx or $\gamma\sqrt{\alpha t}$. It is therefore concluded that at sufficiently large values of time or depth, the effect of diathermancy becomes negligible. This analysis strictly applies only to cases involving monochromatic radiation. It may, however, be extended to cover

cases where various portions of the incident flux are characterized by different γ's. In such situations, one merely computes the temperature rise at any depth and time produced by each fraction of the incident flux acting independently and sums them arithmetically.

Based on the results of experiments on non-symmetrical heating, Weatherford, Sheppard and Valtierra (48) suggested that a fixed fuel-generation-rate criterion must be satisfied in order to achieve sustained piloted ignition in the presence of a heat source. Because of the scatter in their data, which was believed to be caused by the effect of substantial influence of physical and thermal properties, they concluded that a more quantitative definition of fixed fuel-generation-rate as an ignition criterion was not feasible.

Koohyar (14) noted that prior to his investigations all previous studies of ignition of combustible solids by radiation utilized radiation sources such as gas-fired panels, tungsten lamps, carbon arcs, solar furnaces, graphite panels, etc. All these radiation sources emit the major portions of their energy in the visible and near infrared regions of the wavelength spectrum. Koohyar devised a method and experimental apparatus to utilize direct radiation from free burning diffusion flames. The basic objectives in Koohyar's work were to:

1. Develop a new method for the experimental study of the ignition process by irradiating the samples with radiation from buoyant diffusion flames.
2. To obtain experimental data relative to surface temperature at the time of flaming ignition.
3. To obtain experimental sample weight loss data as a function of sample exposure time.

In the experiments Koohyar obtained a continuous recording of the specimen surface temperature throughout the radiation exposure interval. His work was among the first reported experimental determinations of the sample surface temperatures. Efforts prior to this work were limited to analytical determination of surface temperatures. Table II-1 presents a tabulation of the experimentally determined surface temperatures at the time of flaming ignition for the range of wood samples tested.

As shown above, ignition occurred over a relatively wide temperature range for the noted heating conditions, not at a fixed surface temperature as postulated by prior investigators. For example, Muir (32) reported that Lawson and Simms (18) and Simms (42) considered the temperature of the surface of the sample to be a prime factor in determining the time required for pilot ignition to occur. The

TABLE II-1

KOOHYAR'S (14) EXPERIMENTAL SURFACE TEMPERATURES AT IGNITION

Experimental Condition	Average Temp. ~ °C	Range of Temp. ~ °C
One-sided Heating--		
Spontaneous Ignition	402	330-495
One-sided Heating--		
Pilot Ignition	361	280-450
Two-sided Heating--		
Spontaneous Ignition	360	290-450
Two-sided Heating--		
Pilot Ignition	300	240-378

temperature at the surface of an irradiated specimen was calculated from the following equation:

$$\theta = \frac{I}{\psi} (1 - e^{B^2} \text{ erfc } B) \qquad \text{(II-25)}$$

where θ = temperature rise of the sample exposed surface

I = intensity of radiation on the exposed surface

ψ = rate of loss of heat from unit surface per degree temperature rise

erfc = complementary error function

$B = (\psi/K)(\alpha t)^{1/2}$

K = thermal conductivity

α = thermal diffusivity $(K/\rho c$

c = specific heat

t = time

The validity of this equation depends upon the following assumptions:

1. That the exothermic and endothermic reactions that take place during the pyrolysis of the sample do not materially affect the temperature of the sample.
2. That the net radiant energy is uniformly absorbed by the surface of the sample and is independent of the temperature of the surface of the sample.

3. That the rate of loss of heat to the surroundings per unit area of the sample surface per degree difference in temperature was constant.
4. That the sample is infinitely thick so that the convective and radiative heat losses from the rear surface are negligible.

A consideration of these assumptions indicates that most of them will not be met under practical conditions. For example, the calculated net radiant energy absorbed by the surface of the sample decrease about 18 percent during the exposure time when the temperature of the surface of the sample rises from 20°C to 400°C and when the effective blackbody temperature of the radiant energy source is 750°C. Also under these conditions the calculated convective heat transfer coefficient increases from a negligible value to a substantial one. Since heat is lost to the surroundings by radiation, reflection and natural convection, the rate of heat loss cannot be adequately calculated by a linear relationship. Thus, to the extent that Koohyar's results (14) are valid he has apparently confirmed experimentally that ignition does not occur at a fixed surface temperature. It appears that the surface temperature controls the ignition process only though its resultant effect upon the rate of volatile gaseous production due to the pyrolysis processes.

Koohyar (14) also reported that the rate of evolution of volatiles from samples at the time of ignition ranged from 1.0×10^{-4} to 21.7×10^{-4} gm/cm^2-sec. The majority of his tests showed a rate of weight loss more than three times the minimum value of 2.5×10^{-4} gm/cm^2-sec reported by Bamford et al. (2) as a criterion for ignition and burning. Koohyar concluded that while a minimum rate of evolution of volatiles is a necessary condition for ignition to occur it is not a sufficient condition. Therefore, an ignition criterion based only on the rate of weight loss cannot be considered as adequate.

Koohyar (14) employed three mathematical models in an attempt to correlate his experimental data. Model 1, which was based on the assumption of an inert solid with Newtonian cooling, gave a poor correlation. It was shown that all the energy losses from the samples as well as the effect of chemical reactions cannot be combined and expressed by an effective constant overall heat transfer coefficient, h. Models 2 and 3, which were based on an inert solid but no heat loss, suggested the dimensionless group $HL/\Delta T_s K$ (irradiance modulus) and $\alpha t/L^2$ (Fourier modulus) and gave correlations. In the correlations the oak data were below the other wood species. Since the physical properties of the samples appear in the dimensionless groups,

Koohyar (14) suggested that the deviation of oak from the other species tested indicates that the rate of pyrolysis and the heat of reaction is also dependent on the density or grain structure of the wood. This conclusion was also presented by Simms (42) and Buschman (5). Koohyar finally concluded that the ignition process of wood could be described by a mathematical model of an inert and opaque solid with constant and uniform properties. Although these conclusions by Simms, Buschman and Koohyar are open to question, the presentation of Koohyar's model will be completed. Thus, Koohyar presented the equation for his model as

$$\alpha \frac{\partial^2 T}{\partial x^2} = \frac{\partial T}{\partial t} \qquad \text{(II-26)}$$

The boundary condition applied by Koohyar for the irradiated surface was

$$-K \frac{\partial T}{\partial x} = \eta H \qquad \text{(II-27)}$$

where H = incident irradiance (constant)

η = constant depending on species

The factor η was determined to be 0.40 for oak and 0.23 for all other species tested by Koohyar. However, as emphasized by Koohyar, although the above equations describe and correlate the overall results of the ignition tests,

they do not provide a very good means for prediction of ignition behavior. In addition to the thermal properties of the material (K, ρ and c) two of the three parameters H, ΔT_s and t must be known before an estimate of the ignition behavior can be made.

The discussions throughout this section refer to only a few of the most pertinent articles on the broad subject of ignition of solid materials. Emphasis has been placed on those areas in which widely divergent efforts have been made to formulate a generalized criterion for ignition behavior. As clearly illustrated a satisfactory generalized criterion for prediction of ignition is yet to be developed for a realistic range of environmental conditions.

Factors Affecting Ignition

From a review of the literature and extensive efforts to correlate different investigators' results on similar samples, it is evident that there are many factors which will greatly affect the occurrence and nature of the ignition and consequently the experimental results. In general, these factors may be classified in two categories:

1. Experimental procedures: Criterion of ignition, kind of radiation source, experimental method and apparatus, nature and size of container,

geometry of the sample, ignition atmosphere, rate of air flow over the sample surfaces, time of exposure, and rate of heating.

2. Properties of the combustible solid: fineness, moisture content, extraneous materials, diathermancy, surface absorptivity, physical and chemical properties, and pretreatment of the material.

The magnitude effects of the more important of these factors is discussed below:

Effect of Radiation Source

In earlier experimental work on the ignition properties of materials a number of different radiant energy sources were used. For example, Simms (39) used a carbon arc and an ellipsoidal mirror. With this system the maximum uniformly irradiated area was 3 cm^2 and the irradiance varied from 1.5 to 12 cal/cm^2-sec . Simms also used a tungsten filament lamp with an ellipsoidal mirror but the maximum area of uniform radiation was only 0.5 cm^2. Bamford et al. (2) used a vertical electric heater composed of 21, one-kilowatt elements forming a rectangle 14 in by 12 in. Lawson and Simms (18) and Simms (42) conducted tests on ignition by radiation with a one-foot square gas-fired surface combustion heater. This source gave uniform irradiance

up to 1.5 cal/cm^2-sec over an area in excess of 60 cm^2.

Simms and Coiley (43) reported on the characteristics of a one-foot square gas-fired radiant panel. The spectral distribution was found to approach that of a blackbody. The effective emissivity of the surface was found to be 0.7 when the absolute effective blackbody temperature of the surface was 1150°K. They also detected convection currents up to a horizontal distance of 13.5 cm from the front surface of the panel. Simms and Coiley concluded that the heat transfer from this type of panel to a point located outside of this region could be calculated from the radiation configuration factor laws and the indicated effective blackbody temperature.

Koohyar (14) reported the results obtained with buoyant diffusion flames using liquid fuels. Irradiance levles from about 0.2 to 0.8 cal/cm^2-sec were obtained. However, the spontaneous igntion data at the higher irradiance levels are questionable due to the very close proximity of the flames to the irradiated specimen. A possible interaction of the flames with the pyrolysis products could have resulted in piloted ignition rather than spontaneous ignition for these conditions. For this reason Kochyar (14) did not state any firm conclusions regarding these particular data.

Effect of Pilot Position

As noted previously, piloted ignition tests require an external energy source to trigger ignition. Piloted ignition occurs more rapidly than will spontaneous ignition, all other parameters being the same. Simms (42) noted that the time for pilot ignition to occur increased as the pilot flame was moved outward from the face of the sample in a perpendicular direction. He also investigated the combined effects of vertical position and, to some degree, flame size. From the calculated value of the Grashof number he deduced that the flow past the sample face was laminar. Simms further concluded that because of the laminar conditions, gradients of the concentration of the combustible volatiles would exist in the flow field which he thought would account for the variation in ignition time with pilot flame position.

Muir (32) conducted a very thorough and systematic evaluation of the effects of pilot flame size and position on pilot ignition times. He found that pilot ignition times increased significantly as the pilot flame was moved away from the sample in either the vertical or horizontal plane. However, as illustrated in Table II-2, pilot ignition continued to occur even with the pilot at a relatively large distance above the sample. At an irradiance of 0.258 cal/cm^2-sec Muir showed that the pilot ignition time for a

TABLE II-2

EFFECT OF SIZE AND POSITION OF PILOT FLAME

Size of Pilot Flame	Pilot flame position		Irradiance			
			0.258 cal/cm^2-sec^1		0.471 cal/cm^2-sec^1	
	Distance above sample[1]	Distance in front of sample[2]	Mean time to pilot ignition[3]	Variance	Mean time to pilot Ignition[3]	Variance
(cm)	(cm)	(cm)	(sec)	(sec^2)	(sec)	(sec^2)
2.5	0.5	0.0	581	793	53.0	12.6
2.5	1.0	0.0	590	949	60.0*	1.5
2.5	2.0	0.0	589	197	65.8*	9.2
2.5	7.5	0.0	596	31*	87.6*	4.3
2.5	10.0	0.0	642*	386	--	--
2.5	0.0	0.65	572	131	63.6*	52.5
2.5	0.0	0.15	608	566	77.0*	8.5
2.5	0.0	1.65	685*	4940	83.2*	129.8*
2.5	0.0	2.15	701*	270	112.6*	126.3*
1.0	0.5	0.0	574	382	52.0	6.2
5.0	0.5	0.0	567	364	53.4	6.0

[1] Distance of bottom of pilot flame above sample.

[2] Distance of center of pilot flame in front of face of sample.

[3] Mean of five or more tests.

*Value is significantly different at the 5% level from the value for the pilot flame 2.5 cm in size, and 0.5 cm directly above the sample face, i.e., values in top line of table.

pilot flame as much as 7.5 cm above the sample was not significantly different from that for his "control position." His tests also showed that when the samples were exposed to high intensity radiation, the pilot flame had to be located within ± 2 mm of the control position, horizontally, in order to obtain consistent results. At low intensities of radiation, the position of the pilot flame was less critical.

Effect of Superimposed Air Flow

It has been mentioned previously that ignition of solid material occurs in the gas phase. Obviously the supply of sufficient air to mix with the volatile gases released from the sample by pyrolysis action is just as important as the production of the gases. Besides the sufficiency, the velocity of the air near the heated surface will determine the mechanism of mixing, i.e., by diffusion in laminar flow or by turbulent mixing. On the other hand, a very high velocity of air will cool the surface by convection, thus carrying away a large amount of energy. These convective losses become more important as the surface temperature increases. At some optimum air flow ignition will occur in a minimum time at a given responsive irradiance level. For example, Brown (3) defined the optimum rate for

air flow as the minimum in his plot of ignition temperature versus air flow.

Simms (40) studied the behavior of the volatile stream by visual observation and high speed photography. He found that at high rates of heating (above 3 cal/cm^2 sec) with a tungsten lamp source, the flow of volatiles appeared to become turbulent very close to its point of emission from the surface of the heated specimen, and ignition usually followed quickly. At lower rates (below 3 cal/cm^2 sec), the flow was clearly laminar near the heated surface and became turbulent above the sample. Simms also showed that the absence or presence of external air movement of a velocity on the order of 25 cm/sec did not affect the time required for ignition at high intensity levels.

Muir (32) also performed a systematic experimental investigation of the effects of super-imposed air flow on pilot ignition of wood. Table II-3 presents his tabulated results. Muir compared these results with those obtained in an ambient medium. He concluded that pilot ignition times were significantly lowered by air currents of 20 to 32 cm/sec at a low irradiance but had little effect at high irradiance levels. Muir also noted that Simms reached a similar conclusion, but he neglected to note that the minimum intensity at which the material would ignite was

TABLE II-3

EFFECT OF SUPERIMPOSED AIR CURRENT

Irradiance					
0.258 cal/cm^2-sec			0.471 cal/cm^2-sec		
Forced air velocity	Mean time to pilot ignition(1)	Variance	Forced air velocity	Mean time to pilot ignition(1)	Variance
(cm/sec)	(sec)	(sec^2)	(cm/sec)	(sec)	(sec^2)
0	581	793	0	53	12.6
10	592	840	10	50	5.4
20	500*	404	20	50	1.5
32	543*	459	36	51	3.8
53	567	880	53	53	9.2
74	614	455	81	61*	9.5
108	873*	1049	112	78*	59.5

(1) Mean value for at least five tests.

*Value is significantly different at the 5% level from the value for no forced air flow.

affected by the air currents. Thus, at relatively low intensities of radiation, a superimposed air current of about 25 cm/sec affects both spontaneous ignition time and pilot ignition times, while at relatively higher intensities there is apparently little or no effect. Simms suggested that at low irradiances the superimposed draft produced mixing of air with the volatile gases, thereby enabling spontaneous ignition to occur at lower irradiances. At low irradiances without a superimposed draft, turbulence developed so far above the sample that the gases were cooled below the spontaneous ignition temperature before they mixed well enough to ignite. At higher irradiances, Simms hypothesized that turbulence developed near the sample due to natural convection so that the superimposed air currents did not improve mixing and, therefore, did not reduce the time required to produce spontaneous ignition.

A similar explanation for the pilot ignition results would also appear to be valid. For pilot ignition to occur, the air and volatiles must be mixed well enough to ignite when they are heated by the pilot flame. At the time of pilot ignition at high irradiances a superimposed draft apparently does not improve the mixing enough to reduced the ignition times significantly. Also, at high irradiances the rate of volatile gas generation is

rapid, causing better mixing due to more turbulence near the sample surface. At low irradiances the temperature of the sample and the composition of the volatile stream change very slowly so that mixing becomes an important factor in the pilot ignition time.

Muir (32) concluded that by directing an air current upward past the exposed face of the sample a minimum variation in pilot ignition test results would be obtained and that test results would more nearly simulate practical conditions.

Effect of Heating Rate

Aside from the variations in composition of the pyrolysis products produced under different heating rates the effects of heating rate on ignition time are of primary importance.

Lawson and Simms (18) and Koohyar (14) showed that there is a "critical heat flux" below which wood cannot be ignited. The reported values were essentially in agreement for similar ignition conditions (approximately 0.3 and 0.6 cal/cm^2-sec for the cases of pilot and spontaneous ignition respectively). These values were found by extrapolation of heat fluxes to infinite time. Pilot and spontaneous ignition are strongly dependent upon the heating rate, but sustained flaming depends upon the thickness of the material

as well. Thus, when the rate of heating is increased, a level depending on the thickness of material is reached at which ignition might be sustained, i.e., the burning may continue after the removal of the external heating source.

The dependence of ignition time on the irradiance level has been found by several investigators at different ranges of irradiances for similar materials. However, as discussed in the next section, widely divergent results exist and a satisfactory means for correlating different investigator experimental data is yet to be found.

Effect of Moisture Content

In general, it has been determined that for a given set of initial conditions, an increase in sample moisture content will increase the ignition times. Thomas, Simms and Law (47) conducted extensive experimental investigations into the effects of moisture content on ignition times. They concluded, and other investigators agree, that moisture contents below 20 percent do not materially effect ignition times. However studies underway at this laboratory by Murthy indicate a linear relationship between piloted ignition time and percent moisture content from essentially zero percent to 25 percent. Experimental data on balsa, white pine, and oak have been obtained to date for two different absorbed irradiances. Murthy has also indicated

that for given levels of irradiance and moisture content the ignition time also increases with increasing density.

Effect of Absorptivity

One of the most important single factors affecting the ignition process, yet the least investigated, is the surface absorptivity. Most organic materials reflect part or most of the incident energy in the near visible region between 0.3 to 1.0 μ. Gordon (12) and Williams (49) estimated the amount of absorbed energy from a heat balance in a certain period of time. Gardon reported the apparent absorptivities to be in the interval 44-70 percent. Williams, in a sample calculation, reported the corresponding value for birch to be 66 percent. In these calculations the effect of chemical reactions have been ignored, and the heat balances were calculated using the measured temperature in the sample. Simms (41) found that in heating wood to ignition, absorptivity is dependent on exposure time. He then suggested the application of an empirical absorption factor corresponding to different exposure times. This factor is obtainable by comparing the intensities of irradiation required to ignite the natural material with those required when the material is artificially blackened by carbon black.

Earing and Smith (10) reported experimental measurements of reflectance for some woods including oak and

redwood. Based on their results oak has an absorptivity in excess of 80 percent for wavelengths above 2 microns and only 20 percent in the 1 micron region. Hence, a radiation source emitting primarily in the visible region will have initially at least 80 percent of the emitted energy reflected by an oak sample.

Comparison of Existing Experimental Wood Pilot Ignition Data

Table II-4 presents a summary of factors that affect ignition for some of the more representative pilot ignition investigations reported in the literature.

Figure II-1 presents a graphical comparison of the pilot ignition data for dried woods as reported by the investigations summarized in Table II-4. It might be noted that the data reported are represented by data envelopes which include all the data points reported rather than the individual data points.

As clearly illustrated by Figure II-1 a very wide divergence is evident within the published literature regarding pilot ignition behavior of oven dried wood samples. In general, the lower the incident irradiance the greater the deviation in the reported data. As noted in Table II-4 the primary differences in the reported data appeared to be due to

TABLE II-4

SUMMARY OF REPRESENTATIVE PILOT IGNITION DATA FOR WOODS

Investigator	Buschman (5)	Simms (42)	Lawson and Simms (18)	Koohyar (14)
Materials Tested	Woods	Woods	Woods	Woods
Density Range	.16 to 1.1 gm/cm^3	.24 to .72 g/cm^3	.24 to .72 g/cm^3	.3 to .9 g/cm^3
Specimen Size	2¼" x 2¼"	5 cm by 5 cm	2" x 2"	4" x 4"
Specimen Thickness	1/4"	1.9 cm	3/4"	3/4"
Moisture Content	Conditioned for 48 hrs. @ 75°F and 50% R.H.	Oven dried for 24 hrs. @ 95°C	Oven dried for 24 hrs @ 95°C	Oven dried for 24 hrs @ 105°C
Method of Irradiance	Gas Heated Panel	Gas Fired Panel	Surface Combustion Heater	Buoyant Diffusion Flames
Irradiance Range	.34 to 89 cal/cm^2-sec	.25 to 1.50 cal/cm^2-sec	.75 to 1.50 cal/cm^2-sec	.2 to .85 cal/cm^2-sec
Spectral Characteristics	Blackbody at 670°C	Blackbody	Approximates a Blackbody	Diffusion Flame
Measurement Method	Copper Sheet Calorimeter	Thwing-Type Pyrometer*	Total Radiation Pyrometer	Predetermined Position at Burner
Pilot Method	Flame	Flame	Flame	Flame

TABLE II-4 (continued)

Pilot Size	Not stated	1¼ cm	1½" long	½" long
Pilot Position	Contacting Surface	1¼ cm above 1¼ cm out	½" above & out	½" above and out
Air Movement	Not stated	Not stated	Not stated	2-3 fps
Convective Effects	None by visual observations	No comment	None	None
Comments on Reflectivity	None	Wood reflec. is low for infrared	None	None

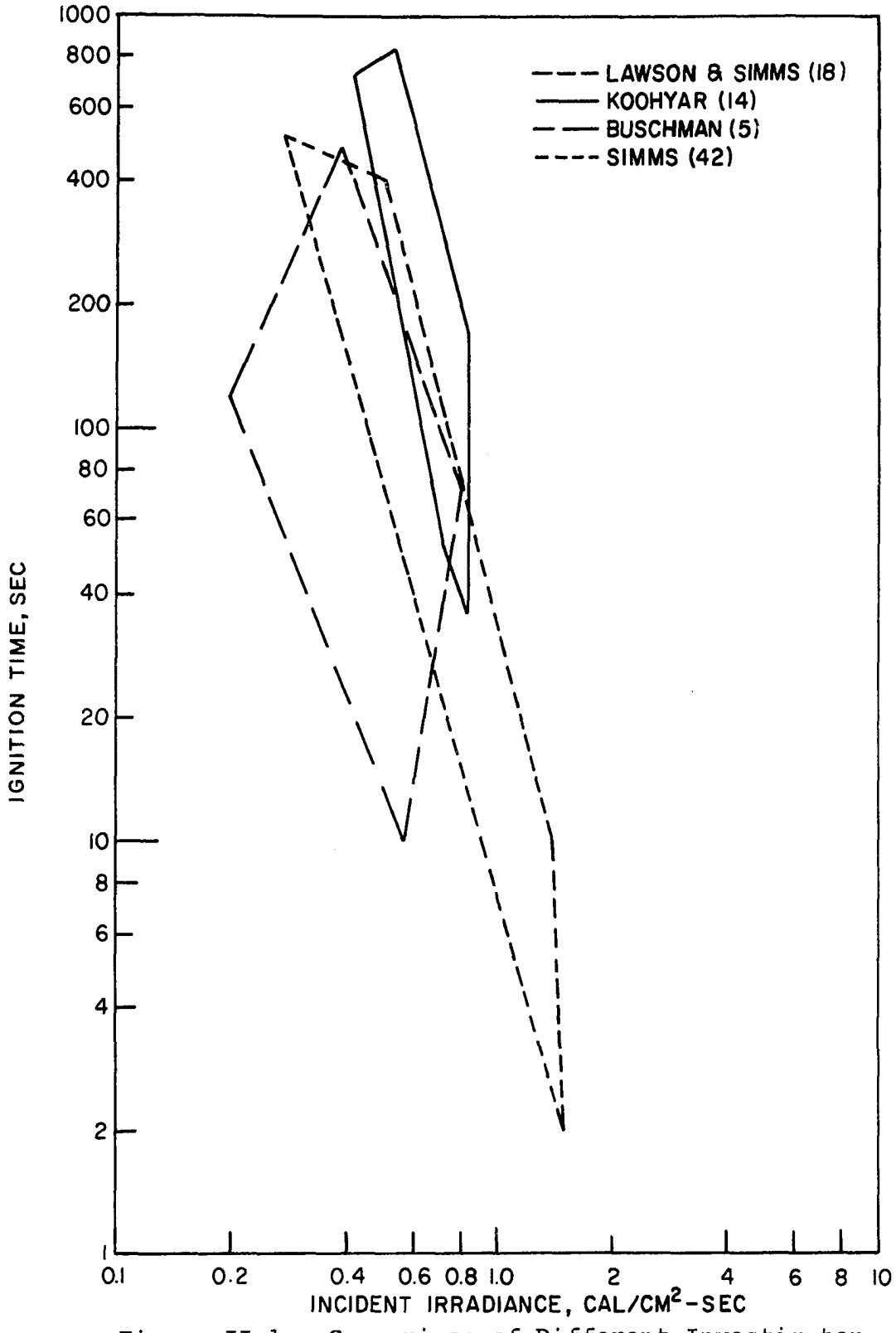

Figure II-1. Comparison of Different Investigator Pilot Ignition Results Obtained on Dried Woods.

a. Different types of radiation sources.

b. Possible minor differences in pilot flame location within the volatile gas-air mixing zones.

c. Different air flow conditions across the sample irradiated surfaces.

The range of the reported data at a given irradiance is also due to the range of densities. Simms (42) presented data on the effect of density on ignition times and concluded that pilot ignition times were dependent upon the intensity of radiation, the density of the wood, position of the pilot flame and possibly the size of the pilot flame. Muir (32) demonstrated that pilot flame sizes from 1 to 5 cm in length did not significantly affect the ignition results. While Simms (42), Muir (32), and Buschman (5) have all reported pilot ignition data with density as a possible parameter, no effort has been reported on systematic efforts to determine the magnitude of the density effect or possible reasons for density being an important factor in the overall ignition process. Simms (42) made an observation that the residual effect of density might be due to the rate of production of volatiles not being a unique function of the temperature but also depending on a number of physical and chemical constants. However, he also reported that density apparently had no such effect on spontaneous ignition. Simms (42) also

correlated his extrapolated data on minimum intensity required for pilot ignition of wood and found a reasonably good relationship. In general, his data indicated a linear increase of minimum intensity required to obtain pilot ignition as the wood density increases.

CHAPTER III

EXPERIMENTAL APPARATUS AND PROCEDURES

Although a voluminous literature has been compiled on the ignition of cellulosic materials in furnaces, by hot gases and radiation sources, such as carbon arcs, radiation panels and solar furnaces, only one source of data on ignition by radiation from flames is available. Due to the previously discussed, widely divergent differences in the pilot ignition behavior of materials exposed to flame radiation as compared to other types of radiation, it was desirable to define and evaluate these differences in ignition behavior under carefully controlled experimental conditions. Therefore, the ignition cabinet used in the one published result (15) was adapted to utilize both flame radiation and tungsten filament radiation for incident radiation sources.

Experimental Apparatus

Figure III-1 presents a front and left side view of the modified ignition cabinet, and Figure III-2 shows a rear and right side view. The schematic diagram of

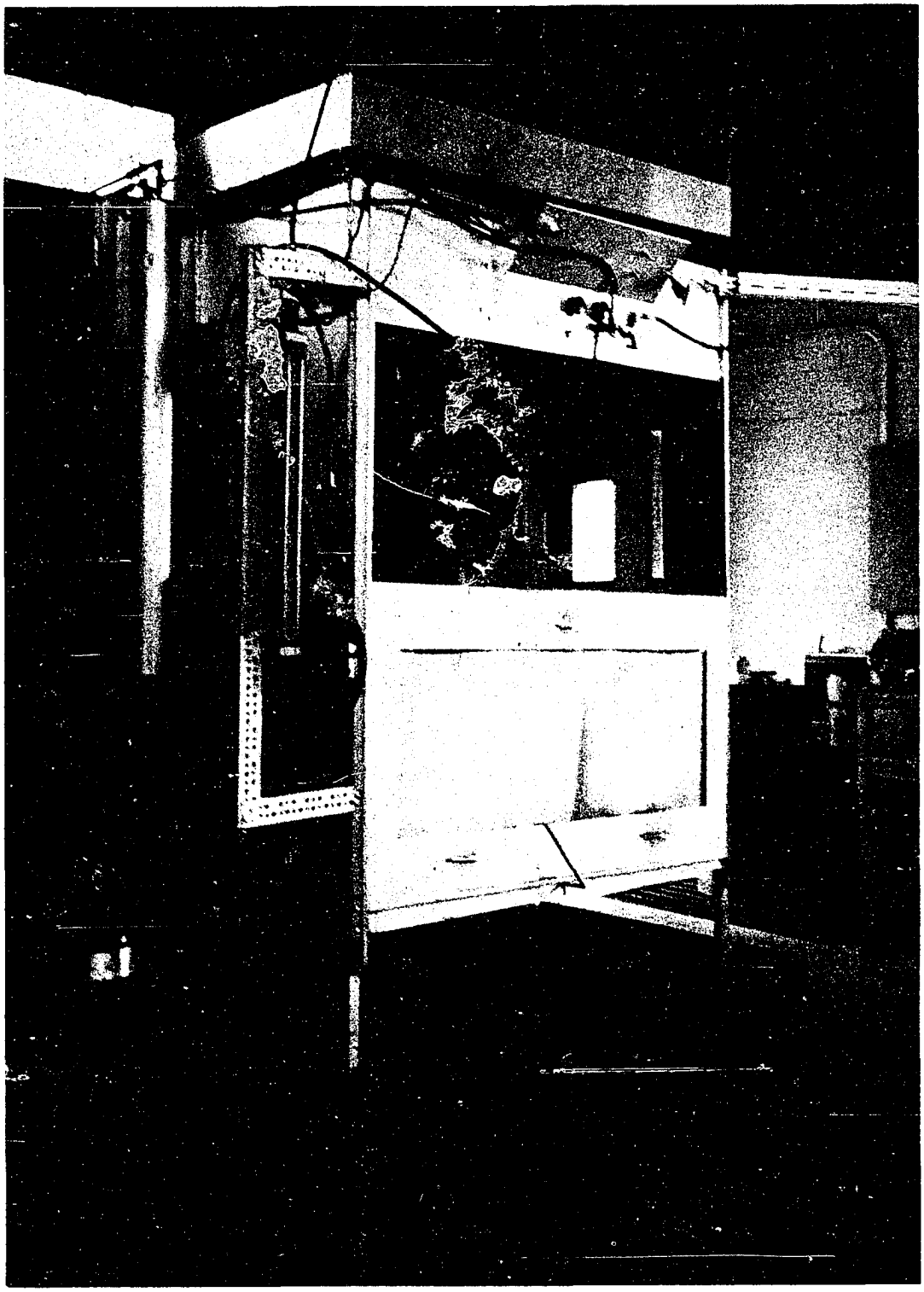

Figure III-1. Front and Left Side View of the Ignition Cabinet.

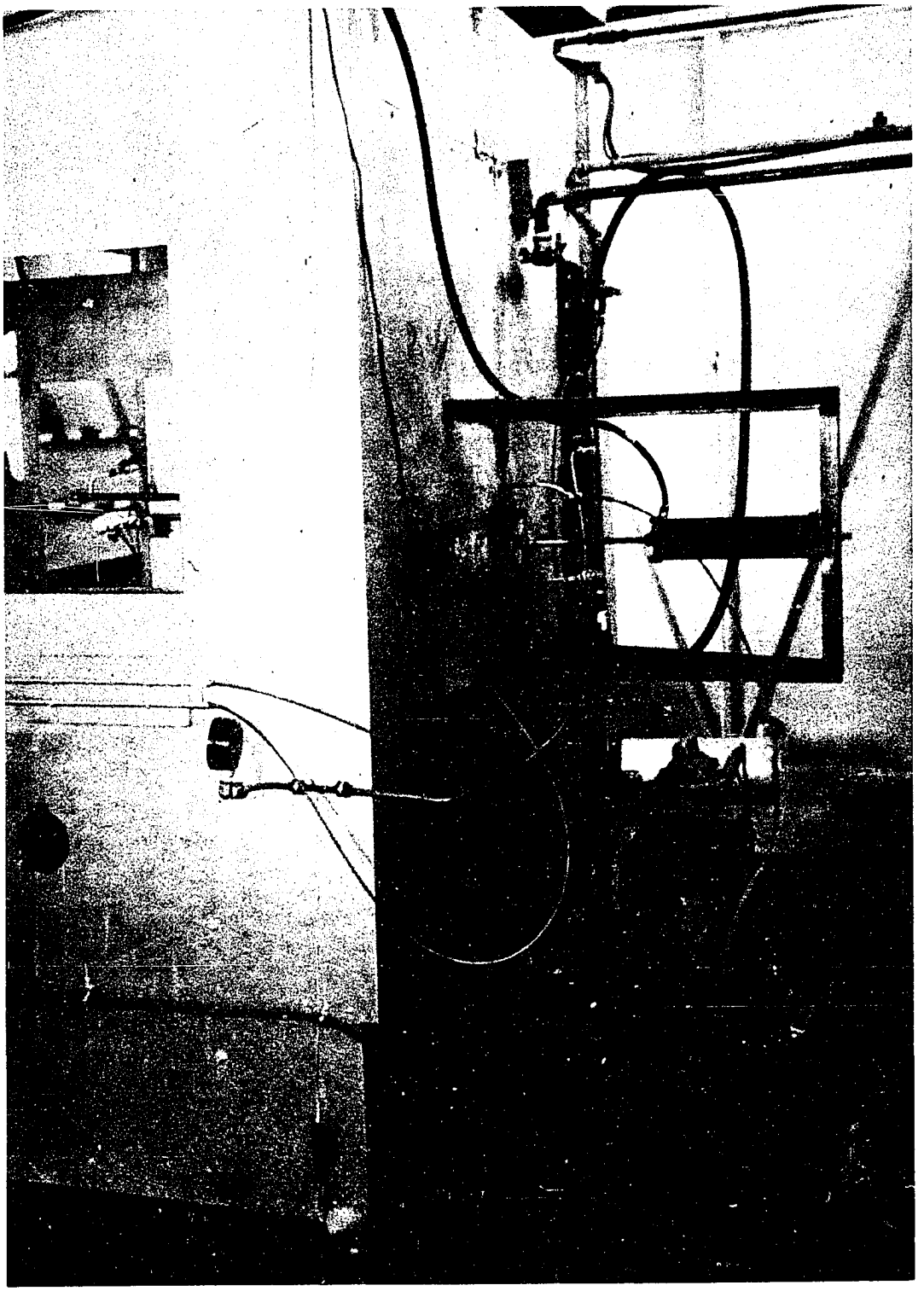

Figure III-2. Rear and Right Side View of the Ignition Cabinet.

Figure III-3 shows a cross section of the front view of the apparatus. As indicated, a sample of test material (A) is supported by a fixed vertical panel of "Fiberfrax" laminated ceramic board (B). A liquid fuel channel burner is mounted on the right side for flame radiation tests. For tungsten filament radiation tests, the liquid fuel burner serves as a support base for the tungsten lamp holder attachment. The fuel burner is 2" wide and 20 inches long and is made from galvanized steel. As illustrated by Figure III-4 a stainless steel tube 1/2 inch outside diameter by 20 1/4 inches long is welded at one end inside the burner near the top. The other end of the oxygen tube is fitted in a guide to permit differential expansion between the tube and the burner. The top of this tube is provided with 0.025-inch drilled holes on 0.25-inch centers for distribution of pressure regulated oxygen gas along the flame base. This addition of regulated oxygen gas flow is to obtain higher heating rates than could be obtained otherwise.

The tungsten filament panel is 6 inches high and 12 1/4 inches wide and contains eight 2000-watt or eight 1000-watt tungsten filament quartz lamps. The lamps operate at 2500°K at rated voltage and have a blackbody radiation distribution as illustrated in Figure III-5.

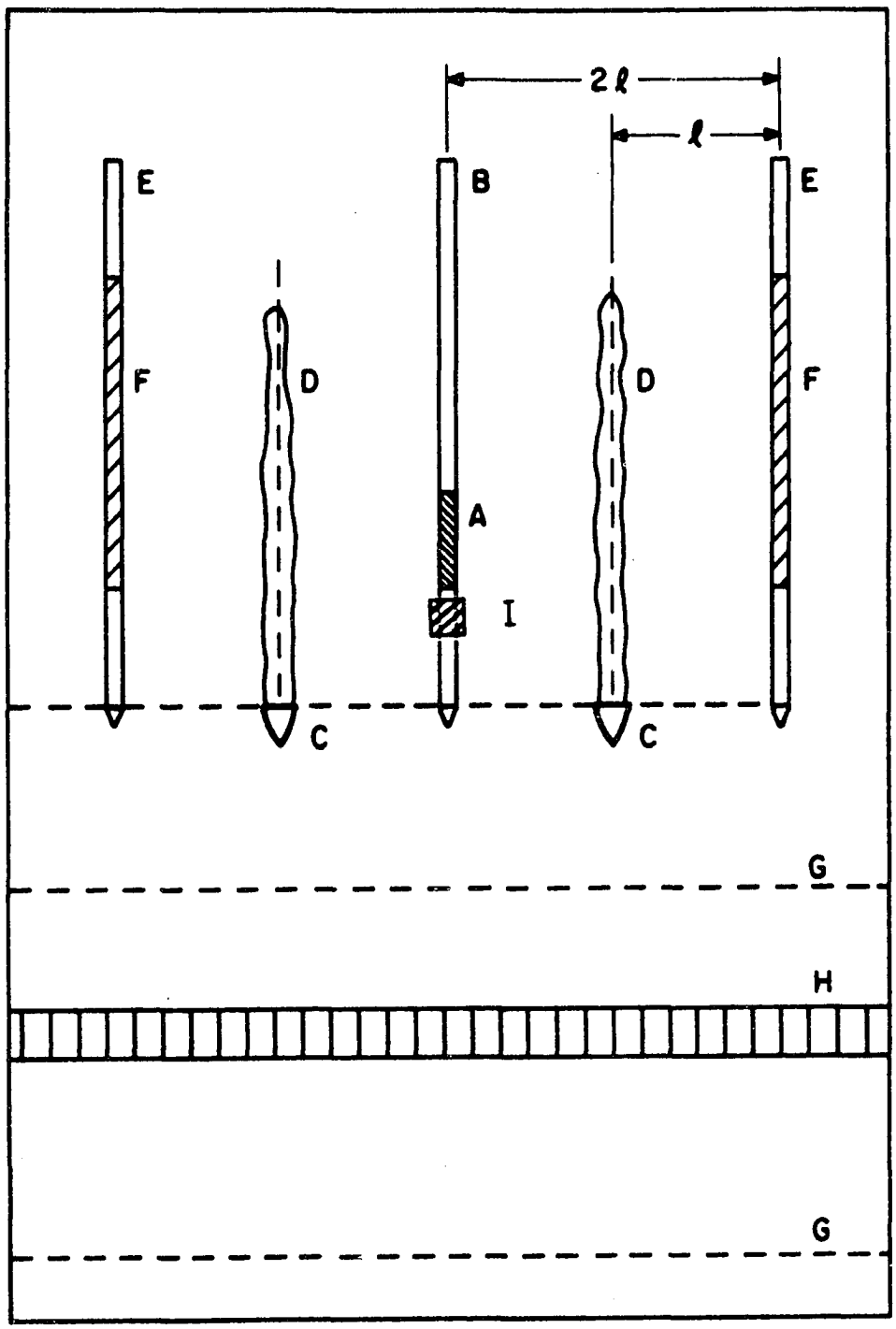

Figure III-3. Schematic Diagram of Ignition Cabinet.

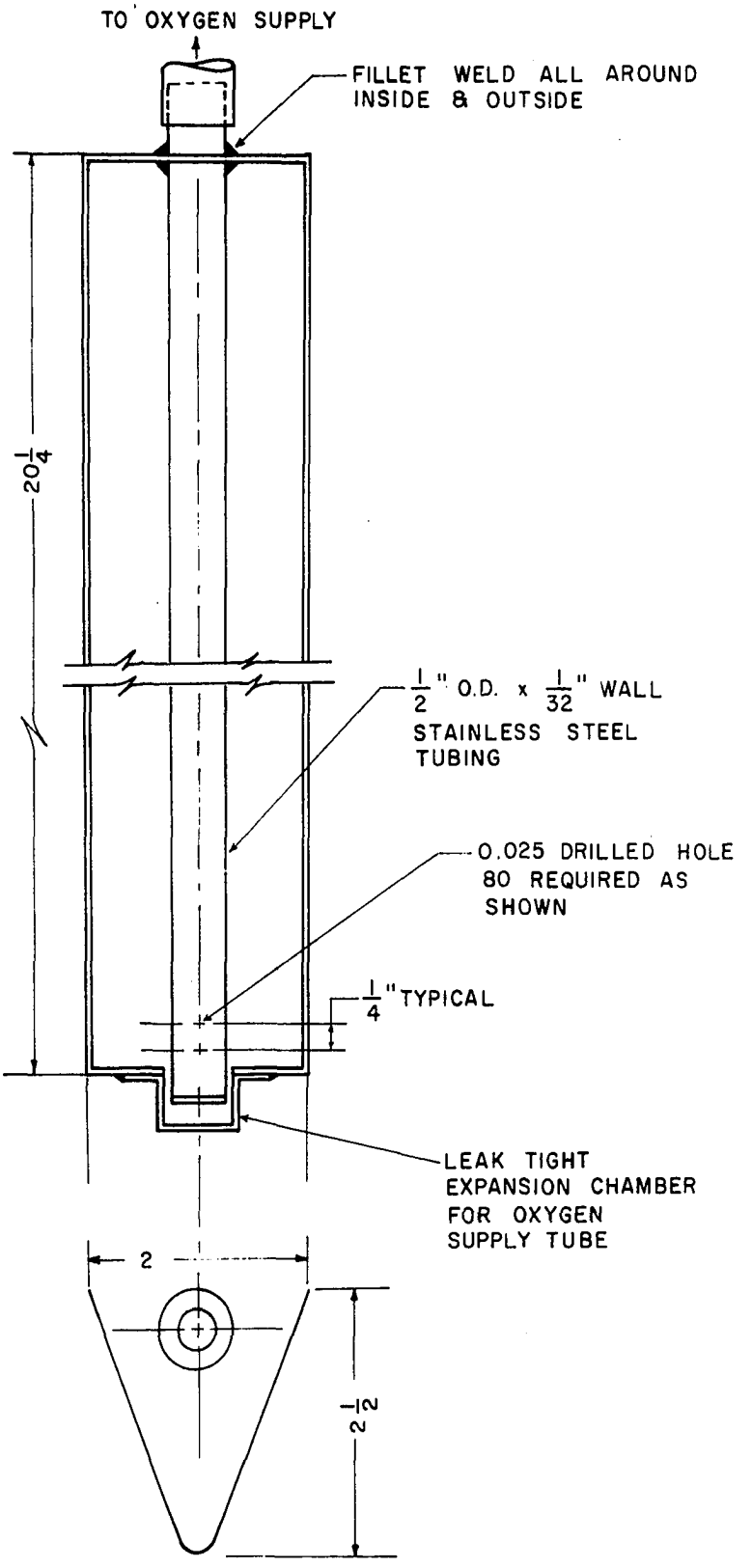

Figure III-4. Schematic of Liquid Fuel Burner and Oxygen Supply Tube Configuration.

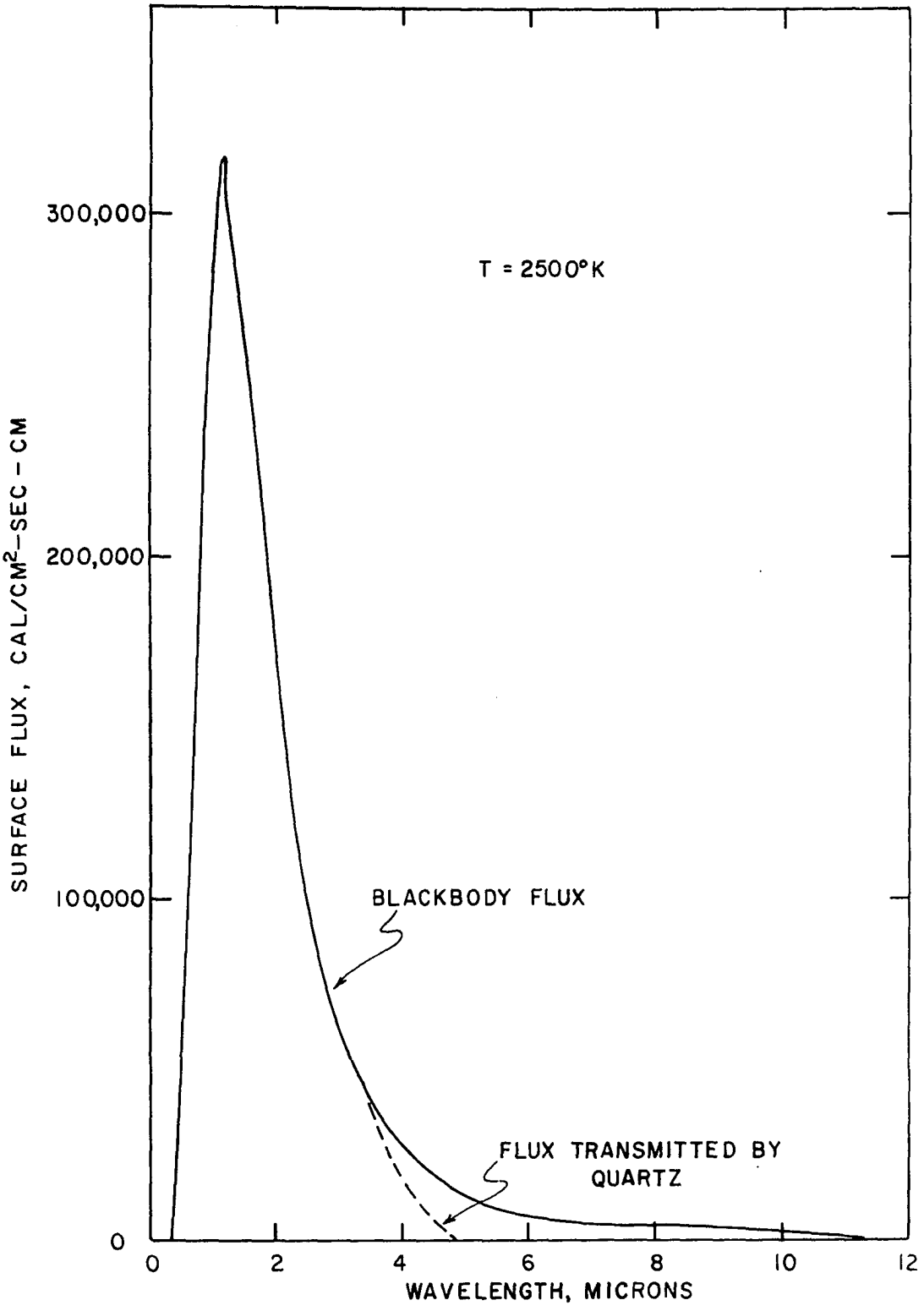

Figure III-5. Spectral Distribution Characteristics of Tungsten Filament Quartz Lamps Operating at 2500°K.

Preliminary experiments showed that if the flames were brought close to a wall,they leaned toward the wall. To counteract this leaning characteristic of flames near walls, two guide panels of "Fiberfrax" laminated ceramic board (E), each containing a high temperature glass observation window (F), were mounted on the opposite side of the flames (D) from the sample. Since the guide panels were very close to the flames, "Vicor" glass, which can be used for a maximum working temperature of 1200°C, was used for the observation windows.

In order to alter the irradiance at the sample position, arrangements were made to vary the separation distance between the radiation source and the sample. In addition, when using flames, the combustion efficiency can be increased from that associated with free-burning conditions by the injection of a regulated flow of oxygen gas along the base of the flames. The fuel burner is supported on each end on rollers which travel horizontally in channels mounted on the apparatus framework. By means of gears and a chain-sprocket arrangement, connected to an electrically driven pulley mounted on the left side of the cabinet as shown in Figure III-1, the burner and guide panel (E) can be simultaneously moved toward or away from the sample. The burner

and guide panel are geared such that the burner is always equidistant from the sample panel (B) and the guide panel (E). To permit these movements, the burners were connected to the fuel tank through flexible tubes.

In the original investigations with the ignition cabinet (14) it was necessary to adjust burner position, fuel level and exhaust fan position to pre-determined combinations in order to obtain and maintain uniform desired irradiance levels since a means of directly determining and recording irradiance levels at the sample position was not incorporated. In order to standardize the significant effects of exhaust fan air flow on the mixing characteristics of the volatile gases with the air as well as on sample surface cooling, it is necessary to utilize a fixed exhaust fan damper position. Further, to simplify the testing procedures and to provide a continuously calibrated means for determination of irradiance during each test run, a radiometer (I) was installed in the fixed vertical panel (B) on the center line of the sample and immediately adjacent to the sample holder (A). Since a sapphire window is utilized to protect the radiometer from physical internal damage and the radiometer is located a short distance from the sample center, it was necessary to calibrate the output of the permanently installed radiometer as a function of the measured irradiance

at the sample surface. This requirement was accomplished by using another radiometer installed temporarily in the center of the sample holder (A). Both radiometers were of the same water cooled type and were initially factory calibrated at the same time by the same procedures to minimize instrumentation artifacts. The outputs of each radiometer at varying burner distances, different liquid fuels and varying oxygen amount supplied to the combustion zone was recorded and a correlation of the two radiometers was established. Figures III-6, III-7, and III-8 present this correlation over the entire range of sample center irradiance levels that were used in the investigations reported herein.

As noted above, an even flow of air upward through the ignition cabinet during flame radiation investigations was necessary to assist in controlling flame stability. This flow of ambient air is also required for smoke removal and to prevent an accumulation of fuel vapors in the ignition cabinet and laboratory space. To provide this influx of ambient air an exhaust fan was installed in the hood above the cabinet. The air velocity required to provide steady flame sheets was determined experimentally by adjusting the position of a damper installed in the exhaust duct. In order to streamline the inlet air flow, the fuel burner

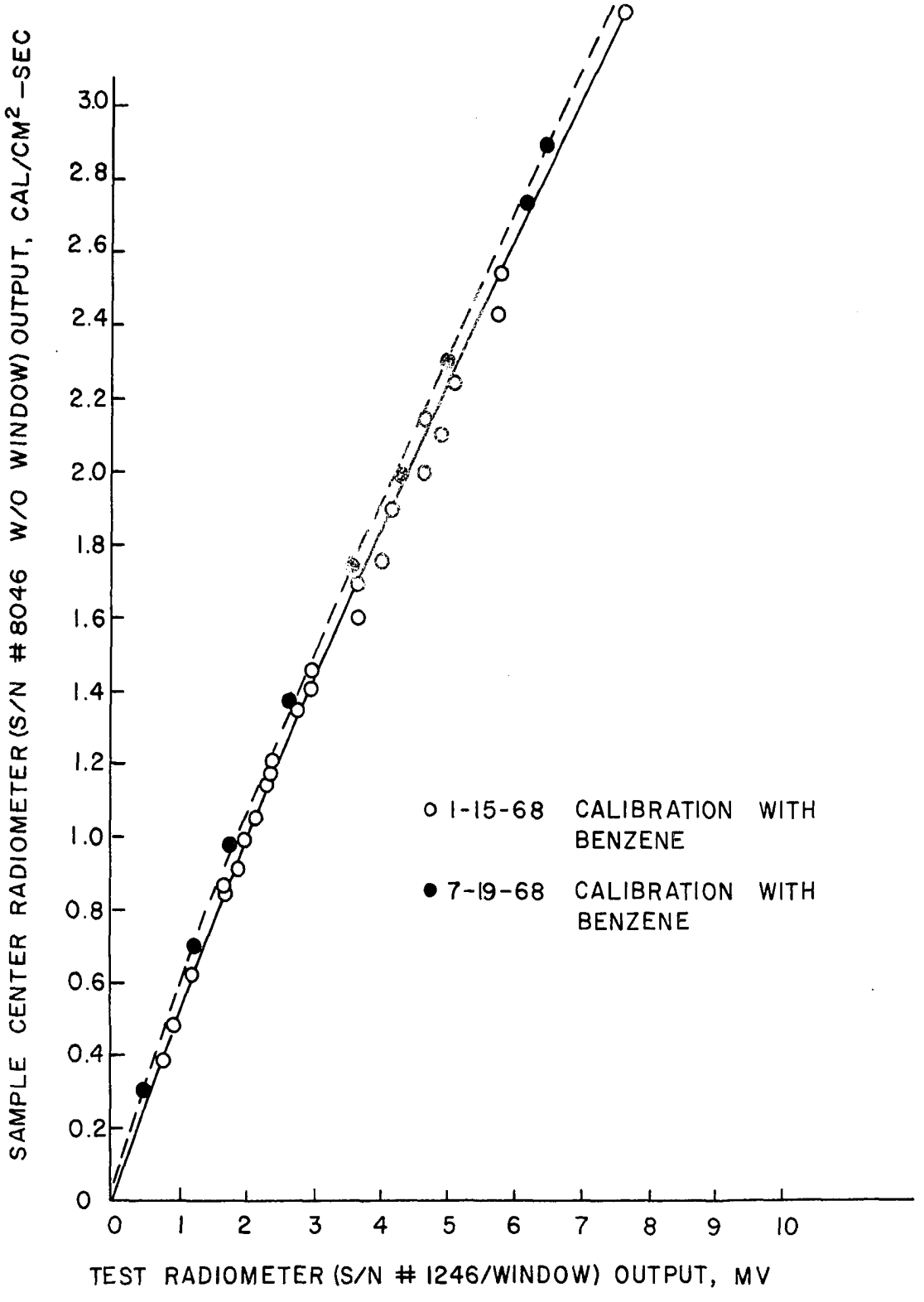

Figure III-6. Radiometer Calibration Curve for Benzene Flames.

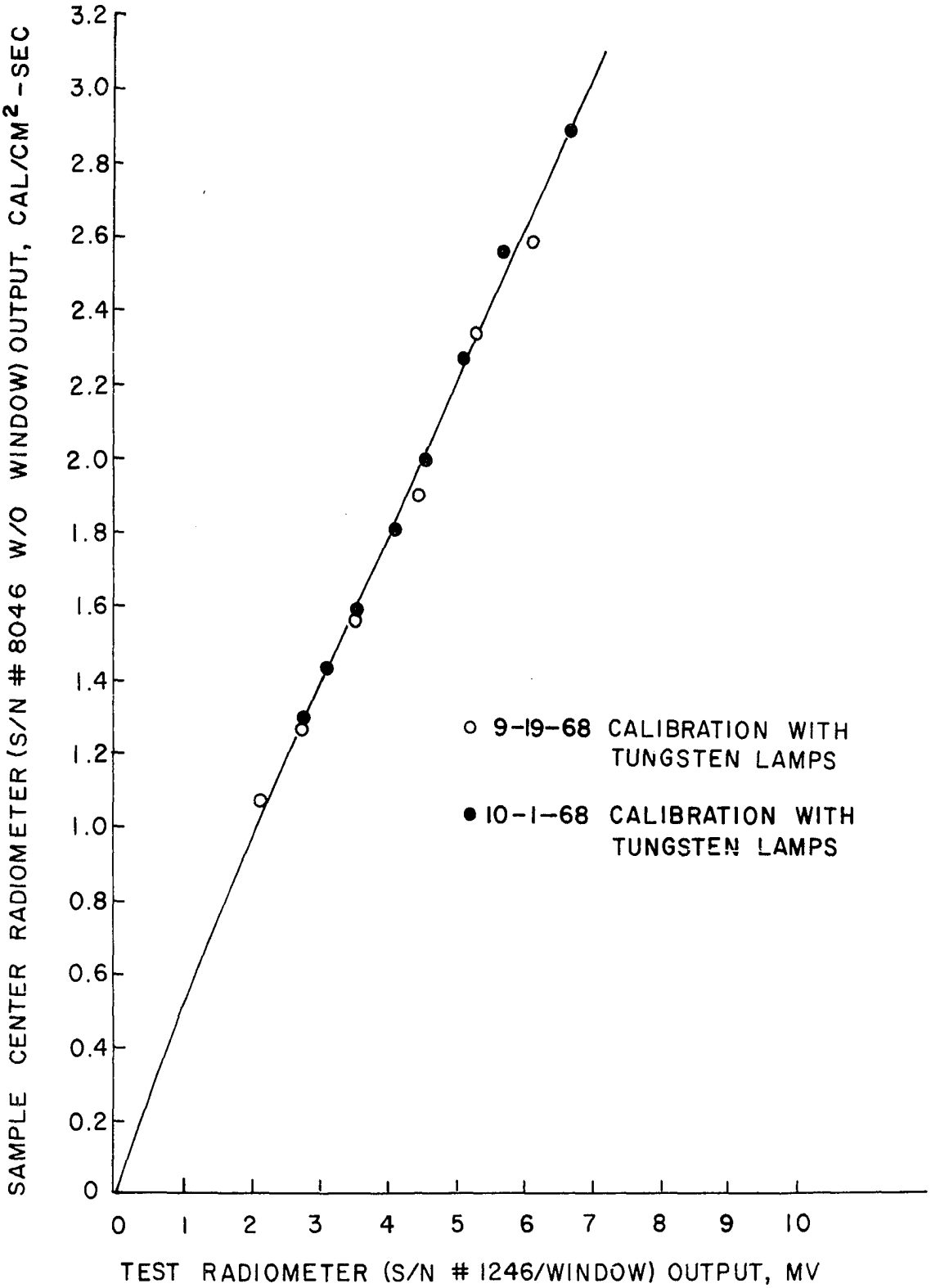

Figure III-7. Radiometer Calibration Cruve for 8-2000 Watt Tungsten Filament Quartz Lamps.

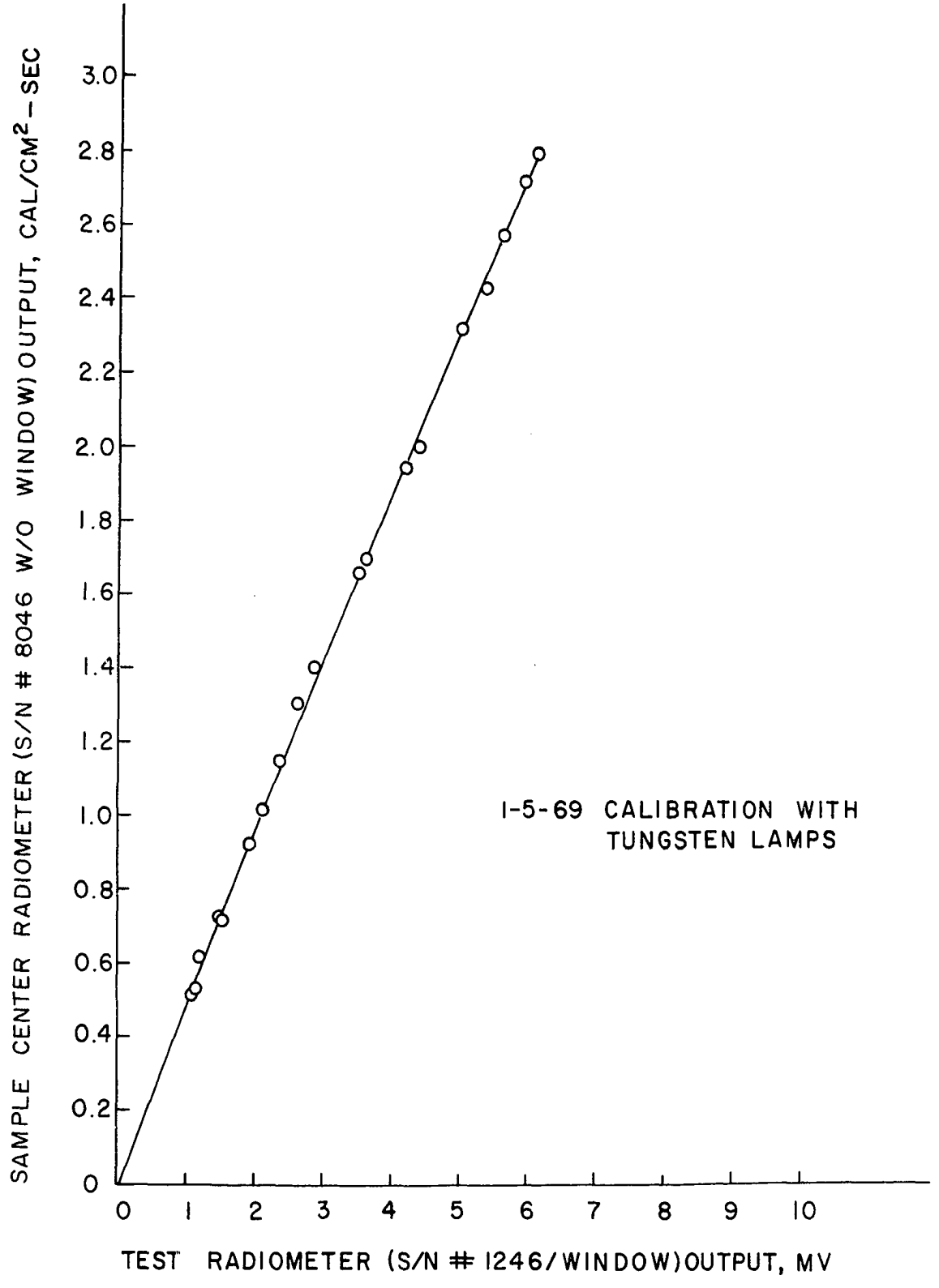

Figure III-8. Radiometer Calibration Curve for 8-1000 Watt Tungsten Filament Quartz Lamps.

and guide panels were curved on the bottoms. In addition, the air supply to the cabinet entered from beneath the burner area through a specially-designed, metal honeycomb section (H). Two fine mesh screens (G) were also provided to decrease the turbulence of the air, one below the honeycomb, and one above it. It should be emphasized that the air velocities utilized in both the flame radiation and tungsten filament quartz lamp radiation investigations were kept below 3 fps to avoid any significant "cooling effects" on the sample surface as well as to standardize the significant test variable of air flow available for mixing with the volatile gases produced by pyrolysis processes within the sample.

The cabinet itself was made of galvanized sheet metal and is insulated inside. It is 5 feet wide, 3 feet deep and 7 feet high, and is open at the top and bottom. The windows in the cabinet sides and front as shown in Figures III-1 and -2, are Herculite tempered plate glass for visual observations and photography. Herculite glass has a thermal endurance of 210°C differential and is safe under a maximum working temperature of 290°C.

A schematic diagram of the liquid fuel and oxygen supply system used in the flame radiation investigations is shown in Figure III-9. The fuel reservoir was made from a 6-inch diameter aluminum pipe with a capacity of about 5

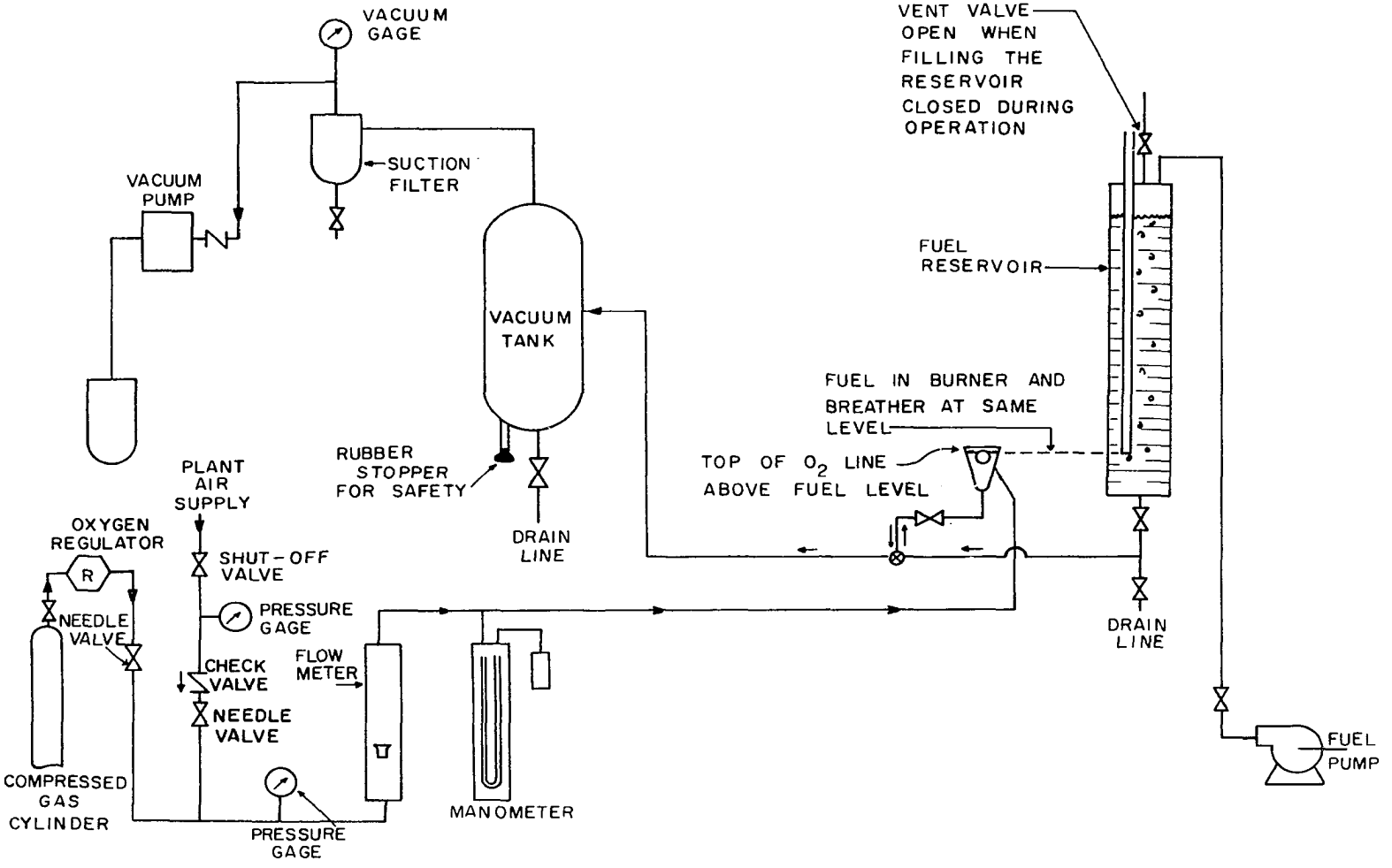

Figure III-9. Schematic Diagram of Fuel and Oxygen Supply and Control Systems.

gallons. This reservoir was mounted on the left side of the cabinet (see Figure III-1). The fuel reservoir and burner function on the principle of a constant head siphon which uses the liquid fuel in the supply line as a liquid seal between the burner and the reservoir. The end of the breather tube is positioned at the same level as that desired in the burner (i.e., approximately level with the centerline of the oxygen distribution tube to provide cooling of the tube). When liquid flows into the burner, and as the level in the burner approaches the breather's level, the head between the burner and the tank balances, and the flow of fuel stops. The liquid level inside the tank is under a slight vacuum induced by the removal of the fuel. As the fuel burns, and the level in the burner starts to fall, air is drawn in through the breather tube. As the pressure rises slightly, more fuel flows into the burner.

If a given irradiance level causes ignition to occur, it is logical to assume that surface flaming after ignition, plus continued external heating from the source, will cause the sample to burn more or less completely depending on thickness. However, it is of interest to ascertain whether or not sustained ignition has occurred. It is therefore necessary to remove the incident energy from the sample surface immediately upon ignition of the sample. Extinguishment

of the flames was accomplished with the aid of the vacuum tank shown in the diagram of Figure III-9. At the moment flaming ignition occurred, a three-way valve was actuated to isolate the fuel reservoir and to draw the fuel from the burner into a vacuum tank. As soon as the three-way valve was turned and the oxygen supply turned off, a strap of sheet-metal, guided by a slit provided in the front door of the cabinet, was also slid manually across the top of the burner. With this method the flames could be extinguished in less than 5 seconds.

The following precautions were taken as safety measures when using the liquid fuel system:

1. A section of screen wire was installed over the fuel inlet-outlet of the burner to prevent a flash-over into the fuel tank.
2. The vacuum pump on the fuel drawn down tank was kept running throughout each test until the burner fire was extinguished. This procedure was followed to keep oxygen out of the fuel exhaust system. A vacuum gauge was installed at a conspicuous location to provide a visual indication of the vacuum in the tank, which was maintained at about 20 inches of mercury throughout each test run.

3. Two check valves were utilized in the system. One of these was installed at the vacuum tank inlet. It was used to prevent a blowback of the hot fuel from the burner in the unlikely event of an explosion in the vacuum tank upon arrival of the fuel. The second check valve was used at the suction to the vacuum pump to prevent a backward flow of air in the event of a vacuum pump malfunction.
4. A rubber stopper, lubricated with vacuum grease, was held at a drain hole in the bottom of the vacuum tank while the vacuum pump was started. The stopper was thus "sucked-in" giving a good seal. Likewise, the stopper could be blown out at a very low positive pressure head. Effectively it served as a rupture disc to vent the vacuum tank in the event of a fire or explosion inside the tank.
5. To prevent possible burn injuries to the operating personnel, an operating procedure was setup so that fuel should not be allowed into the burner until the exhaust fan was turned on and the cabinet front door closed. Ignition of the fuel was accomplished by an electrical spark, manually initiated from outside the cabinet.

6. As shown in Figures III-1 and -2, the ignition cabinet was installed inside a heavy gauge sheet metal pan to contain the liquid fuel in the event of an overflow or spillage from the burner, rupture in fuel feed line, etc.
7. Fire extinguishers (dry chemical and CO_2 types) and a fire blanket were kept near the ignition cabinet at all times.

During the early stages of operation of either the flames or the quartz lamps, the irradiance is increasing. In order to expose the samples to a uniform irradiance of a known magnitude, the sample was shielded during the transient warm-up period by a water-cooled, high reflectance surface placed immediately in front of the sample.

Figure III-10 shows the relative position of the sample and this water-cooled shield. The shield was made of an aluminum base and a polished aluminum cover with the cooling water passageways in the aluminum base next to the sample. Thus, the polished cooled reflective cover and the air space adequately protected the sample during the warm-up period. Preliminary runs with thermocouples mounted in the air space indicated a temperature rise of less than 15°F above ambient during a typical warm-up period. The shield is installed in guides and can be moved horizontally to cover or expose the sample as desired.

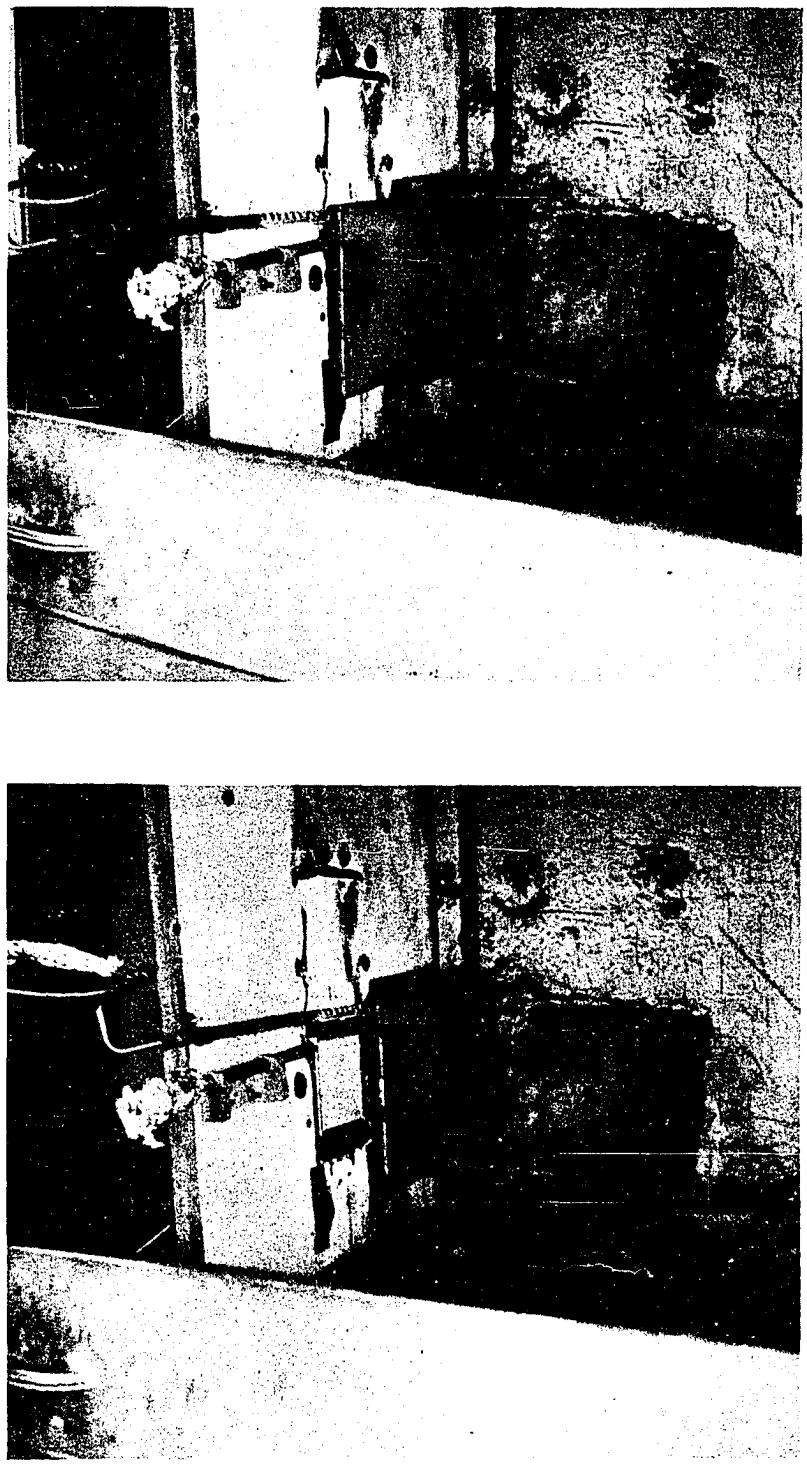

Figure III-10. Photograph of Water Cooled Sample Shield Installation.

At the higher incident irradiance levels (above 2.5 cal cm-2 sec-1) ignition of some woods, plastics, fabrics, etc. would occur in a second or less. To insure as uniform an irradiance level as possible over the entire surface area of the sample a fast acting double stroke air cylinder arrangement operating off the laboratory air supply system was used to move the shield. Less than 0.1 second was required to expose the entire sample. Air cushions within the cylinder avoided excessive forces on the ignition cabinet structure.

While some spontaneous ignition studies were made, the vast majority of tests were concerned with pilot ignition behavior. As previously noted, a review of the literature indicated that the physical location of a small "pilot flame" was a critical factor on sample ignition behavior. A careful review of Koohyar's work (14) also indicated that a single pilot flame would not necessarily "sense" the most representative volatile gas-air mixing conditions since it appears that volatile gas evolution does not always occur uniformly across the entire sample surface. Therefore, to preclude the possible adverse effects of non-uniform mixing of the volatile gas and the air, a fine nichrome resistance heating wire coil was installed just above and across the entire top edge of the sample. Figure III-11 presents a photograph of the pilot heater with the sample in the exposed position.

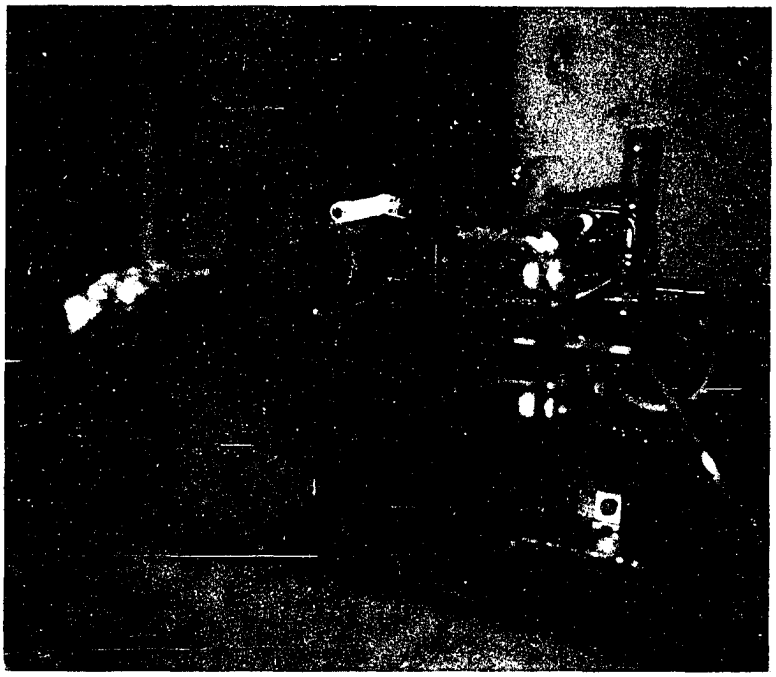

IGNITION DETECTOR AND PILOT HEATER INSTALLATION

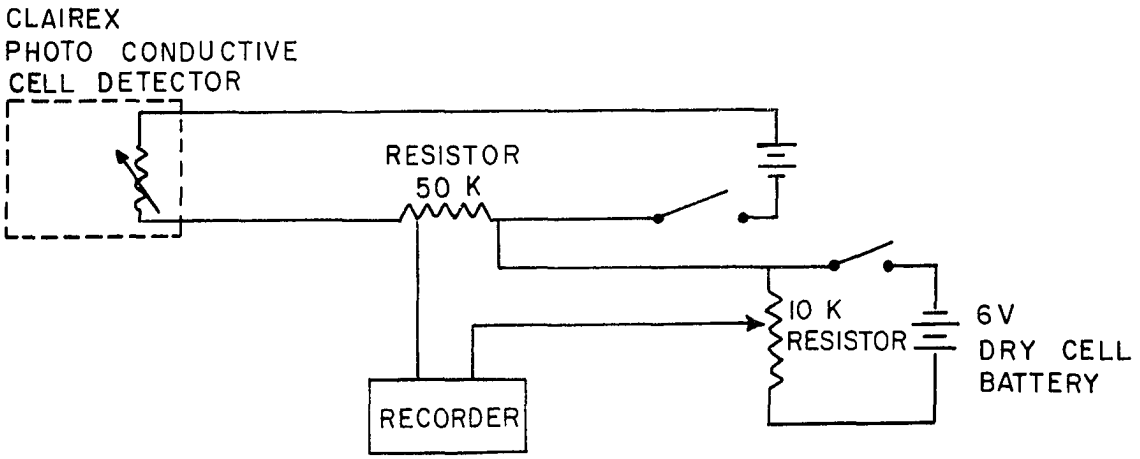

SCHEMATIC WIRING DIAGRAM OF IGNITION DETECTOR

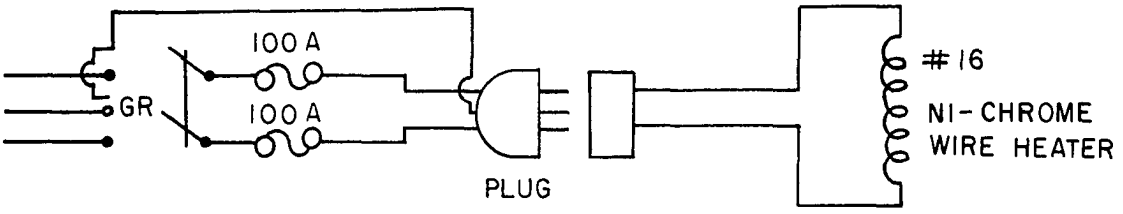

SCHEMATIC WIRING DIAGRAM OF PILOT HEATER

Figure III-11. Photograph and Wiring Schematics for Pilot Heater Coil and Photo-conductive Cell Ignition Detector.

Instrumentation

The only instrumentation requirements during actual test runs were those associated with the measurement of the incident irradiance on the sample surface and the time required for ignition to occur. Since Koohyar's work clearly illustrated that cellulosic pilot ignition could not be predicted from only surface temperature conditions and/or rate of sample weight loss, no provisions were included for determination of sample weight as a function of exposure time or sample surface temperature.

As discussed in the preceeding section, the incident irradiance was measured directly by a water cooled Heat Technology Laboratory Inc. Model GTW-10-64-573 radiometer. This particular type of radiometer utilized a water-cooled copper body with a constantan foil membrane. Copper thermocouple leads attached to the cooled copper body and the center of the heated constantan foil provide the differentials required. The range of the radiometer was 0-10 cal/cm^2-sec. The accuracy of the radiometer is within ± 1% of calibration. A sapphire window with a 150° viewing angle is utilized for physical protection of the constantan foil membrane.

The radiometer output was recorded on a two-channel Honeywell Electronik 19 potentiometric recorder. The

accuracy of the recorder was ± 0.25% of span or 1 microvolt whichever was greater. The speed of recorder pen was reported to be less than 0.5 second for full scale step response. This pen movement was considered to be fast enough to monitor the continuous irradiance measurements.

The other instrumentation system used in this study was a provision for determination of the sample ignition times. This system utilized a photoconductive cell bulk effect type of sensing (see Figure III-11). These cells are made of Cadmium Selemide (CdSe) which changes resistance when it is illuminated. In this respect it is analogous to a thermistor except the heat is replaced by light. The photoconductive cell decreases in resistance as the light level increases and increases in resistance as the light level decreases. An important characteristic of the photoconductive cell is the dependency of the sensitivity on the wavelength of the incident light. Each photoconductive material has a unique response curve which indicates the portion of the light spectrum it is sensitive to. The particular photoconductive cell utilized (Clairex Model CL 603 AL) has a characteristic peak response at 7350 Angstroms (near infrared). A slightly longer wavelength would be more desirable but the CL 603 AL is the longest

wavelength sensitive cell currently available. The photoconductive cell is installed inside a tube which is painted black to avoid incident light from the flames when the flames are close to the sample surface. The photoconductive cell is installed to "look" across the upper edge of the sample surface since ignition always occurred just above the sample and flashed down from the sample surface. At the instant of flaming ignition the sensitivity of the photoconductive cell increases due to the light from the resultant flames. The output of the photoconductive cell through a 50 K-ohm Type J resistor is recorded on the second channel of the Honeywell Electronik 19 potentiometric recorder. A typical trace of the continuous recordings of incident irradiance and photoconductive cell outputs is shown in Figure III-12. As shown, opening of the water-cooled shield results in a slight increase in the radiometer output since the shield partly obstructs the radiometer field of view. The initial photocell output trace is used as the start of exposure. As also shown, flaming ignition results in a sharp increase in the photoconductive cell-resistor output. This point is used to define the instant of ignition. Recording of the chart speed and the distance between these two points adequately define the ignition time for the recorded incident irradiance level.

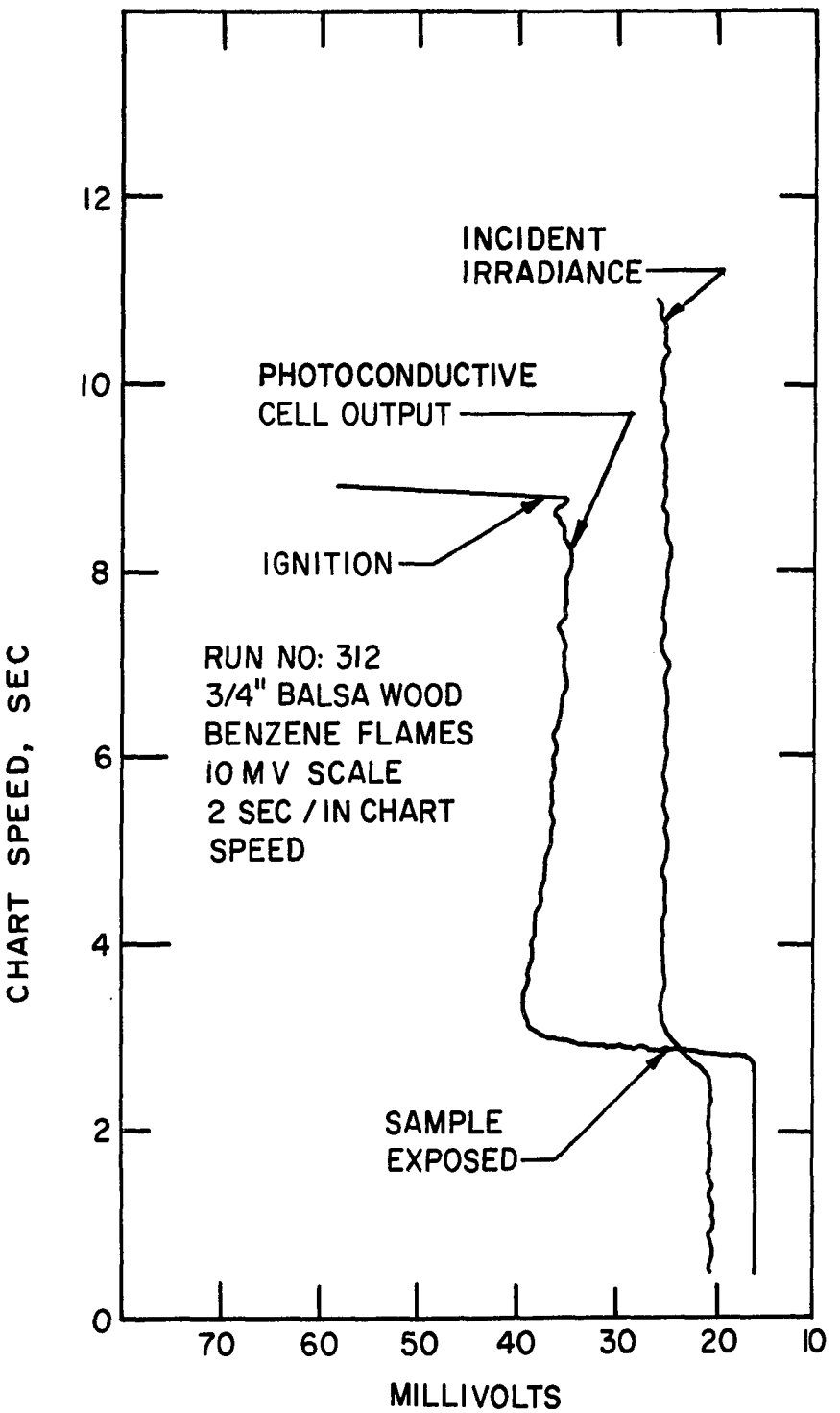

Figure III-12. Typical Recorder Output During Experimental Run.

Experimental Procedure

The experimental technique used in this investigation differed from those used in previous ignition studies that used approximate blackbody energy sources and was similar in some respects to that used by Koohyar (14) in his original flame radiation investigations. Therefore, in the interests of completeness and to explain the differences between these studies and those conducted by Koohyar the work will be discussed along with the experimental procedure.

The present study utilized one-dimensional samples of twelve different woods and three different fabrics. Wood samples for each species were cut from the same board in several different thicknesses. For three different woods (Alaskan cedar, cottonwood and oak) thickness ranging from 0.3 cm to 2.54 cm were utilized. Thickness of 1.97 cm and 2.54 cm were used for the remainder of the woods. The nominal exposed area of the samples was 9.9 by 9.9 cm. The shape of the wood samples and the method of attachment is shown in Figure III-13. Preliminary tests by Koohyar (14) showed that some of the wood samples used in his study, especially oak and fir, crack along the grain and bend after they have been heated for some time. In order not to disturb the conditions for uniform irradiance and one-dimensional

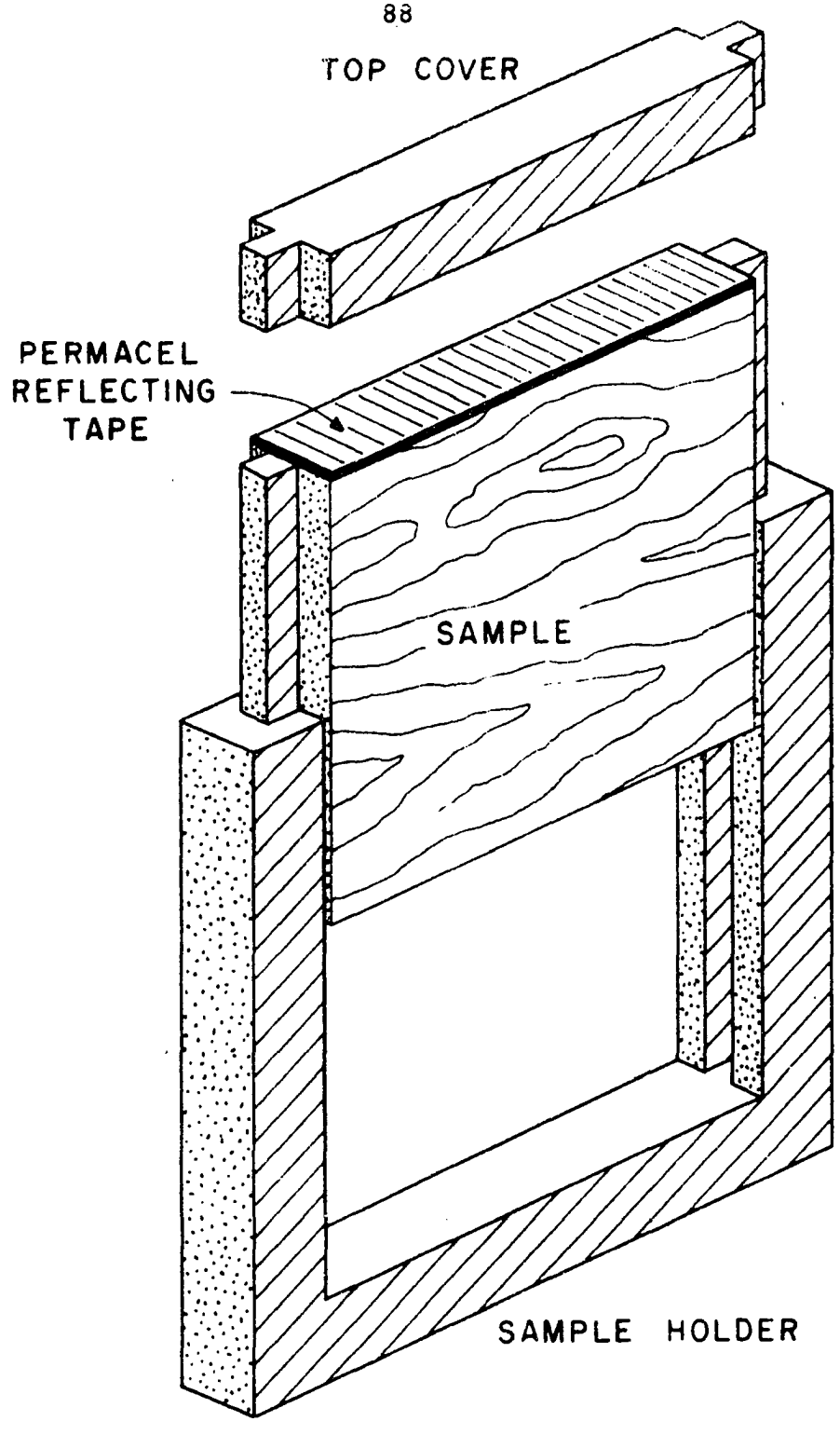

Figure III-13. Position of Sample in Sample Holder.

heating the samples were maintained vertical in the holder throughout the tests by a tongue and groove joint as shown in Figure III-13. This same type of sample-holder arrangement was utilized in the investigations reported herein. Likewise, since some of the samples will expand upward during the heating process, the sides of the sample holder were made longer than the samples. A block of insulating material was used as a top cover, as shown in Figure III-13, to prevent heating from the top. The sample was otherwise free to move in the tongue and groove joint to accommodate shrinkage and expansion. To prevent end effects, a piece of Permacel reflecting tape was applied to the top such that about 1/8 inch extended down on the surface of the sample (see Figure III-13). The Permacel tape (Type PE-100) used in these experiments was an aluminum-coated glass cloth 6.5 mils thick and is specifically designed to reflect radiant heat. The tape was coated with a silicone pressure sensitive adhesive which did not significantly deteriorate prior to ignition.

All samples were oven dried at 102°C for 24 hours. Each was then individually wrapped in a polyethylene bag and sealed to insure that dryness was maintained. Approximately one-half of the wood samples were spray painted with Krylon flat black enamel prior to being placed in the drying oven.

In order to insure a one-dimensional heating condition for the fabrics a different sample holder configuration had to be used. As shown in Figure III-14 a holder with two spring loaded dowel pins was utilized. The holder assembly was constructed of stainless steel to insure a relatively free sliding action. The cloth material was looped and stitched along each side to provide a section for sliding over the dowel pin. Since the double thickness and contact with the holder dowel pins constitute a different thermal condition than the center of the fabric, Permacel tape was used as a heat reflector for the sample side areas.

A typical test was carried out as follows:

1. The water supply for cooling the sample shield and radiometer was turned on. A sight glass provided means for observing that water flow was obtained through both items.
2. The exhaust fan was turned on and the damper adjusted to the "fixed position" used for all test runs.
3. The electronic equipment was turned on and allowed to warm up.
4. The fuel tank was filled with fuel and the vacuum pump was started.

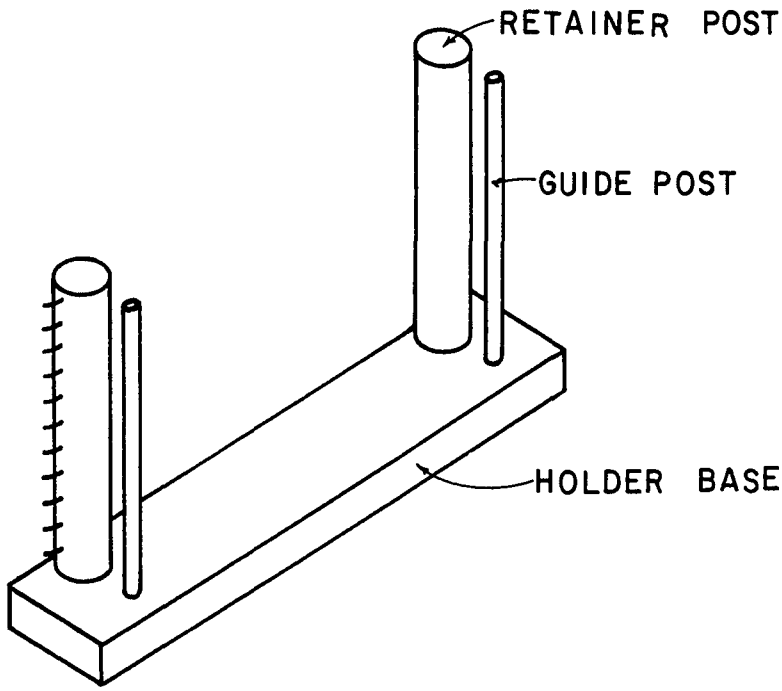

Figure III-14. Fabric Sample Holder

5. After the instruments were warmed up and the zero settings checked, the photoconductive cell output was checked by holding a lighted match in front of the viewing tube and the recording checked for the required characteristic break. The radiometer was similarly checked.
6. The wood sample was then taken out of the polyethylene bag and installed in the sample holder as illustrated in Figure III-13, and the sample shield was positioned in front of the sample.
7. The ignition cabinet door was then closed and the fuel system three-way valve opened.
8. After the fuel burner was filled to the desired level, the electric spark ignitor manual switch was closed and the fuel ignited remotely.
9. The recorders were started and the fuel burner-sample distance and oxygen flow adjusted to provide the desired irradiance level.
10. After the irradiance level stablized, the pilot heater was turned on and stablized.
11. The recorded speed was then adjusted to the desired rate and the sample shield retracted remotely.

12. Immediately following ignition of the sample, the pilot heater and oxygen supply were turned off and the burner fire extinguished.
13. The vacuum pump was turned off as soon as the fire was extinguished. At the conclusion of the test run the contents of the vacuum tank were drained into a safety can and the vacuum pump filter, which had trapped the condensed fuel vapors, was drained.
14. The ignition cabinet door was opened, and the burnt sample removed. The system was then ready for the next test run.

The shutdown of the cabinet at the end of the testing day consisted of cooling the cabinet, turning off the photoconductive cell, turning the recorder to standby position, draining the fuel system into safety cans and turning the exhaust fan and cooling water supply off as well as closing the oxygen cylinder valve.

CHAPTER IV

DISCUSSION OF THE RESULTS

A review of the previous work on the ignition of combustible solids, as briefly discussed in Chapter II, indicates that:

1. The previous studies on ignition of combustible solids by thermal radiation have utilized radiation sources including tungsten filament lamps, gas-fired refractory panels, carbon arcs, solar furnaces and diffusion flames. However, a satisfactory correlation of the reported results using proposed ignition criteria cannot be obtained. Further, an acceptable correlation of different investigative efforts using similar radiation sources could not be determined using the reported data.
2. The work of Koohyar (14) indicates that the criterion of a fixed rate of evolution of volatiles is required for ignition is a necessary but not sufficient condition for ignition to occur. His

work likewise indicates that the criterion of a fixed surface temperature for ignition of cellulosic materials may not be valid.

3. Some of the more recently published results on cellulosic materials indicate a very strong dependency of ignition times on the density of the materials being studied.
4. Experimental evidence also indicates a significant difference between the ignition times of thermally thick and thinner woods.
5. It is quite apparent that the pilot ignition results from the absorption of incident energy with the time required to obtain ignition being dependent in part upon the following:
   a. The rate of energy absorption
   b. The external mixing process of the volatile gases produced by the pyrolysis processes and the surrounding air.
   c. The velocity of airflow in the mixing zone.
   d. The position of the pilot ignition source.
   e. Test set-up configuration influences.

Experimental Validation of Preliminary Conclusions

Based on the work of previous investigators, it is clear that the ignition characteristics of a combustible

material exposed to an external radiating source is strongly dependent on the thickness, density and energy absorptance charactertistics of the sample.

The role of thickness was recognized by others, including Simms (39, 41) and Koohyar (14). Fundamentally, the thickness enters the heat conduction equation in the form of the Fourier modulus. For thin woods some of the absorbed energy will be conducted through the wood and lost by convection at the exit surface before ignition occurs. For thick woods the absorbed energy will not have adequate time to be conducted through the wood and lost by convection at the exit surface before ignition occurs.

The role of density is evident from a review of the work of Simms (42) and Koohyar (14). The latter's investigation particularly emphasized some of the unavoidable complexities in dealing with wood samples. For example Koohyar found that a density variation of the order of 20 to 40 percent between different samples of a given species of wood is not uncommon. In fact, density variations of 10 to 20 percent were found in samples cut from the same board.

Unlike the parameters of thickness and density, which had been generally accepted as principal variables in the ignition process, prior to the work of Koohyar (14),

energy absorptance appears to have been relegated to a minor role. In order to assess the relative contribution of energy absorptance to the ignition process, some preliminary experiments were undertaken on the ignition of colored cotton fabrics. Fabrics were chosen primarily because as a first approximation the parameters of thickness and density could be neglected. The results of these studies, which have been reported previously (49) are summarized herein since they constitute the principal justification for the subsequent studies on ignition of woods.

Several different cotton fabrics which had been used previously by Lee and Alvares (20) in a series of ignition tests using a tungsten filament lamp source operating at 2500°K were selected for these initial flame tests. The cotton fabrics exposed to the flame radiation were manufactured to the same specifications as those used by Lee and Alvares. Two white cotton fabrics and one black cotton fabric were used.

Figure IV-1 presents the ignition behavior of the untreated white cotton fabric by flame radiation and compares the results with those of Lee and Alvares (20) for ignition by a tungsten filament lamp source. The flame source is seen to cause ignition in about one-third the time that is required for the tungsten source. As shown

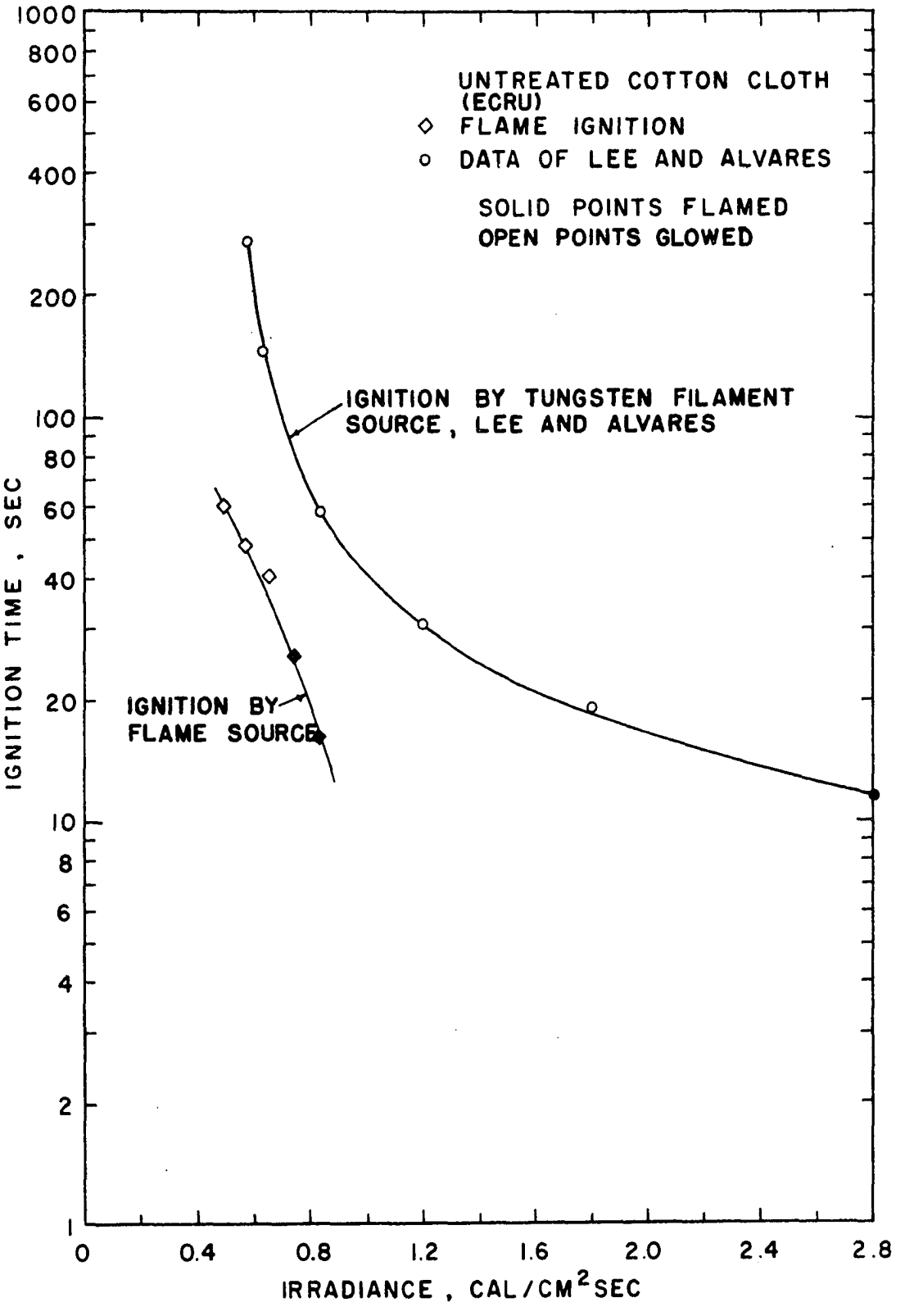

Figure IV-1. Ignition Behavior of Untreated Cotton Cloth.

in Figure IV-2 the treated white cotton fabric behaved similarly, with ignition by the flame source being more rapid than ignition by the tungsten source.

Figure IV-3 presents a comparison of the ignition response times for both the flame radiation and tungsten source for the black cotton cloth. In this case close agreement between the two ignition sources resulted, as expected, since the black cloth more nearly approximates a blackbody absorber than do either of the two white samples and, thus, absorbs essentially the same fraction of incident energy at all wavelengths. As shown, the data compare favorably over the entire range of irradiance for which flame data were obtained.

From the preceding results it is evident that the ignition behavior of flammable materials should be strongly dependent upon the spectral distribution of the incident radiation and the monochromatic absorptance characteristics of the materials being irradiated. This strong dependence suggests that a single correlation can be developed for relating the ignition behavior as a function of the net energy absorbed for materials having essentially the same thickness and density. By way of verification a preliminary correlation (neglecting density and thickness variations within the cotton fabrics) based only upon the net energy

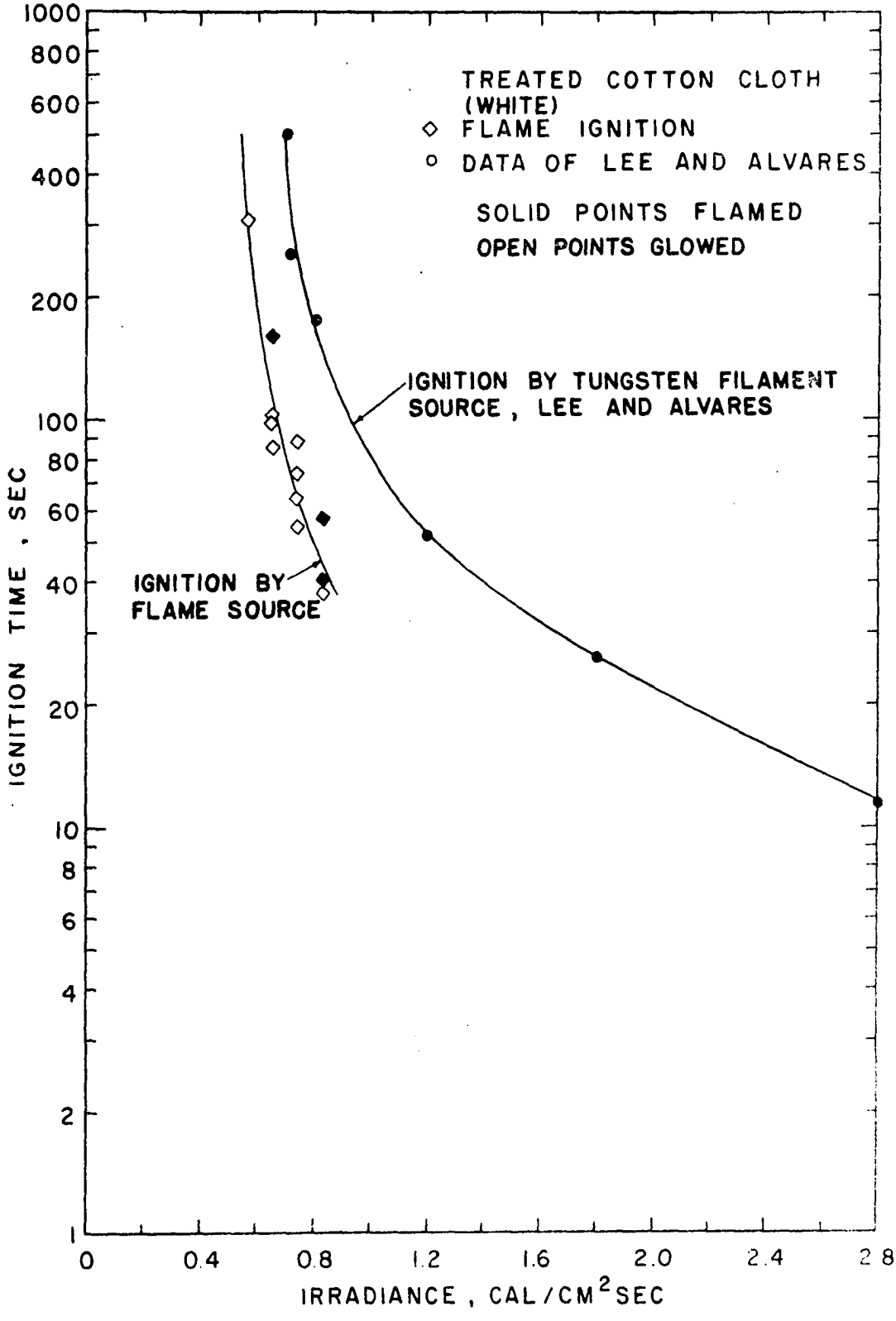

Figure IV-2. Ignition Behavior of Treated Cotton Cloth.

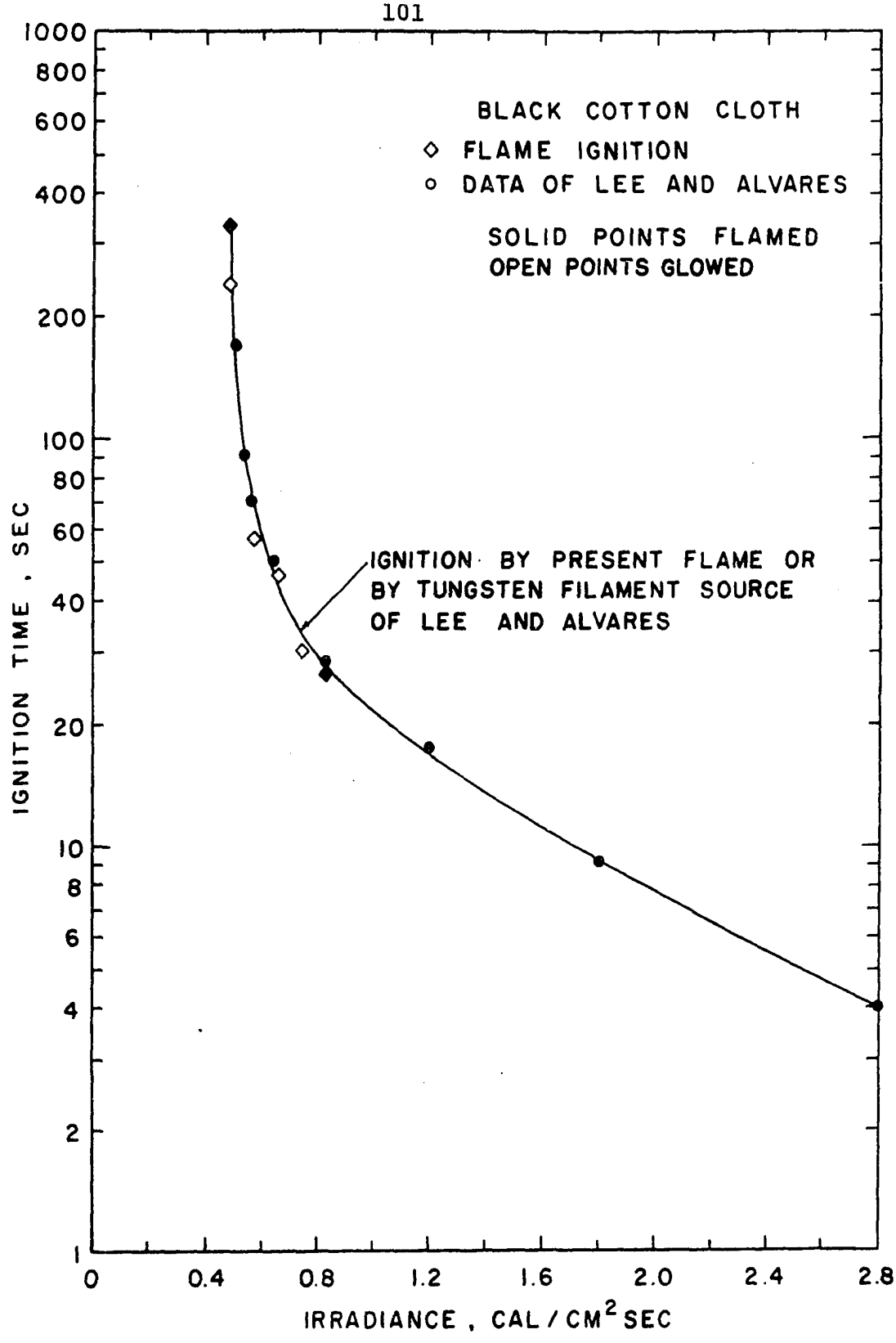

Figure IV-3. Ignition Behavior of Black Cotton Cloth.

absorbed from the incident radiation was made for the different cotton fabrics considering flame and tungsten irradiance. This correlation also neglected any effects of decomposition and pyrolysis. In addition, the effects of cooling at the surface by convection and reradiation and the loss or gain of energy due to pyrolysis reactions and energy transmitted through the cotton fabrics were judged to be about equal for the two different irradiances and were neglected in the correlation. Based on these simplifying assumptions, Figure IV-4 presents a schematic of the mathematical model for the energy balance on a target exposed to a constant level of incident irradiance. As shown, the energy absorbed by the samples can be expressed as

$$H_a = H_i - \int \rho_\lambda \, e_{\lambda i} \, d\lambda - \int \tau_\lambda \, e_{\lambda i} \, d\lambda - \epsilon_f \sigma \, T_f^{\,4} - \epsilon_r \sigma (T_r^{\,4} - T_{a_2}^{\,4}) - h_f (T_f - T_{a_1}) - h_r (T_r - T_{a_2}) + (\Delta H)_{CR} \qquad \text{(IV-1)}$$

where H_a = absorbed energy

H_i = measured incident irradiance

$\int \rho_\lambda \, e_{\lambda i} \, d\lambda$ = integrated reflected energy losses over applicable range of wavelengths

$\int \tau_\lambda \, e_{\lambda i} \, d\lambda$ = integrated transmitted energy losses over applicable range of wavelengths

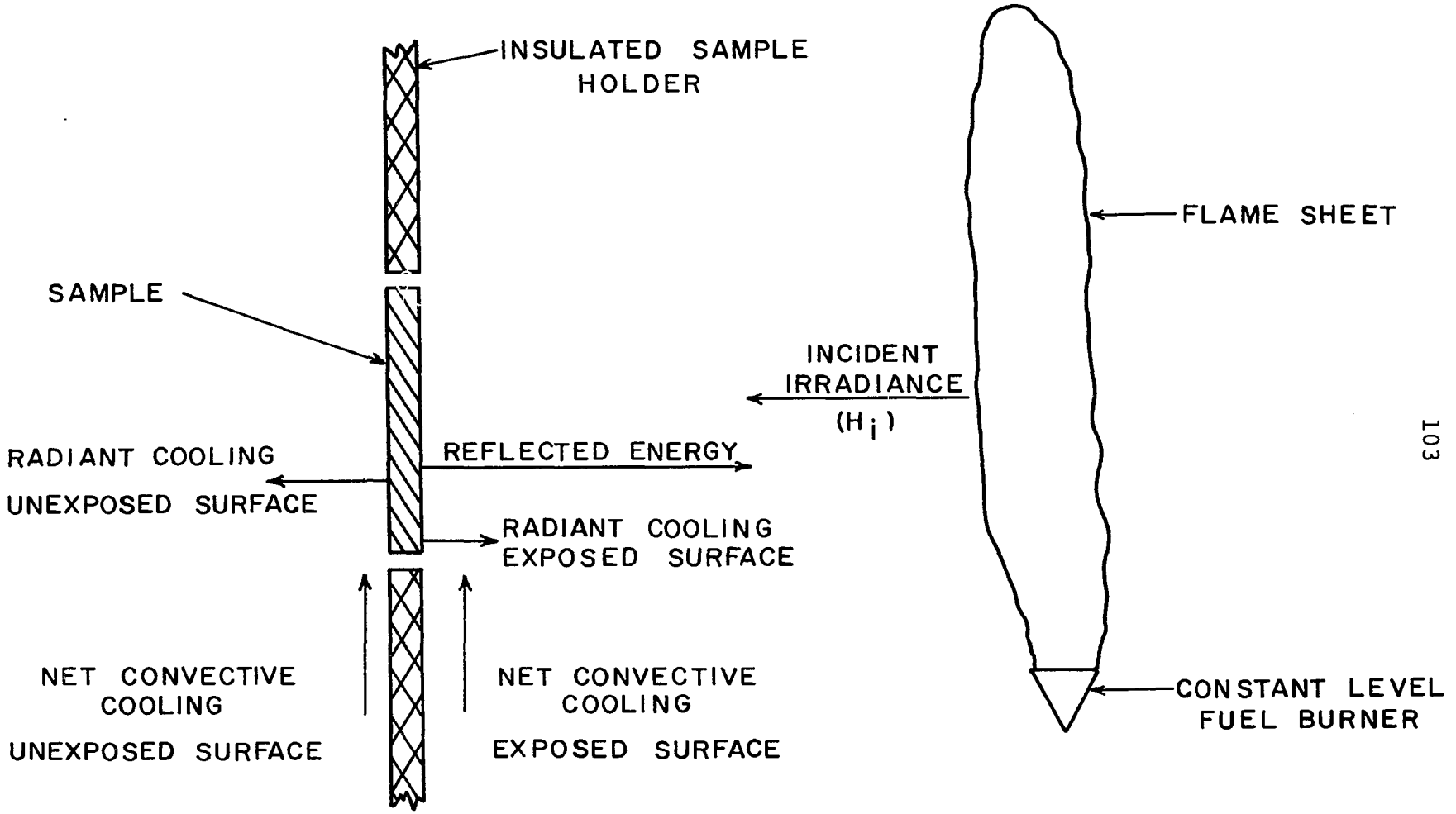

Figure IV-4. Sample Total Energy Balance Model.

$\epsilon_f \sigma (T_f^4 - T_{a_1}^4)$ = reradiated energy losses from target front surface

$\epsilon_r \sigma (T_f^4 - T_{a_2}^4)$ = reradiated energy losses from target rear surface

$h_f (T_f - T_{a_1})$ = convective energy losses from front surface

$h_r (T_r - T_{a_2})$ = convective energy losses from rear surface

$(\Delta H)_{CR}$ = energy generation or absorption due to chemical reactions

ρ_λ = reflectivity of target at wavelength λ

$e_{\lambda i}$ = emissive power of irradiation source at wavelength λ incident on sample surface

τ_λ = transmissivity of target at wavelength λ

ϵ = emissivity of the target

σ = Stefan-Boltzman constant

h = convective heat transfer coefficient

T = absolute temperature

Subscripts

λ = wavelength

s_1 = sample front surface

s_2 = sample rear surface

a = ambient

In order to obtain a very preliminary confirmation of this approach to establishing a comparison of ignition data it was necessary to obtain data regarding the energy losses noted above. It was not possible to extract from the data reported by Lee and Alvares (20) values on the transmitted, reradiated and convective cooling losses associated with the cotton fabric tests using the 2500°K tungsten lamp source. However, since these losses should be quite small in relation to the absorbed and reflected energies and since they should be on the same order of magnitude for both the tungsten lamp and flame irradiance tests, it was decided to neglect these effects in attempting to compare the two sets of data as a function of absorbed energy.

Since a significant fraction of the energy incident on the fabric surface would be reflected, as clearly illustrated by the differences in ignition times in Figures IV-1 and 2, it is of primary importance to evaluate the magnitude of the effect of reflection of energy from the irradiated surface. Fortunately, absorptance data on the black cotton cloth and the treated white cotton cloth were available from Lee (19). These two fabrics were essentially the

same in every respect except color. These data were obtained and then utilized to approximate the fraction of energy absorbed for both the flame radiation and blackbody type of radiation supplied by the tungsten source. Lee's data permitted computation of the spectral absorptance of the black and treated fabrics for wavelengths from only about 0.4 microns to about 2.6 microns. Beyond 2.6 microns, the absorptance was assumed to be constant. Figure IV-5 presents plots of the absorptance used for these two fabrics.

For the emissive power of the flame source the data of Ryan, Penzias and Tourin (34) were used (see Figure IV-6). Although these data are for hexane flames, whereas cyclohexane was used as the fuel in the actual tests, very little difference in the emissive powers of the two fuels is expected.

As discussed previously, the energy absorbed by the fabric samples is a function of both the spectral absorptance and the spectral emissive power of the source. An average total absorptance for a given sample-radiation source configuration can be defined as

$$\alpha_{avg} = \frac{\int_{\lambda_1}^{\lambda_2} \alpha_\lambda \, e_\lambda \, d\lambda}{\int_{\lambda_1}^{\lambda_2} e_\lambda \, d\lambda} \qquad \text{(IV-2)}$$

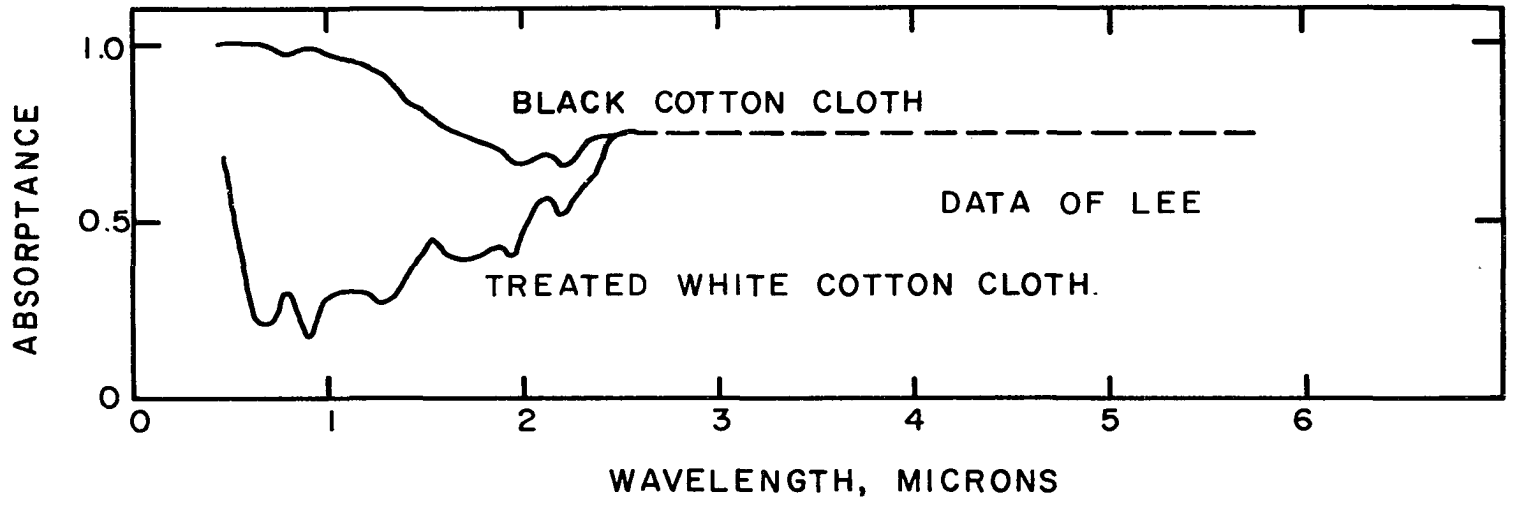

Figure IV-5. Monochromatic Absorptance Characteristics of White and Black Cotton Cloth.

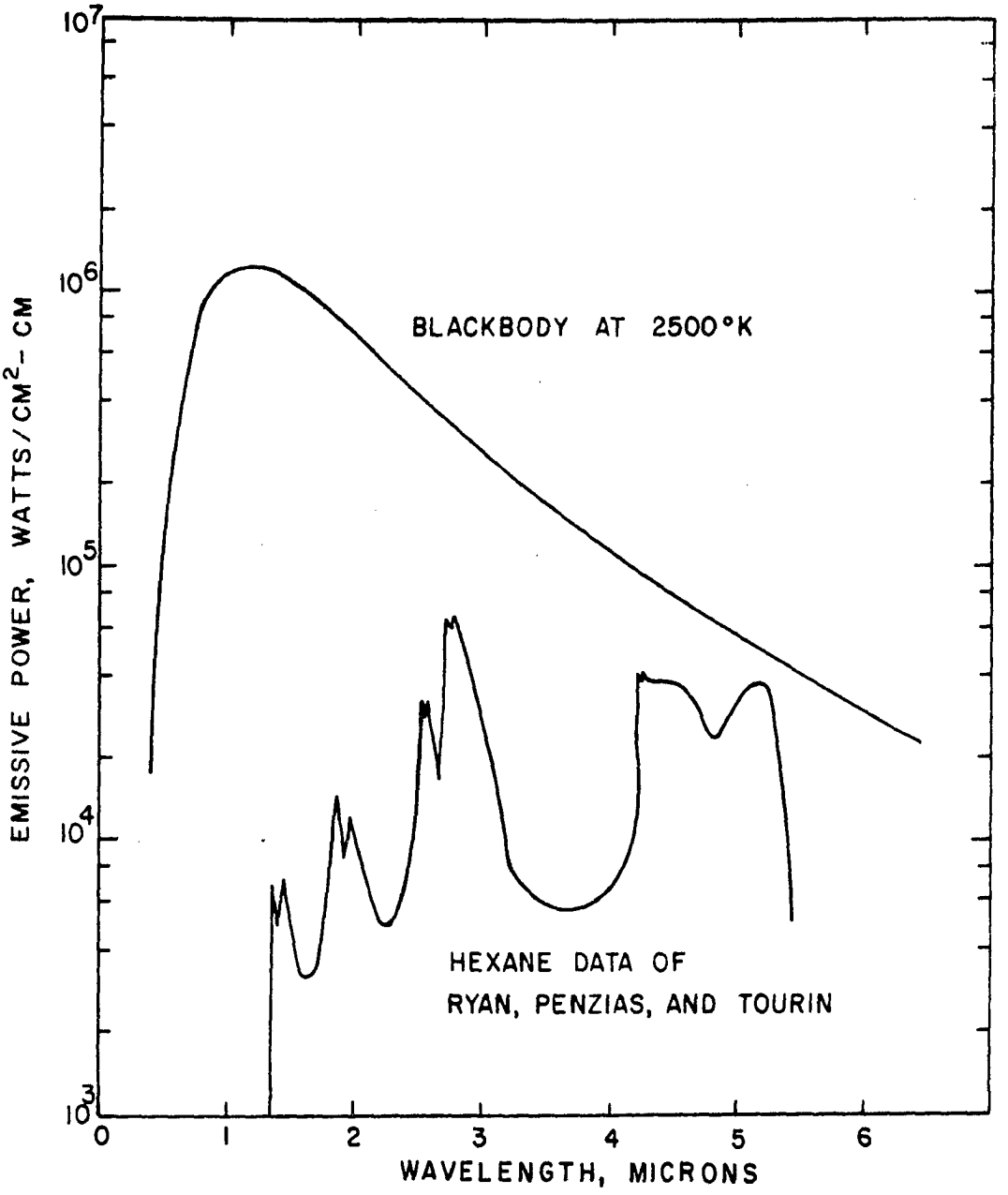

Figure IV-6. Comparison of Emissive Powers of a Blackbody Irradiance Source with a Flames Irradiance Source.

where α_{avg} = average total absorptance for the sample-irradiation source configuration under consideration

α_{λ} = absorptance of sample at wavelength λ

e_{λ} = emissive power of radiation source at wavelength λ.

The integration limits λ_1 and λ_2 are those wavelengths which include all of the energy in the spectrum for the given radiation source. For the purpose of the current comparison, the approximation

$$\alpha_{avg} = \frac{\Sigma \alpha_{\lambda} \, e_{\lambda} \, \Delta\lambda}{\Sigma e_{\lambda} \, \Delta\lambda} \qquad \text{(IV-3)}$$

was used to obtain values of α_{avg} for the four sets of experimental conditions producing the data shown in Figures IV-1 and IV-2. These computations are summarized in Table IV-1.

Once the values of α_{avg} were obtained for each of the fabric-radiation source configurations, it was possible to plot the fabric ignition time as a function of the absorbed irradiance, H_a. The absorbed irradiance was calculated as

$$H_a = \alpha_{avg} \, H_i \qquad \text{(IV-4)}$$

TABLE IV-1

COMPUTATIONS FOR AVERAGE ABSORPTANCE, α_{avg}, USING FABRIC ABSORPTANCE DATA FROM LEE (19) AND FLAME SPECTRAL DATA FROM RYAN, *et al.* (34) FOR HEXANE

λ_1 (μ)	λ_2 (μ)	$\Delta\lambda$ (μ)	$\bar{I}_\lambda \times 10^{-4}$ (cal/cm^2-sec-cm)	$\bar{\alpha}_\lambda$	$\bar{\alpha}_\lambda \bar{I}_\lambda \Delta\lambda$ (cal/cm^2-sec)	$\bar{I}_\lambda \Delta\lambda$ (cal/cm^2-sec)
I. White Fabric-Flames (Hexane, Ryan *et al.*)						
1.30	1.50	0.2	0.60	0.35	0.042	0.120
1.50	1.95	0.45	0.70	0.41	0.129	0.315
1.95	1.10	0.15	1.10	0.50	0.082	0.165
2.10	2.20	0.10	0.50	0.53	0.026	0.050
2.20	2.40	0.20	0.55	0.62	0.102	0.165
2.40	2.50	0.10	1.60	0.75	0.120	0.160
2.50	2.60	0.10	3.00	0.75	0.225	0.300
2.60	2.65	0.05	2.20	0.75	0.082	0.110
2.65	2.70	0.05	4.80	0.75	0.180	0.240
2.70	2.80	0.10	6.15	0.75	0.461	0.615
2.80	3.20	0.40	2.80	0.75	0.840	1.120
3.20	4.15	0.95	0.70	0.75	0.499	0.665
4.15	4.20	0.05	2.80	0.75	0.105	0.145
4.20	4.60	0.40	3.80	0.75	1.140	1.520
4.60	4.80	0.20	2.80	0.75	0.420	0.560
4.80	5.10	0.30	3.00	0.75	0.675	0.900
5.10	5.50	0.40	2.30	0.75	0.690	0.920
					5.818	8.065

$$\alpha_{avg} = \frac{\Sigma \bar{\alpha}_\lambda \bar{I}_\lambda \Delta\lambda}{\Sigma I_\lambda \Delta\lambda} = \frac{5.818}{8.065} = 0.721$$

TABLE IV-1 (Continued)

λ_1 (μ)	λ_2 (μ)	$\Delta\lambda$ (μ)	$\bar{I}_\lambda \times 10^{-4}$ (cal/cm^2-sec-cm)	$\bar{\alpha}_\lambda$	$\bar{\alpha}_\lambda \bar{I}_\lambda \Delta\lambda$ (cal/cm^2-sec)	$\bar{I}_\lambda \Delta\lambda$ (cal/cm^2-sec)
II. Black Cotton Cloth-Flames (Hexane-Ryan *et al.*)						
1.3	1.50	0.20	0.60	0.84	0.101	0.120
1.5	1.95	0.45	0.70	0.73	0.230	0.315
1.95	2.10	0.15	1.10	0.66	0.109	0.165
2.10	2.20	0.10	0.50	0.65	0.032	0.050
2.20	2.40	0.30	0.55	0.70	0.115	0.165
2.40	2.50	0.10	1.60	0.75	0.120	0.160
2.50	2.60	0.10	3.00	0.75	0.225	0.300
2.60	2.65	0.05	2.20	"	0.082	0.110
2.65	2.70	0.05	4.80	"	0.180	0.240
2.70	2.80	0.10	6.15	"	0.461	0.615
2.80	3.20	0.40	2.80	"	0.840	1.120
3.20	4.15	0.95	0.70	"	0.499	0.665
4.15	4.20	0.05	2.80	"	0.105	0.140
4.20	4.60	0.40	3.80	"	1.140	1.520
4.60	4.80	0.20	2.80	"	0.420	0.560
4.80	5.10	0.30	3.00	"	0.675	0.900
5.10	5.5	0.40	2.30	"	0.690	0.920
					6.024	8.065

$$\alpha_{avg} = \frac{\Sigma \bar{\alpha}_\lambda \bar{I}_\lambda \Delta\lambda}{\Sigma I_\lambda \Delta\lambda} = \frac{6.024}{8.065} = 0.747$$

TABLE IV-1 (Continued)

λ_1 (μ)	λ_2 (μ)	$\Delta\lambda$ (μ)	$\bar{I}_\lambda \times 10^{-4}$ (cal/cm^2-sec-cm)	$\bar{\alpha}_\lambda$	$\bar{\alpha}_\lambda \bar{I}_\lambda \Delta\lambda$ (cal/cm^2-sec)	$\bar{I}_\lambda \Delta\lambda$ (cal/cm^2-sec)
III. White Cotton Fabric - Blackbody @ 2500°K (Lee & Alvares)						
0.30	0.50	0.20	0.05	0.8	0.008	0.010
0.50	0.60	0.10	0.55	0.365	0.021	0.055
0.60	0.70	0.10	1.11	0.20	0.022	0.111
0.70	0.80	0.10	1.72	0.265	0.046	0.172
0.80	0.90	0.10	2.35	0.22	0.052	0.235
0.90	1.00	0.10	2.75	0.26	0.071	0.275
1.00	1.20	0.20	3.00	0.29	0.174	0.600
1.20	1.30	0.10	2.98	0.225	0.082	0.298
1.30	1.50	0.20	2.78	0.35	0.159	0.455
1.50	1.95	0.45	2.10	0.41	0.387	0.945
1.95	2.10	0.15	1.61	0.50	0.120	0.241
2.10	2.20	0.10	1.45	0.53	0.077	0.145
2.20	2.50	0.30	1.20	0.62	0.223	0.360
2.50	3.00	0.50	0.80	0.75	0.300	0.400
3.00	3.50	0.50	0.50	"	0.188	0.250
3.50	4.00	0.50	0.33	"	0.124	0.165
4.00	4.50	0.50	0.225	"	0.084	0.112
4.50	5.00	0.50	0.160	"	0.060	0.080
5.00	5.50	0.50	0.115	"	0.044	0.058
5.50	6.00	0.50	0.085	"	0.032	0.042
6.00	7.00	1.00	0.055	"	0.041	0.055
					2.315	5.064

$$\alpha_{avg} = \frac{\Sigma \bar{\alpha}_\lambda \bar{I}_\lambda \Delta\lambda}{\Sigma I_\lambda \Delta\lambda} = \frac{2.315}{5.064} = 0.457$$

TABLE IV-1 (Continued)

λ_1 (μ)	λ_2 (μ)	$\Delta\lambda$ (μ)	$\bar{I}_\lambda \times 10^{-4}$ (cal/cm^2-sec-cm)	$\bar{\alpha}_\lambda$	$\bar{\alpha}_\lambda \bar{I}_\lambda \Delta\lambda$ (cal/cm^2-sec)	$\bar{I}_\lambda \Delta\lambda$ (cal/cm^2-sec)
IV. Black Cotton Cloth - Blackbody @ 2500°K (Lee & Alvares)						
0.3	0.5	0.2	0.05	1.0	0.010	0.010
0.5	0.6	0.1	0.55	1.0	0.055	0.055
0.6	0.7	0.1	1.11	1.0	0.111	0.111
0.7	0.8	0.1	1.72	0.99	0.170	0.172
0.8	0.9	0.1	2.35	0.99	0.233	0.235
0.9	1.0	0.1	2.75	0.98	0.270	0.275
1.0	1.2	0.2	3.00	0.95	0.570	0.600
1.2	1.3	0.1	2.98	0.92	0.274	0.298
1.3	1.5	0.2	2.78	0.84	0.382	0.455
1.5	1.95	0.45	2.10	0.73	0.690	0.945
1.95	2.1	0.15	1.61	0.66	0.160	0.241
2.1	2.2	0.1	1.45	0.65	0.094	0.145
2.2	2.5	0.3	1.20	0.70	0.252	0.360
2.5	3.0	0.5	0.80	0.75	0.300	0.400
3.0	3.5	0.5	0.50	"	0.188	0.250
3.5	4.0	0.5	0.33	"	0.124	0.165
4.0	4.5	0.5	0.225	"	0.084	0.112
4.5	5.0	0.5	0.160	"	0.060	0.080
5.0	5.5	0.5	0.115	"	0.044	0.058
5.5	6.0	0.5	0.085	"	0.032	0.042
6.0	7.0	1.0	0.055	"	0.041	0.055
					4.144	5.064

$$\bar{\alpha}_{avg} = \frac{\Sigma \bar{\alpha}_\lambda \bar{I}_\lambda \Delta\lambda}{\Sigma \bar{I}_\lambda \Delta\lambda} = \frac{4.144}{5.064} = 0.818$$

where H_i is the incident irradiance. The results of the plot of ignition time versus absorbed irradiance are presented in Figure IV-7. Considering the scatter in the original flame data and the assumptions necessary to compute α_{avg}, the agreement among all four sets of data is remarkable.

Analyses of these results revealed that the large differences in the observed ignition times (see Figures IV-1, IV-2 and IV-3) could be quantitatively attributed to the spectral emission characteristics of the radiation source and the spectral absorptance of the cloth. Briefly, the spectral emission from the flame source occurs primarily in the infrared region where the cloth displays maximum absorptance. Conversely, the spectral emission of the tungsten lamps occurs at shorter wavelengths where the cloth has lower absorptance. Another important observation from these studies was that even though the cloth charred prior to flaming ignition, the rate of approach to a blackbody (perfect absorber of all energy, regardless of spectral distribution) was never sufficient to alter significantly the ignition times as predicted from the (initial) spectral absorption characteristics of unexposed white cloth.

It should again be noted that this comparison has neglected several of the parameters which are known to influence ignition behavior, for example, the effect due to

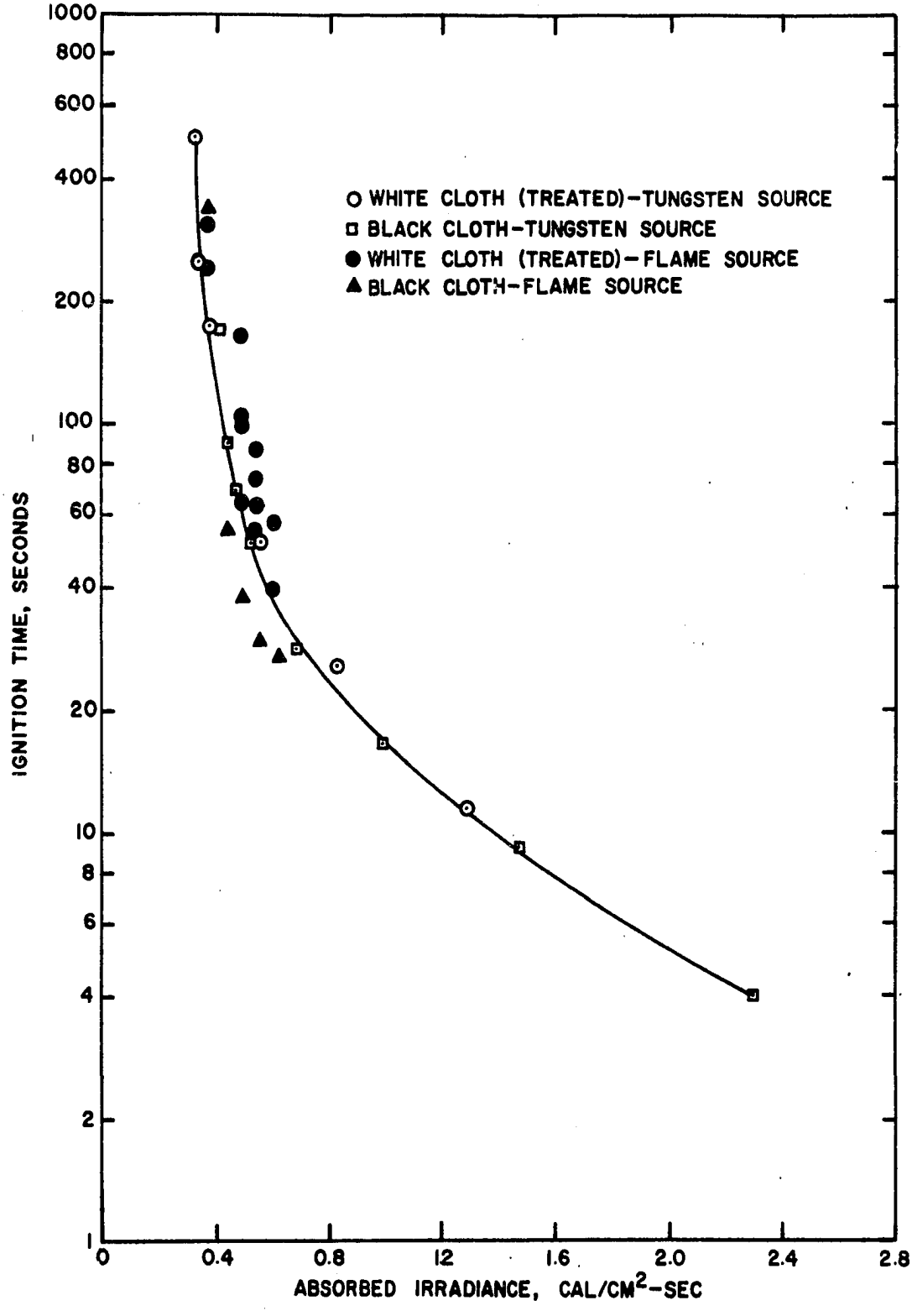

Figure IV-7. Cotton Cloth Ignition Times as a Function of Absorbed Irradiance.

pyrolysis reactions and reradiation. In addition, α_{avg} was calculated based on the absorption data for unexposed samples. The absorptances will change continuously during exposure, particularly for light colored fabrics which will blacken as they char prior to ignition. Nevertheless, the differences in the ignition times based on incident irradiance, as shown in Figures IV-1, IV-2 and IV-3, have been largely explained by taking into account energy absorptance.

In summary, these preliminary studies on ignition of cotton fabrics have emphasized the need for taking into account the parameter of absorptance. In addition, as noted before, any meaningful study of the ignition process should also delineate the role of thickness and density. Considering these three factors, combined with the widespread interest in the ignition of woods, an extensive investigation of the ignition of a variety of wood species was undertaken.

Ignition Data

A complete summary of the ignition data is given in Appendix B. Measurements have been made for the incident irradiance and the ignition time t_i.

A typical recorder output for incident irradiance and ignition time measurements was presented in Figure III-12. For completeness a similar recorder output is also presented in Figure IV-8. The curve ABCD shows the radiometer output

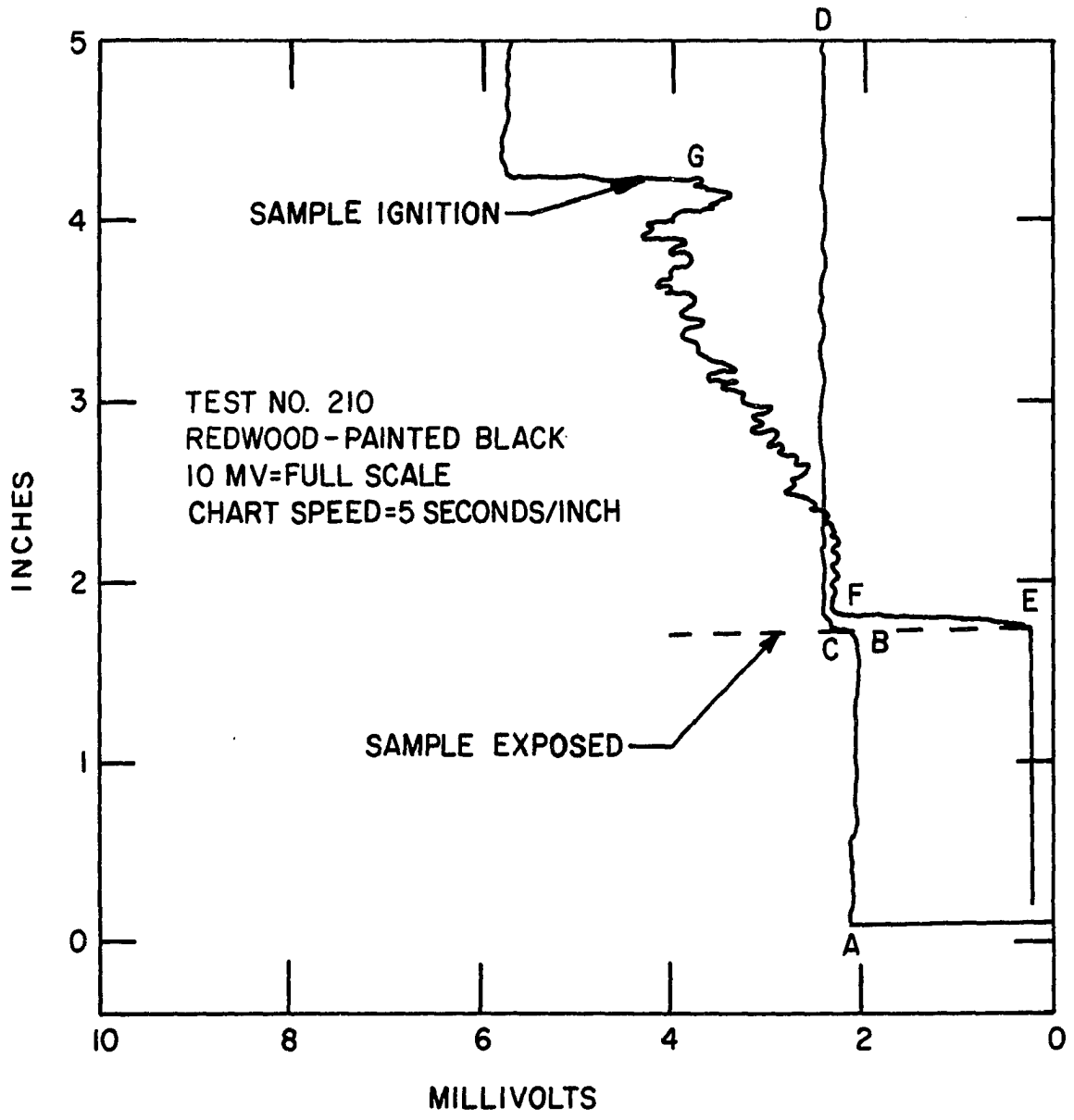

Figure IV-8. Typical Recorder Output for an Ignition Experiment (ABCD-Incident Irradiance; EFG-Ignition Time).

for the incident irradiance measurement and the curve EFG shows the output of the photoconductive cell used to determine the time interval between initial exposure of the sample to radiant energy and sample ignition. Point B indicates the irradiance level with the water-cooled shield in its sample protective position. Due to the shield position the radiometer's field of view is partially obscured. As soon as the shield is retracted (a fraction of a second) the radiometer output increases quickly to that output corresponding to the incident energy on the sample surface. The variation of the flame irradiance during the sample exposure period is quite small as illustrated by the line CD. The photoconductive cell output exhibits a sharp increase as soon as the shield is retracted as illustrated by the line EF. This abrupt change is due to the edge of the shield almost completely obscuring the cell's field of view in the closed position of the shield. Thus, the sharp increase is due to energy reflected by the sample and defines the instant of sample exposure. The photoconductive cell output then continues to rise in a relatively erratic pattern due to changes in the reflection from the pyrolysis products and smoke as well as possible flickers of flame. At the instant of flaming ignition another sharp increase in the photoconductive cell output occurs due to the large increase

in light from the flame front. This sharp increase in output is used to define the instant of ignition. The recorder speed and the linear difference between the two aforementioned sharp increases in photoconductive cell output is used to define the ignition time. The radiometer millivolt output and the applicable calibration curve is then utilized to determine the incident irradiance level at the sample exposed surface.

As noted in Tables B-1, II, III, IV, and V, ignition experiments were carried out on twelve different woods. Nearly 500 ignition tests were made. The variation in the experimental conditions included one-sided piloted and spontaneous ignition tests, natural wood finishes, flat black painted finishes, two sources of flame radiation, and two sources of blackbody type radiation.

Irradiance and Ignition Time Relationship

Figure IV-9 presents a typical relationship between incident irradiance and ignition time for pilot ignition tests. The data points shown on Figure IV-9 are single data points using acetone and benzene flames for the radiant energy source. As illustrated, the ignition time decreases as the incident irradiance level increases. At high irradiance levels the ignition time becomes asymptotic. As also shown, the ignition time rises quite rapidly with a reduction in the incident irradiance below about 1.0 cal/cm^2-sec. The left hand side of the curve becomes asymptotic to

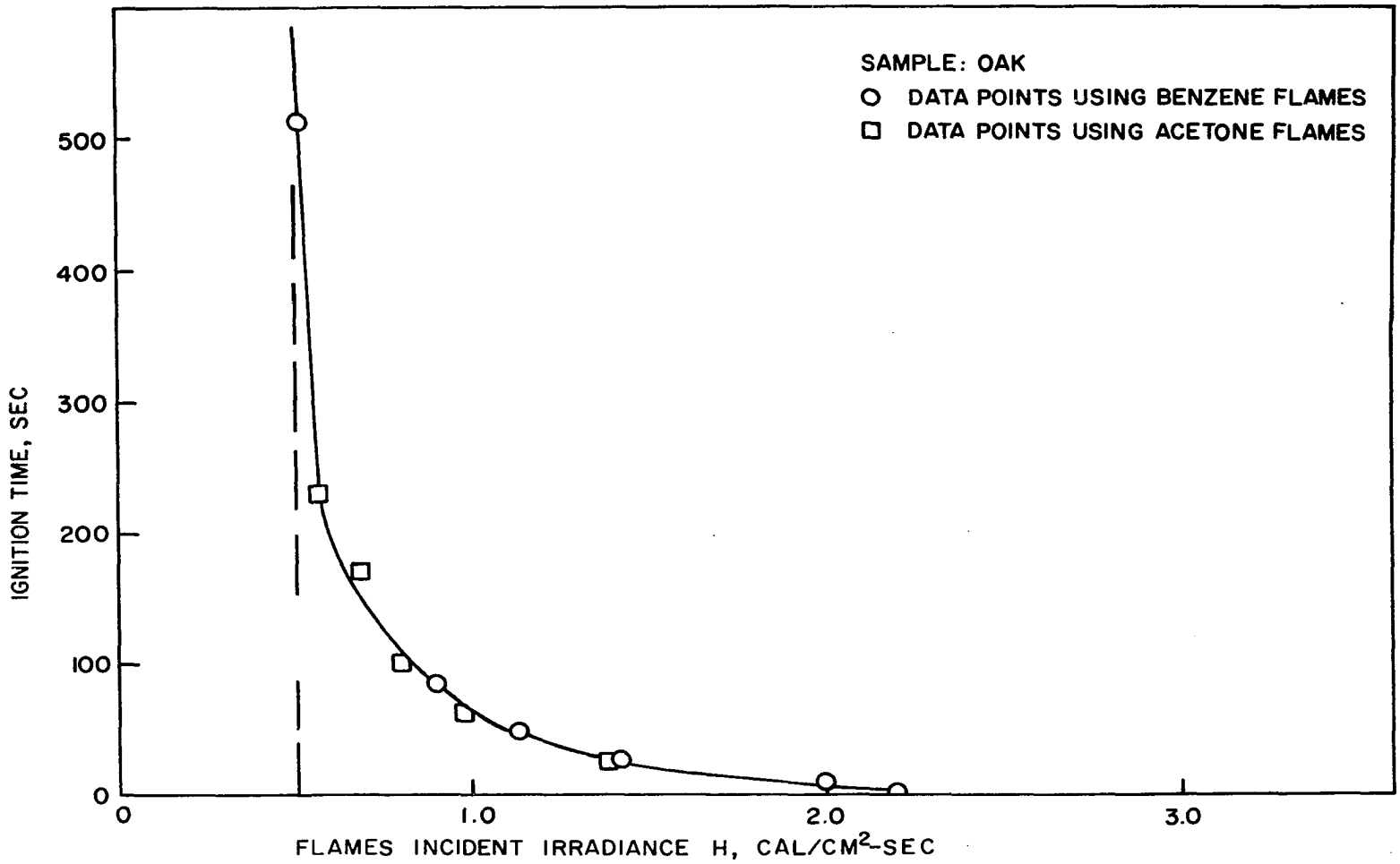

Figure IV-9. Typical Relationship Between Irradiance and Ignition Time (One-Sided Heating, Pilot Ignition of Oak with Flames).

the line $H = H_o$ indicating that below H_o flaming ignition will not occur for the test conditions utilized. In general, if the volatile products of pyrolysis are essentially exhausted before the required conditions of flaming ignition can be satisfied in the gas phase near the irradiated surface, flaming ignition will not occur and the sample will be reduced to char material.

Density as a Parameter and Correlation of Density Effects

Simms, in his pilot ignition experiments on various woods, reported data (42) which showed that the more dense woods required longer exposure periods to gas fired radiation panels in order to achieve flaming ignition. He concconcluded that this density effect could be due to the rate of production of volatiles, which in turn was dependent on a number of physical and chemical constants characteristic of each wood species and, therefore, was not describable by a unique function of surface temperature. Further, Simms found that the density of oven-dried woods significantly affected the minimum incident irradiance required to produce pilot ignition. A closer inspection of these data revealed that this minimum intensity is approximately proportional to the one-third power of the wood density. Based on this

result and the subsequent work of Koohyar, et al. (16) it was decided to explore this density effect more thoroughly.

The differential equation for heat conduction for an inert semi-infinite solid with constant properties is

$$\alpha \frac{\partial^2 T}{\partial x^2} = \frac{\partial T}{\partial t} \qquad \text{(IV-5)}$$

The initial conditions for all x are $T = T_o$, and the boundary conditions are:

$$t > 0;\ x = 0:\quad H = - K \frac{\partial T}{\partial x} \qquad \text{(IV-6)}$$

$$t > 0;\ x = L:\quad \frac{\partial T}{\partial x} = 0 \qquad \text{(IV-7)}$$

The surface temperature rise for this case is given by Carslaw and Jaeger (7, page 75) as

$$\Delta T_s = \left[\frac{2H_i}{K}\right]\left[\frac{\alpha t}{\pi}\right]^{1/2} \qquad \text{(IV-8)}$$

Rewriting this expression in a generalized form gives

$$H_i \sqrt{t} = f\left[\Delta T_s,\ \sqrt{K \rho c}\right] \qquad \text{(IV-9)}$$

where H_i = incident irradiance

t = exposure time

ΔT_s = irradiated surface temperature rise

ρ = material density

K = material thermal conductivity

c = material specific heat

As previously stated, Koohyar (14) experimentally measured a range of surface ignition temperatures for one-sided ignition by flame radiation of 280 to 450°C. However, Koohyar's data are not consistent in the variations, i.e., the variations could be due as much to experimental error as real causes. Simms (42), among others, has postulated a constant surface temperature criterion for ignition of woods. Therefore, the assumption is made that the surface temperature rise up to the instant of flaming ignition is essentially constant for all woods. Based on this assumption Equation IV-9 may be reduced to the functional form of

$$H_i \, t^n = f\left[K \rho \, c\right] \qquad \text{(IV-10)}$$

where the exponent of t has been changed for the completely general case.

Since c is essentially a constant for the different woods and MacLean (24) has shown the thermal conductivity, K, to be a linear function of the density, ρ, Equation IV-10 may be further reduced to

$$H_i \, t^n = k\rho^a \qquad \text{(IV-11)}$$

or, rearranging terms

$$t^n = \frac{k\rho^a}{H_i} \qquad \text{(IV-12)}$$

or

$$t = \frac{k\rho^b}{H_i^c} \qquad \text{(IV-13)}$$

where t = ignition time

k = a constant

ρ = material density

H_i = incident irradiance

Thus, Equation IV-13 states that it should be possible to correlate the ignition time of different woods as a function only of the parameter ρ^a/H_i^c for wood subject to the following restrictions.

a. Uniform irradiance

b. Constant moisture content

c. Constant external effects such as airflow velocity over irradiated surface, fixed pilot position, etc.

Based on the results obtained on the cotton fabrics (49), it is anticipated that each different type of incident irradiance

will give a different correlation due to the constant k and possible the c exponent being different.

Typical test results for the pilot ignition of woods by acetone and benzene flames are presented in Figure IV-10 for low, intermediate and high density woods with the specimen thickness ranging from 1.97 to 2.54 cm. As will be shown later (p. 118) sample thickness beyond 2 cm is not an ignition variable. The fact that the ignition times correlated remarkably well as a function of incident irradiance, with density as a parameter, confirms the previous conclusions by Koohyar, et al. (16) and Simms (42). Furthermore, this result can be reconciled with the analytical considerations enumerated above.

Based on Equation IV-13, data obtained from some 200 tests on twelve different woods exposed to flame radiation from liquid fuel fires were subjected to a linear regression analysis. This analysis indicated that these data could be best represented by the general equation

$$t_i = 80\left[\frac{\rho^{1/3}}{H_i}\right]^3 \qquad \text{(IV-14)}$$

The results of this correlation are presented in Figure IV-11; only part of the data points are included in the interest of clarity. The omitted data points lie within

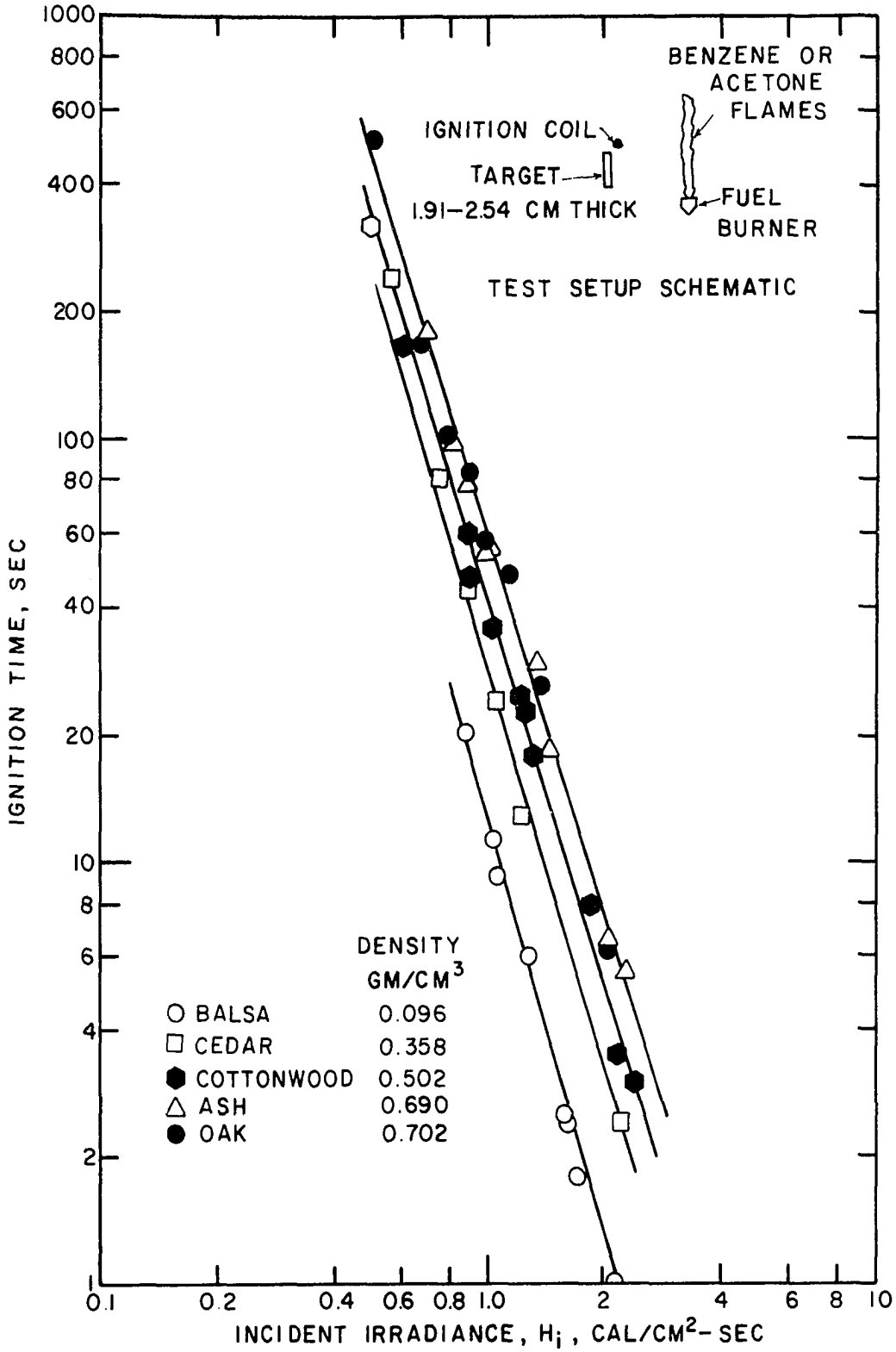

Figure IV-10. Correlation of Pilot Ignition Data for a Variety of Oven-Dried Woods using Flames Irradiance.

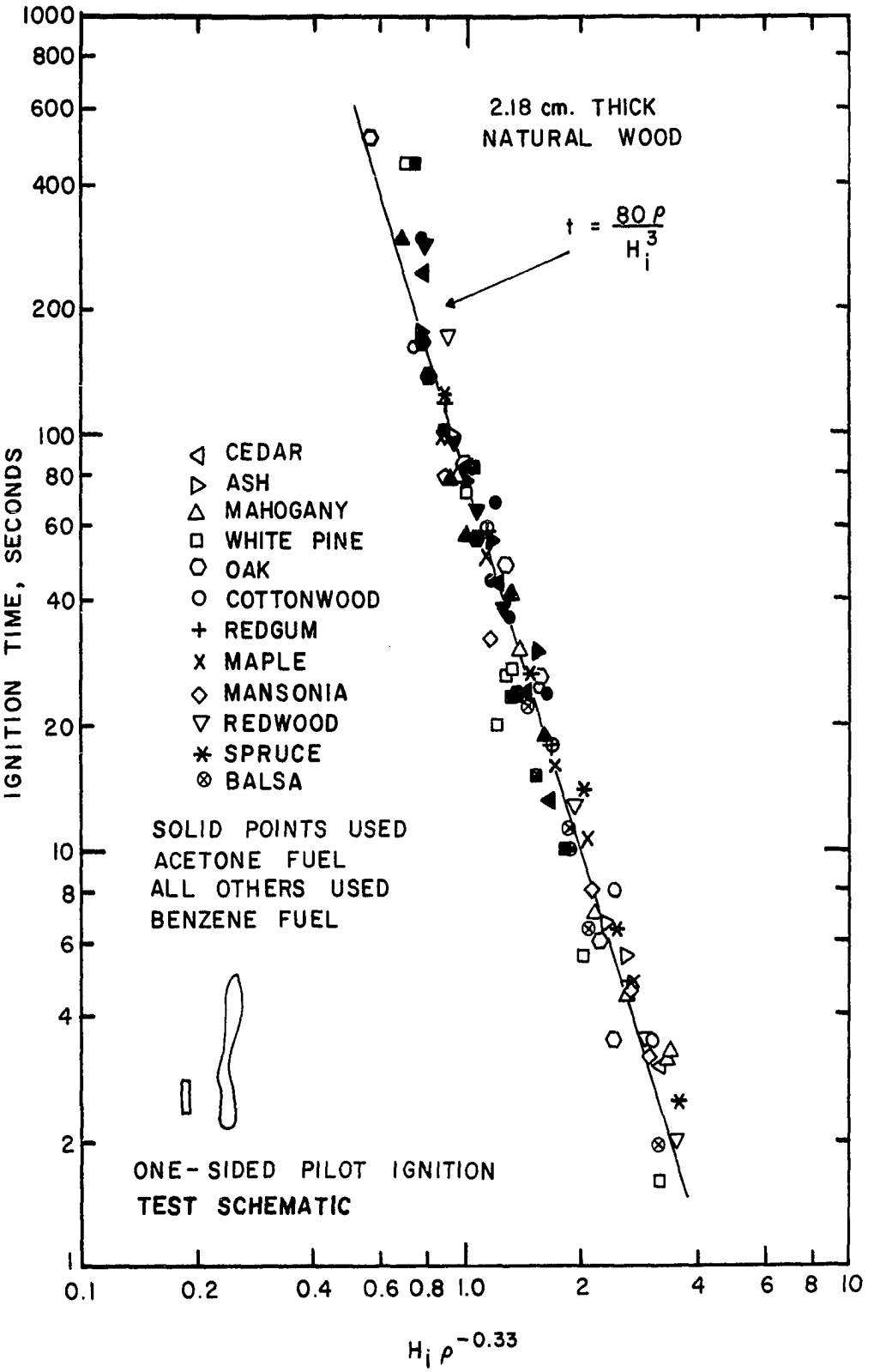

Figure IV-11. Correlation of Natural Finish Wood Piloted Ignition Data for One-Sided Heating by Flames.

the envelope established. The results adequately show that the assumptions made regarding the effects of density on ignition behavior and the use of a mathematical model based on an inert, semi-infinite solid, with the noted initial and boundary conditions, can be used to define the functional parameters required for a good correlation of experimental data obtained on wood equal to or greater than 2 cm in thickness exposed to a specific type of incident irradiance.

Thickness as a Parameter and Correlation of Effects

As noted in the introductory comments of this chapter and the section on Experimental Validation of Preliminary Conclusions, the use of density as the sole parameter in correlating wood ignition times for a given type of incident irradiance serves only as a first approximation in some thickness ranges. The effect is due to the appearance of the thickness in the heat conduction equation in the form of the Fourier modulus. For analysis purposes, the one-dimensional model for heat conduction through an inert, opaque, infinite slab exposed to a constant heat flux on one face and no heat loss on the opposite face is considered adequate since the primary objective is not to use the analytical solution directly, but rather, to obtain the functional form of the parameters for correlating the data.

The differential equation for one-dimensional heat conduction through an inert, opaque, infinite slab is given by:

$$\alpha \frac{\partial^2 \Delta T}{\partial x^2} = \frac{\partial \Delta T}{\partial t} \qquad \text{(IV-15)}$$

The initial condition for all values of x is $\Delta T = 0$, and the boundary conditions are:

$$t > 0;\ x = L:\quad H = - K \frac{\partial \Delta T}{\partial x} \qquad \text{(IV-16)}$$

$$t > 0;\ x = 0:\quad \frac{\partial \Delta T}{\partial x} = 0 \qquad \text{(IV-17)}$$

where it is assumed that all incident irradiance is absorbed. This is not a good assumption for the real case since an appreciable portion of the incident irradiance may be lost due to reflection and cooling effect, but should be adequate when only the functional parameters are desired.

The solution to Equation IV-15, with the stipulated initial and boundary conditions is given by Carslaw and Jaeger (7) for the irradiated surface temperature rise as

$$\Delta T_s = \frac{2 H_i t^{1/2}}{(K \rho c)^{1/2}} \sum_{n=0}^{\infty} \text{ierfc} \frac{2 nL}{2(\alpha t)^{1/2}} + \text{ierfc} \frac{(2n + 2)L}{2(\alpha t)^{1/2}} \qquad \text{(IV-18)}$$

where $\text{ierfc}\ \frac{2\ nL}{2(\alpha t)^{1/2}} = \frac{1}{\sqrt{\pi}}\ e^{-\left[\frac{2\ nL}{2(\alpha t)^{1/2}}\right]^2} - \frac{2\ nL}{2(\alpha t)^{1/2}}\ \text{erfc}\ \frac{2\ nL}{2(\alpha t)^{1/2}}$ (IV-19)

Equation IV-18 may be rewritten in the functional form

$$H_i\sqrt{t} = \left\{ f\ \Delta T_s,\ (K\rho c)^{1/2},\ \text{erf}\left(\frac{L}{2\sqrt{\alpha t}}\right) \right\} \qquad \text{(IV-20)}$$

where $\text{erf}\left[\frac{L}{2\sqrt{\alpha t}}\right]$ is utilized for convenience in lieu of $\text{ierfc}\left[\frac{L}{2\sqrt{\alpha t}}\right]$.

As in the analysis of density effects, assuming the specific heat, c, is a constant for the woods tested and that the thermal conductivity, k, of wood is dependent on the density, ρ, (24), Equation IV-20 becomes

$$H_i\sqrt{t} = \left\{ f\ \Delta T_s,\ \rho,\ \text{erf}\ \left(\frac{L}{2\sqrt{\alpha t}}\right) \right\} \qquad \text{(IV-21)}$$

As previously stated, it will be assumed that the surface temperature rise at ignition is relatively constant. Thus, Equation IV-21 may be modified to

$$H_i\ t^a = A\left[\rho^b\ \text{erf}\ \left(\frac{L}{2\sqrt{\alpha t}}\right)\right]^c \qquad \text{(IV-22)}$$

if the functional form of the equation is assumed to follow a power law distribution. The ignition time, t_i, and the sample thickness, L, are used in the power law expression. Rearranging Equation IV-22 to define the ignition time results in

$$t_i = B\left[\frac{\rho^b \operatorname{erf}\left(\frac{1}{2\sqrt{F}}\right)^c}{H_i}\right]^{1/a} \qquad \text{(IV-23)}$$

where $F = \alpha t/L^2$ is the Fourier modulus. Thus, Equation IV-23 relates the ignition time to the incident irradiance, the wood density and the Fourier modulus which contains the sample thickness, L. The Fourier modulus may be thought of as a measure of the age of the process; thus a small value of F simply means that sufficient time has not elapsed for the radiant energy absorbed at the surface to penetrate very deeply into the specimen.

Equation IV-23 states that the ignition time for a given type of incident irradiance cannot be correlated using only density and incident irradiance except for the case where the quantity $(\operatorname{erf} \frac{1}{2\sqrt{F}})$ is a constant (thermally thick woods). Fortunately it is characteristic of the error function of a given parameter to approach unity as an upper limit for values of the argument greater than 2.5. In the case of wood samples 1.97 cm thick or greater, the para-

meter $1/2\sqrt{F}$ is greater than 3.75 for ignition times up to 500 seconds and the value of $1/2\sqrt{F}$ is essentially equal to unity. Hence, as the value of the wood thickness increases toward 1.97 cm the effects due to thickness equates to a constant as desired and as previously concluded by others (14,42). Use of Equation IV-23 should, therefore, correlate the experimental data insofar as thickness effects alone are concerned. Based on the results obtained in the cotton fabrics (49), it is anticipated that different correlations for each type of incident irradiance will result.

In the preceding section on density effects Equation IV-13 was used to establish the effect of ignition times at various levels of irradiance. Equation IV-13 considers the Fourier modulus to be a constant. The effect of thickness on the samples (which is contained in the Fourier modulus) on the ignition time at various levels of irradiance should be obtainable from pilot ignition experiments at constant density. However, two complications must be resolved:

a. Specimens of the same kind of wood in various thicknesses frequently exhibit density variations as much as 25 percent. This difficulty, however, can be easily circumvented by the correlation presented in Figure IV-11 wherein the density variable is collapsed into a unique function by raising the density to the 1/3 power.

b. The Fourier modulus contains, in addition to the thickness of the specimen, the thermal diffusivity and ignition time. Although the heat capacity, c, for most woods does not vary appreciably, the thermal conductivity is a function of density. Consequently, the Fourier modulus is a function of density as well as thickness; this density dependency is not eliminated by the 1/3 power correction as noted above. Although the thermal diffusivity does not vary greatly from one kind of wood to another, its effect on ignition time is not always negligible as will be now demonstrated.

To ascertain the effect of thickness on pilot ignition time, a series of tests using a bank of tungsten filament lamps as the radiation source was made on oak specimens of thicknesses from 0.318 cm to 2.54 cm and of densities from 0.632 gm/cm^3 to 0.776 gm/cm^3. The results are shown in Figure IV-12. Note that in this case the abscissa contains, in addition to the incident irradiance, the density normalizer, $\rho^{-1/3}$, which has the effect of eliminating density as a variable insofar as it appears explicitly in Equation IV-23 but not as it appears implicitly in the Fourier modulus, F. Figure IV-12 shows clearly that the ignition time increases with increasing thickness up to a thickness of about 1.91 cm.

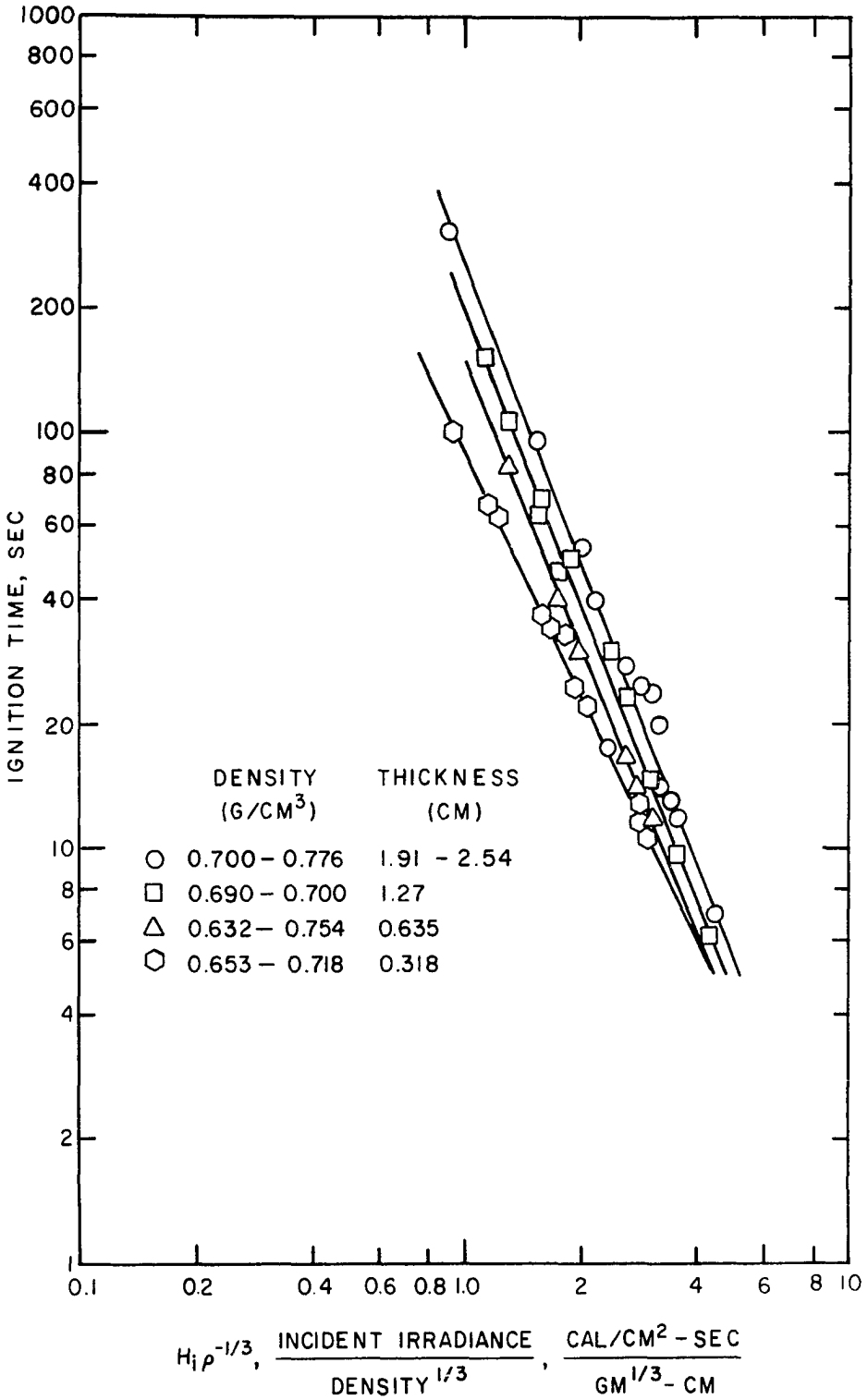

Figure IV-12. Relationship Between Thickness, Density, Incident Irradiance and Pilot Ignition Time for Oak Samples using 2500°K Tungsten Filament Quartz Lamps (One-Sided Heating).

As explained previously, the erf $\frac{1}{2\sqrt{F}}$ approaches a value of unity and remains constant thereafter for sample thicknesses greater than 1.9 cm. Consequently, it can be expected that the ignition time is not dependent on thickness for samples thicker than 1.9 cm. This cut-off point is often referred to in the literature as a "thermally-thick" specimen. Table IV-2 presents a summary of the wood properties utilized in determination of the Fourier moduli.

TABLE IV-2

THERMAL AND PHYSICAL PROPERTIES OF DRIED WOOD SAMPLES*

Type of Wood	Density gm/cm^3	Thermal Conductivity-Avg. $cal/cm^2\text{-}sec\text{-}°C/cm$	Thermal Diffusivity-Avg. cm^2/sec
Ash	0.66→0.69	0.000346	0.001473
Balsa	0.07→0.11	0.000066	0.0001765
Birch	0.53→0.55	0.000290	0.00158
Cedar	0.36→0.56	0.000174	0.001431
Cotton-wood	0.45→0.60	0.000304	0.001780
Mahogany	0.51→0.55	0.000328	0.001780
Mansonia	0.56→0.60	0.000308	0.001562
Maple	0.65→0.68	0.000350	0.001555
Masonite	1.02	0.000515	0.001515
Oak	0.63→0.78	0.000373	0.001555
Redgum	0.60→0.63	0.000292	0.001398
Redwood	0.33→0.35	0.000192	0.001398
Spruce	0.35→0.37	0.000188	0.0015425
White Pine	0.32→0.36	0.000206	0.001786

*Specific heat of wood = 0.34 cal/gm-°C.

To determine whether thermal diffusivity has a measureable effect on ignition time, similar pilot-ignitions were measured for cottonwood which has a thermal diffusivity of 0.001780 cm^2-sec as compared to 0.00155 cm^2-sec for oak. The results are summarized in Figure IV-13. A close comparison of Figures IV-12 and IV-13 reveals that for any prescribed value of the abscissa, the spread in ignition time over a corresponding thickness range is less for oak than for cottonwood. This difference is attributed to the differences in thermal diffusivities of oak and cottonwood since the density correction has been applied in both instances. However, as will be shown later, the effect of thermal diffusivity on ignition time can be normalized by adjusting the exponent on the error function of the Fourier modulus term.

To complete the correlation on thickness, the lines with thickness as a parameter as shown on Figure IV-13, for example, should be reducible to a single line subject to the following limitations:

a. The sample is thick enough to be considered opaque.

b. The spectral distribution of the incident energy is the same for all samples.

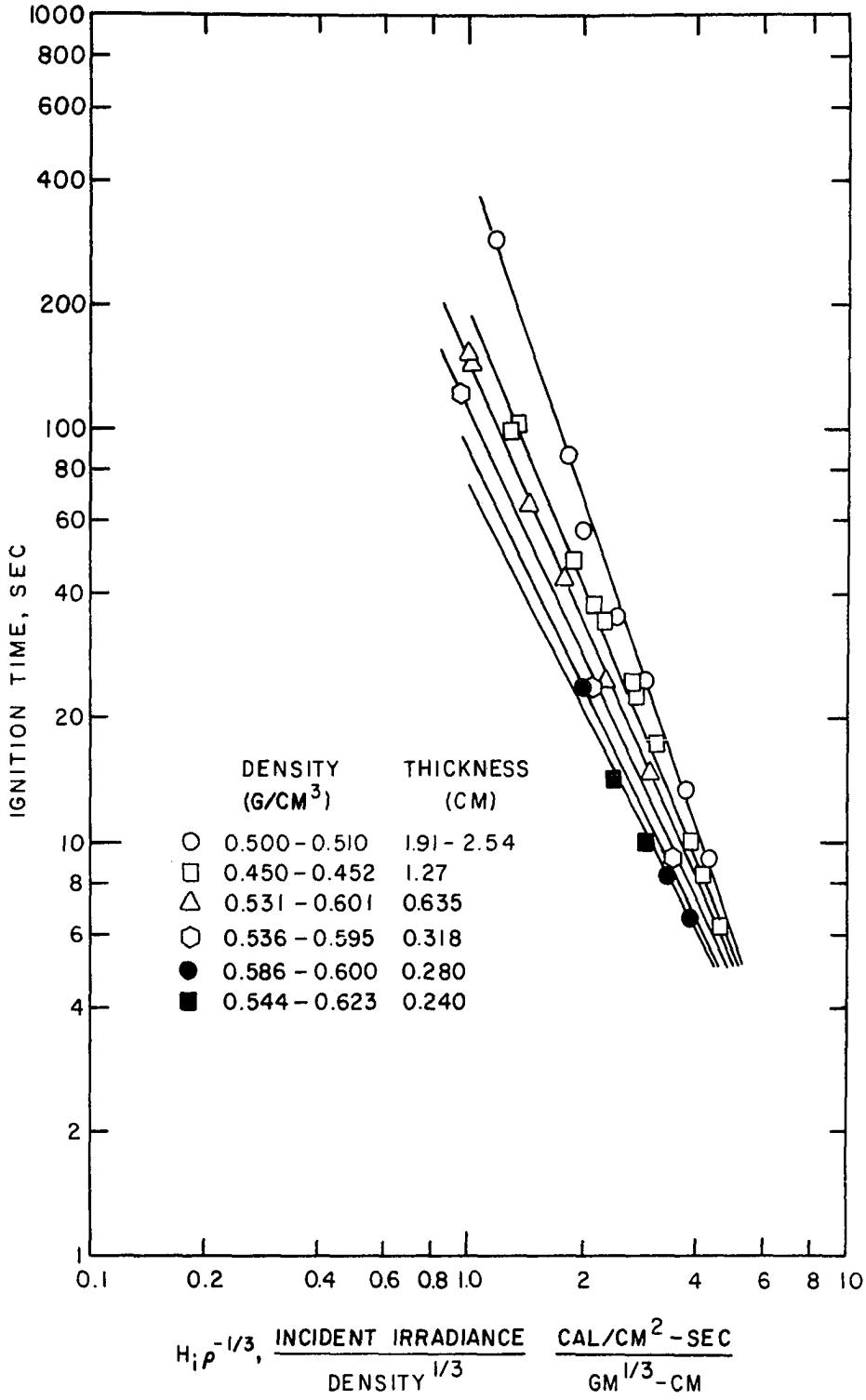

Figure IV-13. Relationship Between Thickness, Density, Incident Irradiance and Pilot Ignition Time for Cottonwood Samples using 2500°K Tungsten Filament Quartz Lamps (One-Sided Heating).

c. The moisture content is constant.

d. External effects (such as airflow and pilot coil position) are constant.

Based on the form suggested by Equation IV-23, the experimental data obtained on ignition by tungsten lamp radiation of three different woods were subjected to a linear regression analysis. The results showed that these ignition data could best be correlated by the expression

$$t_i = 340 \left[\frac{\rho^{1/3} \ \text{erf} \ \frac{1}{2\sqrt{F}}}{H_i} \right]^{3/4}{}^{2.75} \qquad \text{(IV-34)}$$

The results of this correlation for the three different woods are presented in Figure IV-14. The data in Figure IV-14 are based on a density range of 0.36 to 0.78 g/cm^3, a thickness range of 0.24 to 2.54 cm and tungsten lamp incident irradiance levels of 0.5 to 3.5 cal/cm^2-sec.

The correlation presented in Figure IV-14 can now be used to normalize the combined effects of wood density and thickness. The next step is to investigate the effects of energy absorptance on the ignition times. Both the energy that is initially absorbed, neglecting the front surface energy losses, and the retained energy will be evaluated.

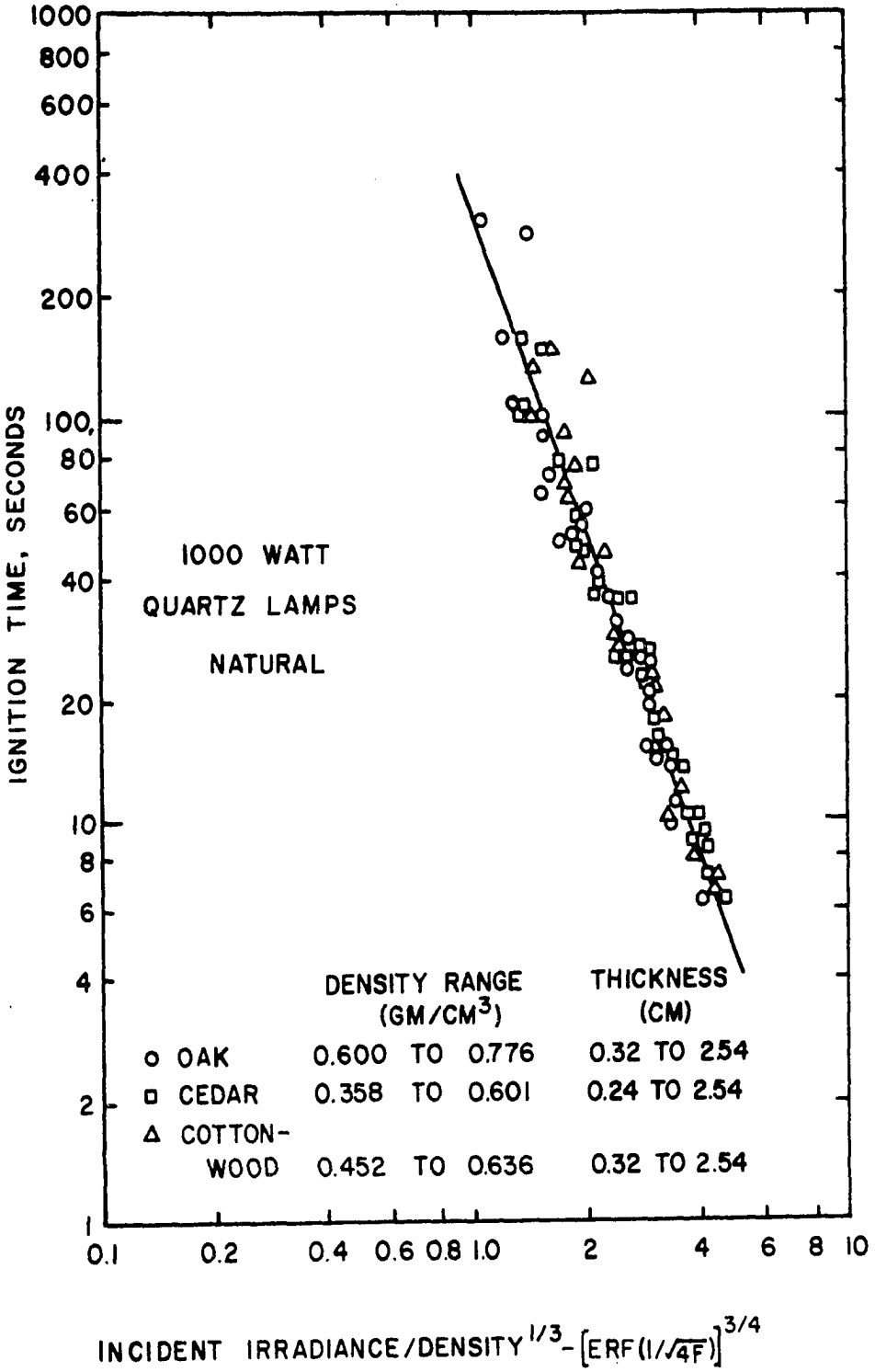

Figure IV-14. Correlation of Thickness, Density and Incident Irradiance Effects upon the Pilot Ignition Behavior for Three Oven-Dried Woods using 2500°K Tungsten Filament Quartz Lamps for Irradiance (One-Sided Heating Only).

Surface Absorptance as a Parameter

In these investigations principal attention is directed to the ignition behavior of combustible cellulosic solids exposed to two different sources of radiant energy, a 2500°K blackbody radiator and diffusion flames from a pool of burning liquid hydrocarbons. The review of the prior work clearly illustrates that in order to obtain flaming ignition, a certain rate of volatile gas production is a necessary condition. It is also evident that the production of these volatile gases results from pyrolysis processes within the irradiated solid and that the pyrolysis process is initiated and sustained by the absorption of energy incident upon the exposed solid surfaces. Two factors are of prime importance in the determination of the energy absorbed by an object: (1) the wavelength range and associated emissive powers of the radiant energy source and (2) the absorptance characteristics of the surface exposed to this radiative energy. While excellent sources of information are available on each of these particular topics (12, 13, 23, 46), the salient features of each will be summarized herein for continuity and ease of reference.

Monochromatic Emissive Characteristics of Energy Sources

For a blackbody radiator the emissivity, ϵ_λ, is equal to unity for all wavelengths. If the value of ϵ_λ is

less than unity and is a constant for all wavelengths, then the radiator is referred to as a graybody. However, in actual practice, radiative energy sources, such as diffusion flames, do not approximate either of these conditions. According to Gaydon and Wolfhard (13) the emissivity for fully aerated flames is quite low (near zero) for most wavelengths. However, it will reach quite high values (near unity) for a limited number of emission bends. The strongest emissions occur in the infrared region of the spectrum. With the single exception of the flame ignition studies reported by Koohyar (14), the majority of prior ignition studies on woods which have been reported in the literature have utilized radiation sources approximating a blackbody radiator. Furthermore, in these reported investigations the radiant energy sources have had their peak intensity in or near the visible region of the spectrum (1.0 to 1.5 microns). For example, the tungsten filament lamps used in some of the investigations reported herein as well as those used by Lee and Alvares (20) in their studies on the ignition of cotton fabrics had an effective blackbody temperature of 2500°K and the peak intensity occurred at a wavelength of about 1.15 microns. However, as previously illustrated by the comparison presented in Figure IV-6, data reported by Ryan, Penzias, and Tourin (34) for hexane flames show essentially no radiation below about 1.3

microns, but show four emission peaks above 1.3 microns. The two weaker peaks near 1.5 and 2.5 microns are apparently related to continuum radiation which is generally emitted by hot solid bodies (in the case of flames by the carbon particles contained therein). The latter two bands, 2.6 to 3.0 microns and 4.3 to 5.3 microns, are due to emissions from hot water and carbon dioxide gases and contain most of the total energy liberated from flames by radiation. According to Gaydon and Wolfhard (13) this characteristic is due to the fact that none of the ordinary molecules which are stable products of combustion, such as H_2O, CO_2, or CO possesses electron energy levels which give spectra of appreciable strength in the visible or ultraviolet regions. The only strong feature in the ultraviolet region of the spectrum appears to be the OH band system. The main combustion products of H_2O and CO_2 do, however, posses very strong vibration-rotation bands in the near infrared as illustrated by the data of Ryan, Penzias, and Tourin (34). Hence, it becomes evident that very little of the total radiant energy emitted from a diffusion flame occurs outside the region of the spectrum from about 1.3 to 5.3 microns. Yet, it is generally accepted that the total radiation emitted by flames from liquid hydrocarbons in this region of the spectrum (1.3 to 5.3 microns), is in excess of 20 percent of the heat of combustion.

Monochromatic Absorptance of Wood Surface

Another equally important and inseparable consideration in the ignition process is the spectral absorptance characteristics of the material being exposed to the energy radiating source. Simms (42), for example, assumed that the wood samples used in his experiments could be accurately modeled as semi-infinite solids which were inert, opaque, and totally absorbing. Hence based on this conclusion it would not make any difference what the spectral emission characteristics of the radiative source were. On the other hand, experimental evidence such as that reported by Earing and Smith (10), shows that reflectance properties of woods cannot even be roughly approximated by the gross assumption that wood absorbs like a blackbody. Further, as stated by Love (23) and Sparrow and Cess (46), this type of analysis can only approach reality when the radiant energy participating in the interchange is confined to a limited range of wavelengths within which the spectral emittance is essentially uniform. Thus, in order to make an accurate accounting of the wavelength dependence of the radiation interchange the computations must be performed monochromatically and then integrated over the applicable range of wavelengths. It then becomes apparent that to compute the total absorbed energy, it is mandatory that the spectral distribution of both the incident energy and the surface absorptance be evaluated.

At this point it should be noted that the use of the terms reflectance and absorptance refer to the radiative properties associated with a real surface. As a result of this real surface configuration, the reflection will be somewhat non-uniform and a monodirectional flux will contribute to the reflected intensities in many directions as illustrated in Figure IV-15 below.

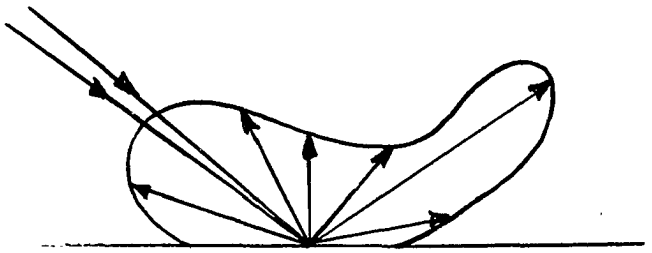

Figure IV-15. Schematic Graph Illustrating the Reflection and Relative Intensities of a Pencil of Rays from a Real Surface.

As illustrated in Figure IV-15, the reflection from a real surface may be described in terms of a function of two directions and the characteristic frequency of the radiation. Love (23) has defined this quantity as a "reflection function". This reflection function relates the energy incident from one direction to the reflected energy in another direction in such a manner that if the intensity distribution of an incident flux is known, the intensity distribution in the reflected flux may be determined. The reflection function is defined mathematically as:

$$I_\lambda(\mu, \Phi)_{\text{Reflected}} = \frac{1}{\pi}\int_0^{2\pi}\int_0^{1} I_\lambda(\mu', \Phi')\,\rho_\lambda(\mu, \Phi, \mu', \Phi')\,\mu'\,d\mu'\,d\Phi' \qquad \text{(IV-35)}$$

where $\rho_\lambda(\mu, \Phi, \mu', \Phi')$ = reflection function

$I_\lambda(\mu', \Phi')$ = incident intensity

μ' = Cosine of polar angle the incident intensity makes with the normal to the surface

$d\mu'\,d\Phi'$ = solid angle

μ = Cosine of polar angle from the surface normal

Φ = Azimuthal angle.

However, accounting for the directional properties of real surfaces in actual radiative heat transfer computations is very involved and has only been accomplished for a very few simplified cases. In general, when the surface has irregularities approximately an order of magnitude greater than the wavelength of the incident radiation or greater, the real surface will reflect in approximately a diffuse manner, i.e., the surface will reflect and, therefore absorb, radiative energy equally in all directions at each monochromatic intensity. Since the wood essentially possesses

such a property, it was tentatively assumed that the wood samples used in this study reflect diffusely. A diffusely reflecting surface is illustrated below in Figure IV-16.

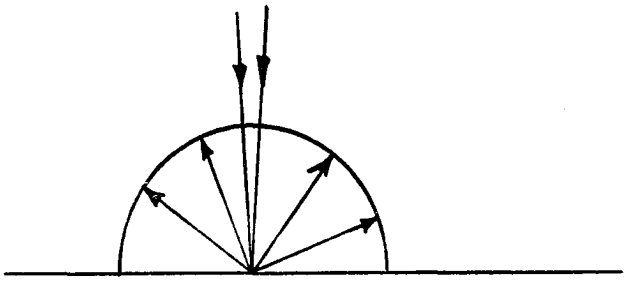

Figure IV-16. Schematic Graph Illustrating the Reflection and Relative (Equal) Intensities of a Pencil of Rays from a Diffuse Surface.

In addition to this tentative assumption (to be validated by experimental data), extreme care was taken in the experimental investigations to insure that the irradiated sample surface was parallel to the radiating surface in order to achieve as nearly a uniform irradiance on the sample surface as possible.

Since diffuse reflectance is not dependent upon direction, the reflection function may be expressed as:

$$\rho_\lambda (\mu, \Phi, \mu', \Phi')_{diffuse} = \rho_\lambda \quad \text{(IV-36)}$$

Likewise the relationship between the emittance and the reflectance for a diffuse surface may be expressed as:

$$\epsilon_\lambda (\mu, \Phi) = 1 - \rho_\lambda = \epsilon_\lambda \qquad \text{(IV-37)}$$

As noted, the total hemispherical reflectance is required for the energy balance correlation proposed herein. The total hemispherical reflectance, ρ, is usually defined as the fraction of the total hemispherically incident radiation that is reflected back into the hemispherical space above the irradiated surface. In terms of the incident spectral energy, H_λ, and the monochromatic reflectance, ρ_λ, the total reflected and incident irradiance are expressed, respectively, as:

$$\int_0^\infty \rho_\lambda H_\lambda \, d\lambda \qquad \text{(IV-38)}$$

and

$$\int_0^\infty H_\lambda \, d\lambda . \qquad \text{(IV-39)}$$

Since these investigations are primarily concerned with the ultraviolet, visible and near infrared regions of the spectrum in producing ignition by radiative heat transfer, the

limits of integration in Equations IV-38 and IV-39 may be revised from 0 to ∞ to about 0.3 to 6.0 microns. As illustrated by Figure IV-6, outside these limits, the spectral energy emissive powers are quite small (near zero). Hence, exclusion of energy outside the limits will not materially affect the total absorbed energy levels.

Although the monochromatic reflectance, ρ_λ, is a property of the surface, the spectral energy emissive power, H_λ, depends upon the nature of the incident irradiance. Hence, the total average reflectance, which is not in itself uniquely a surface property, is generally expressed as:

$$\rho_\lambda = \frac{\int_{0.3}^{6.0} \rho_\lambda H_\lambda \, d\lambda}{\int_{0.3}^{6.0} H_\lambda \, d\lambda} \qquad \text{(IV-40)}$$

A review of the literature indicated an almost complete lack of spectral reflectance data on natural finish woods. The data which are available covered only the range of about 0.8 microns to 1.5 microns. Earing and Smith (10) present limited reflectance data for oak and redwood, freshly sanded. Figure IV-17 presents these data. As shown, the monochromatic reflectance varies from about 75 percent at 1 micron to about 12 percent at 1.75 microns for oak and from 90 percent at 1 micron to 35 percent at 1.5 microns for red-

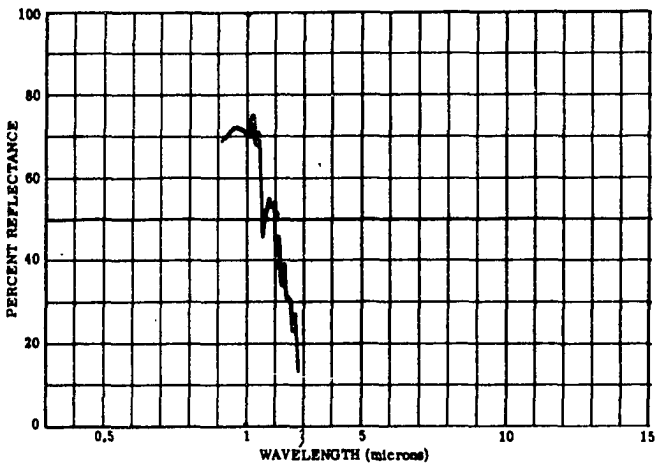

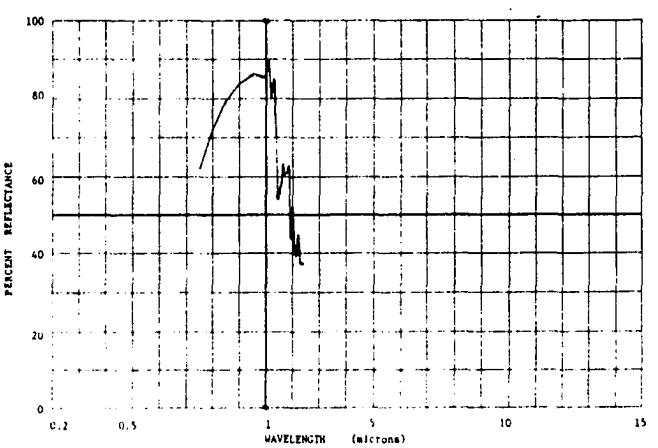

Figure IV-17. Measured Reflectance Data as a Function of Wavelength for Oak and Redwood.

wood. Hence, not only does the monochromatic reflectance vary significantly as a function of wavlength, but it also varies somewhat at equivalent wavelengths for different woods. This review of the literature confirmed the original conclusion that adequate spectral reflectance data for the woods used in these studies were not available in the literature. Fortunately, an experimental program by Mr. J. R. Hallman of this laboratory (as a part of his Ph.D. Dissertation, currently in progress) at the General Dynamics, San Diego Division facilities made the required data available. The reader is referred to his work for full details concerning the experimental procedures, discussion of the test setup and complete tabulation of the pertinent test data. Appendix C presents a brief summary of the salient features applicable to this specific study. It is sufficient to state here that all twelve woods utilized in these investigations were subjected to isotropic incident radiation. Normal monochromatic reflectance data were obtained over the wavelengths of 0.3 to 2.0 microns for all wood samples and from 2.0 to 11.0 microns for four wood samples. However, only the data through 5.6 microns were used herein since the radiation sources used had essentially zero emissive powers beyond this wavelength. Reflectance data were also obtained at different viewing angles up to 45 degrees from

the normal. Although the experimental configuration raises doubts as to the absolute precision of these directional measurements, the insignificant variations with viewing angles justifies neglecting the directional effect.

In addition to the twelve natural finished wood specimens, three selected species of wood (very smooth grain structure, normal grain structure and very rough grain structure) were spray-painted with a flat black enamel paint, and normal reflectance data were obtained. Figures IV-18 through IV-25 present the monochromatic absorptance factor as a function of wavelength for the natural finish wood samples. Figure IV-26 presents similar data for the three black-painted wood samples. As illustrated by Figures IV-18 through IV-25, the monochromatic absorptance characteristics vary quite significantly with wavelength from one color of wood to another in the visible region of the spectrum. Much less variation is evident between woods for wavelengths in the infrared region. The black-painted woods experienced considerably less variation of monochromatic reflectance and almost no variation with grain structure. This result was not expected from the review of prior investigations which concluded that grain structure could be important in the ignition process (14).

Figure IV-27 presents the monochromatic reflectance data for ash for three different viewing angles (normal, 18

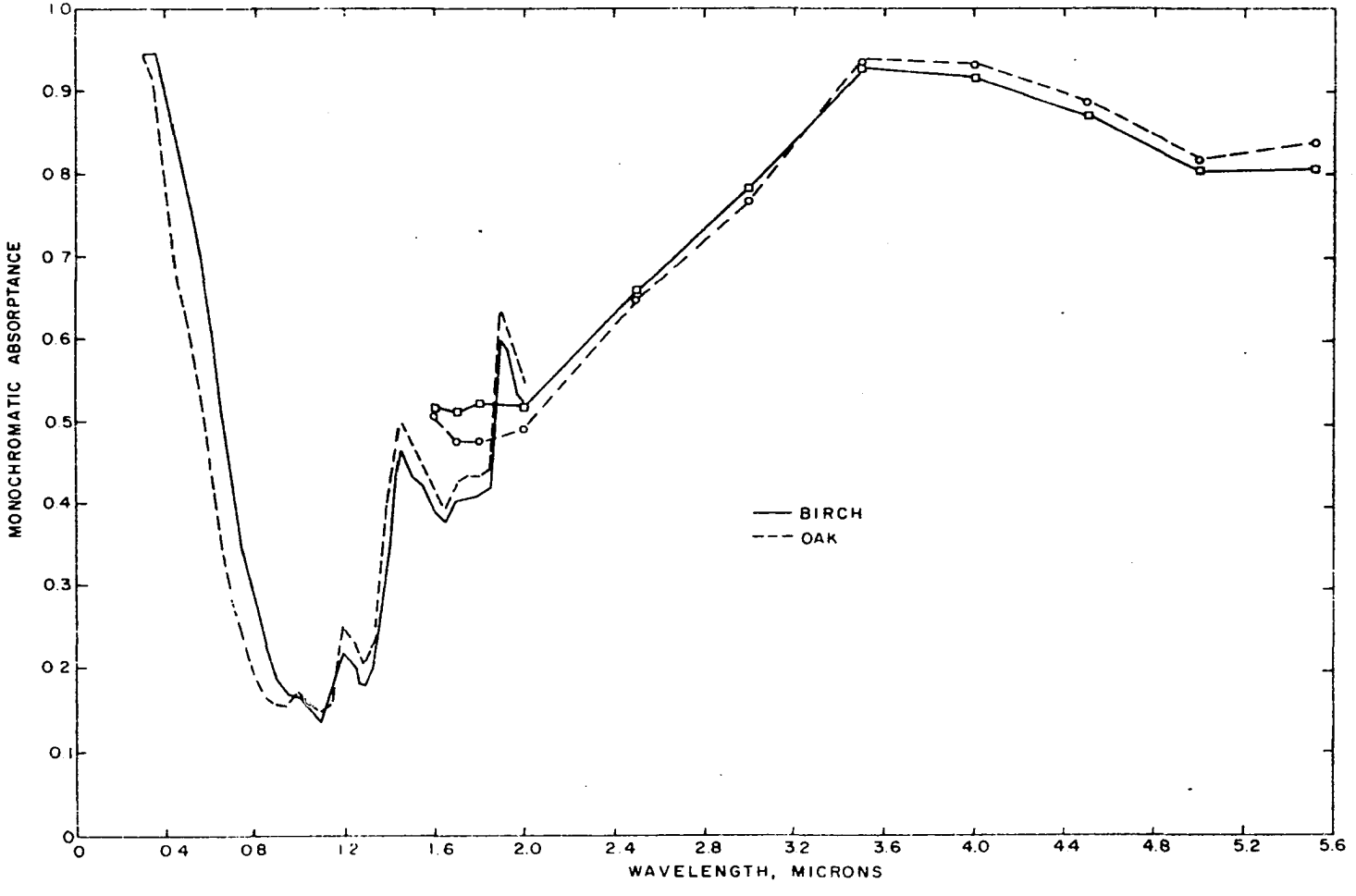

Figure IV-18. Absorptance Characteristics of Natural Finish Oak and Birch Woods.

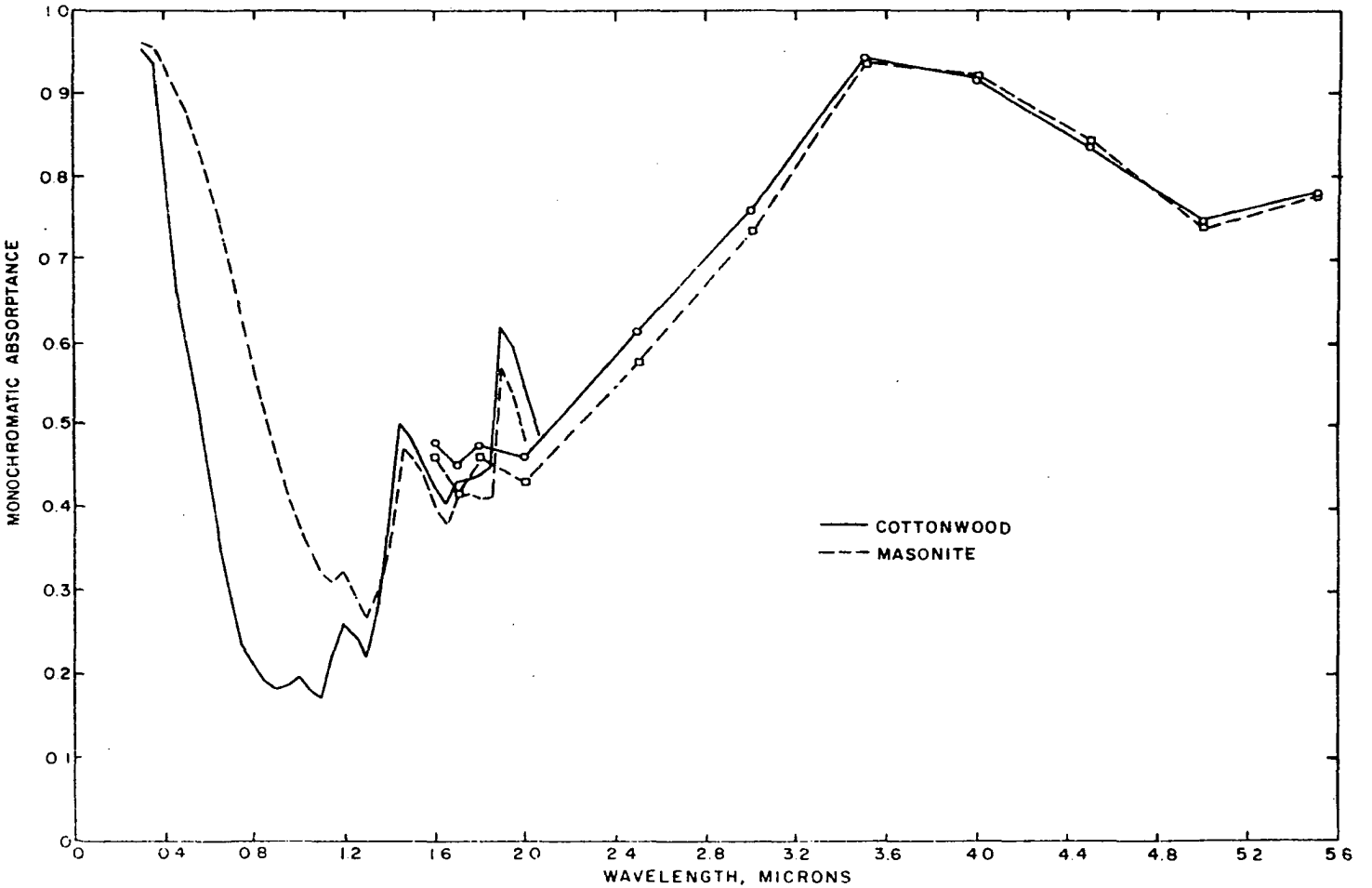

Figure IV-19. Absorptance Characteristics of Natural Finish Cottonwood and Masonite.

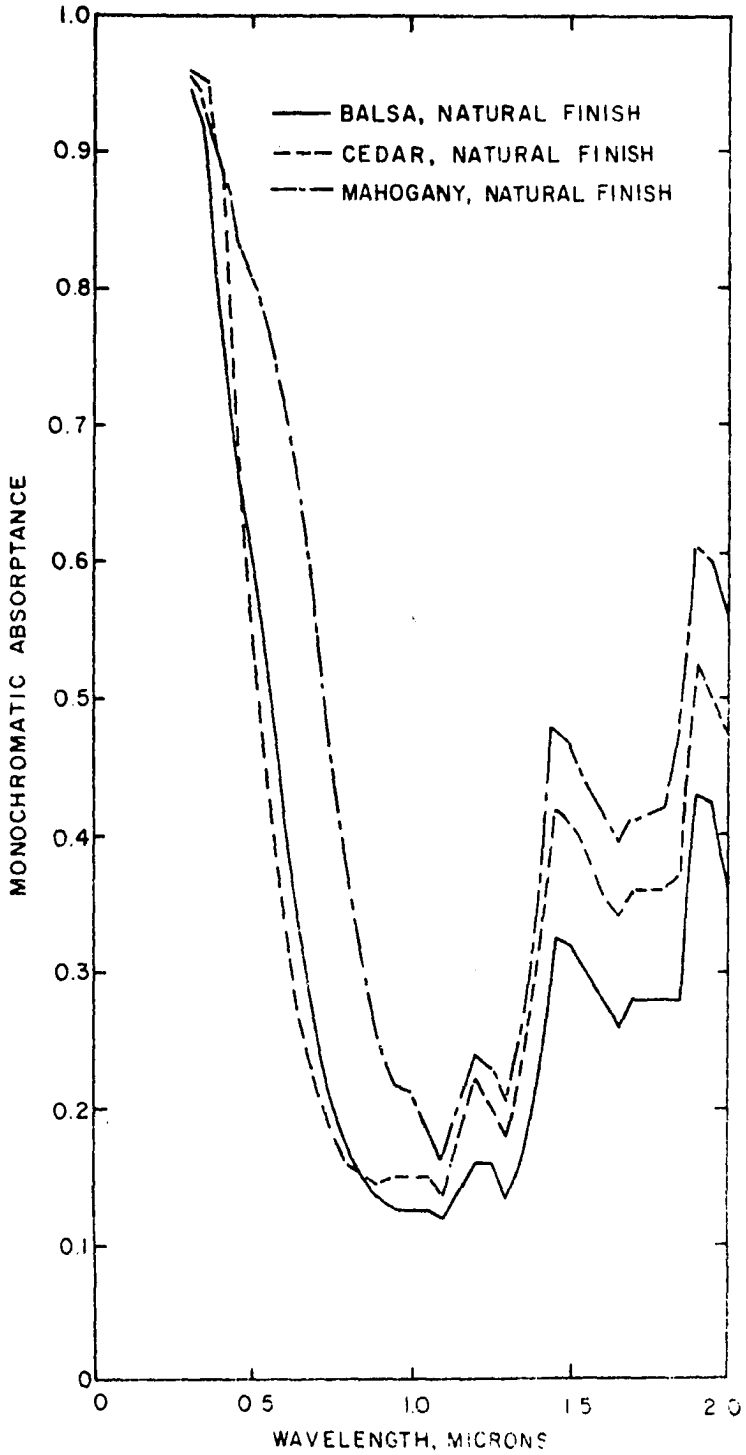

Figure IV-20. Absorptance Characteristics of Various Natural Finish Woods with Normal Viewing Angles.

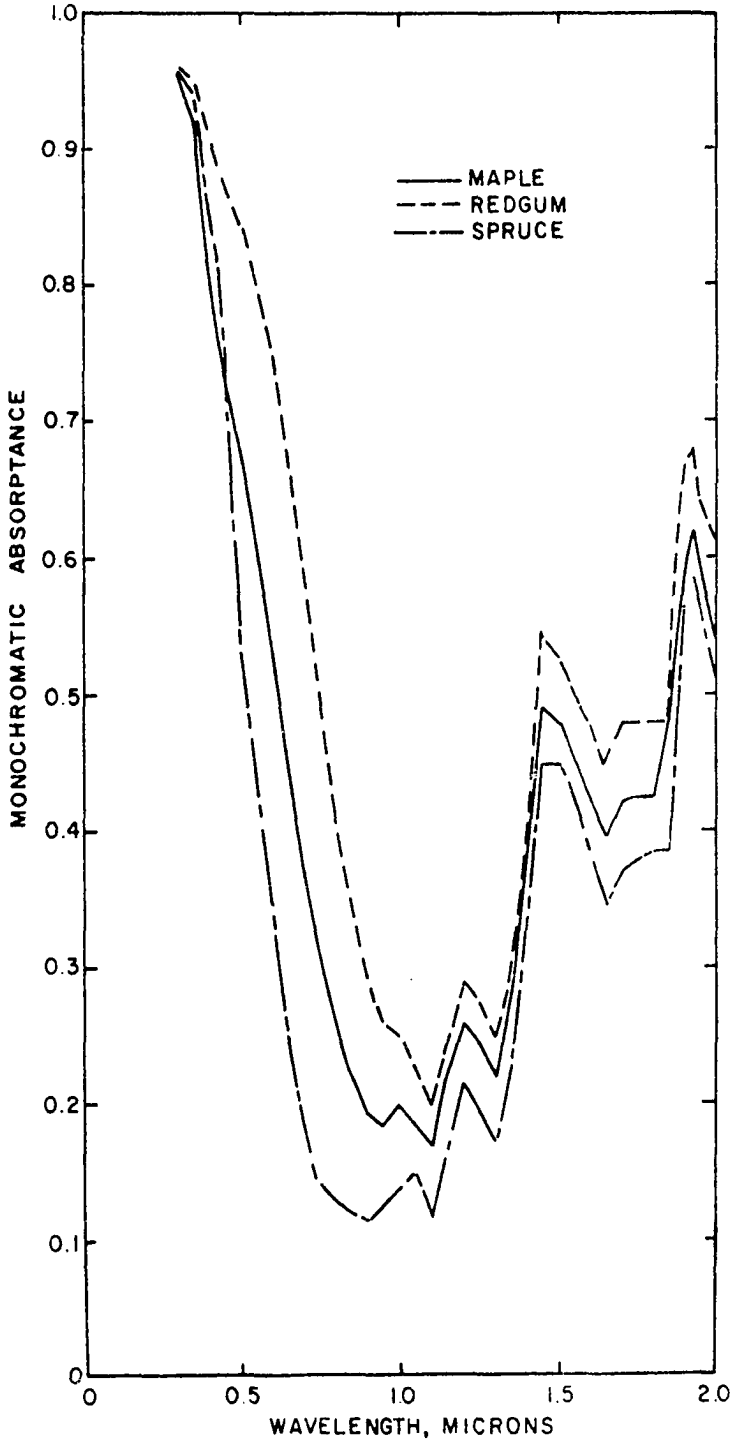

Figure IV-21. Absorptance Characteristics of Various Natural Finish Woods with Normal Viewing Angles.

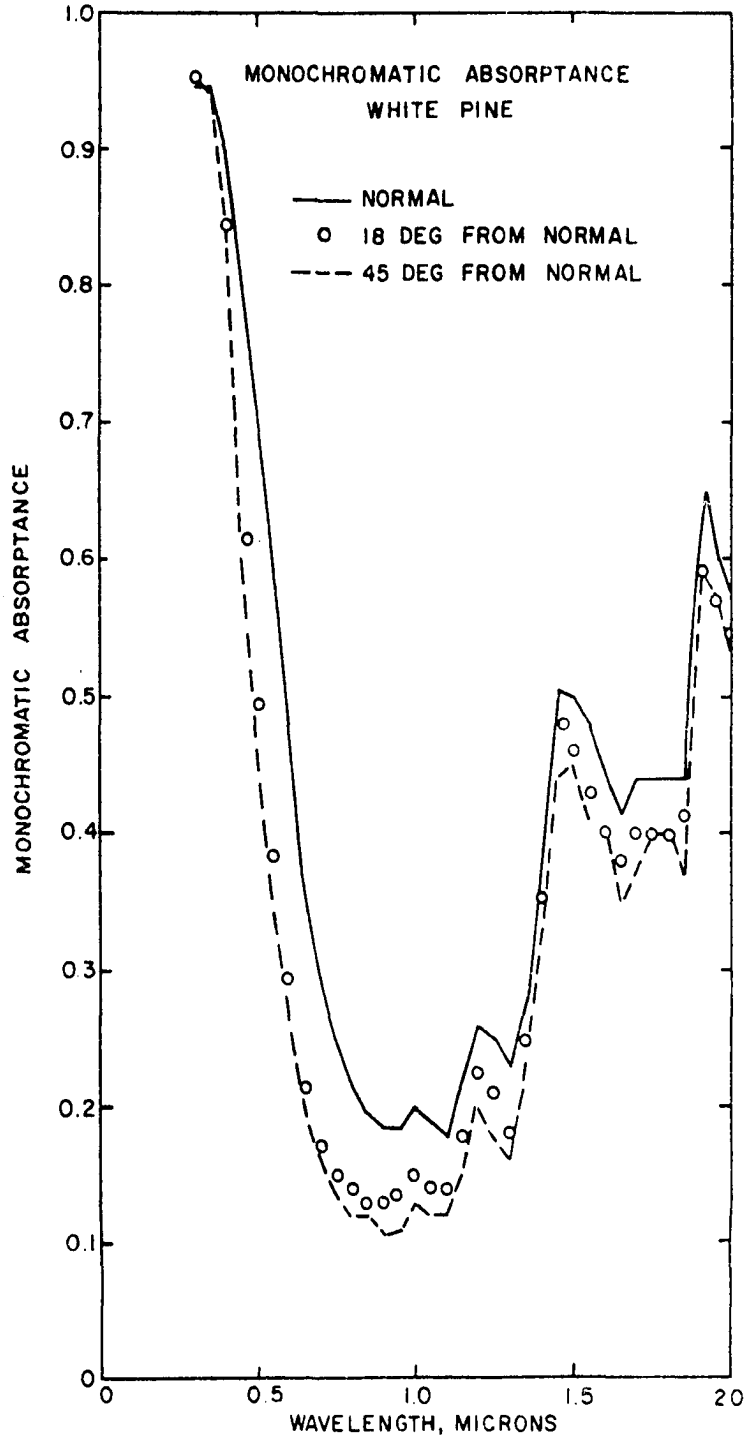

Figure IV-22. Absorptance Characteristics for Various Viewing Angles-Natural Finish White Pine.

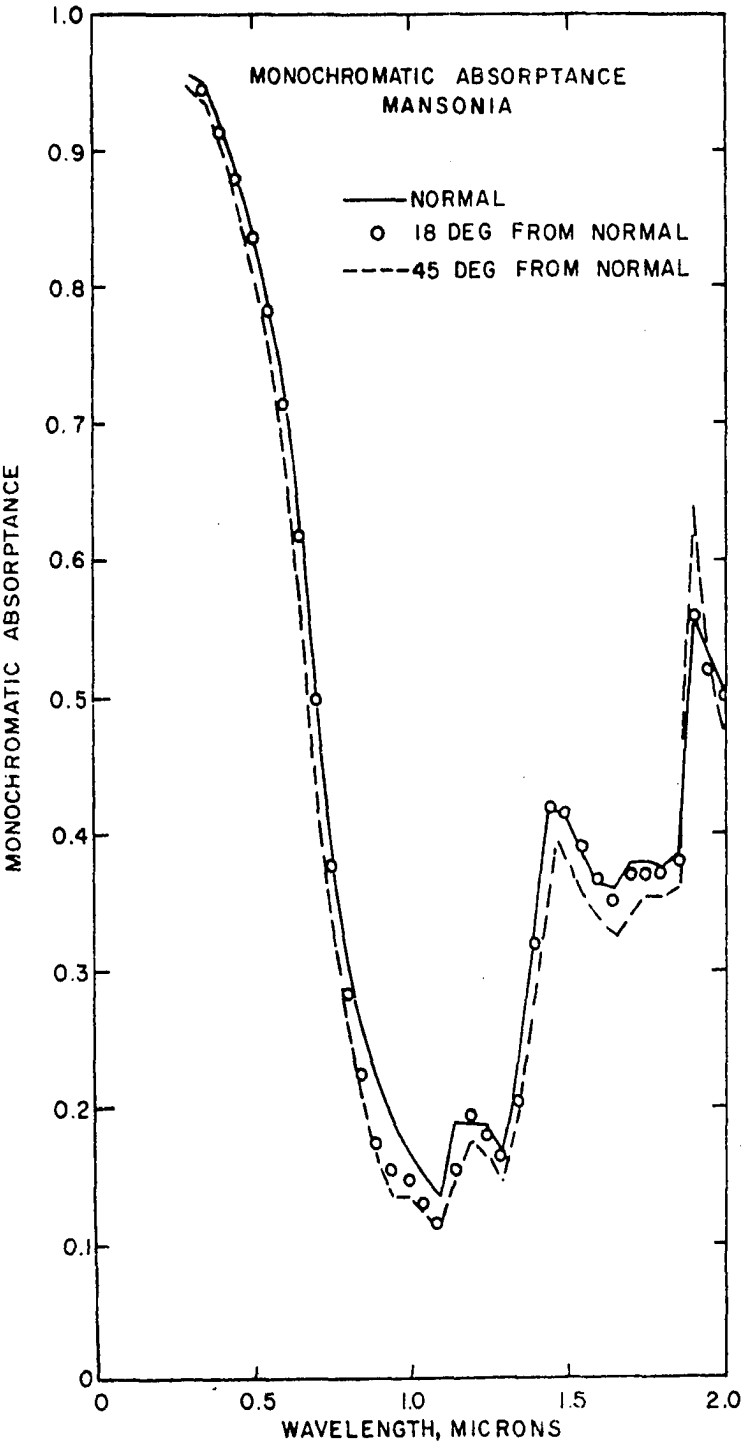

Figure IV-23. Absorptance Characteristics for Various Viewing Angles-Natural Finish Mansonia.

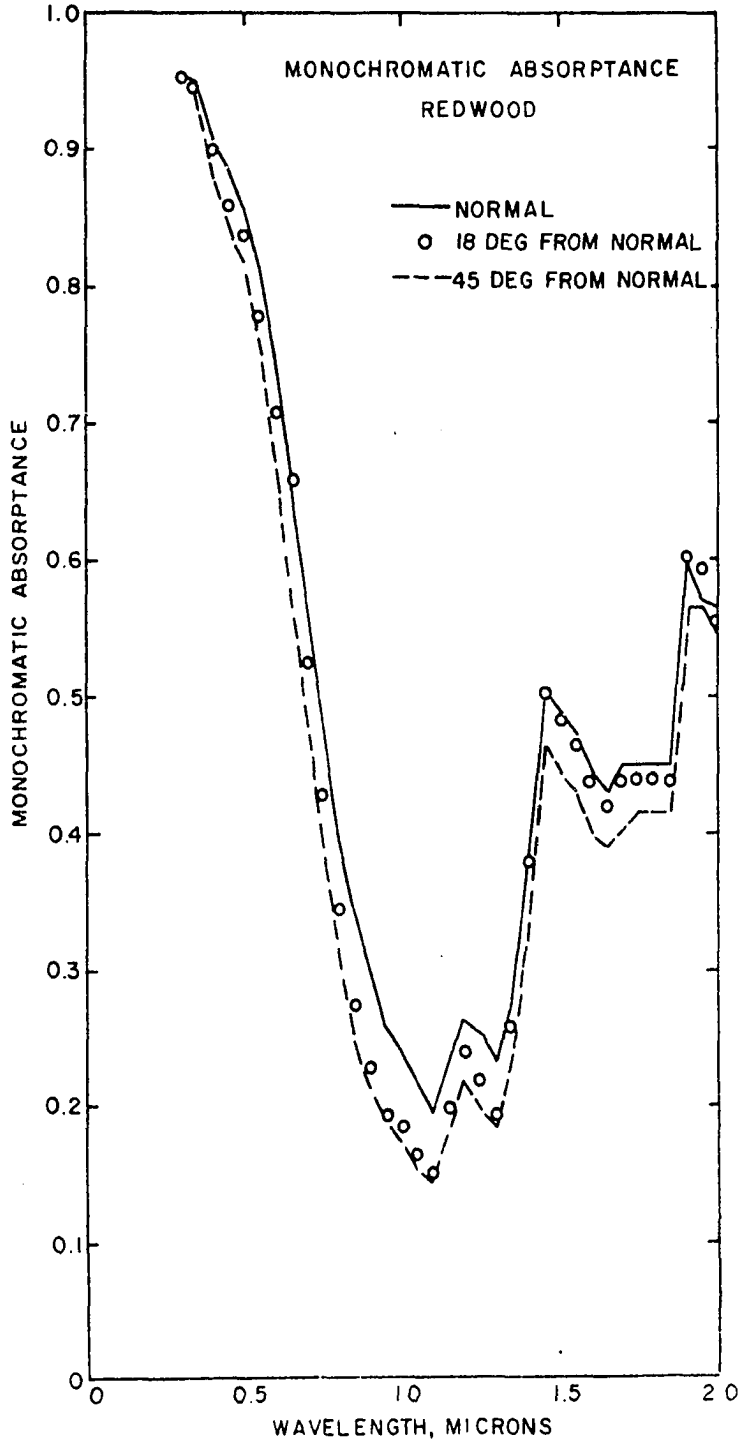

Figure IV-24. Absorptance Characteristics for Various Viewing Angles-Natural Finish Redwood.

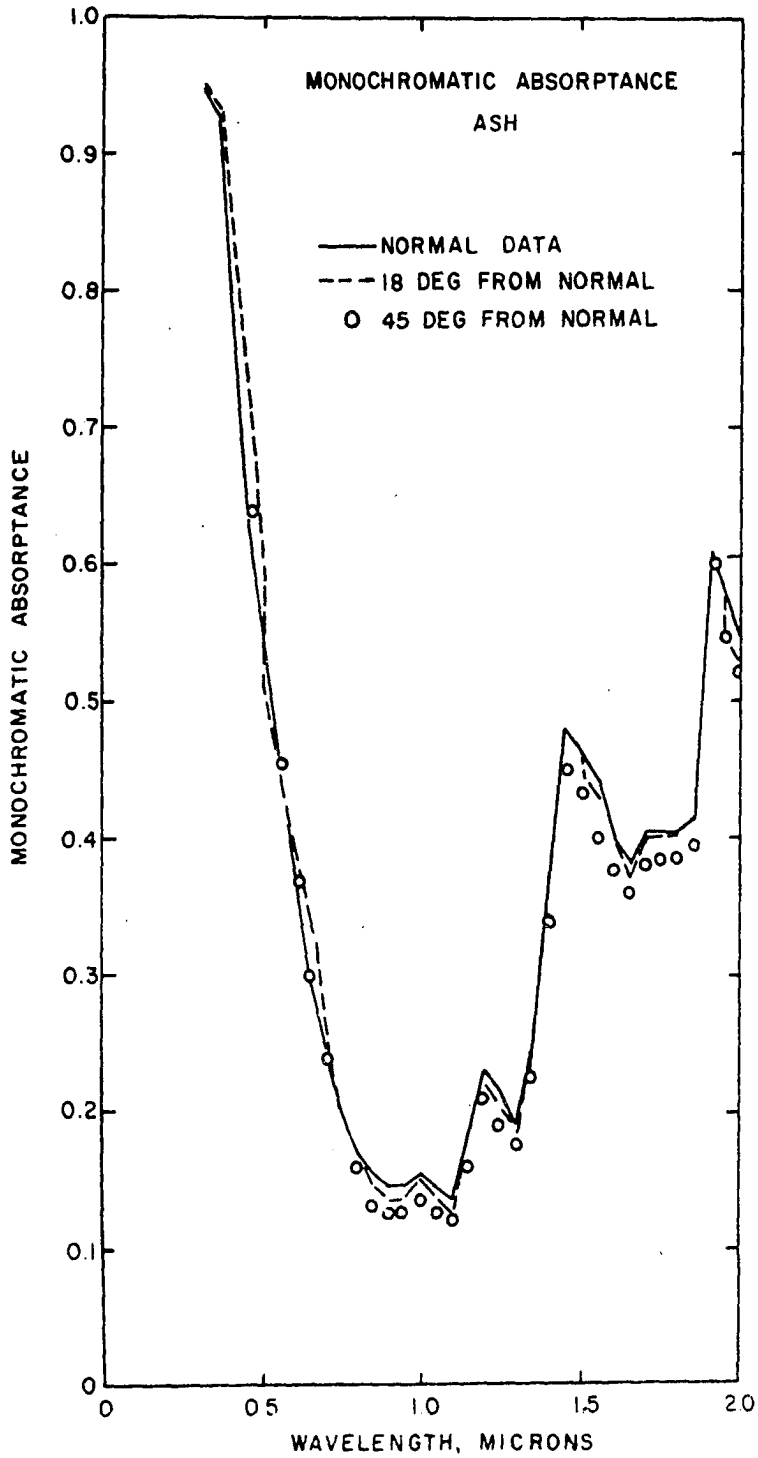

Figure IV-25. Absorptance Characteristics for Various Viewing Angles-Natural Finish Ash.

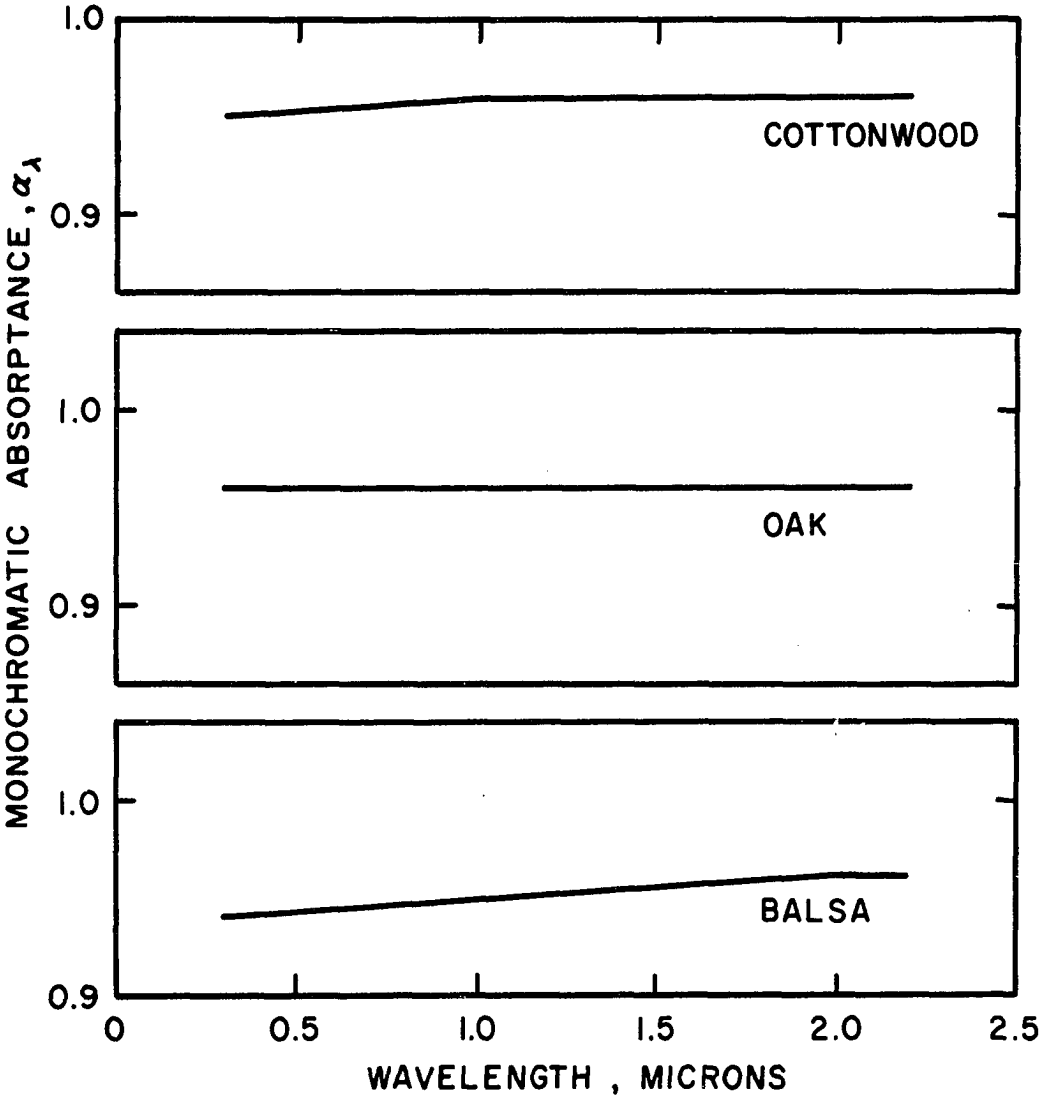

Figure IV-26. Absorptance Characteristics of Various Black Painted Woods with Normal Viewing Angle.

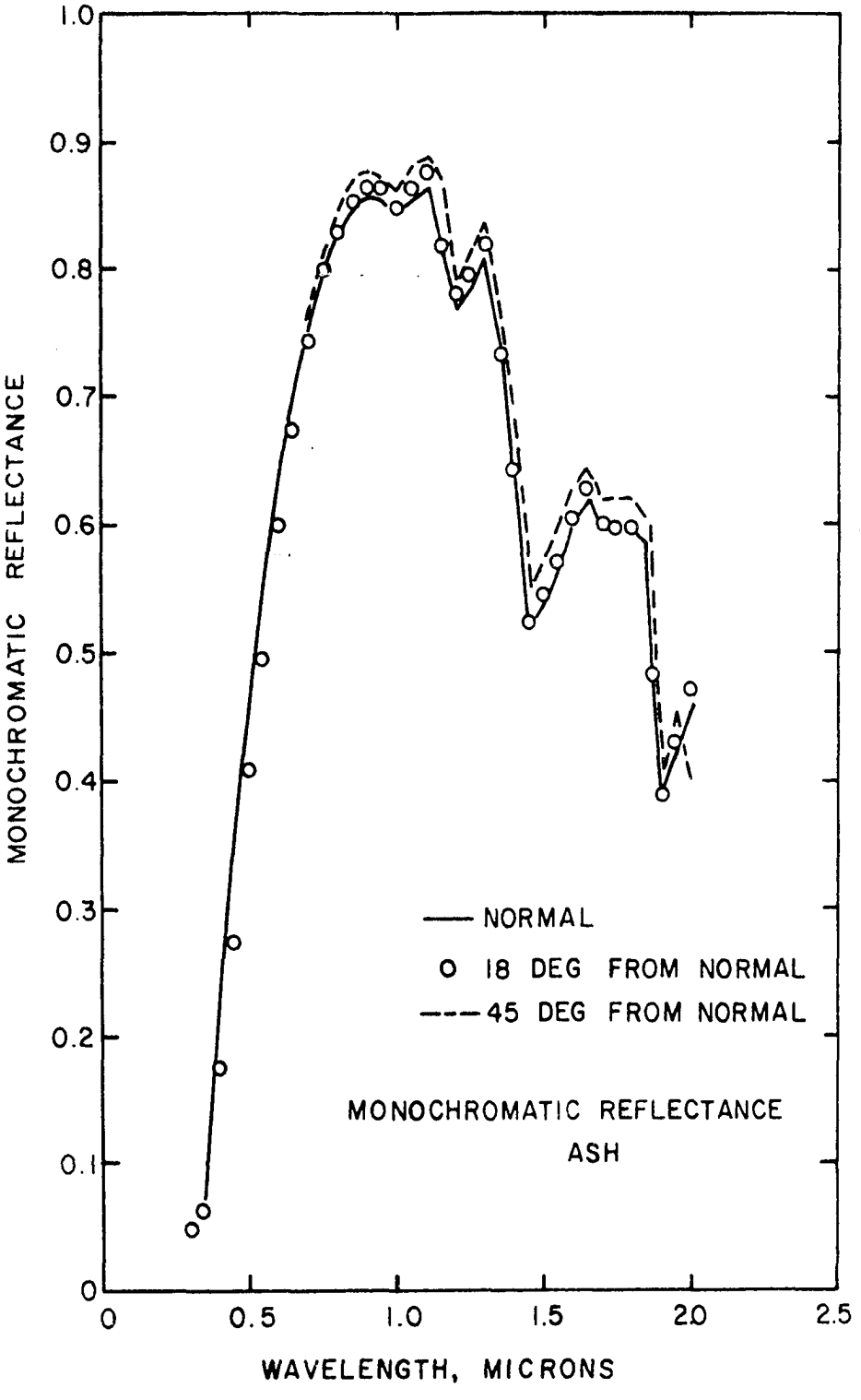

Figure IV-27. Monochromatic Reflectance Characteristics for Various Surface Viewing Angles-Natural Finish Ash Wood.

degrees from normal and 45 degrees from normal). As shown, very little variation was found at the different viewing angles even though the absolute precision of the non-normal data may be questionable due to the experimental configuration. However, the closeness of the data tends to confirm the generally accepted conclusion that wood reflects diffusely. Based on the data presented in Figure IV-6 on the relative emissive powers of a blackbody radiator and of diffusion flames, and the data presented in Figures IV-18 through IV-25 on the monochromatic absorptance characteristics of wood as a function of wavelength, it appears that the ignition times of wood should exhibit marked differences with the two different radiant energy sources at equivalent incident irradiance levels.

However, it is anticipated that the total absorptance factor will vary during the exposure period due to surface changes from normal conditions to a charred condition. For this reason it may be necessary to determine also the integrated average absorptance factor representative of the entire exposure period in order to obtain a good correlation. Such normalized total absorptance factors are not available in the literature; only a few unexposed total absorptance factors for woods are listed. Thus, from a practical view point, a correlation based on the average unexposed absorptance fac-

tors would appear to be not only more useful but also attainable for the following reason. While the average absorptance factors increase during the exposure period, the resultant increase in absorbed energy rate causes a higher surface temperature, which in turn increases the surface energy losses due to convective and reradiative cooling effects. Hence, at the lower incident irradiance levels where ignition times should be relatively long and the surface losses represent an appreciable percentage of the incident irradiances, the retained energy rate would tend to be more uniform. Thus, it appears reasonable to assume, for the time being, that it will be possible to correlate the data as a function of the initially absorbed energy, uncorrected for surface losses.

Correlation of Data on an Initially Absorbed Irradiance Basis

In deriving Equation (IV-23) the incident irradiance, H_i, was treated as a lumped energy term with no allowances for the spectral distribution. In the preliminary studies on the ignition of cotton fabrics, it was found that the ignition of white cloth by flame occurred in about 20 percent of the time required for ignition by tungsten lamps at the same level of incident irradiance. On the other hand, the ignition times for the black cloth for both the flame

and tungsten lamp irradiances were essentially the same at all irradiance levels used in the tests.

To determine the magnitude of the effects of the spectral distribution of the irradiance source and the spectral absorptances of the various wood surfaces, all of the pilot-ignition data obtained in these investigations, using both flame and tungsten lamps on 3/4-inch and greater thickness woods, (natural finish and black-painted woods) were subjected to a linear regression analysis. Figure IV-28 presents a comparison of the ignition data for natural finish woods using both flame and tungsten lamp radiation. As shown a good correlation of the test data was obtained, with ignition by flame radiation occuring in about 1/4 of the time required for ignition by tungsten lamps at comparable levels of incident irradiance. The linear regression analysis showed that the two sets of data could be best represented by the relationships:

For Flame Radiation:

$$t_i = 80 \left[\frac{\rho^{1/3} \left(\text{erf} \ \frac{1}{2\sqrt{F}} \right)^{3/4}}{H_i} \right]^3 \qquad \text{(IV-41)}$$

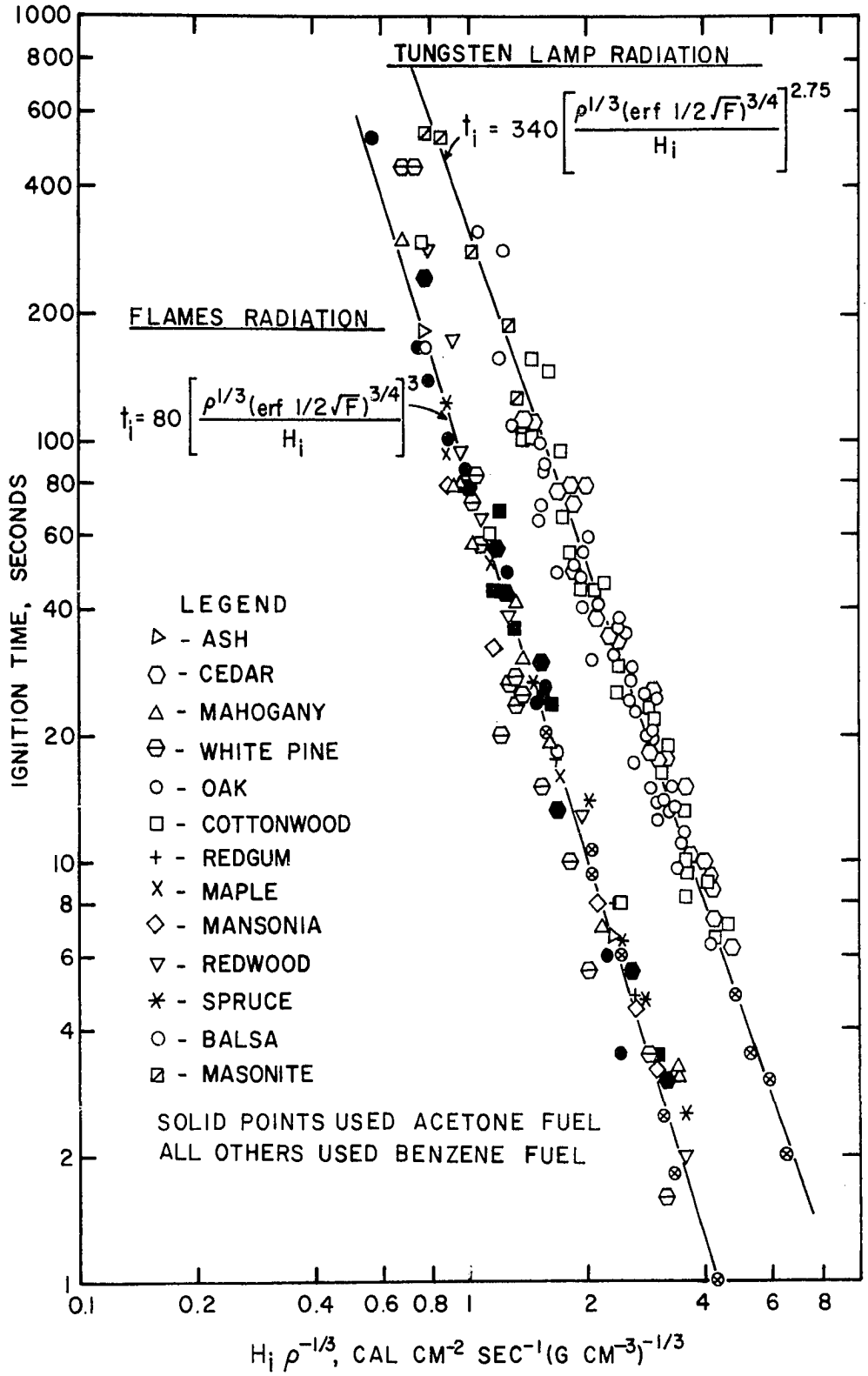

Figure IV-28. Comparison of Flames Ignition Data with Tungsten Filament Quartz Lamp Ignition Data for Natural Finish Woods.

For Tungsten Lamp Radiation:

$$t_i = 340 \left[\frac{\rho^{1/3} \left(\text{erf} \frac{1}{2\sqrt{F}} \right)^{3/4}}{H_i} \right]^{2.75} \qquad \text{(IV-42)}$$

Figure IV-29 presents a comparison of the ignition data for black-painted woods using both flame and tungsten lamp radiation. As shown a good correlation of the test data was obtained, with ignition by flame radiation occurring in about 1/2 of the time required for ignition by tungsten lamps at comparable levels of incident irradiance.

A comparison of the flame ignition data for natural and black-painted woods is presented in Figure IV-30. Similar data for tungsten lamp radiation are presented in Figure IV-31. Figure IV-32 presents a comparison of all four sets of test data. For the purposes of clarity the test points shown in Figures IV-29 through IV-31 are not reproduced, only the line correlations are presented. As shown, black-painted woods exposed to flame radiation ignited in the shortest time and natural finish woods exposed to tungsten lamp radiation took the longest time to ignite at all incident irradiance levels utilized in the tests.

Presumably, if the spectral absorptance characteristics of the woods previously presented were accounted for, it should be possible to collapse the line correlations of

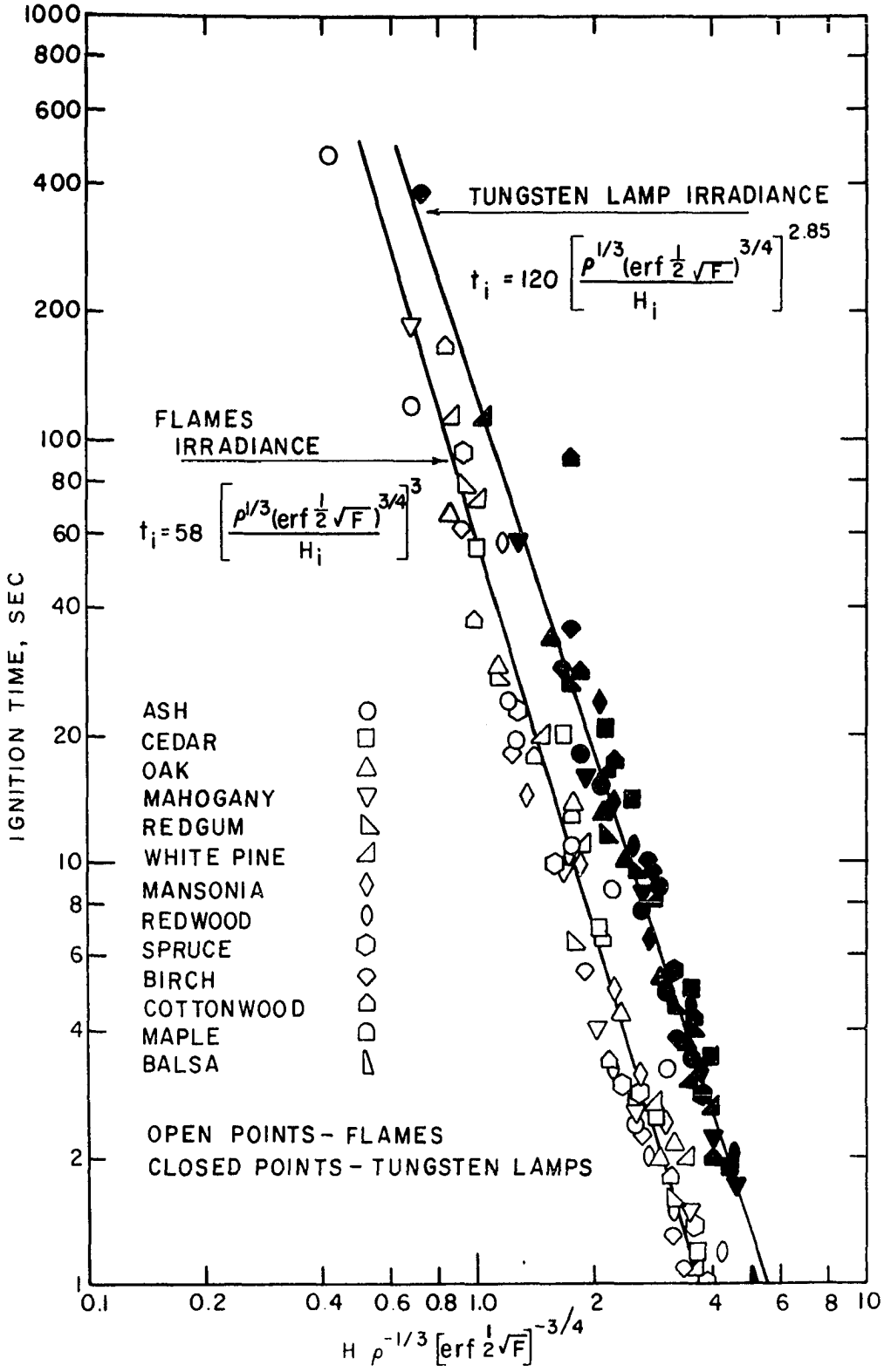

Figure IV-29. Comparison of Black Painted Wood Ignition Data Obtained with Flames and Tungsten Lamp Irradiances.

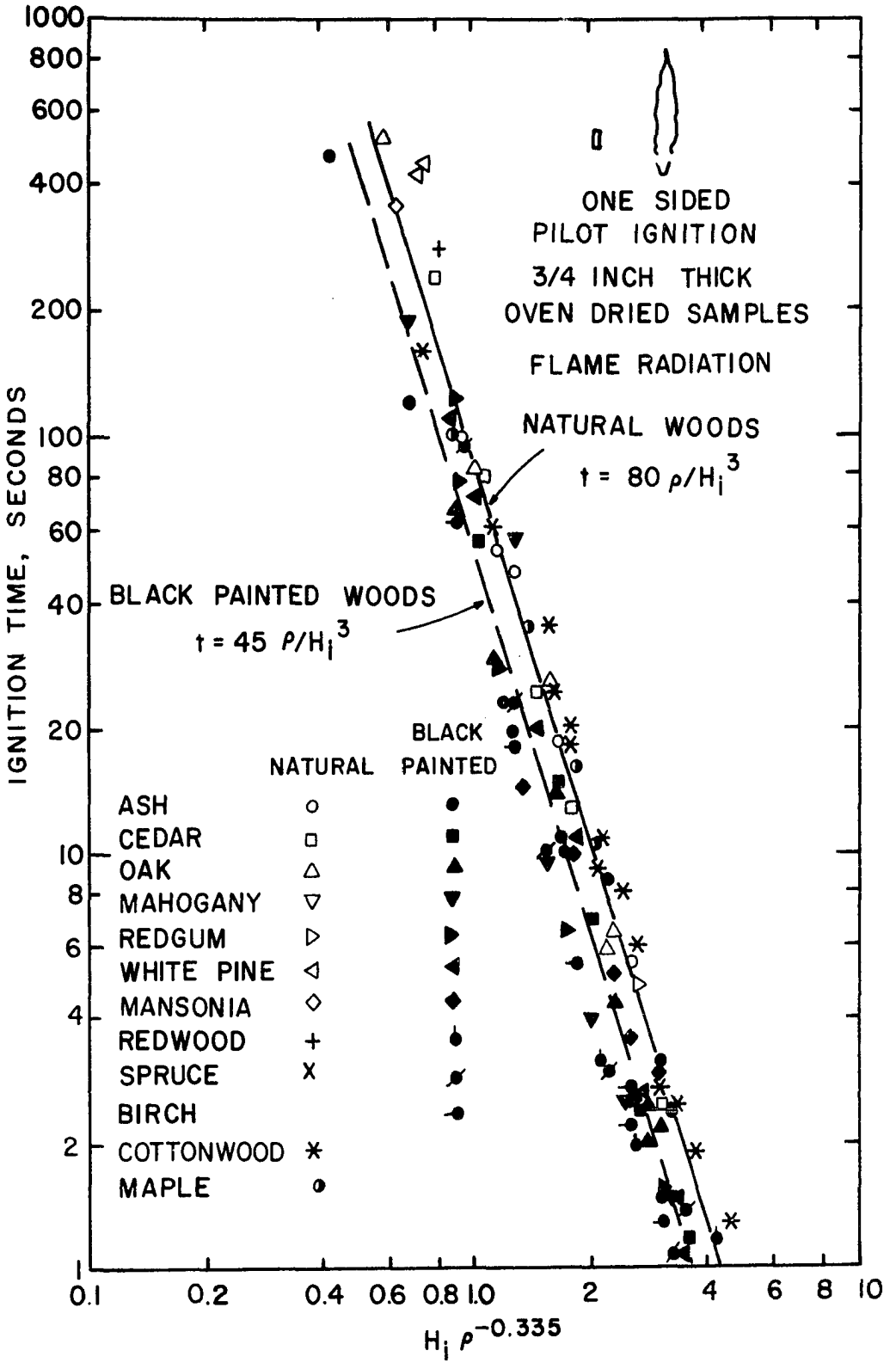

Figure IV-30. Comparison of Flames Ignition Data for Natural Finish Wood with the Data for Black Painted Woods.

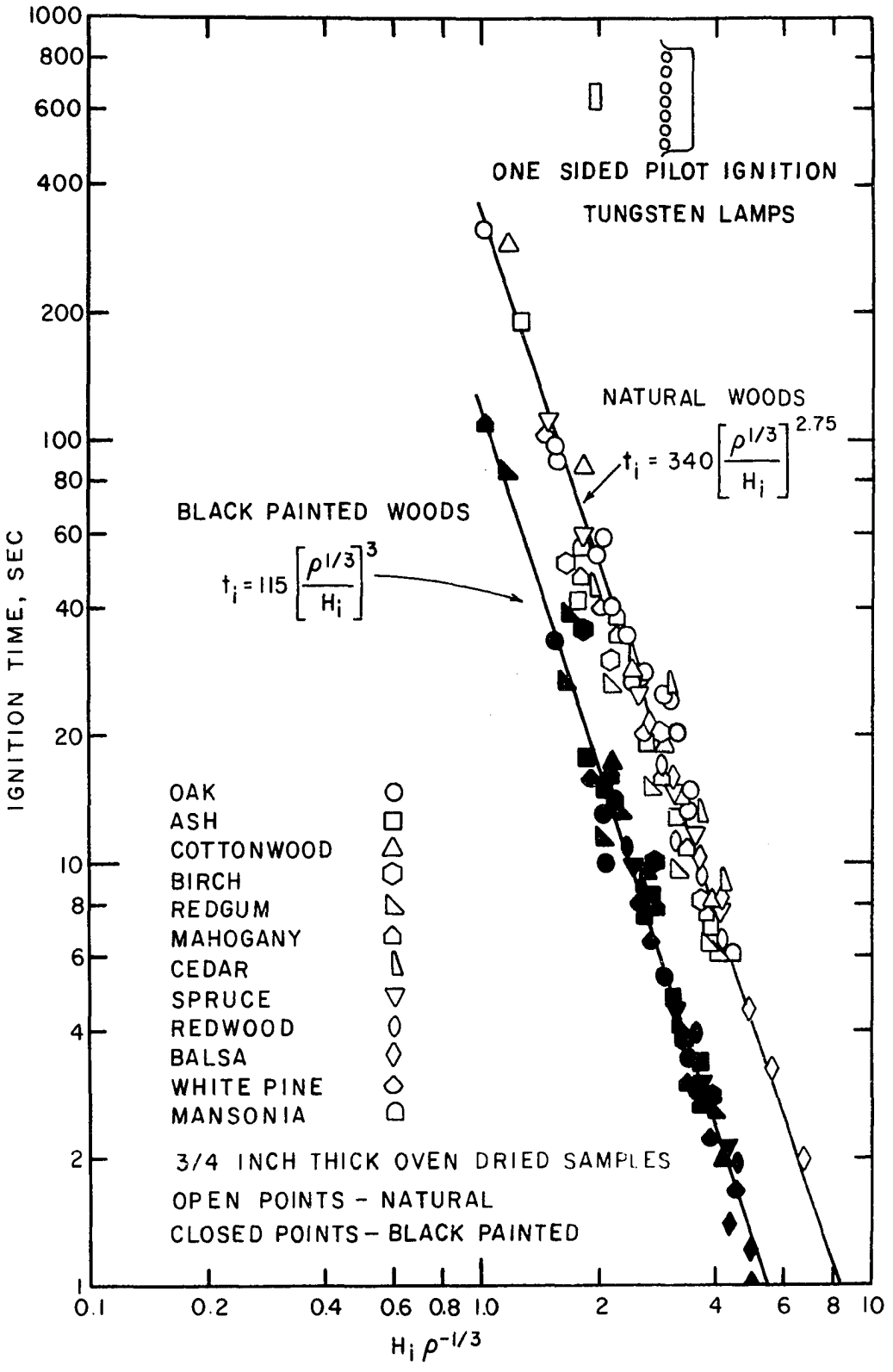

Figure IV-31. Comparison of Tungsten Lamp Ignition Data for Natural Finish Woods with the Data for Black Painted Woods.

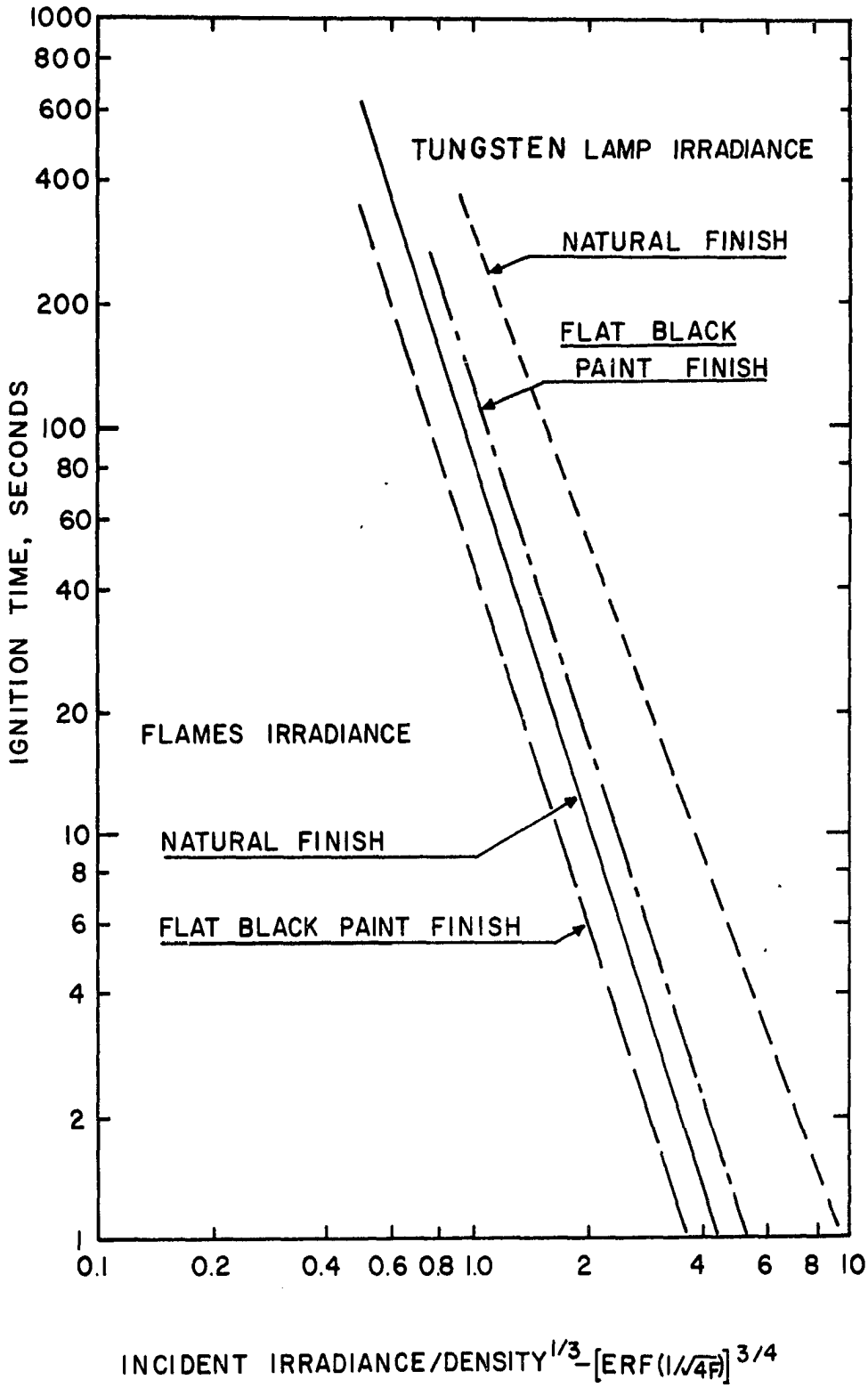

Figure IV-32. Comparison of Flames and Tungsten Lamp Ignition Data Correlations for Natural and Black Painted Woods.

Figure IV-32 into a single correlation by replacing the incident irradiance term in the abscissa with the absorbed irradiance. This same technique proved successful in obtaining a single correlation for the cotton fabrics discussed earlier in this chapter, irrespective of sample color and nature of the radiation source.

As discussed previously, spectral reflectance measurements in the range of 0.3 to 2.0 microns were made on all twelve woods subjected to ignition tests. Reflectance data on four of these twelve woods were also obtained in the range of 2 through 11 microns. However, only data through 5.6 microns were utilized herein since the radiation sources for the ignition tests did not possess any significant emissive power beyond 5.6 microns.

Based on the relatively small variations in the over-all spectral absorptance of these four widely different woods (color as well as grain structure) in the 2 through 5.6 micron range as shown in Figures IV-18 and IV-19, it was concluded that all woods tested could be represented by these four samples in the 2 through 5.6 micron range. The data obtained for each separate wood were utilized in the 0.3 to 2.0 micron range. Since there were minor differences for the twelve woods in the 1.3 through 2.0 micron range, minor differences in the average absorptance factors

for woods exposed to flame radiation (1.3 to 5.3 microns) were anticipated. Larger differences in the average absorptance factors for the woods exposed to tungsten lamp radiation were expected due to more significant spectral absorptance factor variations in the 0.5 to 1.3 micron range which contained the maximum emissive powers of the tungsten lamps.

According to Equation IV-4 the energy initially absorbed by the sample is a function of both the spectral absorptance of the samples and the spectral emissive powers of the energy source. An average total absorptance for a given sample-radiation source configuration can be expressed as

$$\bar{\alpha} = \frac{\int_{\lambda_1}^{\lambda_2} e_\lambda \, \alpha_\lambda \, d\lambda}{\int_{\lambda_1}^{\lambda_2} e_\lambda \, d\lambda} \qquad \text{(IV-43)}$$

However, due to the relative values of e_λ, as shown in Figure IV-6, and α_λ, as shown in Figure IV-18 through IV-25 it was decided to utilize the approximation

$$\bar{\alpha} = \frac{\Sigma \alpha_\lambda \, e_\lambda \, \Delta\lambda}{\Sigma e_\lambda \, \Delta\lambda} \qquad \text{(IV-44)}$$

with $\Delta\lambda$'s on the order of 0.05 microns. This small incremental value of $\Delta\lambda$ gives a very close approximation to an

actual integrated value of $\bar{\alpha}$. Table IV-3 presents a summary of the unexposed average absorptance factors obtained using this approximation technique. As shown, and expected, minor variations resulted in the average absorptance facotrs for natural finished wood exposed to flame radiation. Larger variations resulted for the woods exposed to tungsten lamp radiation.

TABLE IV-3

CALCULATED VALUES FOR UNEXPOSED WOOD AVERAGE ABSORPTANCE FACTORS

Type of Wood	Average Absorptance Values			
	Flames Radiation		Tungsten Lamp Radiation	
	Natural Finish	Black-Painted Finish	Natural Finish	Black-Painted Finish
Cottonwood	0.760	0.870	0.482	0.930
Mahogany	0.796	0.870	0.495	0.930
Balsa	0.753	0.870	0.408	0.930
Cedar	0.760	0.870	0.441	0.930
Redgum	0.766	0.870	0.526	0.930
Maple	0.762	0.870	0.485	0.930
Spruce	0.765	0.870	0.437	0.930
Ash	0.765	0.870	0.464	0.930
Redwood	0.764	0.870	0.510	0.930
Minsonia	0.760	0.870	0.467	0.930
White Pine	0.770	0.870	0.488	0.930
Oak	0.773	0.870	0.567	0.930
Birch	0.771	0.870	0.471	0.930
Masonite	0.750	0.870	0.526	0.930

These average absorptance factors were then used to obtain a correlation of the ignition data on an initially absorbed energy basis. This correlation does not consider

the irradiated surface energy losses due to convective or reradiative cooling effects. Figure IV-33 shows one correlation for the ignition data obtained on natural woods by both flame and tungsten lamp radiation and the ignition data of black-painted wood by flame radiation only. The pilot ignition time for this particular correlation can be expressed by

$$t_i = 35 \left[\frac{\rho^{0.9} \left(\operatorname{erf} \frac{1}{2\sqrt{F}} \right)^{1.2}}{2.8} \right] \qquad \text{(IV-45)}$$

$$\bar{\alpha} H_i$$

Another correlation for the ignition of black-painted wood by tungsten lamp radiation is also shown on Figure IV-33, but it is not included as part of the correlation given by Equation IV-45 for the following reasons. It is apparent from the darkening of natural wood samples as they pyrolyze and char that their absorptance is increasing, at least in the visible region of the spectrum. The effect of this change in absorptance is apparently not sufficient to affect the correlation in Figure IV-33 for natural woods and/or black-painted woods using flame radiation. If the tungsten lamp radiation is used for black-painted wood, however, the ignition time is greater than that predicted by the correlation in Figure IV-33. The reason for this behavior, which

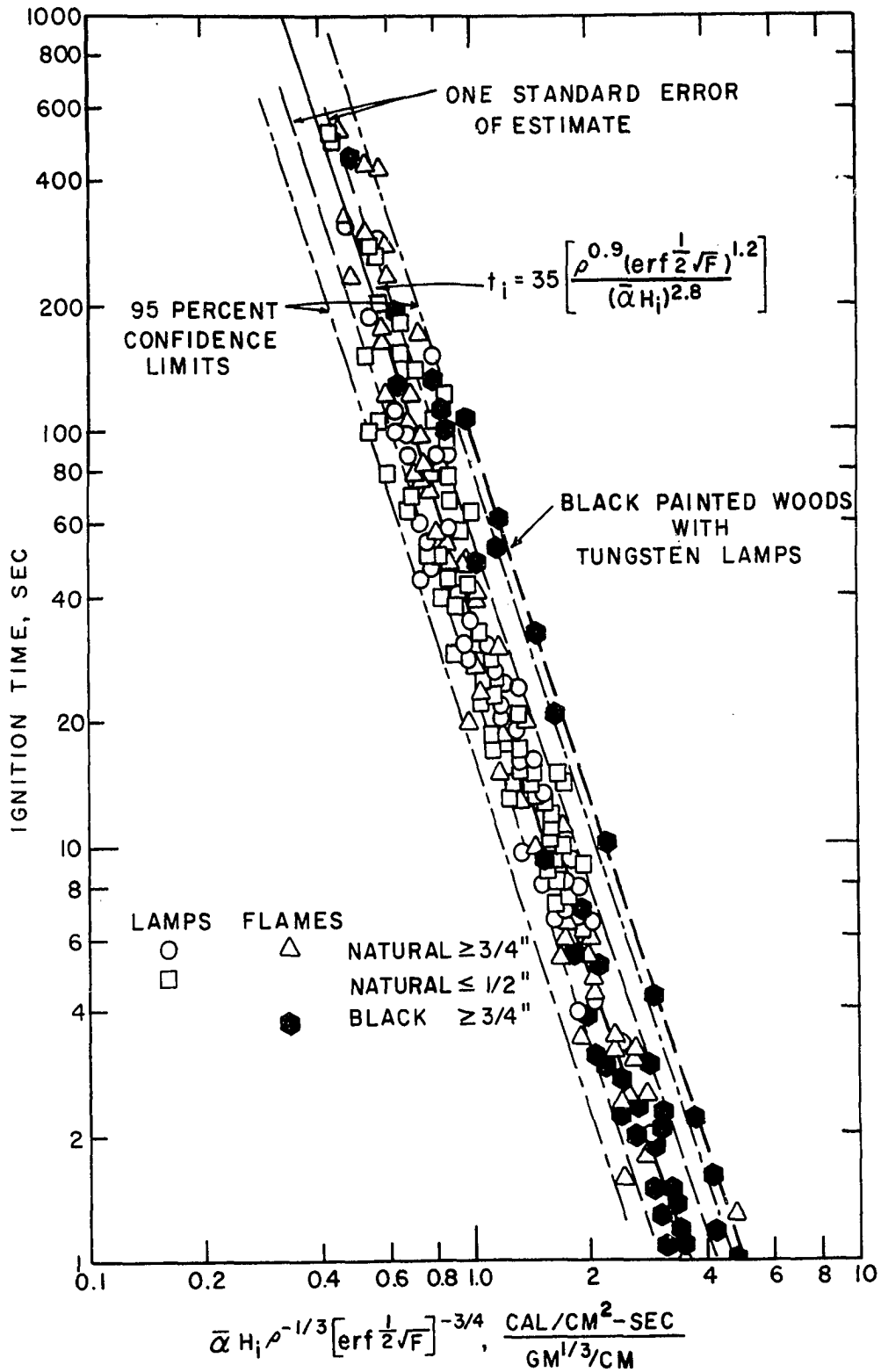

Figure IV-33. Correlation of Ignition Data using Initially Absorbed Irradiance Corrected for Wood Density and Thickness Effects.

will be discussed in detail in the section on Correlation of Data on a Retained Irradiance Basis, is due to the decrease in average absorptance of the black-painted samples with heating, both by flame and tungsten lamp radiation. This decrease in absorptance of the black-painted wood is relatively unimportant for the flame radiation since the change occurs primarily for the longer wavelengths where the absorptance is high for even uncharred wood samples. However, as can be shown by a comparison of Figures IV-6 and IV-34, the decreasing absorptance, due to the degradation of the black paint, occurs in the region of the spectrum where the peak emissive power of the tungsten lamps is located. The absorbed energy, therefore, is abnormally low for the tungsten lamp ignition tests on black-painted woods, which results in an effective retarded ignition time.

Experimental data on the monochromatic reflectance characteristics of wood, just prior to charring, and the spectral emissive powers of the tungsten lamp give, by Equation IV-44, an average absorptance factor of 0.75. Similar data for black-painted wood indicate an average absorptance of 0.93. Based on the work of Muir (32), who also investigated the effects of paint coatings on ignition times for cedar, it is concluded that the paint coating itself did not materially effect the ignition time insofar as energy

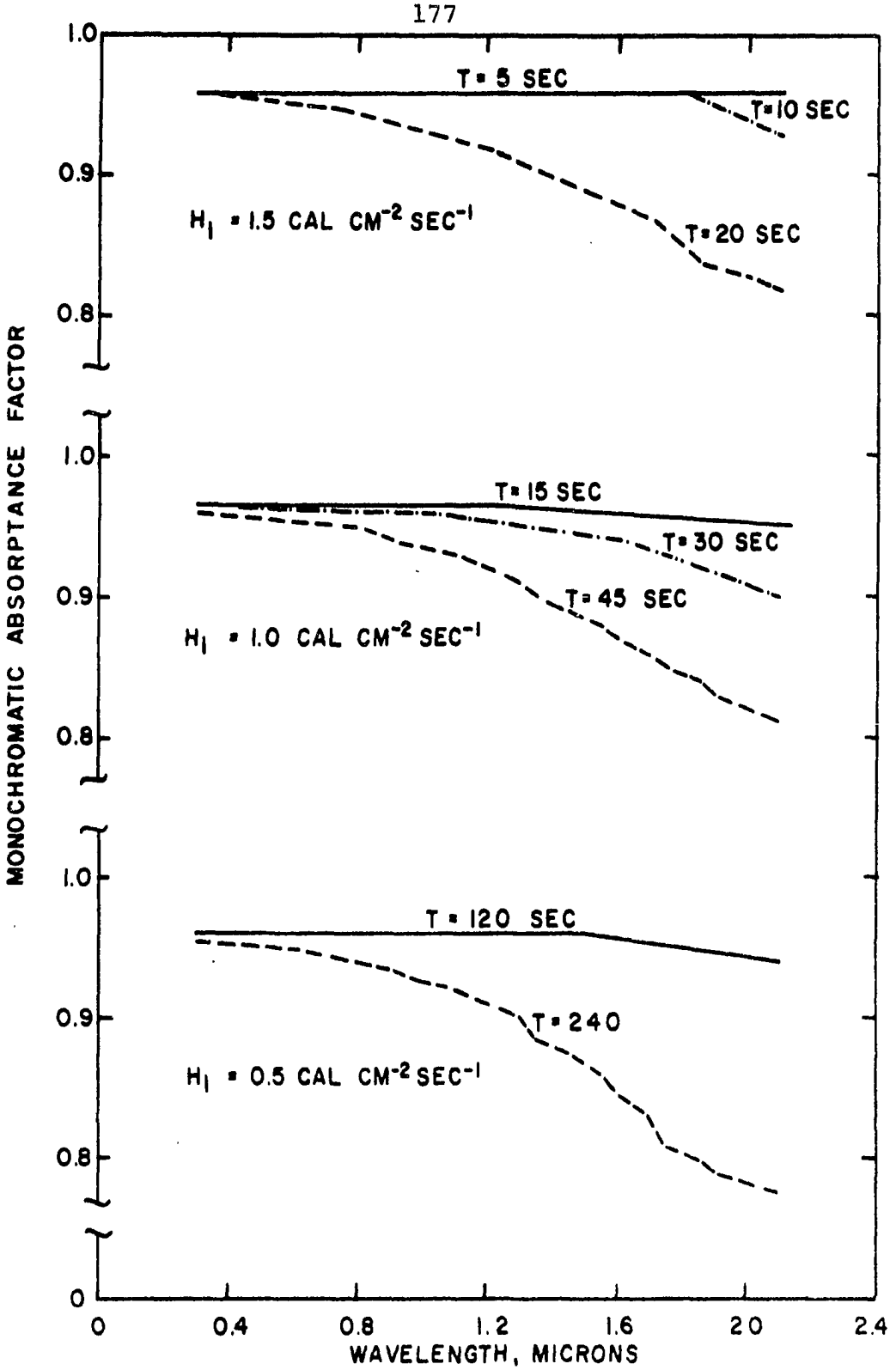

Figure IV-34. Monochromatic Absorptance of Black Painted Oak Exposed for Varying Time Periods to Tungsten Lamp Irradiance (1000 W Lamps).

requirements to pyrolyze the coating. Therefore, if the average absorptance factor of 0.75, determined for wood blackened by heating effects, were used in lieu of the 0.93 factor determined for the black-painted woods, the ignition data obtained for the black-painted woods exposed to tungsten lamp radiation (as shown in Figure IV-33) would fall with the general recommended correlation presented in Figure IV-33. The 95 percent confidence limits are also presented by Figure IV-33.

Discussion of Initially Absorbed Irradiance Correlation

It may be recalled from preceding discussions in this chapter that an inert solid (no net heat effect due to decomposition) and constant uniform properties were assumed. In this section the results of the correlation presented in Figure IV-33 are compared with the predictions of a graphical technique for the solution of the wood ignition problem (33). For completeness and ease of reference this graphical method is reproduced in its entirety in Appendix (C). Briefly, the analysis for an opaque, semi-infinite, one-dimensional material subjected to constant radiant heating at the surface with heat loss due to reradiation and convective cooling from this irradiated surface was considered.

Based on the experimentally determined physical and thermal properties of white pine as determined by Havens (13), the ignition times for a range of absorbed irradiances were

graphically determined for an assumed constant surface ignition temperature of 450°C. As shown by Figure IV-35 very good agreement between the graphical predictions and the experimental data correlations were obtained.

The 450°C surface ignition temperature is in fair agreement with the surface temperatures experimentally determined by Smith (45) and discussed in detail in the following section. Further, the work of Havens (13) indicated that at a heating rate of 20°C/min the maximum sample weight loss rate, and hence, maximum rate of pyrolysis production, occurs at a surface temperature of about 380°C. Haven's data also indicated a possible increase in the temperature at which this maximum rate of pyrolysis occurs with an increase in the heating rate. Since the actual surface temperature rises in this study varied from about 40°C/min (ignition in about 600 seconds) to over 26,000°C/min (ignition in less than one second), exact conclusions or extrapolation of these data cannot be made. However, an assumed ignition temperature of 450°C does not appear to be unreasonable in view of Smith (45) and Havens (13).

Correlation of Data on a Retained Irradiance Basis

As illustrated by the overall energy balance model presented in Figure IV-4, part of the incident energy will be absorbed by the irradiated material. Of that portion of

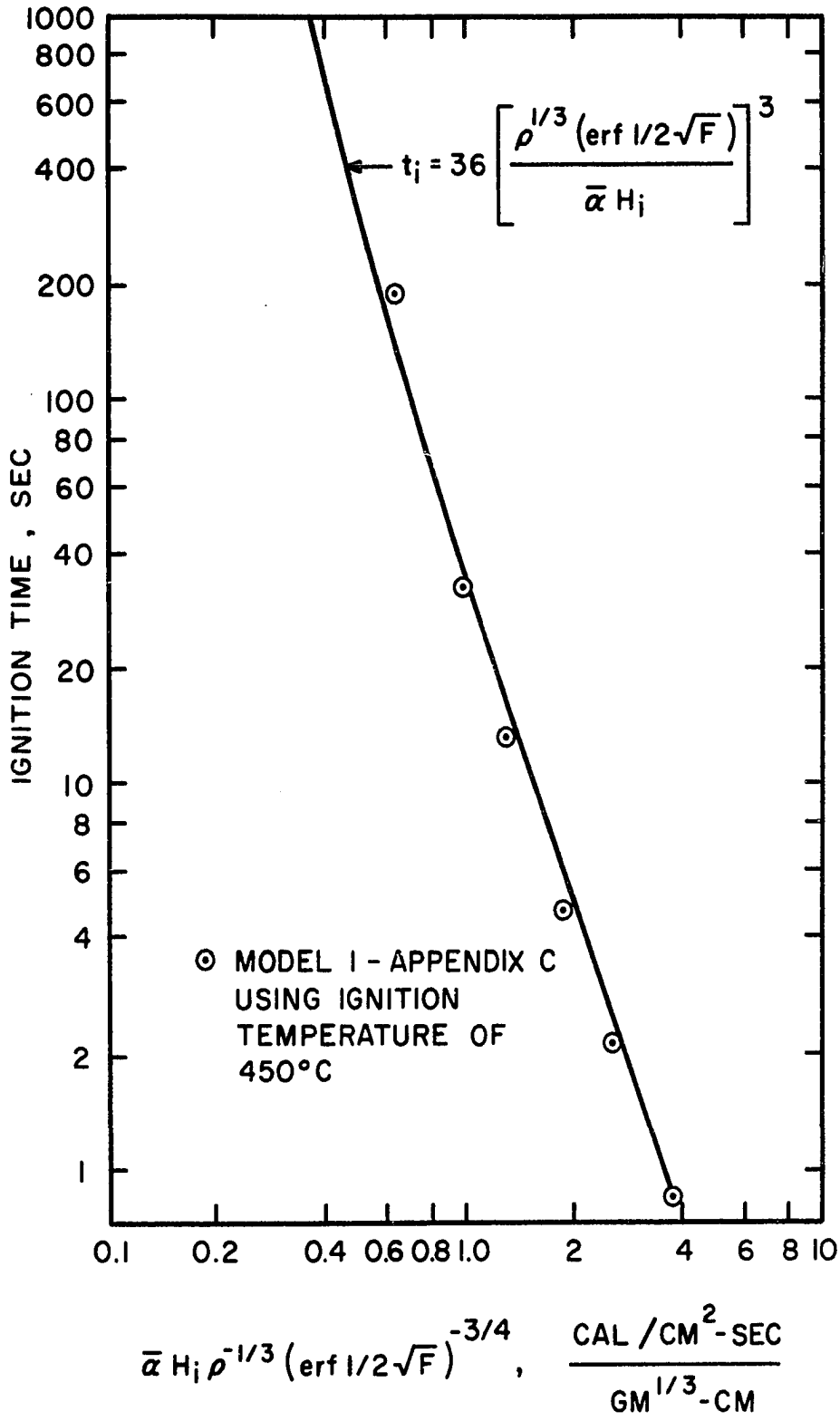

Figure IV-35. Comparison of Ignition Data Correlation and Ignition Behavior Predicted by Model 1-Appendix C.

the incident energy that is initially absorbed, part will be reradiated as the irradiated surface temperature rises, part will be lost due to convective cooling effects, and the remainder will be retained within the material. In order to evaluate the relative magnitudes of this distribution of the energy that is initially absorbed, it is necessary that the exposed surface temperatures as a function of exposure time, the exposed surface convective heat transfer film coefficients and the irradiated surface reflectances be determined during the exposure period.

Rear Surface (Non-Irradiated) Energy Losses

The rear surface of the wood samples will experience a loss of the energy that is initially absorbed by the irradiated surface and is subsequently conducted through the sample during the exposure period. The magnitude of this energy loss will depend upon the rate of energy absorption, the thermal properties of the wood, the exposure time, the thickness of the wood and the convective film coefficient at the rear surface. Airflow measurements performed by Koohyar (14), and reconfirmed in these investigations, showed a very uniform distribution of airflow throughout the ignition cabinet. The supplemental spot measurements indicated a velocity variation of less than 5 percent (within instrumentation accuracy) around the area of the cabinet containing the sample material.

The mean value of the convective heat transfer coefficient was estimated by the Pohlhausen Equation (29, page 224) derived from boundary layer theory; thus,

$$\left[\frac{h_c}{c_p V \rho}\right]\left[\frac{C_p \mu}{K}\right]^{2/3} = \frac{2}{3}\left[\frac{h V \rho}{\mu}\right]^{-1/2} \qquad \text{(IV-49)}$$

where all the quantities are the properties of air at average film conditions,

C_p = heat capacity of air at constant pressure

V = free stream air velocity

ρ = air density

μ = air viscosity

K = air thermal conductivity

h = height of the test sample

The average film temperature was determined by averaging the free stream temperature T_o and an assumed range of surface temperatures T_s, i.e. $(T_s + T_o)/2$. For the surface temperatures a range of 50°C to 600°C was assumed to account for the difference between irradiated and nonirradiated surfaces. The air temperature in the cabinet under test conditions was measured to be consistently less than 40°C. The free stream velocity at the

fixed exhaust damper position used for all experiments was measured to be 3.40 ft/sec. For these conditions, h_c was calculated by Equation IV-49 for the range of assumed surface temperatures and the results are tabulated in Table IV-4 below. As anticipated the calculated values of h_c are essentially constant over the entire range of assumed surface temperatures, and the assumption of a uniform h_c for both irradiated and nonirradiated surfaces appears to be valid.

TABLE IV-4

CALCULATED VALUES OF h_c FOR VARIABLE SURFACE TEMPERATURES OF SAMPLE SURFACES

T_s (°C)	$T_s - T_o$ (°C)	h_c (cal/cm^2-sec-°C x 10^4)
50	10	3.0
100	60	3.0
200	160	3.0
300	260	2.95
400	360	2.95
500	460	2.90
600	560	2.90

The rear surface convective heat losses were then approximated by the conventional relationship

$$q_c = h_c (T_s - T_o) \qquad \text{(IV-50)}$$

where q_c = convective heat loss rate

h_c = convective heat transfer coefficient

T_s = rear surface temperature

T_o = rear surface surrounding air temperature

Since the rear surfaces did not undergo any significant physical or coloring change up to the time of ignition on the front surface, the total normal emissivity would not be expected to change. Further, due to the diffuse nature of the wood samples, the total normal emissivities should be very representative of total hemispherical values based on the literature, woods have a normal total emissivity value range of 0.895 to 0.95. The maximum value was assumed. Hence, the radiative losses from the rear surface were approximated by the conventional relationship

$$q_r = \sigma\epsilon (T_s^4 - T_o^4) \qquad \text{(IV-51)}$$

where q_r = radiative energy loss rate

σ = Stefan-Boltzmann constant

ϵ = total normal emissivity

Since most woods, particularly those of light density such as balsa, cottonwood, cedar, etc. are fairly

good thermal insulators, it was anticipated that only very small rear surface temperature rises would result prior to ignition at the irradiated surface. However, the magnitude and time history of these temperature rises determine the relative magnitude of the convective and radiative energy losses. It follows that if these effects are small, the energy losses from the rear surface will be small and can possibly be neglected in the final correlations. To confirm this tentative conclusion rear surface temperatures as a function of exposure time for typical test runs on the most dense and minimum thickness samples (0.318 cm oak) were obtained experimentally. These data are summarized in Table B-IX.

As shown by Figure IV-36 the time averaged heat losses from the rear surface was approximately 3 percent of the incident irradiance. The energy losses for less dense and thicker woods were calculated to be less than 1.5 percent of the incident irradiance over the entire exposure period. It was, therefore, concluded that the convective and radiative energy losses could be neglected since their contributions were within the overall range of experimental error.

Front (Irradiated) Surface Energy Losses

Since the convective and reradiated energy losses from the front (irradiated) surface are determined by the

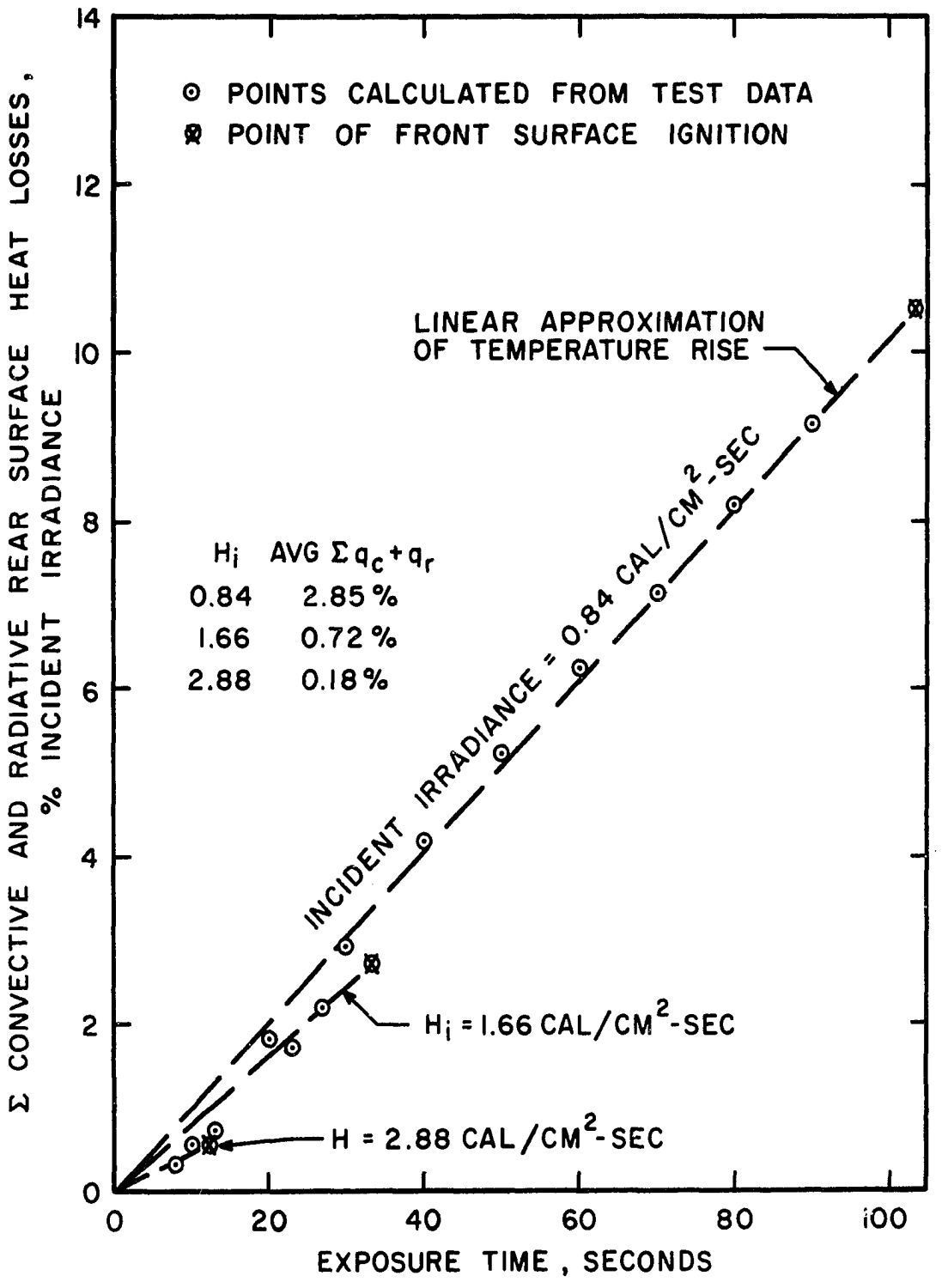

Figure IV-36. 0.318 cm Oak Samples Convective and Radiative Transient Heat Losses from the Rear Surface During the Front Surface Exposure Period.

magnitude and time history of the associated temperature rises during the exposure period prior to the appearance of flaming ignition, it is imperative that realistic data for surface temperatures be obtained. As reported in the literature and observed during these experimental investigations, the determination of irradiated surface temperatures is extremely difficult and the results of different studies usually do not agree with each other. The techniques that have been used consist of the following:

1. The most common procedure is to attach a thermocouple to the surface of the sample. While this technique was used for the measurements discussed above for nonirradiated (rear) surface temperature rises, the results for irradiated surface temperature rises would be most difficult and questionable to interpret because: (a) An unknown portion of the recorded signal is due to direct absorption of radiant energy by the thermocouple. (b) The thermocouple bead may lose its intimate contact with the surface as soon as charring, shrinkage and cracking starts. (d) The thermocouple bead senses a temperature which is different from the surface temperature because it is only in partial contact with the surface.

2. A second method is to place thermocouple junctions at various depths in the sample and extrapolate the measurements to the surface. The results of this method are also questionable, due to the nature of contact, depth of energy penetration for extremely short exposure periods, the distance from the surface and the extrapolating technique.
3. The third general method is by means of radiation pyrometers which allow remote measurements of the surface temperature and do not require physical contact. This last method appears to be more feasible and is broadly classified in two groups: (a) optical pyrometers, which are instruments in which the brightness (for a narrow wavelength interval) of a hot object is visually compared to that of a source of standard brightness, and (b) radiation pyrometers, which measure the rate of energy emission per unit area over a relatively narrow range of wavelengths.

A pyrometer of the latter type was used for surface temperature measurement of samples used in the flames ignition cabinet. The instrument covered the range of incandescent and nonincandescent temperatures and also incorporated a sufficiently rapid response to permit measurement of rapidly

varying temperatures (surface temperature rises of 500 to 26,000 °C/min will occur). However, if an instrument of this type is employed, the optical properties of the samples must be clearly known or measured. Koohyar (14) used a similar setup in measuring the surface temperature rises of wood samples during the exposure period to flames radiation. Figure IV-37 presents Koohyar's data on the pilot ignition temperatures for five wood species. As shown a relatively constant band of ignition temperatures (290°C to 450°C) was obtained for the range of flame irradiance used. However, since this particular type of radiation pyrometer measures both the energy emitted by the hot surface and the energy reflected by the surface, it is necessary to know that portion of the energy emitted in order to determine surface temperatures associated with the measurement. Koohyar's data are further complicated by the fact that due to the close proximity of the flames to the irradiated surface, a grazing angle has to be used for viewing of the surface by the radiation pyrometer. Hence, the percentage of reflected energy may be quite different for different relative positions of the flames and the irradiated sample. Koohyar attempted to take this effect of variable reflectance into account by a computational technique. He indicated that the overall range of directional reflectance varied from 0.056 to 0.257 and used the expression

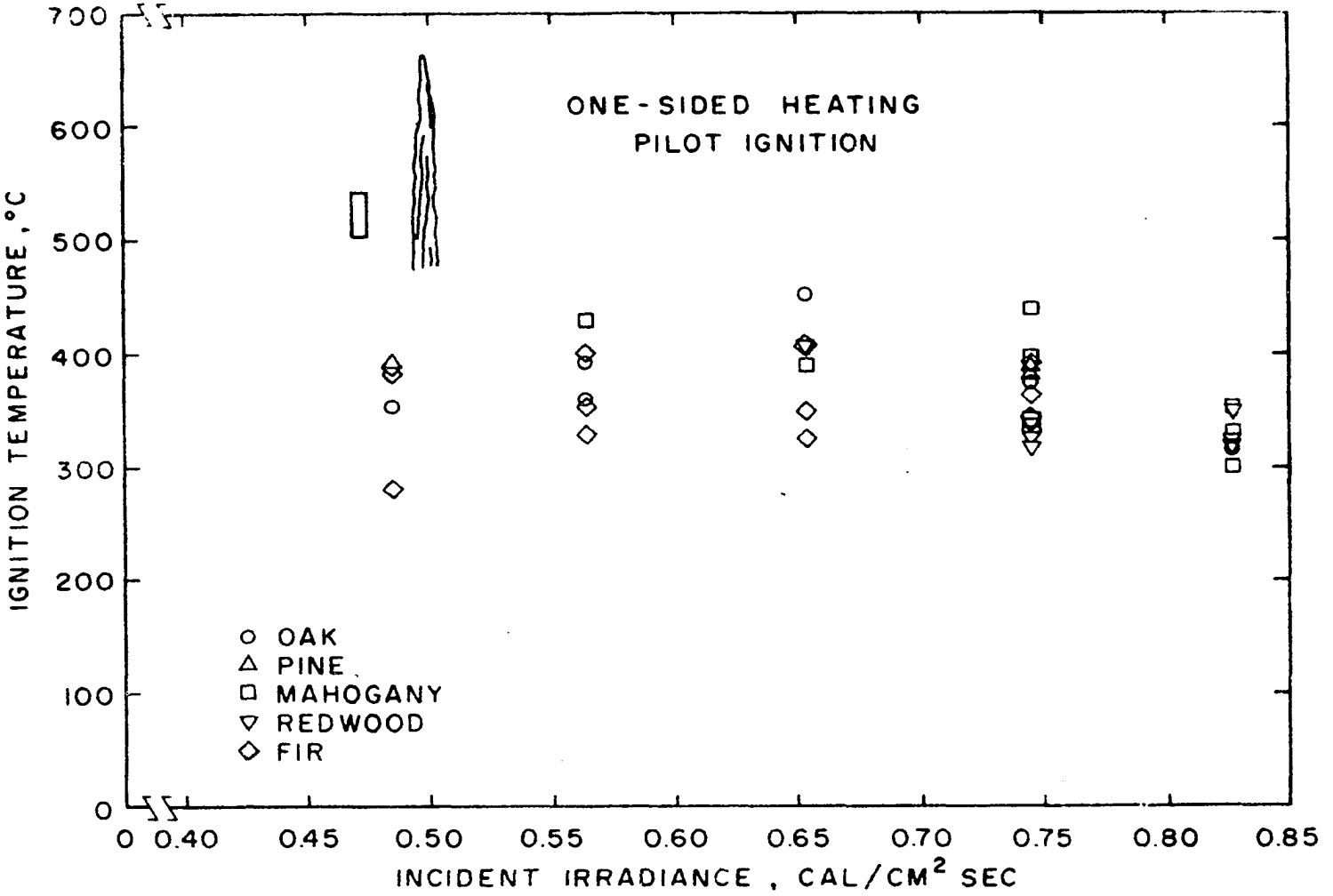

Figure IV-37. Ignition Temperature as a Function of Irradiance (One-Sided Heating, Piloted Ignition) (14).

$$\Delta T_s = \frac{2H}{K}\left(\frac{\alpha t}{\pi}\right)^{1/2} \qquad \text{(IV-52)}$$

in these computations. However, H in this expression is derived from a boundary condition which assumes that all the incident energy is absorbed. For the higher values of directional reflectance significant error might be introduced by using this method for calculating the temperature rise of the surface.

Subsequent to Koohyar's work, Smith (45) conducted ignition tests on natural and blackened pine and made surface temperature measurements during the exposure period using a similar technique. In his experiment Smith (45) used a tungsten filament lamp radiation source consisting of two holders and 16 1000-T3 tungsten filament quartz lamps (similar to the tungsten lamps used in the present investigations) and viewed normal to the irradiated surface by viewing between the two lamp holders. Smith used an Ircon Infrared Pyrometer which was sensitive only to wavelengths between 4.8 and 5.6 microns. Since the tungsten filament quartz lamps only pass radiation shorter than 3.5 microns, the Ircon pyrometer cannot "see" any of the significant direct lamp radiation, and hence is not affected by the reflected radiation from the lamps or wood samples. It

can, therefore, sense essentially only the radiation emitted by the hot specimen and can be used for fairly accurate surface temperature measurements during the exposure period. The measured surface temperatures versus time for incident irradiances of 2.25 to 0.75 cal/cm^2-sec are presented in Figures IV-38 through IV-42. As illustrated, the temperature-time history of the ponderosa pine is quite different for various incident irradiance levels. Hence, the average reradiated and convective cooling losses (based on the average temperature during the total exposure period) will be different for each incident irradiance. It is most interesting to note that these data also confirm the fact that the surface temperature at ignition is not constant but varies with incident irradiance and will likewise vary with the absorbed irradiance as will be shown later. This variation of ignition temperature with incident irradiance is shown in Figure IV-43. However, the very sharp rise in the ignition temperature below an incident irradiance level of 1.0 cal/cm^2-sec (from tungsten lamps) does not appear reasonable considering the ignition temperature variation above 1.0 cal/cm^2-sec. It appears reasonable to assume that this sharp rise could be due to the presence of "glowing ignition" prior to the appearance of "flaming ignition". This situation has been observed visually to exist at low irradiance

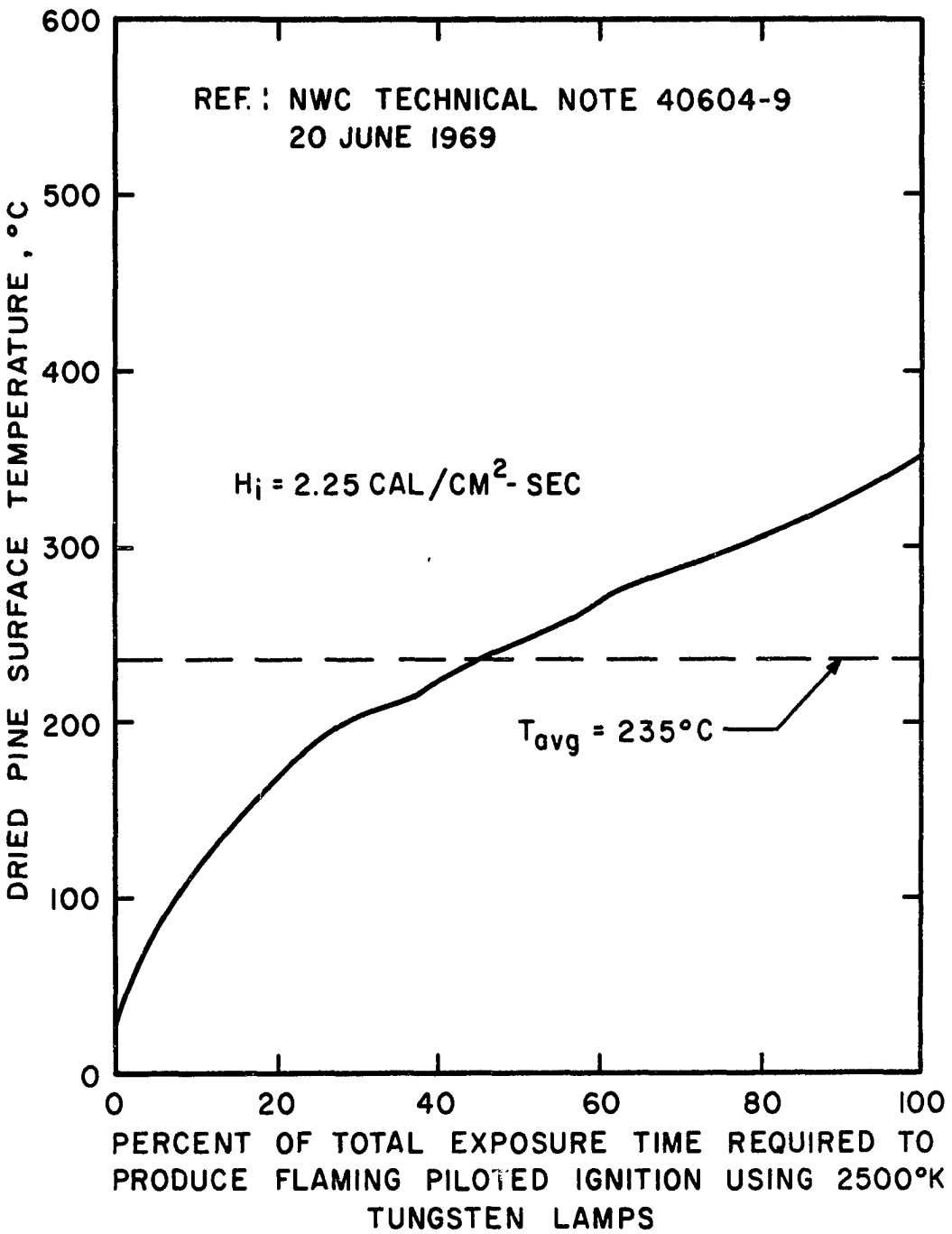

Figure IV-38. Surface Temperature of Ponderosa Pine During Exposure to Tungsten Lamps (H_i= 2.25 cal/ cm^2-sec).

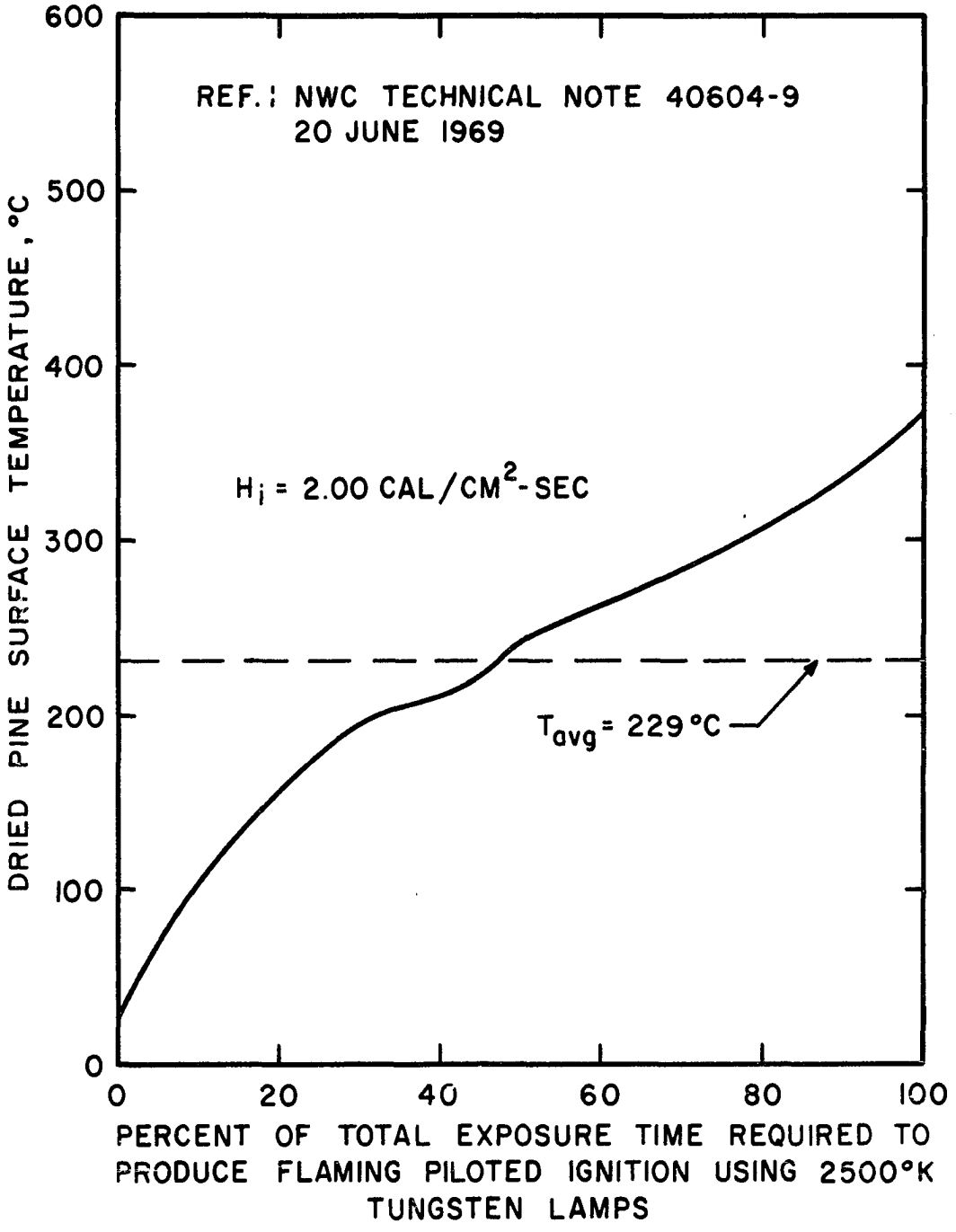

Figure IV-39. Surface Temperature of Ponderosa Pine During Exposure to Tungsten Lamps (H_i = 2.00 cal/cm^2-sec).

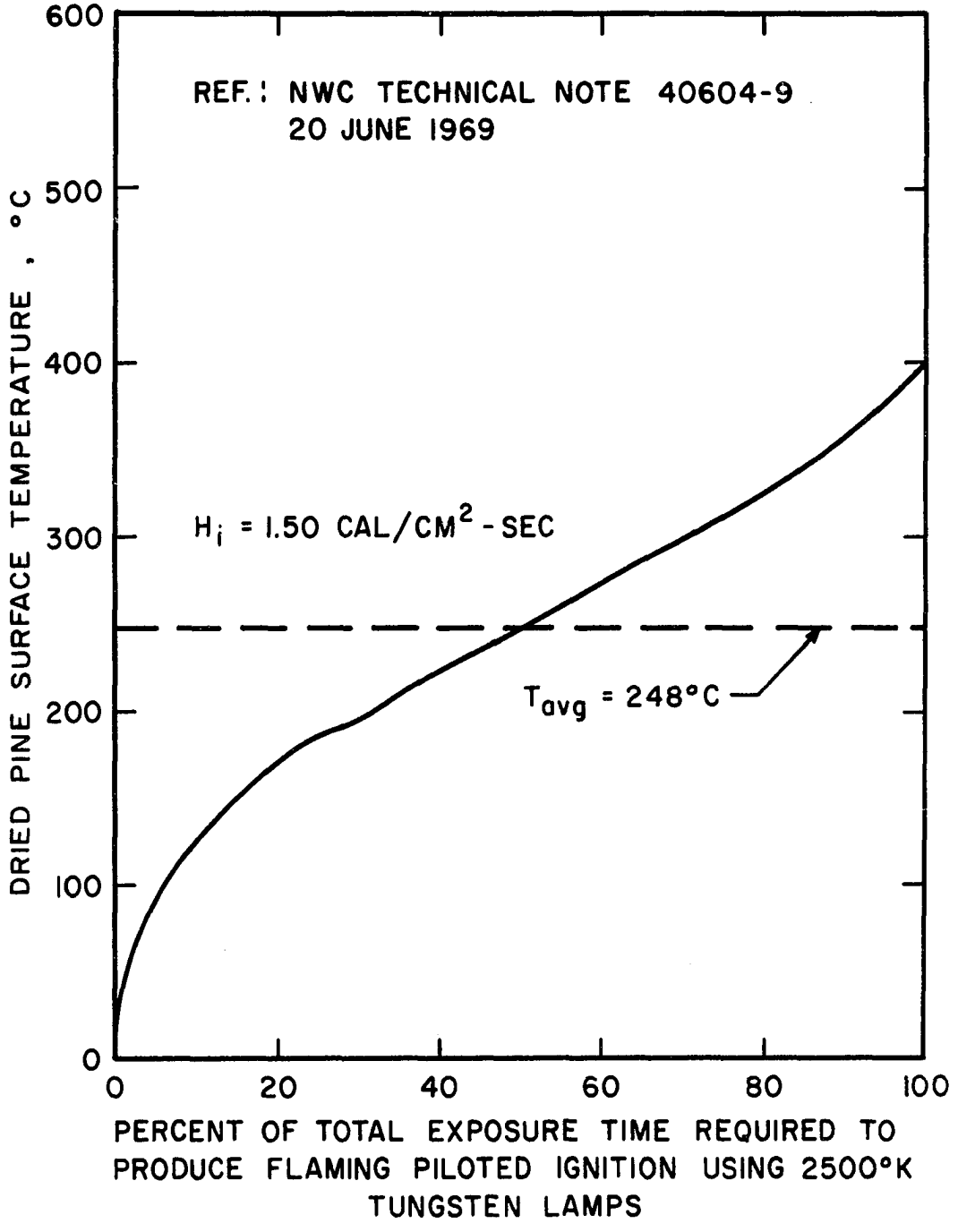

Figure IV-40. Surface Temperature of Ponderosa Pine During Exposure to Tungsten Lamps (H_i = 1.50 cal/cm^2-sec).

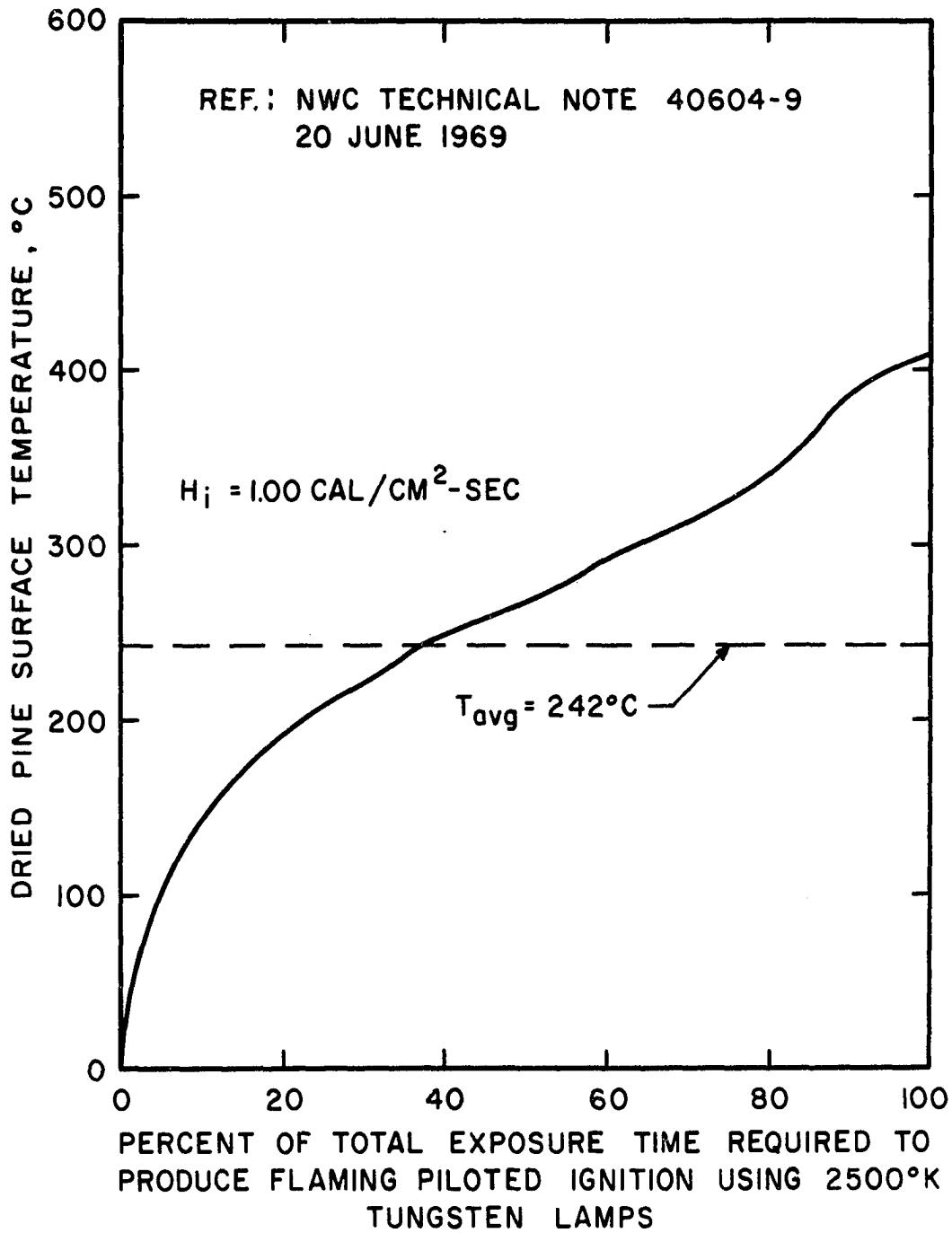

Figure IV-41. Surface Temperature of Ponderosa Pine During Exposure to Tungsten Lamps (H_i = 1.00 cal/cm^2-sec).

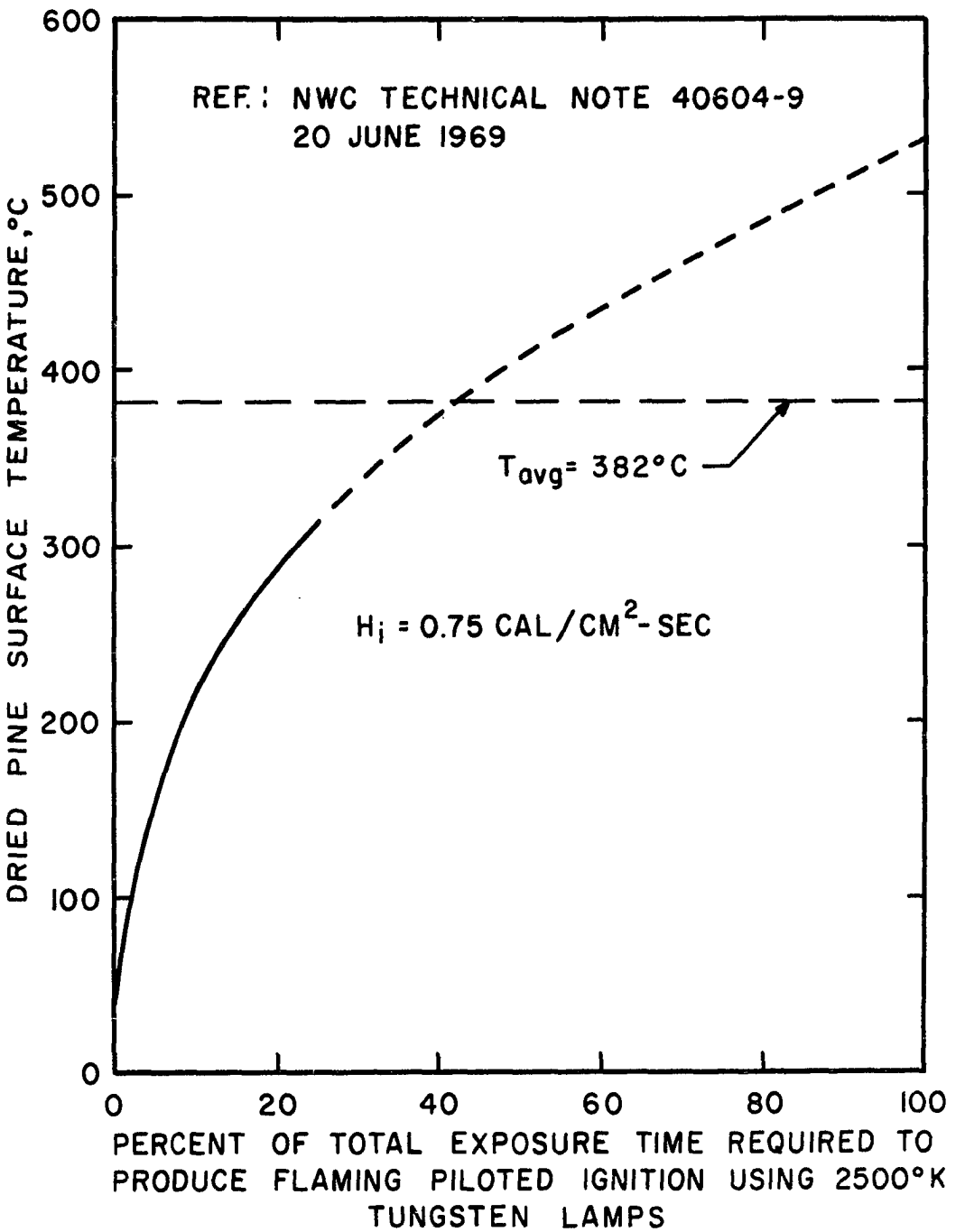

Figure IV-42. Surface Temperature of Ponderosa Pine During Exposure to Tungsten Lamps (H_i = 0.25 cal/cm^2-sec).

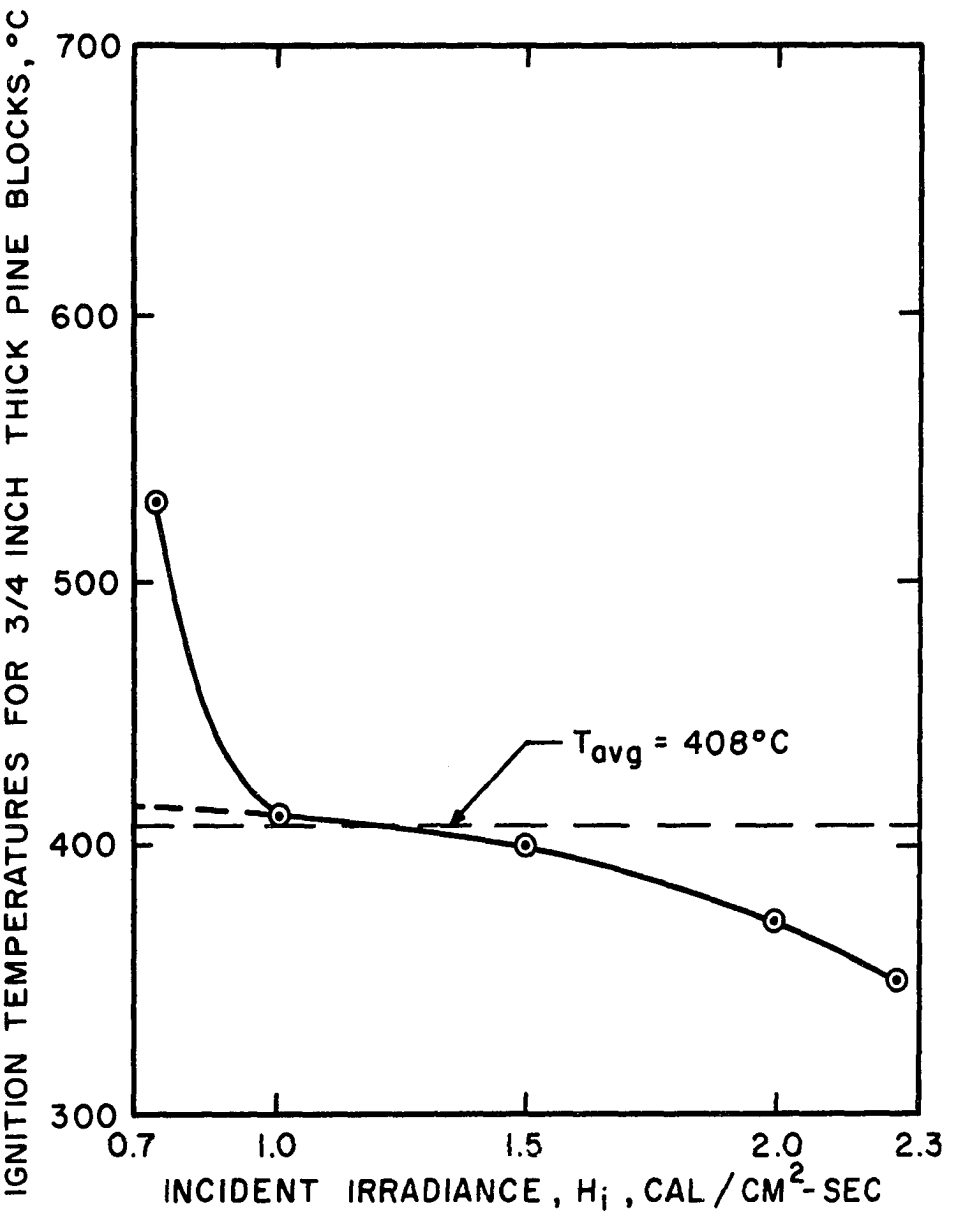

Figure IV-43. Ignition Temperatures of Ponderosa Pine using Tungsten Lamps.

levels using both flames and tungsten lamps in the ignition tests reported herein. Therefore, for the purposes of computing irradiated surface energy losses due to convective and reradiative effects the ignition temperatures below 1.0 cal/cm^2-sec were assumed to vary in accordance with the dashed extrapolated line shown in Figure IV-43 insofar as tungsten lamp irradiance is concerned.

Integration of the data presented in Figures IV-38 through IV-42 provided an integrated average surface temperature representative of the total exposure period for the specified range of tungsten lamp irradiances. These integrated average surface temperatures are presented in Figure IV-44. However, since these data were obtained by Smith with different ignition test apparatus than the ignition cabinet discussed herein, it is pertinent to compare Smith's ignition data on ponderosa pine with the present data on white pine. Tungsten lamps were used as radiation sources in both studies. Figure IV-45 presents this comparison with density corrections applied. As shown, using a density of 0.61 gm/cm^3 for ponderosa pine (29), excellent agreement of the two sets of independently determined experimental data resulted. It is, therefore, concluded that the surface temperature measurements as a function of exposure time, as determined by Smith (45) for ponderosa pine, may be applied to the wood species reported herein.

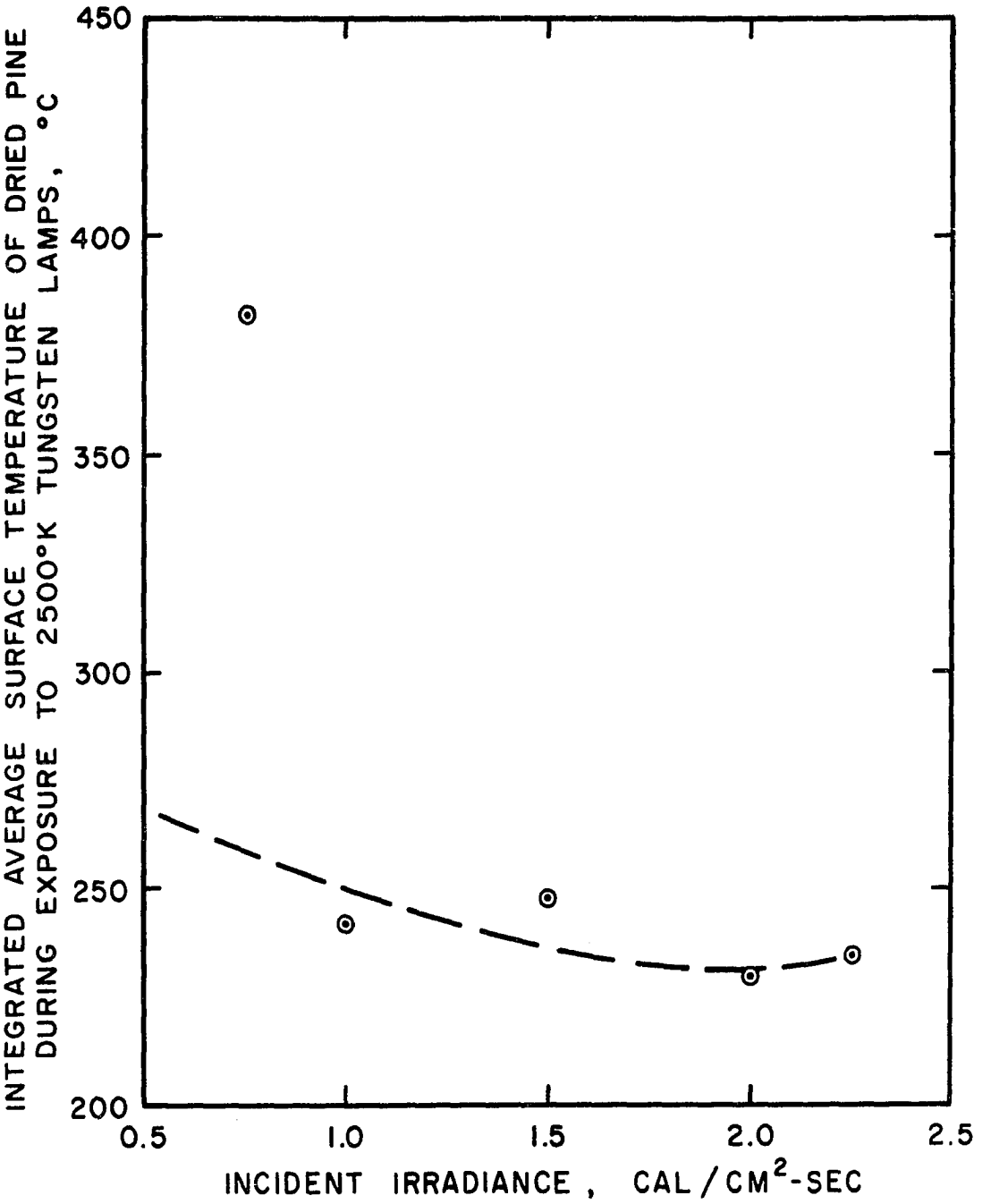

Figure IV-44. Integrated Average Surface Temperature for Ponderosa Pine Exposed to Tungsten Lamp Irradiance.

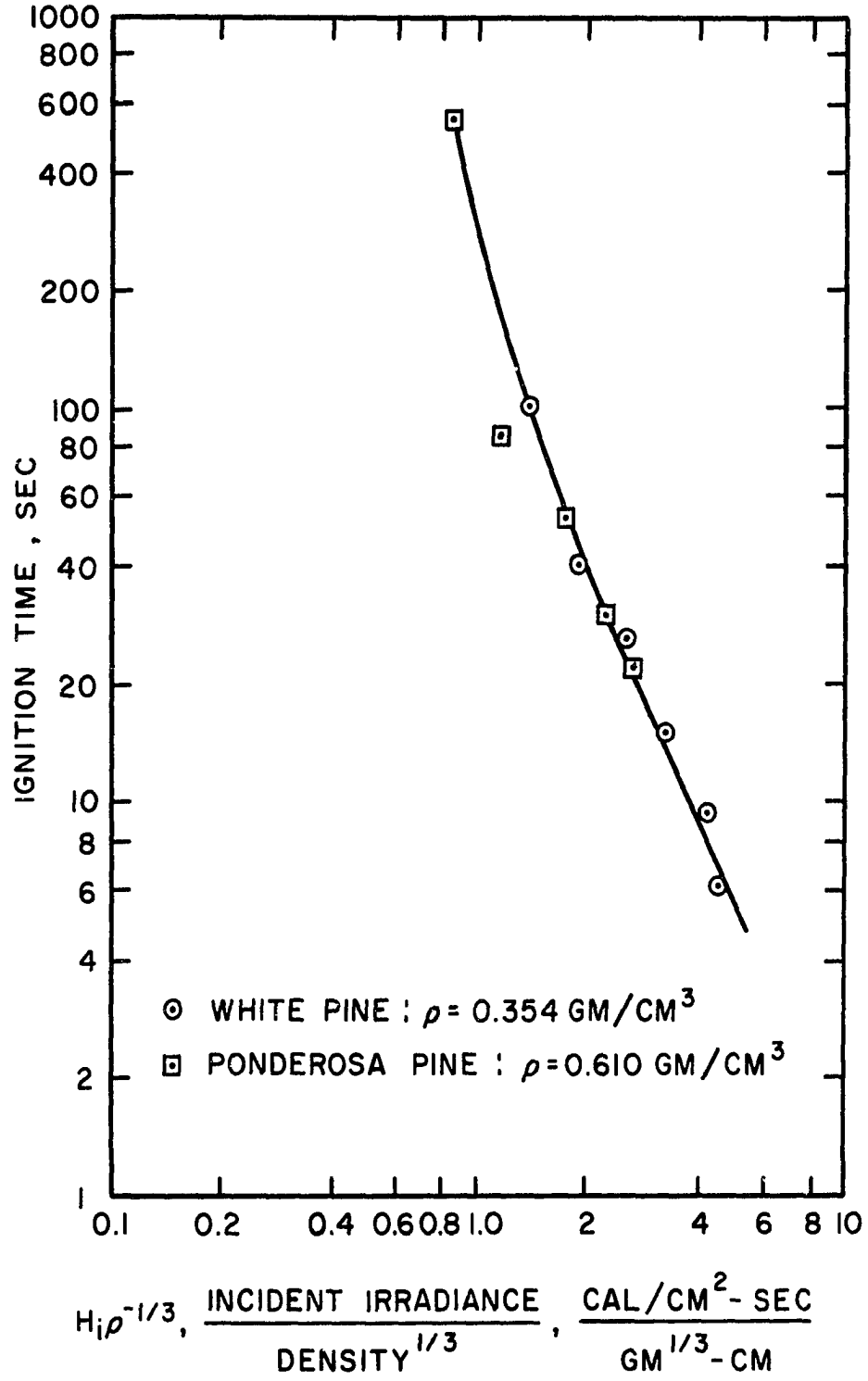

Figure IV-45. Comparison of Smith's (45) Ignition Test Results on Ponderosa Pine with OURI Results on White Pine using Equivalent Tungsten Lamps.

Before the irradiated surface energy losses can be evaluated numerically, it will be necessary to consider the effects of exposure time on the average absorptance factors and to convert the surface temperatures of Figure IV-44 from an incident irradiance basis to an absorbed irradiance. By virtue of this conversion the temperature data can be used with the ignition results obtained either from flames or tungsten lamps in this study.

Effects of Exposure Time on Average Absorptance Factors

As stated previously the failure of black-painted woods irradiated with tungsten lamps to fall within the otherwise generalized correlation of Figure IV-33 was attributed to the change in absorptance of the wood during the exposure period. To ascertain the magnitude of this change in absorptance, several samples of a representative species of wood were exposed for different time periods to preselected incident irradiance levels from both flames and tungsten lamps. Both natural finish and black-painted wood samples were employed. Utilizing the same equipment configurations and test procedures (see Appendix A) as those used for the unexposed wood samples, normal monochromatic reflectance data were obtained over the wavelengths of 0.3 to 2.1 microns. For the wavelength range of 2.1 to 6.0 microns, estimates from the data on unexposed wood samples

were used. Based on the conventional relationship for an opaque, diffuse reflecting surface the spectral absorptance characteristics were evaluated for each wood sample. Figure IV-46 presents the monochromatic absorptance characteristics of natural finished maple samples exposed for various time periods to an irradiance level of 1.65 cal/cm^2-sec from tungsten lamps. Similar data for irradiance levels of 1.04 and 0.5 cal/cm^2-sec are presented in Figures IV-47 and IV-48, respectively. Data for natural finished woods exposed for varying time periods to incident irradiances of 1.95, 1.25 and 0.75 cal/cm^2-sec from flames are presented in Figures IV-49, IV-50 and IV-51, respectively. Figures IV-34 and IV-52 present data for black-painted woods exposed to tungsten lamps and flame radiation, respectively.

As previously noted, the monochromatic absorptance for the black-painted woods decreased significantly with an increase in the tungsten lamp exposure time (see Figure IV-34). This result affirms the earlier premise that the black paint used to simulate a "blackbody" significantly decreased the wood ignition time due to an abnormally higher rate of energy absorption in the visible region of the spectrum.

A computer program based on the relationship

$$\bar{\alpha} = \frac{\Sigma \alpha_\lambda \; e_\lambda \; \Delta\lambda}{\Sigma e_\lambda \; \Delta\lambda} \qquad \text{(IV-3)}$$

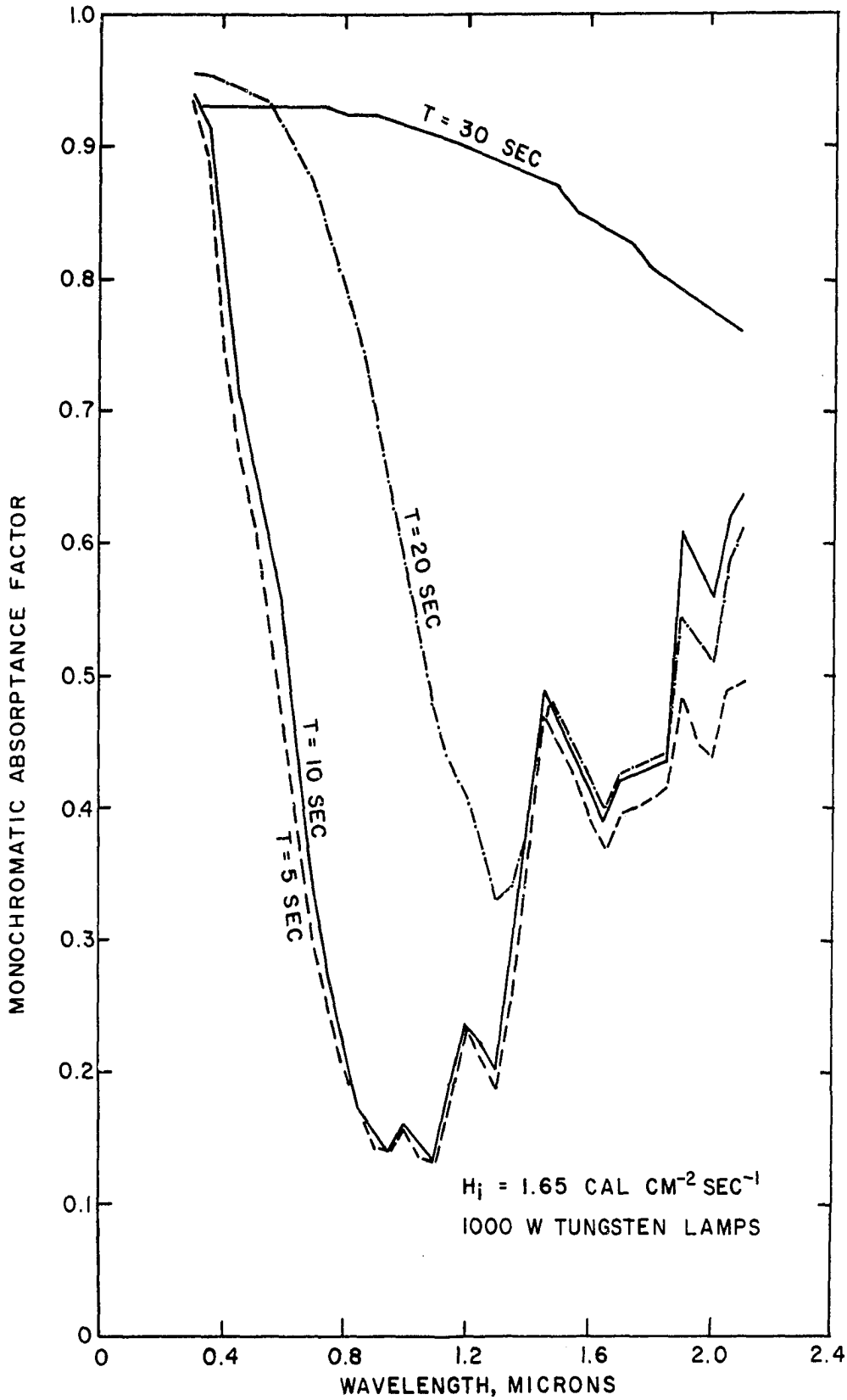

Figure IV-46. Monochromatic Absorptance of Natural Finish Maple Exposed for Varying Time Periods to Tungsten Lamp Irradiance.

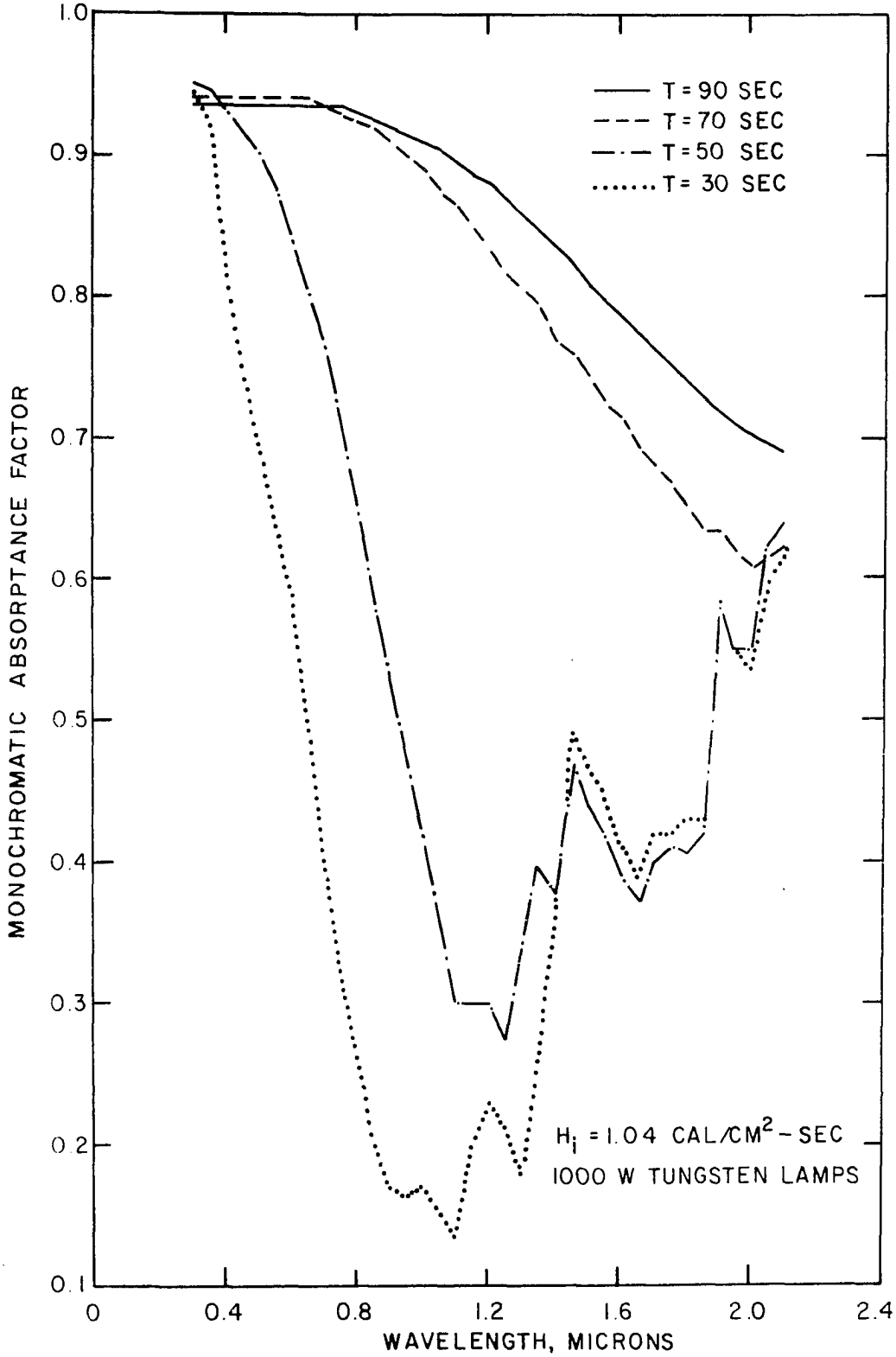

Figure IV-47. Monochromatic Absorptance of Natural Finish Maple Exposed for Varying Time Periods to Tungsten Lamp Irradiance.

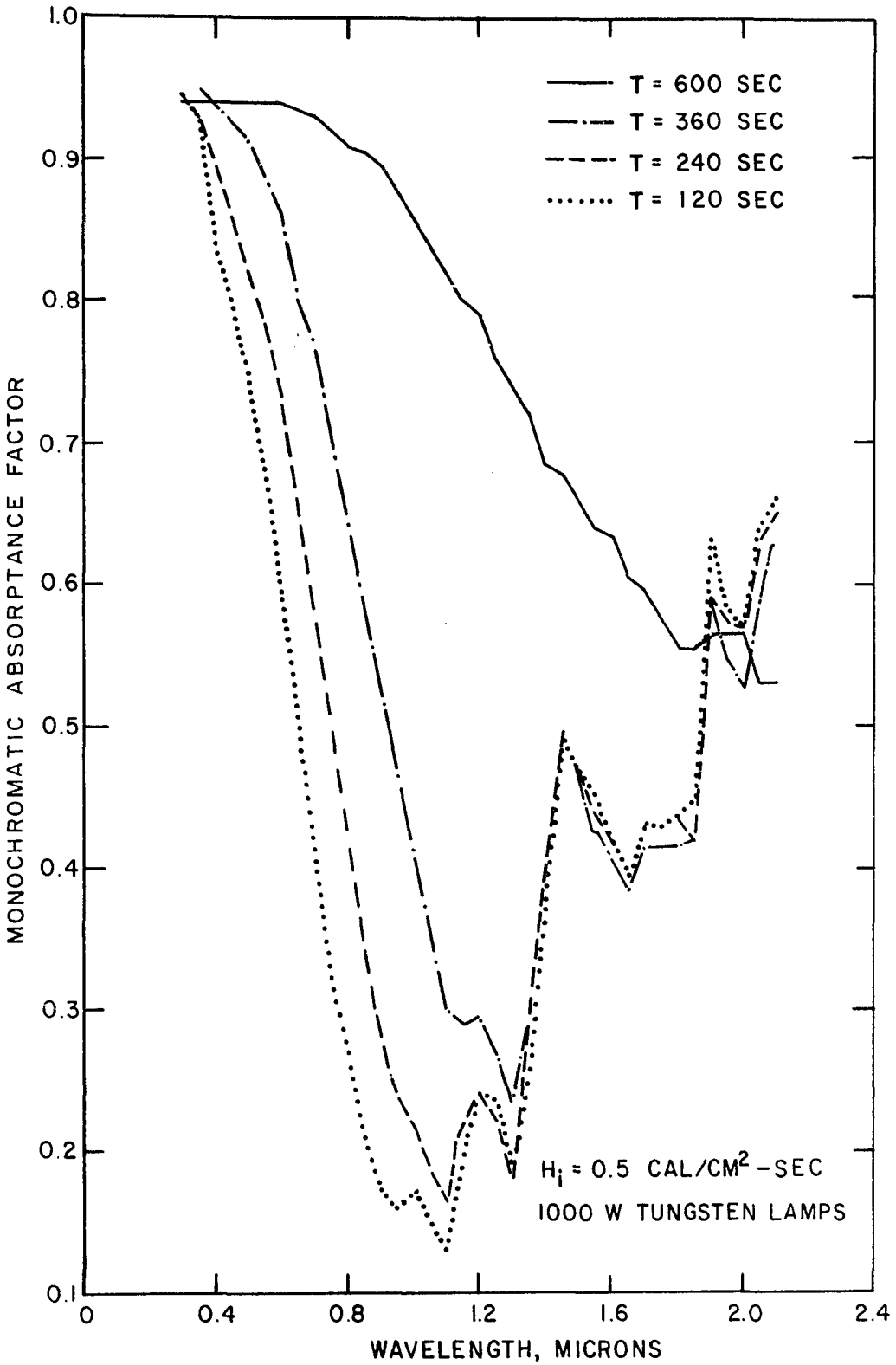

Figure IV-48. Monochromatic Absorptance of Natural Finish Maple Exposed for Varying Time Periods to Tungsten Lamp Irradiance.

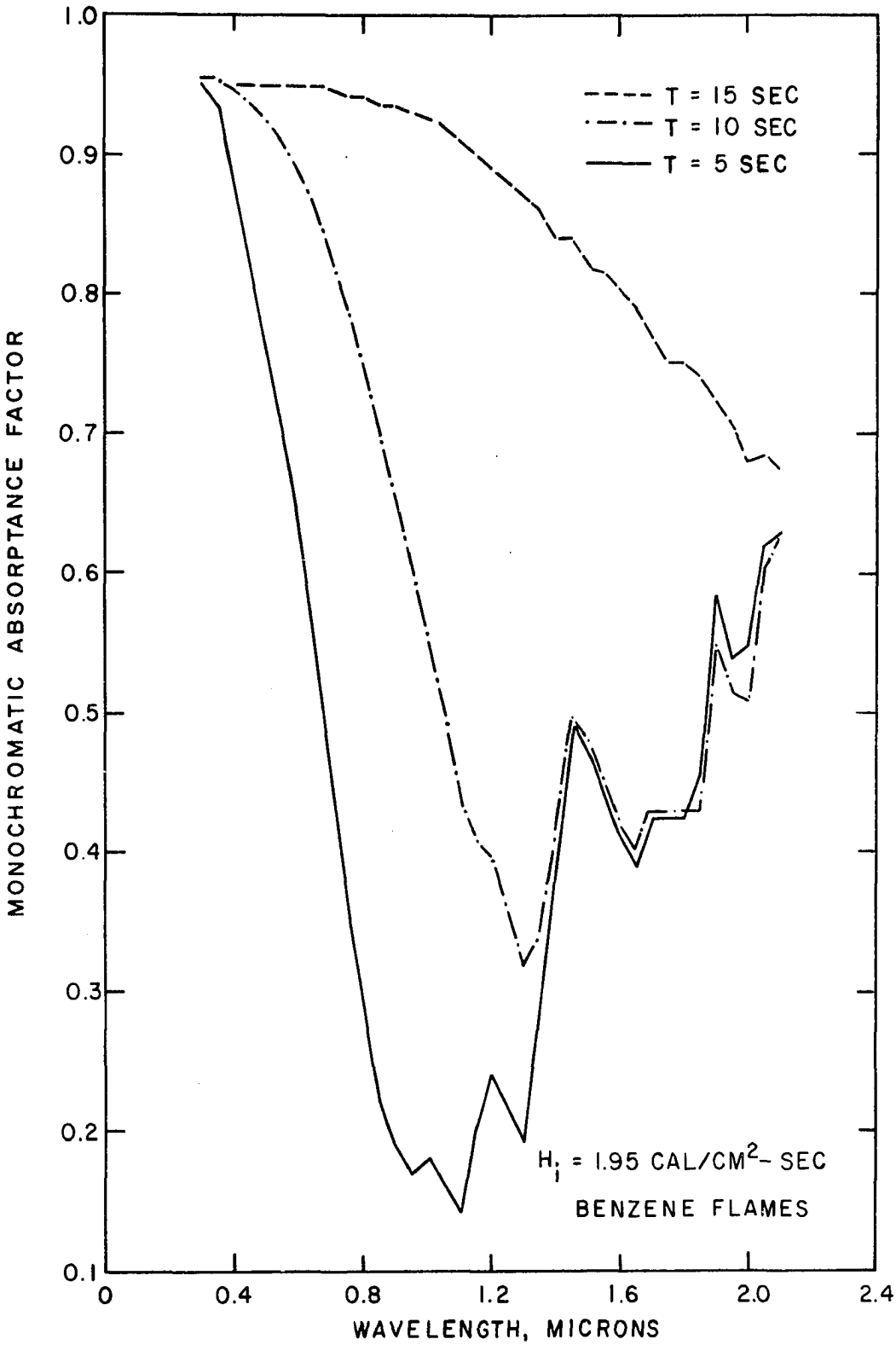

Figure IV-49. Monochromatic Absorptance of Natural Finish Maple Exposed for Varying Time Periods to Flame Irradiance.

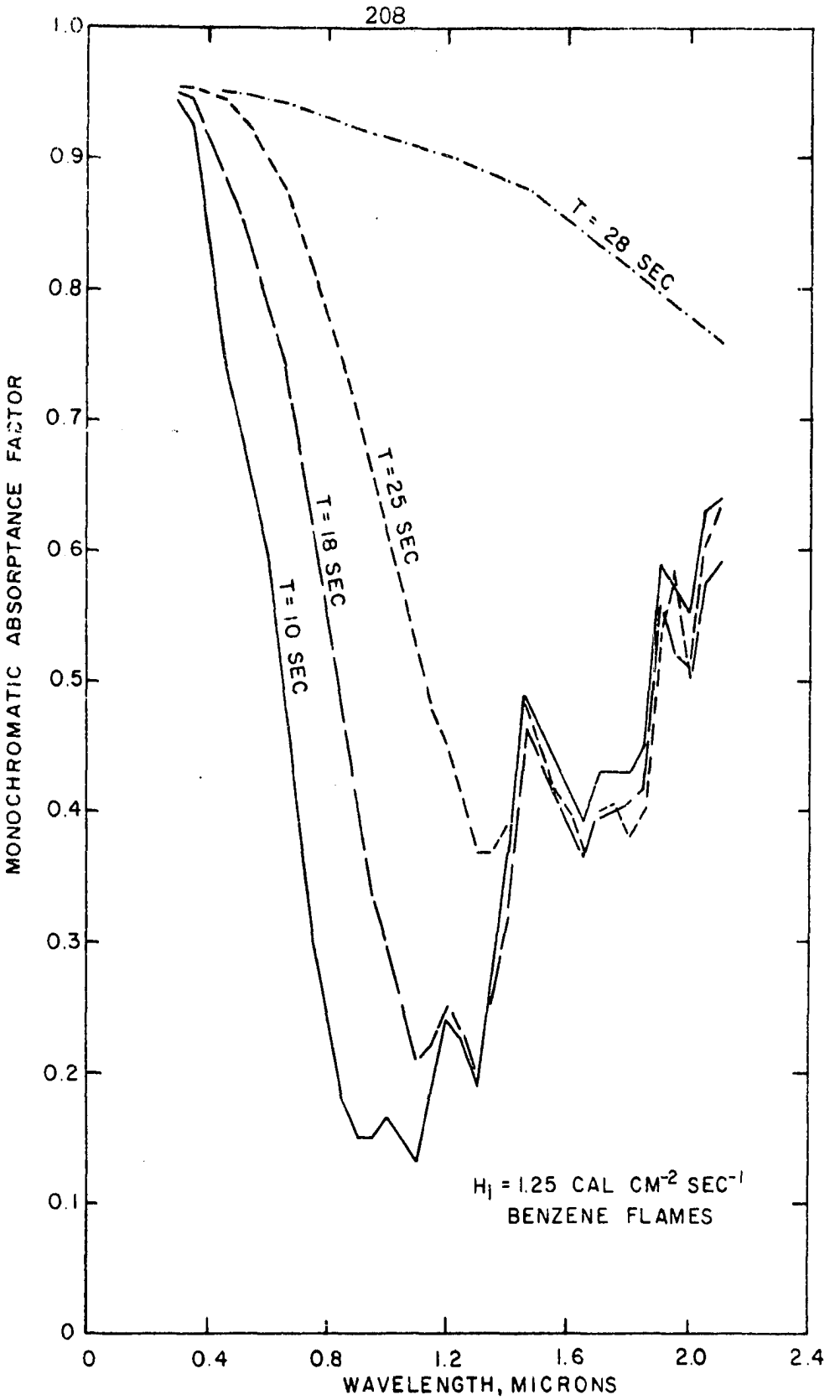

Figure IV-50. Monochromatic Absorptance of Natural Finish Maple Exposed for Varying Time Periods to Flames Irradiance.

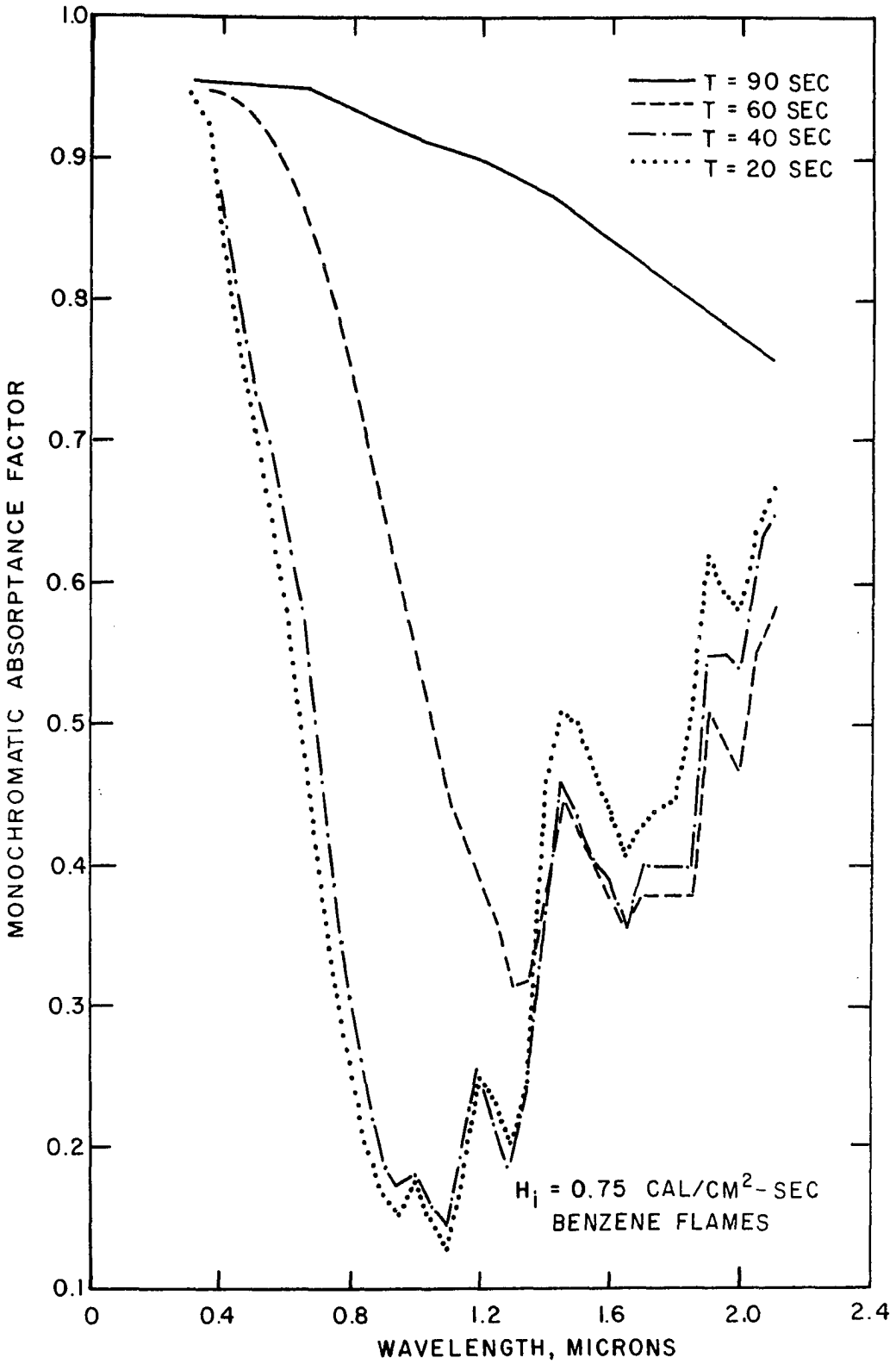

Figure IV-51. Monochromatic Absorptance of Natural Finish Maple Exposed for Varying Time Periods to Flames Irradiance.

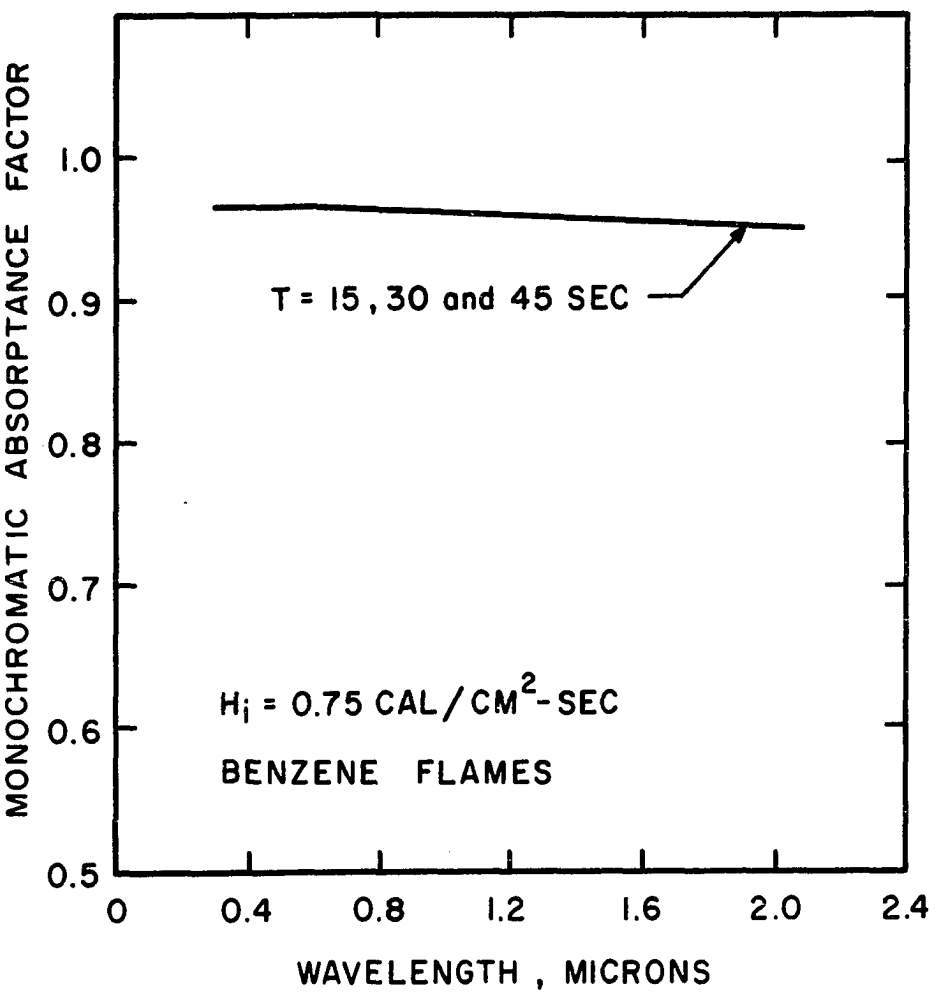

Figure IV-52. Monochromatic Absorptance of Black Painted Oak Exposed for Varying Time Periods to Flames Irradiance.

was then used to obtain the average absorptance factor for each wood sample. A valuable by product of these computations was the generation of average absorptance factors for natural finish woods exposed to a range of incident irradiances which can be represented by equivalent blackbody temperatures between 500°C and 3500°C as presented in Figure IV-53.

The average absorptance factors of the individual wood samples were then correlated as a function of percent of total exposure time to produce ignition. Figure IV-54 presents these data for natural finished woods exposed to tungsten lamp radiation. The results confirm those anticipated earlier based on qualitative visual observations. Thus, the natural surface gradually darkens to a char condition and remains in this state for a short time period prior to the appearance of flaming ignition. Integration of the data of Figure IV-52 then provided the integrated average absorptance factors, representative of the transient period from initial exposure to ignition. As noted, natural finished maple has an average absorptance factor, $\bar{\alpha}$, 0.44 in its unexposed state and an integrated average absorptance factor, $\bar{\bar{\alpha}}$, of 0.595 for the exposure period using tungsten lamp radiation. This change represents an increase of some 35 percent in absorbed irradiance.

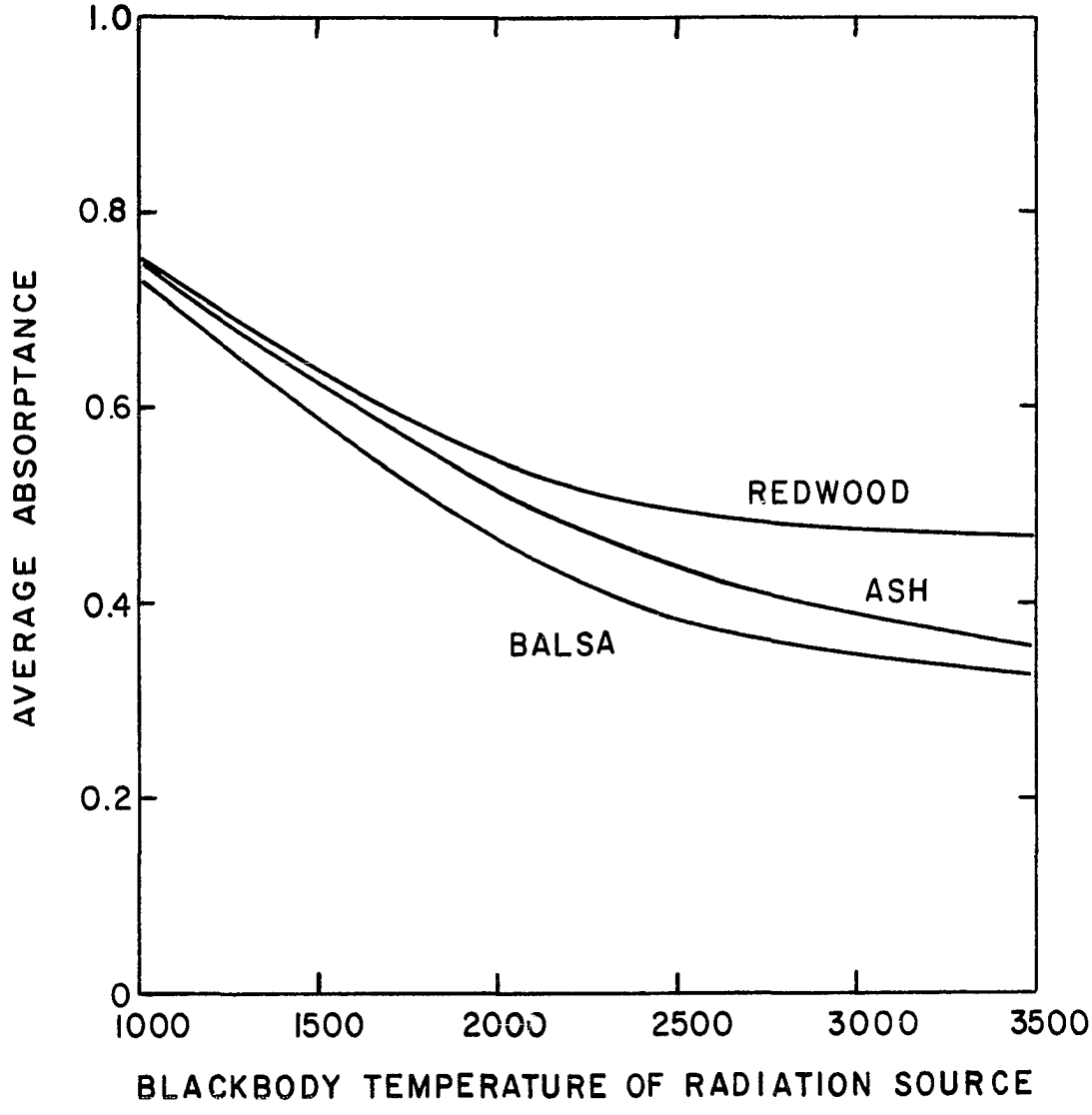

Figure IV-53. Average Absorptance Factors for Natural Finish Woods as a Function of Equivalent Blackbody Incident Irradiances.

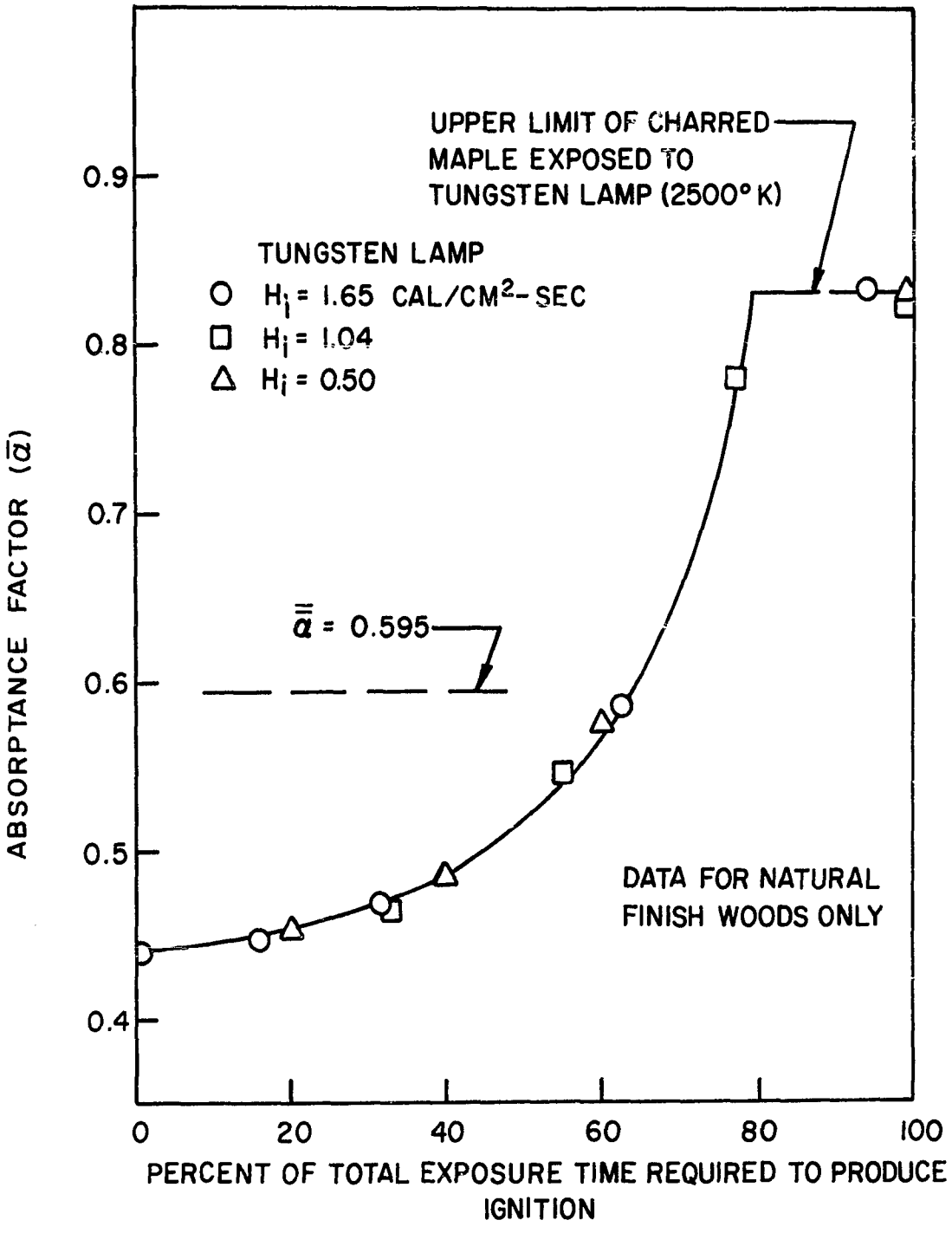

Figure IV-54. Variation of Maple Wood Integrated Absorptance Factor During the Exposure Period to Tungsten Lamp Irradiance.

Data for the natural finish maple exposed to flame radiation are presented in Figure IV-55. The average absorptance factor increases from 0.765 to 0.823, an increase of only 8 percent during the exposure period. It is interesting to point out that the related ratios of the percentage increase in absorptance factors, 3 5/8 or approximately 4:1, is virtually the same as the earlier observed ratio of ignition times for tungsten lamp and flame radiation.

Figure IV-56 presents the variation of the average absorptance factors for the black-painted wood samples exposed to tungsten lamp and flame radiation.

To apply the data of Figures IV-55 and IV-56 to the present analysis it is necessary to assume that the percentage increase in the average absorptance factors due to the exposure period, as determined experimentally for conditioned maple, are applicable to the other species of wood tested. In view of the excellent agreement obtained in the previously discussed data correlations considering ignition time, sample physical and thermal properties and the unexposed average absorptance factors, any deviation due to this assumption should be quite small. Consequently, values for the integrated average absorptance factors for the exposure period were calculated; the results are given in Table IV-5. For any one type of incident irradiance

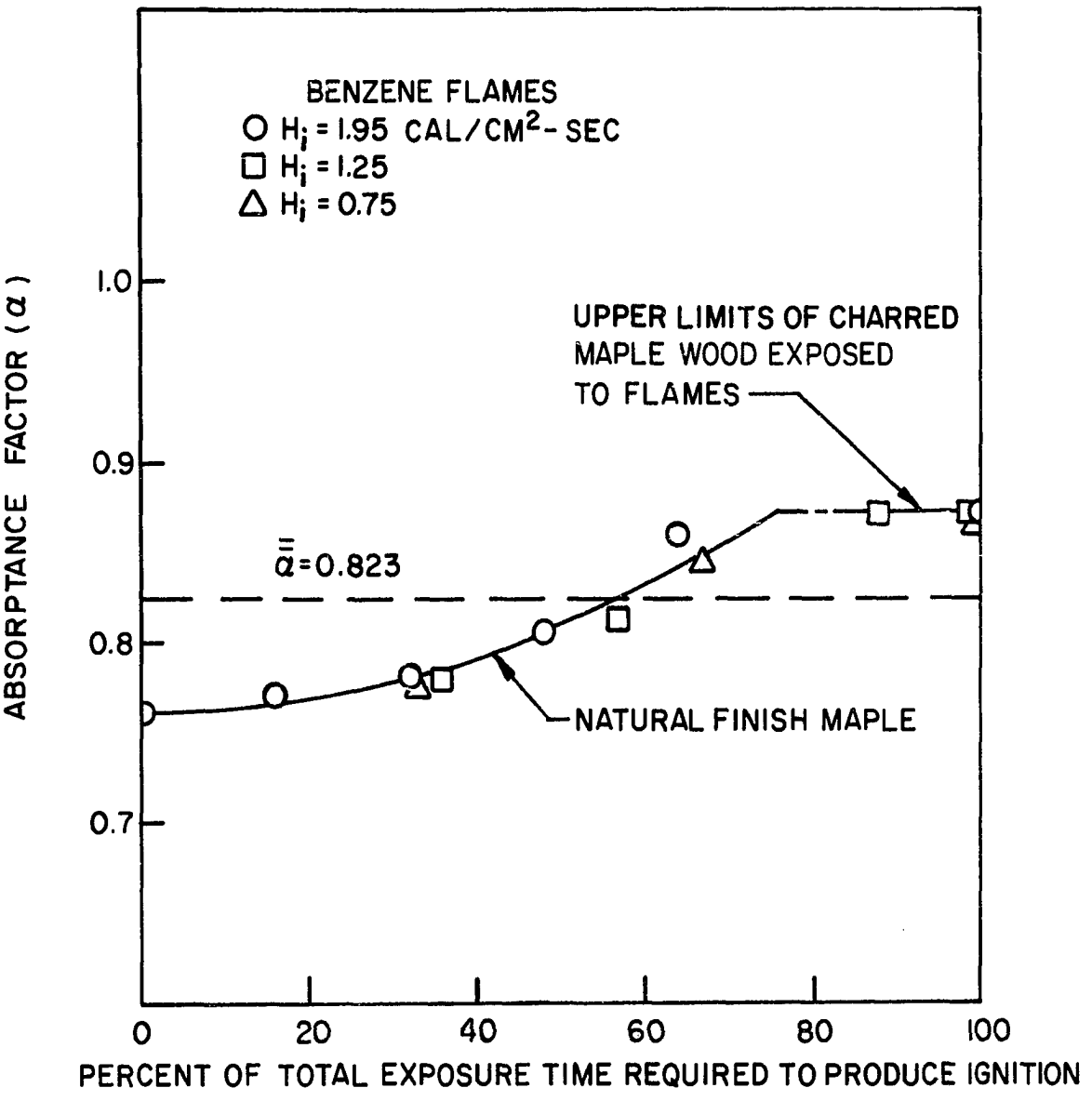

Figure IV-55. Variation of Natural Finish Maple Integrated Absorptance Factor During Exposure to Flames Irradiance.

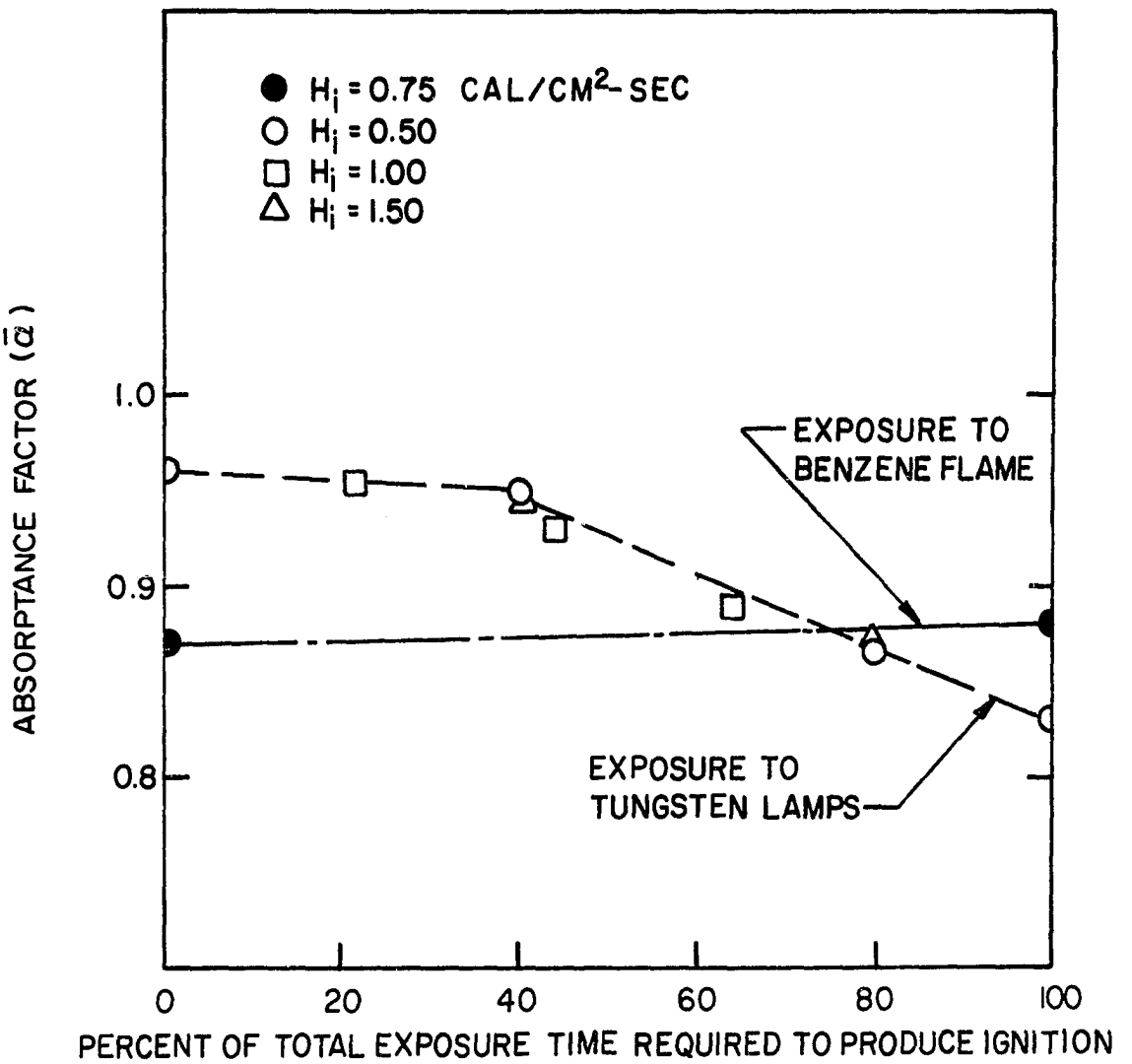

Figure IV-56. Variation of Black Painted Oak Integrated Absorptance Factor During Exposure to Different Irradiance Sources.

TABLE IV-5

CALCULATED VALUES FOR WOOD AVERAGE ABSORPTANCE FACTORS INTEGRATED OVER THE EXPOSURE PERIOD

Type of Wood	Time Integrated Average Absorptance Factors			
	Flame Radiation		Tungsten Lamp Radiation	
	Natural Finish	Black-Painted Finish	Natural Finish	Black-Painted Finish
Cottonwood	0.818	0.872	0.650	0.850
Mahogany	0.826	0.872	0.668	0.850
Balsa	0.810	0.872	0.551	0.850
Cedar	0.818	0.872	0.595	0.850
Redgum	0.825	0.872	0.712	0.850
Maple	0.820	0.872	0.655	0.850
Spruce	0.825	0.872	0.590	0.850
Ash	0.825	0.872	0.626	0.850
Redwood	0.820	0.872	0.690	0.850
Minsonia	0.818	0.872	0.630	0.850
White Pine	0.830	0.872	0.660	0.850
Oak	0.833	0.872	0.765	0.850
Birch	0.831	0.872	0.636	0.850
Masonite	0.808	0.872	0.710	0.850

and initial surface condition (natural or black-painted) there is relatively little variation in the values for the woods. However, between flames and tungsten lamp radiation a major difference still occurs, as would be expected.

Magnitude of Irradiated Surface Energy Losses

The integrated average absorptance factors for tungsten lamp radiation (Table IV-5) and the integrated average surface temperature data (Figure IV-44) can be combined to obtain the integrated average surface temperatures

as a function of the integrated average absorbed irradiance $(\bar{\alpha} H_i)$. This surface temperature can then be used to evaluate the irradiated surface convective and reradiated cooling losses that are representative of the entire exposure period. These time averaged losses as a function of the time averaged absorbed irradiance are presented in Figure IV-57.

Retained Irradiance Correlation

Combining the irradiated surface energy losses of Figure IV-57 and the time-dependent (during exposure) average absorptance factors of Table IV-5 with the results of Figure IV-33 leads to the final data correlation (based upon the actual retained irradiance) presented in Figure IV-58. This correlation adequately confirms the conclusion that the ignition characteristics of woods may be expressed as a function of only the retained irradiance, density and sample thickness. Nevertheless, the correlation of Figure IV-33, which is uncorrected for irradiated surface losses (note that the incident irradiance and unexposed average absorptance factors rather than retained irradiance is used) is more practical for prediction purposes since considerably less input data are required.

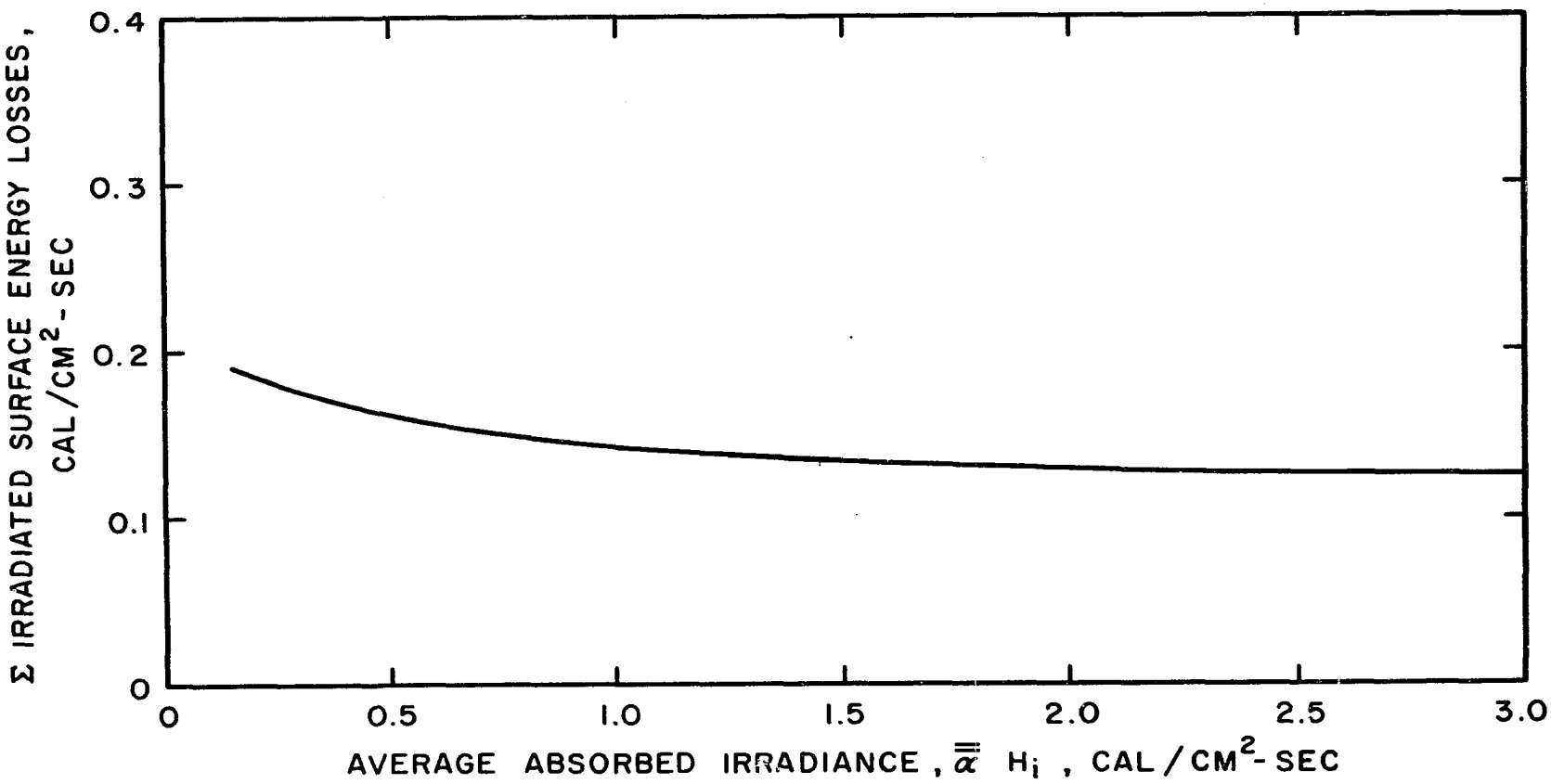

Figure IV-57. Average Irradiated Surface Total Energy Losses Due to Convective and Re-radiative Cooling Effects using Reported Test Data (45) on Surface Temperature Measurements During Exposure to Tungsten Lamps and Time Averaged Absorptance Factors.

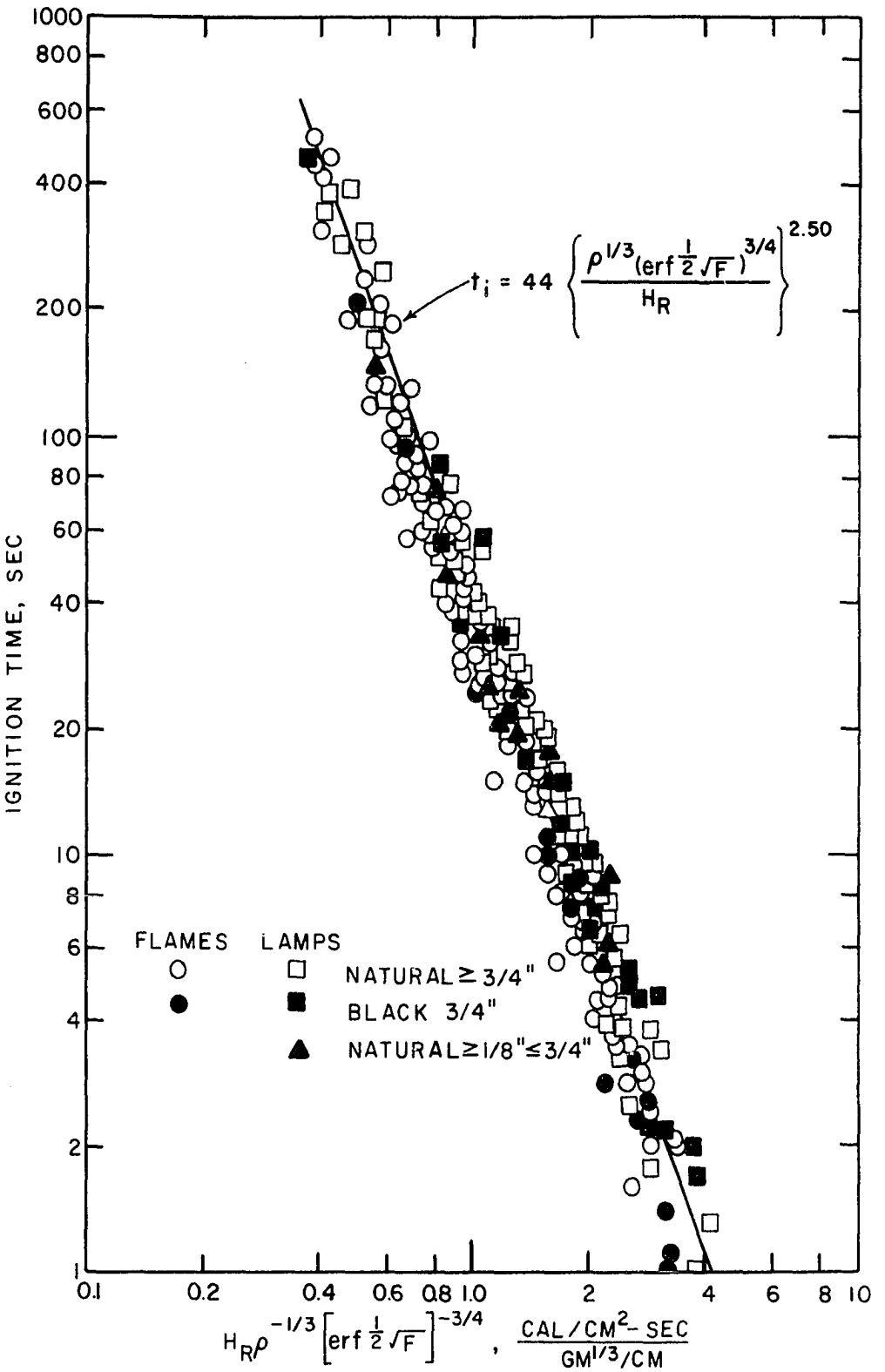

Figure IV-58. Correlation of Ignition Data on a Retained Energy Basis with Corrections for Density and Thickness Effects.

CHAPTER V

SUMMARY AND CONCLUSIONS

This study constitutes the first reported experimental investigations on ignition phenomena in which the effects of material thermal properties, physical properties such as density and thickness, and energy absorptance characteristics associated with different sources of incident radiation were investigated in detail. The study also included an investigation of the transient behavior during the exposure period up to the time of flaming ignition at the irradiated surface. The oven-dried wood samples were subjected to radiation from liquid hydrocarbon pool fires and from tungsten filament quartz lamps operating at 2500°K. The sample densities ranged from 0.07 to 1.08 gm/cm^3 and the sample thicknesses varied from 0.24 to 2.54 cm.

The spectral reflectance characteristics of the samples were determined for un-exposed conditions as well as for several different time periods of the total exposure for both radiation sources (flames and tungsten lamps). The spectral emissive characteristics of the incident radiation

were obtained from the literature. The level of incident irradiance varied from 0.5 to 3.50 cal/cm^2-sec and the ignition times ranged from less than one second to over 500 seconds. The incident irradiance was recorded continuously. The thermal and physical properties of the samples were determined experimentally. Sample ignition times were determined from a continuous chart speed-length relationship from a photoconductive cell device which could view products leaving the irradiated surface.

Surface temperature measurements throughout the exposure period by others (45) on dried ponderosa pine samples exposed to tungsten lamp radiation were shown to be generally applicable to this study. These data indicate that the measured surface temperature at ignition varies somewhat with the level of incident irradiances, decreasing with increasing irradiance levels. However, the reported surface temperatures at ignition were assumed to be relatively constant (approximately 410°C) for analysis purposes. This temperature is in good agreement with the characteristic temperature of 420°C which Havens (13) reported as the temperature at which the decomposition heat effects in pine woods exposed to a heating rate of 20°C/min had decayed to essentially zero.

An analysis based on heat conduction in an infinite, inert, and opaque slab with the initial conditions that for all x, $T = T_o$, and the boundary conditions

$$t > 0;\ x = L;\ H = -K\frac{\partial T}{\partial x} \qquad \text{(V-1)}$$

$$t > 0;\ x = \ ;\ \frac{\partial T}{\partial x} = 0 \qquad \text{(V-2)}$$

indicated that the ignition time, t_i, could be functionally expressed as

$$t_i = B \left[\frac{\rho^a (\text{erf}\ \frac{1}{2\sqrt{F}})^b}{H_i^c}\right] \qquad \text{(V-3)}$$

for a specified type of radiation and an assumed constant surface ignition temperature. The experimental data adequately confirmed this conclusion. Correlation of the test data on an initially absorbed irradiance basis ($\bar{\alpha}H_i$), neglecting the irradiated surface energy losses due to convection and re-radiation, confirmed this functional relationship and showed that the ignition times can be expressed as

$$t_i = 35 \left[\frac{\rho^{0.9} (\text{erf}\ \frac{1}{2\sqrt{F}})^{1.2}}{(\bar{\alpha}H_i)^{2.8}}\right] \qquad \text{(V-4)}$$

except for the black-painted wood exposed to tungsten lamp radiation. It was showed that this lack of agreement, for black-painted wood exposed to tungsten lamp radiation, with the generalized correlation was due to the fact that the black paint had a higher absorptance than does charred wood.

Hence the average absorptance decreased during exposure to radiation rather than increasing, as would be the real case for very dark woods.

The most significant conclusions regarding the correlation expressed by Equation V-4 are:

1. The pilot ignition time of dry woods is inversely proportional to approximately the cube of the absorbed irradiance. The difference in dependence from an inverse square relationship is most likely due to neglecting convection and re-radiation in the theoretical model.
2. The ignition time depends very strongly on the spectral distribution of the incident irradiance. In general, natural finished woods reflects radiation from about 0.6 μ to 2.0 μ quite efficiently, but absorbs radiation at longer wavelengths. The average absorptance for flame radiation is about 0.76, whereas for tungsten lamps at 2500°K the average absorptance is about 0.48. This difference accounts for the observed fact that ignition of wood by radiation from tungsten lamps takes about 4 times as long as for radiation from flames at the same incident irradiance.

3. The ignition time is approximately proportional to wood density.
4. The effect of sample thickness on ignition time can be accounted for by means of the error function of the Fourier modules.

Even though the experimental data gave a good correlation on an initially absorbed irradiance basis, neglecting the irradiated surface convective and re-radiative losses, these energy losses can become a relatively large percentage of the initially abosrbed irradiance, especially at moderate to low irradiance levels. However, it was also concluded that the same functional form of Equation V-3 would apply for correlating on a retained energy basis if the irradiated surface convective and re-radiative losses were accounted for. Figure IV-58 leads to the relationship

$$t_i = 44 \left\{ \frac{\rho^{0.8} \left(\operatorname{erf} \frac{1}{2\sqrt{F}}\right)^{1.07}}{H_R^{2.5}} \right\} \qquad \text{(V-5)}$$

where H_R is the retained irradiance integrated over the entire exposure period which accounts for the integrated average surface energy losses.

Additional significant conclusions are:

5. The correlation of Equation V-5 accounts for all the experimental data including the data on

black-painted woods exposed to tungsten lamp radiation which was excluded from the correlation of Equation V-4 on initially absorbed irradiance. Thus, the correlation of Equation V-5 is more general since it can be used for those instances wherein the average absorptance factors are both increasing and decreasing as a result of exposure to radiation in general. The correlation of Equation V-5 also provides a better understanding of the actual total distribution of the incident radiation and is of value in studies on thermal decomposition of wood and allied problems where the energy distribution within the sample could be of great importance.

Based on the results reported by Muir (32) which showed that ignition times of ordinary painted wooden structures did not differ significantly from un-painted structures, and in view of the good correlation obtained by Equation V-4 (initially absorbed irradiance correlation) it is recommended that it be used for wood ignition predictions since the input data requirements are considerably less than those required by Equation V-5.

Equation V-5 should be used for analysis wherein the actual retained energy is required or where the wood finish is such that it would significantly influence the reflected energy distribution.

6. It should be emphasized that the good agreement between the correlation of white pine ignition data on an initially absorbed energy basis and the Appendix C-Model 1 prediction is due solely to the fact that the experimentally determined density correction, the experimentally determined thickness correction and the experimentally determined surface ignition temperature had to be known before the model could be used. The agreement merely affirms that once these necessary and vital input data are known, the model is useful. Without these data, the model is of limited value.

APPENDIX A

EXPERIMENTAL DETERMINATION OF THE MONOCHROMATIC REFLECTANCE PROPERTIES OF WOOD SAMPLES

During the preliminary analyses of the wood ignition data reported in the literature and the initial test data obtained on the cotton fabrics, it was determined that the absorptance characteristics of the various surface-energy source would significantly influence the ignition time results. This observation indicated that the total absorptance factor for each configuration would be a necessary parameter in any ignition system.

It is well known that different energy sources have different emissive capabilities of different wavelengths. Figures A-1 and A-2 are graphic illustrations of solar spectral irradiance, hexane flame spectral irradiance and tungsten lamp emissive power as a function of wavelength. As shown, the three energy sources have irradiance of quite different magnitudes; the maximum energy level of the

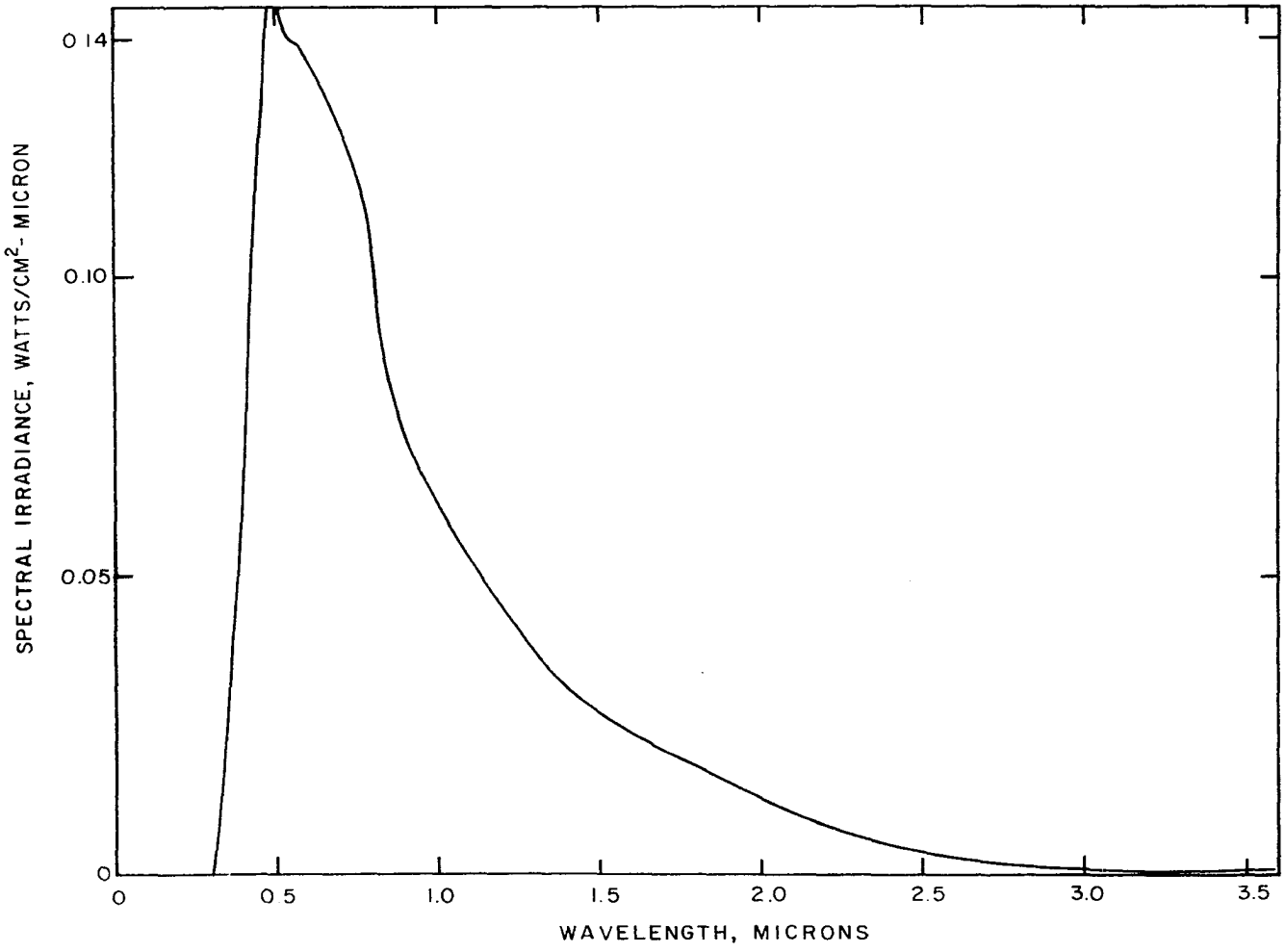

Figure A-1. The Relationship of Solar Spectral Irradiance Radiation With Wave Length At The Earth's Surface.

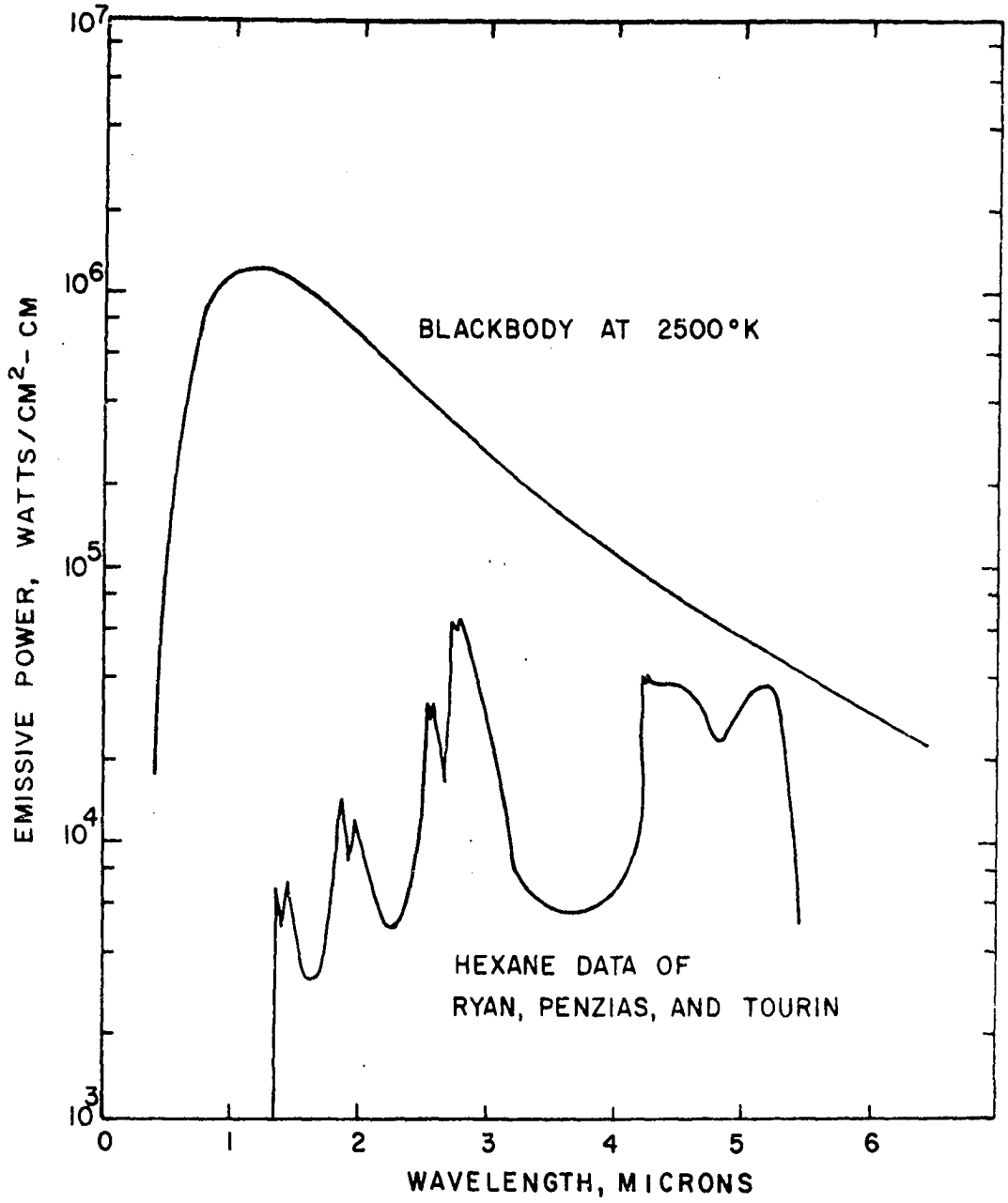

Figure A-2. Relationship between Flames and 1000 Watt Tungsten Lamp Emmissive Powers and Spectral Wave Lengths.

sources occur at different wavlengths. Furthermore, the wavelength span for essentially total energy emission is quite different for each emitting source.

Theoretical Considerations

Kirchoff's general law pertaining to heat radiation incident on an absorbing-reflecting surface is given as

$$\alpha + \tau + \rho = 1 \qquad \text{(A-1)}$$

where α is the absorptance, τ is the transmittance and ρ is the reflectance, the latter being either specular, diffuse or both.

For a material that is opaque, Equation (A-1) reduces to

$$\alpha + \rho = 1 \qquad \text{(A-2)}$$

where it is assumed that the heat radiation has negligible transmittance, i.e., $\tau \cong 0$.

Since radiative heat is not constant but varies with spectral wavelength, as illustrated by Figures A-1 and A-2, Equations (A-1) and (A-2) must be adjusted for this variation which gives

$$\alpha_\lambda + \tau_\lambda + \rho_\lambda = 1 \qquad \text{(A-3)}$$

and

$$\alpha_\lambda + \rho_\lambda = 1 \qquad \text{(A-4)}$$

where the subscript λ indicates the monochromatic absorptance, transmittance, and reflectance of the surface.

With the values of α_λ and ρ_λ varying with individual wavelength and, considering that the incident irradiance also varies with wavelength, it is necessary to obtain an average absorptance, α_{av}, before any realistic energy balances can be obtained.

Define the average absorptance as

$$\alpha_{avg} = \frac{\int_{\lambda_1}^{\lambda_2} \alpha_\lambda e_\lambda \, d\lambda}{\int_{\lambda_1}^{\lambda_2} e_\lambda \, d\lambda} \qquad \text{(A-5)}$$

where e_λ is the monochromatic emissive power of the individual heat source at a particular wavelength. Equation (A-5) has been used to calculate the average absorptances by means of computer computation using the trapazoidal rule for integration. Figures IV-5 through IV-12 are graphic illustrations of the monochromatic variations of the absorptance with wavelength for all of the tested woods.

Measurement of Reflectance and Transmittance

The writer is indebted to his colleage, J. R. Hallman and to General Dynamics Convair, GDC, San Diego, California

for the use of their reflectivity apparatus to obtain the necessary data for computing the wood sample absorptances.

The measurement of directional reflectance in the wavelength region of 0.3 to 2.1 microns was made with the use of a Cary Model 14 spectrophotometer together with an integrating sphere attachment. Figure A-3 is a photograph of the test apparatus. The Cary Model 14 is a double beam instrument with automatic scan and a readout which is linear with wavelength. The monochromator contains a grating in series with a fused silica prism. A photo tube is used as a detector for the range from 0.3 to 0.6 microns and a PbS cell is used from 0.6 to 2.1 microns. The integrating sphere consists of a 7-inch diameter sphere coated on the inside with a thick layer of MgO. The sample, located at the center of the sphere, is uniformly illuminated by a tungsten source. One beam of the Cary spectrophotometer originates from the sample and the other beam originates from the MgO wall. The ratio of these two beams is the reflectance of the sample; it is displayed by the recorder as a function of wavelength. The system is capable of making measurements from normal to 86 degrees.

The measurement of reflectance above the wavelength of 2.1 microns required the use of additional specialized equipment. In this present research the reflectance in the

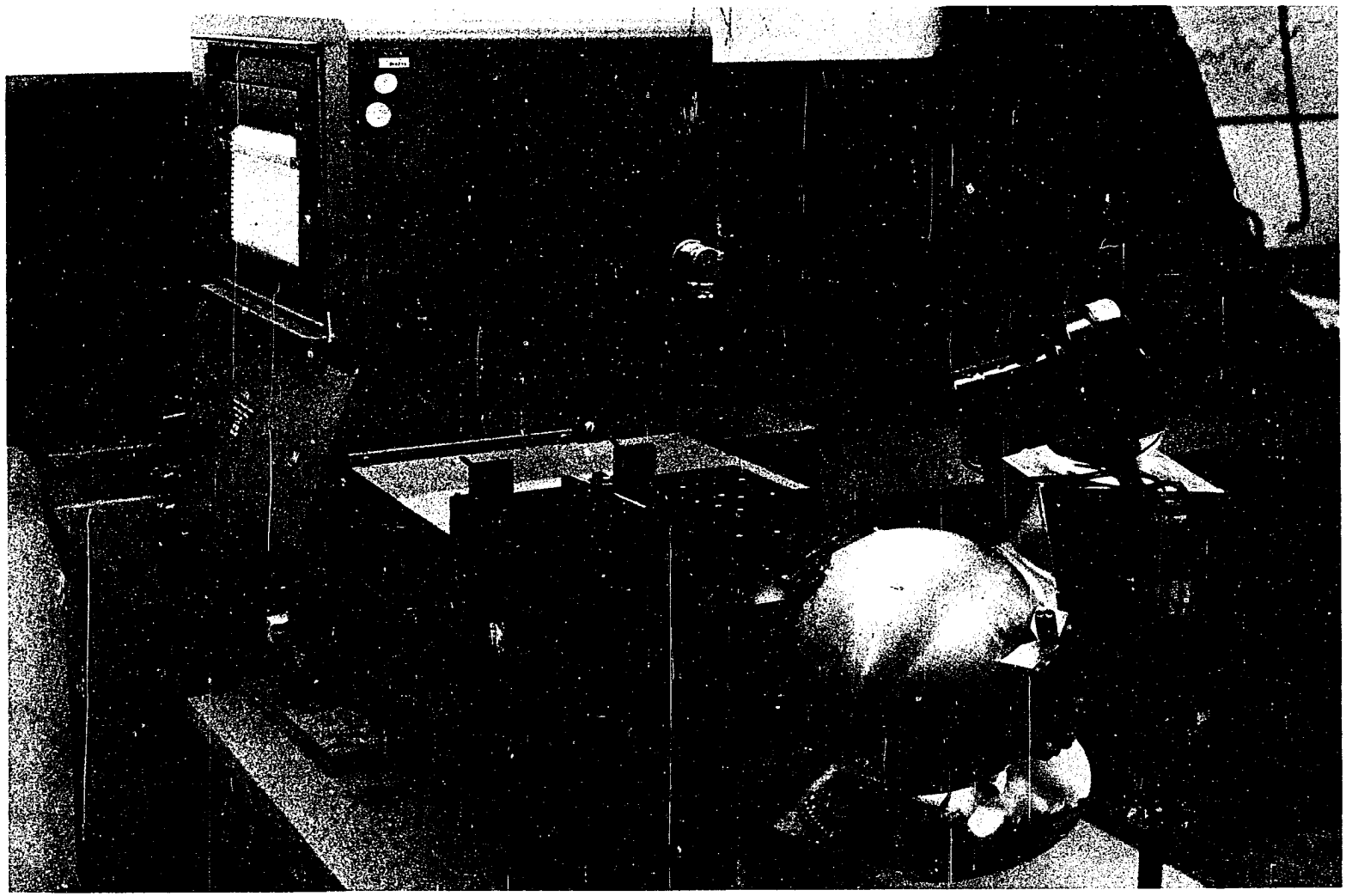

Figure A-3. Photograph of Test Set-Up.

range of 2.0 to 7.0 microns was obtained through the use of a Gier-Dunkle infrared reflectivity Hohlraum in conjunction with a Perkin-Elmer Model 99 double beam spectrometer and associated optics. Figure A - 3 is a photo of the total system while Figure A - 4 is an illustration of the optical path. The basic experimental apparatus consists of a source unit, a light collection system, a chopper, a monochrometer and a detector. The unit works on the single beam principal, wherein light from the sample surface is collected, chopped, passed through a monochrometer and displayed on the detector. The radiation from the sample surface was recorded as a function of wavelength. In later experiments, the output was displayed on a digital voltmeter. The reflectivity of a material was obtained by use of the ratio of the reflectance of the sample to the reflectance of gold at the same wavelength. The Hohlraum cavity was operated at a temperature of 700°F. A thermocouple detector was used throughout the spectral testing region of 1.6-7.0 microns.

Calculation of Absorptance

As previously described, Equation (A-5) was adapted for computer calculation using the trapozoidal rule for integration. Discrete values for the monochromatic emissive power e_λ were supplied to the computer in tabular form.

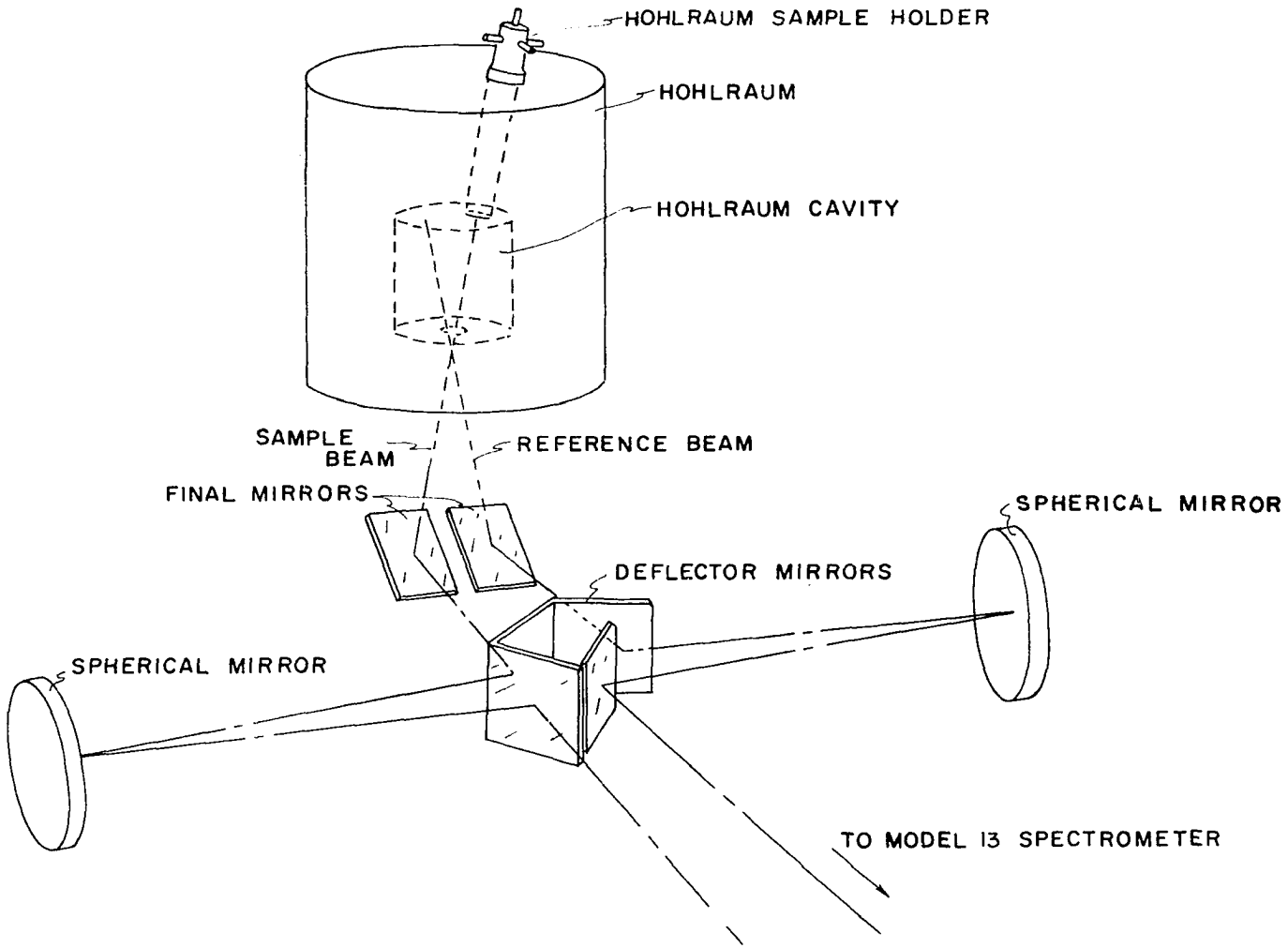

Figure A-4. Reflectivity Measurement Optical Path to Spectrometer.

Values of average absorptance, α_{av}, were obtained for benzene flame, 1000 watt tungsten lamps and solar radiation. Table IV-4 lists the calculated values of average absorptivities as described by Equation (A-5).

APPENDIX B

SUMMARY OF IGNITION DATA FOR OVEN DRIED WOOD SAMPLES

A summary of ignition data for oven dried wood is given in Tables B-1 through B-9 of this appendix. The tables are sub-divided according to type of radiation source, sample thickness and sample surface treatment (natural finish or flat black spray painted).

Table B-9 presents a summary of the data utilized to evaluate the un-exposed (rear) surface, transient, total energy losses during the irradiating period on the sample front surface. Table B-10 presents a summary of the physical and thermal properties, as well as the computations made to establish the effects of sample thickness on ignition behavior.

TABLE B-1

SUMMARY OF IGNITION DATA FOR 1.97 AND 2.54 CM THICK OVEN-DRIED WOODS USING FLAME RADIATION

Run No.	Type of Wood	Type of Ignition	ρ Sample Average Density (gm/cm^3)	Source of Irradiance	Nominal Sample Thickness (cm)	H_i Heating Rate (cal/cm^2-sec)	t Ignition time (seconds)
1	Cedar	Piloted	.358	Benzene	2.54	2.35	3.0
2	Mahogany	"	.553	"	"	2.80	3.3
3	Cedar	Spontaneous	.358	"	"	2.75	3.8
4	Cedar	"	"	"	"	2.25	6.5
5	Cedar	"	"	"	"	2.06	8.0
6	Cedar	"	"	"	"	1.45	78.0
7	White Pine	Piloted	.352	"	"	2.25	1.6
8	"	"	"	"	"	1.45	5.5
9	"	"	"	"	"	0.80	20.0
10	"	"	"	"	"	0.94	27.0
11	"	"	"	"	"	0.72	72.0
12	"	Spontaneous	"	"	"	2.25	4.5
13	"	"	"	"	"	1.65	7.5
14	"	"	"	"	"	1.35	180.0
15	"	"	"	"	"	1.20	no ignition
16	"	"	"	"	"	1.25	no ignition
17	Ash	Piloted	.686	"	"	2.30	5.5
18	"	"	"	"	"	2.05	6.6
19	"	"	"	"	"	1.45	18.5
20	"	"	"	"	"	1.00	54.0
21	"	"	"	"	"	0.82	98.0
22	"	Spontaneous	"	"	"	2.55	1.70
23	"	"	"	"	"	1.95	11.0

TABLE B-1 (Continued)

Run No.	Type of Wood	Type of Ignition	ρ Sample Average Density (gm/cm^3)	Source of Irradiance	Nominal Sample Thickness (cm)	H_i Heating Rate (cal/cm^2-sec)	t Ignition time (seconds)
24	Ash	Spontaneous	.686	Benzene	2.54	1.65	41.0
25	"	"	"	"	"	1.40	no ignition
26	"	"	"	"	"	1.35	no ignition
27		ABORT					
28		ABORT					
29	Oak	Piloted	.709	Benzene	2.54	2.20	3.50
30	"	"	"	"	"	2.00	6.0
31	"	"	"	"	"	1.42	26.0
32	"	"	"	"	"	.51	512.0
33	"	"	"	"	"	1.15	48.0
34	"	"	"	"	"	.90	84.0
35	"	Spontaneous	"	"	"	1.25	no ignition
36	"	"	"	"	"	1.50	40.0
37	"	"	"	"	"	1.72	21.2
38	"	"	"	"	"	2.10	14.2
39	"	"	"	"	"	2.21	8.5
40	"	"	"	"	"	2.60	4.50
41	Cottonwood	"	.502	"	"	2.90	3.0
42	"	"	"	"	"	2.36	5.0
43	"	"	"	"	"	1.94	10.0
44	"	"	"	"	"	1.56	no ignition
45	"	"	"	"	"	1.65	58.0
46	"	Piloted	"	"	"	2.45	3.5
47	"	"	"	"	"	1.95	8.0

TABLE B-1 (Continued)

Run No.	Type of Wood	Type of Ignition	ρ Sample Average Density (gm/cm^3)	Source of Irradiance	Nominal Sample Thickness (cm)	H_i Heating Rate (cal/cm^2-sec)	t Ignition time (seconds)
48	Cottonwood	Piloted	.502	Benzene	2.54	1.35	18.0
49	"	"	"	"	"	1.24	25.0
50	"	"	"	"	"	.90	60.0
51	"	"	"	"	"	.60	162.0
52	Redgum	"	.624	"	"	.76	122.0
53	"	"	"	"	"	.98	48.0
54	"	"	"	"	"	1.43	18.0
55	"	"	"	"	"	2.03	8.0
56	"	"	"	"	"	2.30	4.8
57	"	Spontaneous	"	"	"	2.47	4.8
58	"	"	"	"	"	2.07	10.0
59	"	"	"	"	"	1.65	20.0
60	"	"	"	"	"	1.40	no ignition
61	"	"	"	"	"	1.50	50.0
62	Maple	Piloted	.676	"	"	2.40	4.8
63	"	"	"	"	"	1.84	10.5
64	"	"	"	"	"	1.50	16.0
65	"	"	"	"	"	1.00	52.0
66	"	"	"	"	"	.76	100.0
67	"	Spontaneous	"	"	"	1.30	no ignition
68	"	"	"	"	"	1.46	144.0
69	"	"	"	"	"	1.76	17.0
70	"	"	"	"	"	2.30	6.0
71	"	"	"	"	"	2.52	7.0

TABLE B-1 (Continued)

Run No.	Type of Wood	Type of Ignition	ρ Sample Average Density (gm/cm^3)	Source of Irradiance	Nominal Sample Thickness (cm)	H_i Heating Rate (cal/cm^2-sec)	t Ignition time (seconds)
72	White Pine	Spontaneous	.352	Benzene	2.54	2.04	6.0
73	"	"	"	"	"	1.50	33.0
74	"	Piloted	"	"	"	.50	426.0
75	"	"	"	"	"	.92	27.0
76	Mansonia	"	.598	"	"	.75	78.0
77	"	"	"	"	"	1.00	32.0
78	"	"	"	"	"	1.80	8.0
79	"	"	"	"	"	2.30	4.5
80	"	"	"	"	"	2.55	3.4
81	"	Spontaneous	"	"	"	1.40	no ignition
82	"	"	"	"	"	1.50	36.0
83	"	"	"	"	"	1.80	14.0
84	"	"	"	"	"	2.30	4.8
85	"	"	"	"	"	2.60	3.0
86	Redwood	Piloted	.345	"	"	2.52	2
87	"	"	"	"	"	2.10	3.5
88	"	"	"	"	"	1.37	13.0
89	"	"	"	"	"	.90	38.0
90	"	"	"	"	"	.64	172.0
91	"	Spontaneous	"	"	"	1.26	no ignition
92	"	"	"	"	"	1.56	168.0
93	"	"	"	"	"	2.0	8.0
94	"	"	"	"	"	2.25	4.5
95	"	"	"	"	"	2.96	1.6

TABLE B-1 (Continued)

Run No.	Type of Wood	Type of Ignition	ρ Sample Average Density (gm/cm^3)	Source of Irradiance	Nominal Sample Thickness (cm)	H_i Heating Rate (cal/cm^2-sec)	t Ignition time (seconds)
96	Spruce	Spontaneous	.366	Benzene	2.54	2.48	5.0
97	"	"	"	"	"	2.30	8.0
98	"	"	"	"	"	1.42	no ignition
99	"	"	"	"	"	1.41	no ignition
100	"	"	"	"	"	1.85	20.0
101	"	Piloted	"	"	"	2.60	2.5
102	"	"	"	"	"	1.80	6.5
103	"	"	"	"	"	1.46	14.0
104	"	"	"	"	"	1.08	27.0
105	"	"	"	"	"	.64	126.0
106	Mahogany	"	.533	"	"	.80	78.0
107	"	"	"	"	"	1.15	30.0
108	"	"	"	"	"	1.80	7.0
109	"	"	"	"	"	2.20	4.5
110	"	"	"	"	"	2.80	3.1
111	"	Spontaneous	"	"	"	2.95	2.80
112	"	"	"	"	"	2.18	8.0
113	"	"	"	"	"	1.45	240.0
114	"	"	"	"	"	1.67	21.0
115	"	"	"	"	"	1.30	no ignition
116	Cottonwood	Piloted	.502	Acetone	"	1.32	24.0
117	"	"	"	"	"	.94	44.0
118	"	"	"	"	"	.62	292.0

TABLE B-1 (Continued)

Run No.	Type of Wood	Type of Ignition	ρ Sample Average Density (gm/cm^3)	Source of Irradiance	Nominal Sample Thickness (cm)	H_i Heating Rate (cal/cm^2-sec)	t Ignition time (seconds)
119	Cottonwood	Piloted	.502	Acetone	2.54	.97	68.0
120	"	"	"	"	"	1.04	36.0
121	Mahogany	"	.553	"	"	1.32	19.0
122	"	"	"	"	"	1.10	41.0
123	"	"	"	"	"	.85	57.0
124	"	"	"	"	"	.76	78.0
125	"	"	"	"	"	.56	293.0
126	White Pine	"	.352	"	"	.53	443.0
127	"	"	"	"	"	.76	83.0
128	"	"	"	"	"	.94	23.0
129	"	"	"	"	"	1.09	15.0
130	"	"	"	"	"	1.30	10.0
131	Oak	"	.709	"	"	.68	168.0
132	"	"	"	"	"	.80	100.0
133	"	"	"	"	"	.97	56.0
134	"	"	"	"	"	1.40	26.0
135	"	"	"	"	"	.56	228.0
136	Mansonia	"	.598	"	"	.50	321.0
137	"	"	"	"	"	.80	72.0
138	"	"	"	"	"	.92	60.0
139	"	"	"	"	"	1.18	24.0
140	"	"	"	"	"	.68	137.0

TABLE B-1 (Continued)

Run No.	Type of Wood	Type of Ignition	ρ Sample Average Density (gm/cm^3)	Source of Irradiance	Nominal Sample Thickness (cm)	H_i Heating Rate (cal/cm^2-sec)	t Ignition time (seconds)
141	Redwood	Piloted	.345	Acetone	2.54	.57	282.0
142	"	"	"	"	"	.76	66.0
143	"	"	"	"	"	.90	38.0
144	"	"	"	"	"	.68	96.0
145	Ash	"	.686	"	"	.67	180.0
146	"	"	"	"	"	.90	78.0
147	"	"	"	"	"	1.04	56.0
148	"	"	"	"	"	1.36	30.0
149	Cedar	"	.358	"	"	1.22	13.0
150	"	"	"	"	"	1.04	24.0
151	"	"	"	"	"	.90	44.0
152	"	"	"	"	"	.76	81.0
153	"	"	"	"	"	.56	240.0
306	Balsa	"	.074	Benzene	1.97	2.22	1.3
307	"	"	.089	"	"	1.70	1.8
308	"	"	.086	"	"	1.02	11.2
309	"	"	.070	"	"	.83	26.0
310	"	"	.103	"	"	.88	20.0
311	"	"	.112	"	"	1.05	9.10
312	"	"	.103	"	"	1.29	6.0
313	"	"	.099	"	"	1.56	2.5
314	"	"	.106	"	"	1.58	2.5
315	"	"	.100	"	"	2.12	1.0

TABLE B-II

SUMMARY OF IGNITION DATA FOR BLACK PAINTED 2.54 CM THICK OVEN-DRIED WOODS USING FLAME RADIATION

Run No.	Type of Wood	Type of Ignition	ρ Sample Average Density (gm/cm^3)	Source of Energy	Nominal Sample Thickness (cm)	H_i Heating Rate (cal/cm^2-sec)	t Ignition time (seconds)
154	Ash	Piloted	.686	Benzene	2.54	.36	465.0
155	"	"	"	"	"	.60	120.0
156	"	"	"	"	"	1.06	23.0
157	"	"	"	"	"	1.12	19.5
158	"	"	"	"	"	1.52	11.0
159	"	"	"	"	"	1.99	8.7
160	"	"	"	"	"	2.72	3.25
161	"	"	"	"	"	2.90	2.40
162	Oak	"	.709	"	"	.36	Charred-Run Terminated
163	"	"	"	"	"	.58	Charred-Run Terminated
164	"	"	"	"	"	.76	67.0
165	"	"	"	"	"	1.01	29.0
166	"	"	"	"	"	1.50	14.0
167	"	"	"	"	"	2.06	4.4
168	"	"	"	"	"	2.56	2.0
169	"	"	"	"	"	2.60	2.5
170	"	"	"	"	"	2.85	2.2

TABLE B-II (Continued)

Run No.	Type of Wood	Type of Ignition	ρ Sample Average Density (gm/cm^3)	Source of Energy	Nominal Sample Thickness (cm)	H_i Heating Rate (cal/cm^2-sec)	t Ignition time (seconds)
171	Mahogany	Piloted	.533	Benzene	2.54	.56	189.0
172	"	"	"	"	"	1.06	57.0
173	"	"	"	"	"	1.68	4.0
174	"	"	"	"	"	1.30	9.5
175	"	"	"	"	"	2.10	2.6
176	"	"	"	"	"	2.78	1.5
177	Redgum	"	.624	"	"	.56	glowing-run terminated
178	"	"	"	"	"	.66	glowing-run terminated
179	"	"	"	"	"	1.01	28.0
180	"	"	"	"	"	.80	78.0
181	"	"	"	"	"	1.50	6.5
182	"	"	"	"	"	2.22	2.6
183	"	"	"	"	"	2.68	1.6
184	Birch	"	.548	"	"	2.80	1.1
185	"	"	"	"	"	2.60	1.3
186	"	"	"	"	"	2.10	2.25
187	"	"	"	"	"	1.54	5.5
188	"	"	"	"	"	1.02	18.0
189	"	"	"	"	"	.74	62.0
190	"	"	"	"	"	.56	glowing-run terminated

TABLE B-II (Contined)

Run No.	Type of Wood	Type of Ignition	ρ Sample Average Density (gm/cm^3)	Source of Energy	Nominal Sample Thickness (cm)	H_i Heating Rate (cal/cm^2-sec)	t Ignition time (seconds)
191	White Pine	Piloted	.352	Benzene	2.54	.72	72.0
192	"	"	"	"	"	.62	111.0
193	"	"	"	"	"	1.06	20.0
194	"	"	"	"	"	1.32	11.0
195	"	"	"	"	"	2.03	2.7
196	"	"	"	"	"	2.44	1.5
197	"	"	"	"	"	2.60	1.1
198	Mansonia	"	.598	"	"	2.18	5.2
199	"	"	"	"	"	2.60	3.0
200	"	"	"	"	"	1.95	5.2
201	"	"	"	"	"	1.55	10.0
202	"	"	"	"	"	1.12	14.5
203	"	"	"	"	"	.90	glowing-run terminated
204	Redwood	"	.345	"	"	3.06	1.2
205	"	"	"	"	"	2.20	1.50
206	"	"	"	"	"	1.95	2.0
207	"	"	"	"	"	1.90	2.0
208	"	"	"	"	"	1.54	3.2
209	"	"	"	"	"	1.25	10.0
210	"	"	"	"	"	.76	58.0
211	Cedar	"	.358	"	"	.35	glowing-run terminated
212	"	"	"	"	"	.72	56.0

TABLE B-II (Continued)

Run No.	Type of Wood	Type of Ignition	ρ Sample Average Density (gm/cm^3)	Source of Energy	Nominal Sample Thickness (cm)	H_i Heating Rate (cal/cm^2-sec)	t Ignition time (seconds)
213	Cedar	Piloted	.358	Benzene	2.54	1.20	15.0
214	"	"	"	"	"	1.46	7.0
215	"	"	"	"	"	2.00	2.5
216	"	"	"	"	"	2.60	1.2
217	"	"	"	"	"	2.75	0.9
218	Spruce	"	.366	"	"	2.72	0.8
219	"	"	"	"	"	2.67	1.1
220	"	"	"	"	"	2.60	1.4
221	"	"	"	"	"	1.84	2.8
222	"	"	"	"	"	1.60	3.0
223	"	"	"	"	"	1.10	10.0
224	"	"	"	"	"	.92	23.0
225	"	"	"	"	"	.66	94.0
316	Cottonwood	"	.502	"	"	2.48	1.80
317	"	"	"	"	"	.67	165.0
318	"	"	"	"	"	.56	384.0
319	"	"	"	"	"	.94	37.2
320	"	"	"	"	"	1.16	18.0
321	"	"	"	"	"	1.38	13.0
322	"	"	"	"	"	1.60	6.8
323	"	"	"	"	"	2.07	3.4

TABLE B-III

SUMMARY OF IGNITION DATA FOR 1.97 CM THICK OVEN-DRIED WOODS
USING TUNGSTEN LAMP RADIATION

Run No.	Type of Wood	Type of Ignition	ρ Sample Average Density (gm/cm^3)	Source of Energy	Nominal Sample Thickness (cm)	H_i Heating Rate (cal/cm^2-sec)	t Ignition time (seconds)
226	Oak	Piloted	.709	1000 w Lamps	1.97	3.05	13.5
227	"	"	"	"	"	2.75	24.4
228	"	"	"	"	"	2.78	20.4
229	"	"	"	"	"	2.63	25.0
230	"	"	"	"	"	2.32	28.0
231	"	"	"	"	"	1.90	40.5
232	"	"	"	"	"	1.80	59.0
233	"	"	"	"	"	1.37	98.0
234	"	"	"	"	"	.94	run terminated glowing ignition
235	"	"	"	"	"	3.10	13.5
236	"	"	"	"	"	.90	318.0
237	Ash	"	.686	"	"	3.30	7.0
238	"	"	"	"	"	2.80	13.0
239	"	"	"	"	"	2.32	19.0
240	"	"	"	"	"	1.50	42.0
241	"	"	"	"	"	1.02	terminate @ 390 sec glowing ignition
242	Cottonwood	"	.502	"	"	3.10	8.2
243	"	"	"	"	"	2.32	19.0
244	"	"	"	"	"	1.96	29.0

TABLE B-III (Continued)

Run No.	Type of Wood	Type of Ignition	ρ Sample Average Density (gm/cm^3)	Source of Energy	Nominal Sample Thickness (cm)	H_i Heating Rate (cal/cm^2-sec)	t Ignition time (seconds)
245	Cottonwood	Piloted	.502	1000 w Lamps	1.97	1.44	88.0
246	"	"	"	"	"	.94	291.0
247	Birch	"	.548	"	"	3.00	8.3
248	"	"	"	"	"	2.35	20.0
249	"	"	"	"	"	1.72	30.5
250	"	"	"	"	"	1.34	52.0
251	"	"	"	"	"	.90	glowing ignition
252	Redgum	"	.624	"	"	2.66	9.6
253	"	"	"	"	"	2.28	15.5
254	"	"	"	"	"	1.80	26.5
255	"	"	"	"	"	1.34	39.0
256	"	"	"	"	"	.98	86.0
257	Mahogany	"	.553	"	"	1.0	glowing ignition
258	"	"	"	"	"	1.43	49.0
259	"	"	"	"	"	1.90	25.0
260	"	"	"	"	"	2.36	16.0
261	"	"	"	"	"	2.75	11.0
262	"	"	"	"	"	3.06	8.4
263	Cedar	"	.358	"	"	3.10	9.3

TABLE B-III (Continued)

Run No.	Type of Wood	Type of Ignition	ρ Sample Average Density (gm/cm^3)	Source of Energy	Nominal Sample Thickness (cm)	H_i Heating Rate (cal/cm^2-sec)	t Ignition time (seconds)
264	Cedar	Piloted	.358	1000 w Lamps	1.97	2.66	13.5
265	"	"	"	"	"	2.10	25.0
266	"	"	"	"	"	1.70	35.0
267	"	"	"	"	"	1.34	47.0
268	"	"	"	"	"	.90	glowing ignition
269	Spruce	"	.366	"	"	3.10	8.0
270	"	"	"	"	"	2.62	12.0
271	"	"	"	"	"	2.28	15.5
272	"	"	"	"	"	1.84	25.5
273	"	"	"	"	"	1.24	60.0
274	"	"	"	"	"	1.06	111.0
275	Redwood	"	.345	"	"	2.95	6.6
276	"	"	"	"	"	2.58	9.3
277	"	"	"	"	"	2.20	11.5
278	"	"	"	"	"	1.88	18.0
279	"	"	"	"	"	1.38	27.0
280	"	"	"	"	"	.96	glowing ignition

TABLE B-III (Continued)

Run No.	Type of Wood	Type of Ignition	ρ Sample Average Density (gm/cm^3)	Source of Energy	Nominal Sample Thickness (cm)	H_i Heating Rate (cal/cm^2-sec)	t Ignition time (seconds)
281	White Pine	Piloted	.352	1000 w Lamps	1.97	3.10	6.2
282	"	"	"	"	"	2.92	9.4
283	"	"	"	"	"	2.28	15.2
284	"	"	"	"	"	1.80	26.0
285	"	"	"	"	"	1.34	40.0
286	"	"	"	"	"	.98	100.0
287	Mansonia	"	.598	"	"	3.12	6.6
288	"	"	"	"	"	2.78	14.2
289	"	"	"	"	"	2.31	20.0
290	"	"	"	"	"	1.80	40.0
291	"	"	"	"	"	1.52	53.0
292	"	"	"	"	"	1.04	190.0
293	Redgum	"	.624	"	"	3.06	6.5
294	"	"	"	"	"	3.10	6.2
295	Balsa	"	.0901	"	"	3.25	2.0
296	"	"	"	"	"	3.20	2.0
297	"	"	"	"	"	2.75	3.4
298	"	"	"	"	"	2.35	4.6
299	"	"	"	"	"	1.80	8.3
300	"	"	"	"	"	1.38	15.0

TABLE B-III (Continued)

Run No.	Type of Wood	Type of Ignition	ρ Sample Average Density (gm/cm^3)	Source of Energy	Nominal Sample Thickness (cm)	H_i Heating Rate (cal/cm^2-sec)	t Ignition time (seconds)
301	Oak	Piloted	.734	1000 W Lamps	1.97	1.40	88.0
302	"	"	.762	"	"	1.80	54.0
303	"	"	.700	"	"	2.10	35.5
304	"	"	.723	"	"	2.38	28.8
305	"	"	.776	"	"	3.06	15.2
519	Balsa	"	.0901	"	"	2.03	4.0
520	"	"	"	"	"	1.48	9.4
521	"	"	"	"	"	1.00	20.8

TABLE B-IV

SUMMARY OF IGNITION DATA FOR 1.97 CM THICK BLACK PAINTED OVEN-DRIED WOODS USING TUNGSTEN LAMP RADIATION

Run No.	Type of Wood	Type of Ignition	ρ Sample Average Density (gm/cm^3)	Source of Energy	Nominal Sample Thickness (cm)	H_i Heating Rate (cal/cm^2-sec)	t Ignition time (seconds)
324	Oak	Piloted	.709	1000 W Lamps	1.97	1.38	34.0
325	"	"	"	"	"	1.82	13.0
326	"	"	"	"	"	1.84	10.0
327	"	"	"	"	"	2.66	5.4
328	"	"	"	"	"	3.04	3.8
329	Ash	"	.686	"	"	3.15	3.4
330	"	"	"	"	"	2.66	4.9
331	"	"	"	"	"	2.30	7.6
332	"	"	"	"	"	1.84	15.0
333	"	"	"	"	"	1.38	glowing ignition
334	"	"	"	"	"	1.65	18.0
335	White Pine	"	.352	"	"	3.20	1.7
336	"	"	"	"	"	2.66	2.2
337	"	"	"	"	"	2.28	4.6
338	"	"	"	"	"	1.88	8.0
339	"	"	"	"	"	1.60	7.5
340	"	"	"	"	"	1.20	16.0
341	Redwood	"	.345	"	"	3.25	2.0

TABLE B-IV (Continued)

Run No.	Type of Wood	Type of Ignition	ρ Sample Average Density (gm/cm^3)	Source of Energy	Nominal Sample Thickness (cm)	H_i Heating Rate (cal/cm^2-sec)	t Ignition time (seconds)
342	Redwood	Piloted	.345	1000 W Lamps	1.97	2.60	4.6
343	"	"	"	"	"	1.86	8.1
344	"	"	"	"	"	1.80	11.0
345	Mahogany	"	.553	"	"	3.14	2.6
346	"	"	"	"	"	2.80	3.0
347	"	"	"	"	"	2.24	8.0
348	"	"	"	"	"	1.76	16.5
349	"	"	"	"	"	0.88	210.0
350	Balsa	"	.0901	"	"	3.10	0.5
351	"	"	"	"	"	2.62	0.8
352	"	"	"	"	"	2.28	1.00
353	"	"	"	"	"	1.76	1.40
354	Spruce	"	.366	"	"	3.18	2.10
355	"	"	"	"	"	2.74	2.70
356	"	"	"	"	"	2.35	5.50
357	"	"	"	"	"	1.84	10.0
358	"	"	"	"	"	1.24	36.0
359	Redgum	"	.624	"	"	3.04	3.9
360	"	"	"	"	"	2.66	3.8
361	"	"	"	"	"	2.28	9.6
362	"	"	"	"	"	1.75	11.5
363	"	"	"	"	"	1.43	27.0
364	"	"	"	"	"	1.10	glowing ignition

TABLE B-IV (Continued)

Run No.	Type of Wood	Type of Ignition	ρ Sample Average Density (gm/cm^3)	Source of Energy	Nominal Sample Thickness (cm)	H_i Heating Rate (cal/cm^2-sec)	t Ignition time (seconds)
365	Cedar	Piloted	.358	1000 W Lamps	1.97	3.18	1.90
366	"	"	"	"	"	2.80	3.50
367	"	"	"	"	"	2.52	5.0
368	"	"	"	"	"	1.77	14.0
369	"	"	"	"	"	1.50	21.0
370	Mansonia	"	.598	"	"	1.74	24.0
371	"	"	"	"	"	1.44	glowing ignition
372	"	"	"	"	"	1.88	14.0
373	"	"	"	"	"	2.27	6.6
374	"	"	"	"	"	2.70	4.3
375	"	"	"	"	"	3.14	3.4
376	Birch	"	.548	"	"	1.34	64.5
377	"	"	"	"	"	1.48	37.0
378	"	"	"	"	"	1.88	13.2
379	"	"	"	"	"	2.28	10.0
380	"	"	"	"	"	2.70	3.8
381	"	"	"	"	"	3.25	2.8
382	Cottonwood	"	.502	"	"	1.50	27.0
383	"	"	"	"	"	1.38	90.0
384	"	"	"	"	"	1.84	17.6
385	"	"	"	"	"	2.32	8.8
386	"	"	"	"	"	2.75	4.3
387	"	"	"	"	"	3.20	2.0

TABLE B-V

SUMMARY OF IGNITION DATA FOR 1.97 CM THICK OVEN-DRIED WOODS
USING 2000 W TUNGSTEN QUARTZ LAMPS

Run No.	Type of Wood	Type of Ignition	ρ Sample Average Density (gm/cm^3)	Source of Energy	Nominal Sample Thickness (cm)	H_i Heating Rate (cal/cm^2-sec)	t Ignition time (seconds)
388	Cedar	Piloted	.358	2000 W Lamps	1.97	3.00	7.5
389	"	"	"	"	"	2.60	9.8
390	"	"	"	"	"	3.32	6.1
391	"	"	"	"	"	2.10	15.8
392	"	"	"	"	"	1.64	32.0
393	"	"	"	"	"	1.32	53.5
394	"	"	"	"	"	1.08	73.5
395	Oak	"	.709	"	"	3.36	7.5
396	"	"	"	"	"	3.06	9.8
397	"	"	"	"	"	2.58	13.7
398	"	"	"	"	"	2.20	19.5
399	"	"	"	"	"	1.54	45.0
400	Cottonwood	"	.502	"	"	3.36	4.3
401	"	"	"	"	"	3.10	7.9
402	"	"	"	"	"	2.63	10.0
403	"	"	"	"	"	2.10	16.6
404	"	"	"	"	"	1.70	31.0
405	Oak	"	.749	"	"	2.94	13.7
406	"	"	.749	"	"	2.40	22.0
407	"	"	.756	"	"	1.84	35.5
408	"	"	.739	"	"	1.45	68.0
409	"	"	.738	"	"	1.62	54.0

TABLE B-VI

SUMMARY OF IGNITION DATA FOR 1.27 CM THICK OVEN DRIED WOODS USING 1000 W TUNGSTEN LAMPS RADIATION

Run No.	Type of Wood	Type of Ignition	ρ Sample Average Density (gm/cm^3)	Source of Energy	Nominal Sample Thickness (cm)	H_i Heating Rate (cal/cm^2-sec)	t Ignition time (seconds)
410	Oak	Piloted	.633	1000 W Lamps	1.27	3.72	6.25
411	"	"	"	"	"	3.00	9.70
412	"	"	"	"	"	2.60	14.90
413	"	"	"	"	"	2.10	31.40
414	"	"	"	"	"	1.58	50.50
415	"	"	"	"	"	1.34	64.50
416	"	"	"	"	"	.98	153.0
417	Cedar	"	.471	"	"	3.70	6.30
418	"	"	"	"	"	3.14	10.1
419	"	"	"	"	"	2.54	17.2
420	"	"	"	"	"	2.20	25.0
421	"	"	"	"	"	1.70	38.0
422	"	"	"	"	"	1.06	106.0
423	Cottonwood	"	.452	"	"	3.64	7.10
424	"	"	"	"	"	2.76	13.00
425	"	"	"	"	"	2.54	18.60
426	"	"	"	"	"	2.32	22.00
427	"	"	"	"	"	1.84	29.0
428	"	"	"	"	"	1.38	52.0

TABLE B-VI (Continued)

Run No.	Type of Wood	Type of Ignition	ρ Sample Average Density (gm/cm^3)	Source of Energy	Nominal Sample Thickness (cm)	H_i Heating Rate (cal/cm^2-sec)	t Ignition time (seconds)
429	Cottonwood	Piloted	.452	1000 W Lamps	1.27	1.06	101.5
430	Oak	"	.633	"	"	2.28	23.5
431	"	"	"	"	"	2.65	18.9
432	"	"	"	"	"	1.50	47.8
433	"	"	"	"	"	1.36	70.0
434	"	"	"	"	"	1.10	108.0
435	"	"	"	"	"	.97	282.0
436	"	"	"	"	"	2.80	14.0
437	"	"	"	"	"	3.10	11.0
438	"		(Run Aborted)				
439	"	"	.452	"	"	1.10	80.0
440	"	"	"	"	"	1.40	40.0
441	"	"	"	"	"	2.00	25.0
442	"	"	"	"	"	2.60	15.6
443	"	"	"	"	"	2.96	12.0
444	"	"	"	"	"	3.26	7.0
445	"	"	"	"	"	2.70	14.6
446	Cedar	"	.471	"	"	3.36	8.5
447	"	"	"	"	"	3.00	10.1
448	"	"	"	"	"	2.48	17.5
449	"	"	"	"	"	2.20	23.5
450	"	"	"	"	"	1.85	35.0
451	"	"	"	"	"	1.44	46.0
452	"	"	"	"	"	1.00	100.0

TABLE B-VII

SUMMARY OF IGNITION DATA FOR 0.635 CM THICK OVEN DRIED WOODS USING 1000 W TUNGSTEN LAMPS

Run No.	Type of Wood	Type Ignition	ρ Sample Average Density (gm/cm^3)	Source of Energy	Nominal Sample Thickness (cm)	H_i Heating Rate (cal/cm^2-sec)	t Ignition time (seconds)
453	Cedar	Piloted	.561	1000 W Lamps	0.635	3.96	9.0
454	"	"	.533	"	"	3.44	15.4
455	"	"	.540	"	"	3.31	16.2
456	"	"	.543	"	"	2.68	21.0
457	"	"	.557	"	"	2.02	32.5
458	"	"	.521	"	"	1.32	80.0
459	"	"	.515	"	"	1.00	204.0
460	Cottonwood	"	.531	"	"	.80	156.0
461	"	"	.540	"	"	.92	144.0
462	"	"	.533	"	"	1.20	66.0
463	"	"	.523	"	"	1.43	44.0
464	"	"	.601	"	"	1.96	25.0
465	"	"	.531	"	"	2.66	15.8
466	Oak	"	.745	"	"	2.66	14.8
467	"	"	.754	"	"	1.80	30.0
468	"	"	.747	"	"	1.60	40.0
469	"	"	.745	"	"	2.36	17.0
470	"	"	.667	"	"	.98	82.0
471	"	"	.632	"	"	2.62	12.6

TABLE B-VIII

SUMMARY OF IGNITION DATA FOR 0.318 CM THICK OVEN DRIED WOODS USING 1000 W TUNGSTEN FILAMENT QUARTZ LAMPS

Run No.	Type of Wood	Type of Ignition	$\bar{\rho}$ Sample Average Density (gm/cm^3)	Source of Energy	Nominal Sample Thickness (cm)	H_i Heating Rate (cal/cm^2-sec)	t Ignition time (seconds)
472	Cottonwood	Piloted	.544	1000 W Lamps	0.318	2.78	9.4
473	"	"	.586	"	"	2.72	8.1
474	"	"	.586	"	"	3.36	6.6
475	"	"	.636	"	"	2.48	10.0
476	"	"	.536	"	"	2.01	14.2
477	"	"	.586	"	"	1.60	24.0
478	"	"	.623	"	"	1.06	43.6
479	"	"	.595	"	"	0.81	125.0
480	Cedar	"	.518	"	"	0.82	150.0
481	"	"	.518	"	"	1.00	78.0
482	"	"	.499	"	"	1.36	36.0
483	"	"	.483	"	"	1.66	25.0
484	"	"	.518	"	"	1.94	18.5
485	"	"	.451	"	"	2.38	15.0
486	"	"	.518	"	"	2.96	8.8
487	"	"	.513	"	"	3.30	7.2
488	"	"	.518	"	"	0.77	189.0
489	Oak	"	.696	"	"	2.88	11.8
490	"	"	.653	"	"	2.38	13.0

TABLE B-VIII (Continued)

Run No.	Type of Wood	Type of Ignition	ρ Sample Average Density (gm/cm^3)	Source of Energy	Nominal Sample Thickness (cm)	H_i Heating Rate (cal/cm^2-sec)	t Ignition time (seconds)
491	Oak	Piloted	.707	1000 W Lamps	0.318	2.12	18.0
492	"	"	.710	"	"	1.82	22.0
493	"	"	.717	"	"	1.66	33.0
494	"	"	.714	"	"	1.48	35.0
495	"	"	.600	"	"	1.32	37.5
496	"	"	.714	"	"	1.08	64.0
497	"	"	.718	"	"	.84	103.0
498	"	"	.698	"	"	1.05	68.0
499	"	"	.711	"	"	1.70	27.0
500	"	"	.695	"	"	2.72	11.6
501	Masonite	"	1.02	"	"	2.44	17.4
502	"	"	"	"	"	2.81	12.8
503	"	"	"	"	"	3.18	10.7
504	"	"	"	"	"	3.18	10.6
505	"	"	"	"	"	2.85	13.4
506	"	"	"	"	"	2.33	18.0
507	"	"	"	"	"	1.90	21.7
508	"	"	"	"	"	1.41	44.0
509	"	"	"	"	"	0.95	122.0
510	"	"	"	"	"	0.49	538.0
511	"	"	"	"	"	0.50	525.0

TABLE B-VIII (Continued)

Run No.	Type of Wood	Type of Ignition	ρ Sample Average Density (gm/cm^3)	Source of Energy	Nominal Sample Thickness (cm)	H_i Heating Rate (cal/cm^2-sec)	t Ignition time (seconds)
512	Masonite	Piloted	1.02	1000 W Lamps	0.318	0.85	127.0
513	"	"	"	"	"	0.98	96.0
514	"	"	"	"	"	1.22	57.0
515	"	"	"	"	"	0.59	283.0
516	"	"	"	"	"	0.73	184.0
517	"	"	"	"	"	1.76	29.0
518	"	"	"	"	"	1.72	30.1

TABLE B-IX

SUMMARY OF SAMPLE REAR SURFACE TRANSIENT HEAT LOSS DATA
UP TO THE TIME OF FRONT SURFACE IGNITION

Run No.	H_i Incident Irradiance (cal/cm^2-sec)	t Exposure Time (Seconds)	0.318 cm thick Type of Wood	Rear Surface Temperature °C	Convection Loss (cal/cm^2-sec)	Radiation Loss (cal/cm^2-sec)	% loss of Incident Irradiance
497	0.84	0	Oak	41	0	0	0
"	"	4	"	41	0	0	0
"	"	10	"	52	.00378	.0011	.581
"	"	20	"	71	.00930	.0061	1.835
"	"	30	"	90	.0142	.0104	2.92
"	"	40	"	109	.0197	.0156	4.20
"	"	50	"	123	.0238	.020	5.22
"	"	60	"	137	.0278	.025	6.27
"	"	70	"	146	.0305	.0292	7.11
"	"	80	"	159	.0314	.0342	7.10
"	"	90	"	172	.038	.040	9.15
"	"	103*	"	186	.042	.0466	10.55
493	1.66	0	"	39	0	0	0
"	"	3	"	41	.00058	.000272	.0514
"	"	8	"	48	.00261	.001355	.2398
"	"	13	"	64	.00725	.00461	.715
"	"	23	"	95	.0165	.01205	1.728
"	"	28	"	111	.0208	.0168	2.265
"	"	33*	"	124	.0246	.0209	2.735
489	2.88	0	"	23	0	0	0

*Ignition

TABLE B-IX

Run No.	H_i Incident Irradiance (cal/cm^2-sec)	t Exposure Time (Seconds)	0.318 cm thick Type of Wood	Rear Surface Temperature °C	Convection Loss (cal/cm^2-sec)	Radiation Loss (cal/cm^2-sec)	% loss of Incident Irradiance
489	2.88	2	Oak	25	.00058	.000406	.0343
"	"	4	"	28	.00145	.000812	.0787
"	"	6	"	35	.00346	.00183	.1670
"	"	8	"	46	.00665	.00363	.3575
"	"	10	"	57	.00985	.0057	.540
"	"	11.8*	"	71	.01420	.00865	.794

*Ignition

TABLE B-X

SUMMARY OF CALCULATIONS FOR VARYING WOOD THICKNESSES AND 1000 W TUNGSTEN LAMP ENERGY SOURCE

Run No.	Material	Sample Thickness (cm)	Density (gm/cm^3)	Incident Irradiance $\left[\text{Erf}\ \frac{1}{2\sqrt{F}}\right]^{3/4}$ (cal/cm^2-sec)	α	$\frac{\bar{\alpha}\ H_i}{\rho^{1/3}\left\{\left(\text{erf}\frac{1}{2\sqrt{F}}\right)\right\}^{3/4}}$	Ignition Time (sec)
263	Cedar	1.91	.358	3.10	1.0	.412	1.81	9.3
264	"	"	"	2.66	1.0	"	1.55	13.5
265	"	"	"	2.10	1.0	"	1.22	25.0
266	"	"	"	1.70	1.0	"	.989	35.0
267	"	"	"	1.34	1.0	"	.778	47.0
417	"	1.27	.471	3.70	1.0	"	1.97	6.3
418	"	"	"	3.14	1.0	"	1.66	10.1
419	"	"	"	2.54	1.0	"	1.345	17.2
420	"	"	"	2.20	1.0	"	1.165	25.0
421	"	"	"	1.70	1.0	"	.902	38.0
422	"	"	"	1.06	.985	"	.575	106.0
446	"	"	"	3.36	1.0	"	1.78	8.5
447	"	"	"	3.00	1.0	"	1.59	10.1
448	"	"	"	2.48	1.0	"	1.315	17.5
449	"	"	"	2.20	1.0	"	1.165	23.5
450	"	"	"	1.85	1.0	"	.980	35.0
451	"	"	"	1.44	1.0	"	.762	46.0
452	"	"	"	1.00	.985	"	.538	100.0

TABLE B-X (Continued)

Run No.	Material	Sample Thickness (cm)	Density (gm/cm^3)	Incident Irradiance (cal/cm^2-sec)	$\left[\text{Erf}\ \frac{1}{2\sqrt{F}}\right]^{3/4}$	$\bar{\alpha}$	$\frac{\bar{\alpha}\ H_i}{\rho^{1/3}\left\{\left(\text{erf}\frac{1}{2\sqrt{F}}\right)\right\}^{3/4}}$	Ignition Time (sec)
453	Cedar	.635	.561	3.96	1.0	.412	1.94	9.0
454	"	"	.533	3.44	1.0	"	1.75	15.4
455	"	"	.540	3.31	1.0	"	1.68	16.2
456	"	"	.543	2.68	.985	"	1.33	21.0
457	"	"	.557	2.02	.96	"	1.05	32.5
458	"	"	.521	1.32	.854	"	.796	80.0
459	"	"	.515	1.00	.68	"	.754	204.0
480	"	.318	.518	.82	.482	"	.875	150.0
481	"	"	.518	1.00	.595	"	.875	78.0
482	"	"	.499	1.36	.741	"	.958	36.0
483	"	"	.483	1.66	.814	"	1.075	25.0
484	"	"	.518	1.94	.862	"	1.155	18.5
485	"	"	.451	2.38	.893	"	1.44	15.0
486	"	"	.518	2.96	.97	"	1.57	8.8
487	"	"	.513	3.30	.9775	"	1.74	7.2
242	Cottonwood	1.91	.502	3.10	1.0	.445	1.740	8.2
243	"	"	"	2.32	1.0	"	1.305	19.0
244	"	"	"	1.96	1.0	"	1.100	29.0
245	"	"	"	1.44	1.0	"	.808	88.0
246	"	"	"	.94	.939	"	.561	291.0

TABLE B-X (Continued)

Run No.	Material	Sample Thickness (cm)	Density (gm/cm^3)	Incident Irradiance (cal/cm^2-sec)	$\left[\text{Erf}\ \frac{1}{2\sqrt{F}}\right]^{3/4}$	$\bar{\alpha}$	$\frac{\bar{\alpha}\ H_i}{\rho^{1/3}\left\{(\text{erf}\ \frac{1}{2\sqrt{F}})\right\}^{3/4}}$	Ignition Time (sec)
423	Cottonwood	1.27	.452	3.64	1.0	.445	1.62	7.1
424	"	"	"	2.76	1.0	"	1.23	13.0
425	"	"	"	2.54	1.0	"	1.13	18.6
426	"	"	"	2.32	1.0	"	1.03	22.0
427	"	"	"	1.84	1.0	"	.819	29.0
428	"	"	"	1.38	1.0	"	.615	52.0
429	"	"	"	1.06	.97	"	.472	101.5
460	"	.635	.531	.80	.682	"	.645	156.0
461	"	"	.540	.92	.700	"	.720	144.0
462	"	"	.533	1.20	.846	"	.776	66.0
463	"	"	.523	1.43	.908	"	.870	44.0
464	"	"	.601	1.96	.970	"	1.085	25.0
465	"	"	.531	2.66	1.0	"	1.495	15.8
472	"	.32	.544	2.78	.939	"	1.655	9.4
473	"	.278	.586	2.72	.908	"	1.63	8.1
474	"	.278	.586	3.36	.947	"	1.92	6.6
475	"	.238	.636	2.48	.838	"	1.56	10.0
476	"	.318	.536	2.01	.870	"	1.30	14.2
477	"	.281	.586	1.60	.732	"	1.19	24.0
478	"	.239	.623	1.06	.560	"	.99	43.6
479	"	.319	.595	0.81	.475	"	.905	125.0
226	Oak	1.91	.709	3.05	1.0	.437	1.49	13.5
227	"	"	"	2.75	1.0	"	1.345	24.4
228	"	"	"	2.78	1.0	"	1.310	20.4
229	"	"	"	2.63	1.0	"	1.235	25.0

TABLE B-X (Continued)

Run No.	Material	Sample Thickness (cm)	Density (gm/cm^3)	Incident Irradiance (cal/cm^2-sec)	$\left[\text{Erf}\frac{1}{2\sqrt{F}}\right]^{3/4}$	$\bar{\alpha}\ \frac{\alpha\ H_i}{\rho^{1/3}\left\{(\text{erf}\frac{1}{2\sqrt{F}})\right\}^{3/4}}$	Ignition Time (sec)
230	Oak	1.91	.709	2.32	1.0	.437 1.135	28.0
231	"	"	"	1.90	1.0	" .93	40.5
232	"	"	"	1.80	1.0	" .885	59.0
233	"	"	"	1.37	1.0	" .670	98.0
235	"	"	"	3.10	1.0	" 1.56	13.5
236	"	"	"	.90	.9545	" .464	318.0
301	"	"	.734	1.40	1.0	" .682	88.0
302	"	"	.762	1.80	1.0	" .861	54.0
303	"	"	.700	2.10	1.0	" 1.035	35.5
304	"	"	.723	2.38	1.0	" 1.160	28.8
305	"	"	.776	3.06	1.0	" 1.455	15.2
410	"	1.27	.633	3.72	1.0	" 1.91	6.25
411	"	"	"	3.00	1.0	" 1.54	9.7
412	"	"	"	2.60	1.0	" 1.33	14.9
413	"	"	"	2.10	1.0	" 1.08	31.4
414	"	"	"	1.58	1.0	" .81	50.5
415	"	"	"	1.34	1.0	" .687	64.5
416	"	"	"	.98	.9395	" .534	153.0
430	"	"	"	2.28	1.0	" 1.17	23.5
431	"	"	"	2.65	1.0	" 1.36	18.9
432	"	"	"	1.50	1.0	" .77	47.8
433	"	"	"	1.36	1.0	" .696	70.0
434	"	"	"	1.10	.9775	" .577	208.0
435	"	"	"	.97	.862	" .578	282.0
436	"	"	"	2.80	1.0	" 1.43	14.0
437	"	"	"	3.10	1.0	" 1.59	11.0

TABLE B-X (Continued)

Run No.	Material	Sample Thickness (cm)	Density (gm/cm^3)	Incident Irradiance (cal/cm^2-sec)	$\left[\text{Erf}\ \frac{1}{2\sqrt{F}}\right]^{3/4} \bar{\alpha}$	$\frac{\bar{\alpha}\ H_i}{\rho^{1/3}\left\{\left(\text{erf}\frac{1}{2\sqrt{F}}\right)^{3/4}\right\}}$	Ignition Time (sec)
466	Oak	.635	.745	2.66	1.0 .437	1.27	14.8
467	"	"	.754	1.80	.962 "	.90	30.0
468	"	"	.747	1.60	.9395 "	.825	40.0
469	"	"	.745	2.36	1.0 "	1.14	17.0
470	"	"	.667	.98	.838 "	.594	82.0
471	"	"	.632	2.62	1.0 "	1.34	12.6
489	"	.318	.696	2.88	.924 "	1.54	11.8
490	"	"	.653	2.38	.90 "	1.34	13.0
491	"	"	.707	2.12	.854 "	1.21	18.0
492	"	"	.710	1.82	.814 "	1.10	22.0
493	"	"	.717	1.66	.781 "	1.03	33.0
494	"	"	.714	1.48	.732 "	.99	35.0
495	"	"	.600	1.32	.715 "	.958	37.5
496	"	"	.714	1.08	.530 "	1.00	64.0
497	"	"	.718	.84	.512 "	.80	103.0
498	"	"	.698	1.05	.604 "	.855	68.0
499	"	"	.711	1.70	.781 "	1.055	27.0
500	"	"	.695	2.72	.916 "	1.47	11.6
501	Masonite	"	1.02	2.44	.846 .501	1.44	17.4
502	"	"	"	2.81	.906 "	1.55	12.8
503	"	"	"	3.18	.932 "	1.71	10.7
504	"	"	"	3.18	.9395 "	1.69	10.6
505	"	"	"	2.85	.906 "	1.57	13.4
506	"	"	"	2.33	.87 "	1.34	18.0

TAELE B-X (Continued)

Run No.	Material	Sample Thickness (cm)	Density (gm/cm^3)	Incident Irradiance (cal/cm^2-sec)	$\left[\text{Erf}\ \frac{1}{2\sqrt{F}}\right]^{3/4}$	$\bar{\alpha}$	$\frac{\bar{\alpha}\ H_i}{\rho^{1/3}\left\{\left(\text{erf}\frac{1}{2\sqrt{F}}\right)\right\}^{3/4}}$	Ignition Time (sec)
507	Masonite	.318	1.02	1.90	.838	.501	1.13	21.7
508	"	"	"	1.41	.708	"	1.04	44.0
509	"	"	"	.95	.505	"	.94	122.0
510	"	"	"	.49	.295	"	.415	538.0
511	"	"	"	.50	.30	"	.415	525.0
512	"	"	"	.85	.496	"	.86	127.0
513	"	"	"	.98	.55	"	.89	96.0
514	"	"	"	1.22	.655	"	.93	57.0
515	"	"	"	.59	.373	"	.57	283.0
516	"	"	"	.73	.47	"	.65	184.0
517	"	"	"	1.76	.79	"	1.11	29.0
518	"	"	"	1.72	.782	"	1.10	30.1

APPENDIX C

A GRAPHICAL TECHNIQUE FOR SOLUTION OF THE TARGET IGNITION PROBLEM WITH COMBINED RADIATION AND CONVECTION BOUNDARY CONDITIONS

Every combustible solid has a characteristic relationship between radiant energy flux and time to ignition. In this section a graphical method for obtaining the solution of this nonlinear boundary value problem for the one-dimensional, opaque target is developed. The solution in this instance is based on a fixed surface temperature as the criterion for ignition. Properties of the target material such as thermal conductivity, heat capacity and density, of course, must be known. Once the relationship between radiant energy flux and time to ignition is obtained, then one can determine whether or not ignition will occur for a particular flame-target orientation, and if so, at what time.

Consider the region $a \leq x \leq b$, $(b \neq a)$, containing the solid target material initially at uniform temperature

T_o, where the semi-inifinite case of $b = \infty$ is not excluded. Let heat be absorbed at the target surface $x = a$ by radiation from a source at temperature T_f with a configuration factor F. Further, at the surface $x = a$, heat is lost to the surrounding atmosphere by both radiation and convection. (Note: One will observe in the development which follows that it is not essential to specify a source temperature T_f; in fact, it is preferable to know the radiation flux q_R. The two quantities are related by the expression $q_R = \epsilon_f \sigma F T_f^4$, assuming a uniform, graybody source of radiation.) If the surface at $x = b$ is insulated, then for the general one-dimensional problem, where x is the distance along an axis in any orthogonal set of coordinates, the temperature $T(x,t)$ is given by the solution of the following boundary value problem:

$$P_1(x) \frac{\partial}{\partial x} \left[P_2(x) \frac{\partial}{\partial x} T(x,t) \right] = \frac{\rho c}{K} \frac{\partial}{\partial t} T(x,t) ; \quad a<x<b, \ t>0 \tag{C-1a}$$

$$-K \frac{\partial T}{\partial x} = F\sigma (\epsilon_f T_f^4 - \epsilon_o T_o^4) - \sigma (\epsilon_s T^4 - \epsilon_o T_o^4) - h(T-T_o) ; \quad x = a, \ t>0 \tag{C-1b}$$

$$-K \frac{\partial T}{\partial x} = 0; \quad x = b, \ t>0 \tag{C-1c}$$

$$T(x,0) = T_o \tag{C-1d}$$

where ϵ_f, ϵ_s and ϵ_o = emissivities of the flame, target surface, and ambient air, respectively,

$P_1(x)$, $P_2(x)$ = weighting functions which depend on the coordinate system. ($P_1 = P_2 = 1$, for rectangular coordinates; $P_2 = 1/P_1 = x$, for cylindrical coordinates.)

Restricting the analysis to the opaque, semi-infinite, one-dimensional target as shown in Figure C-1, then

$$\frac{\partial^2 T(x,t)}{\partial x^2} = \frac{\rho c}{K} \frac{\partial T(x,t)}{\partial t} \qquad \text{(C-2a)}$$

$$-K \frac{\partial T}{\partial x} = F\sigma (\epsilon_f T_f^4 - \epsilon_o T_o^4) - \sigma (\epsilon_s T^4 - \epsilon_o T_o^4) - h(T-T_o); \quad x = 0,\ t>0 \qquad \text{(C-2b)}$$

$$-K \frac{\partial T}{\partial x} = 0;\ x = \infty,\ t>0 \qquad \text{(C-2c)}$$

$$T(x,0) = T_o \qquad \text{(C-2d)}$$

From this statement of the problem, it is observed that the thermal properties of the target material are assumed to be constant. Further, the target is assumed to be sufficiently

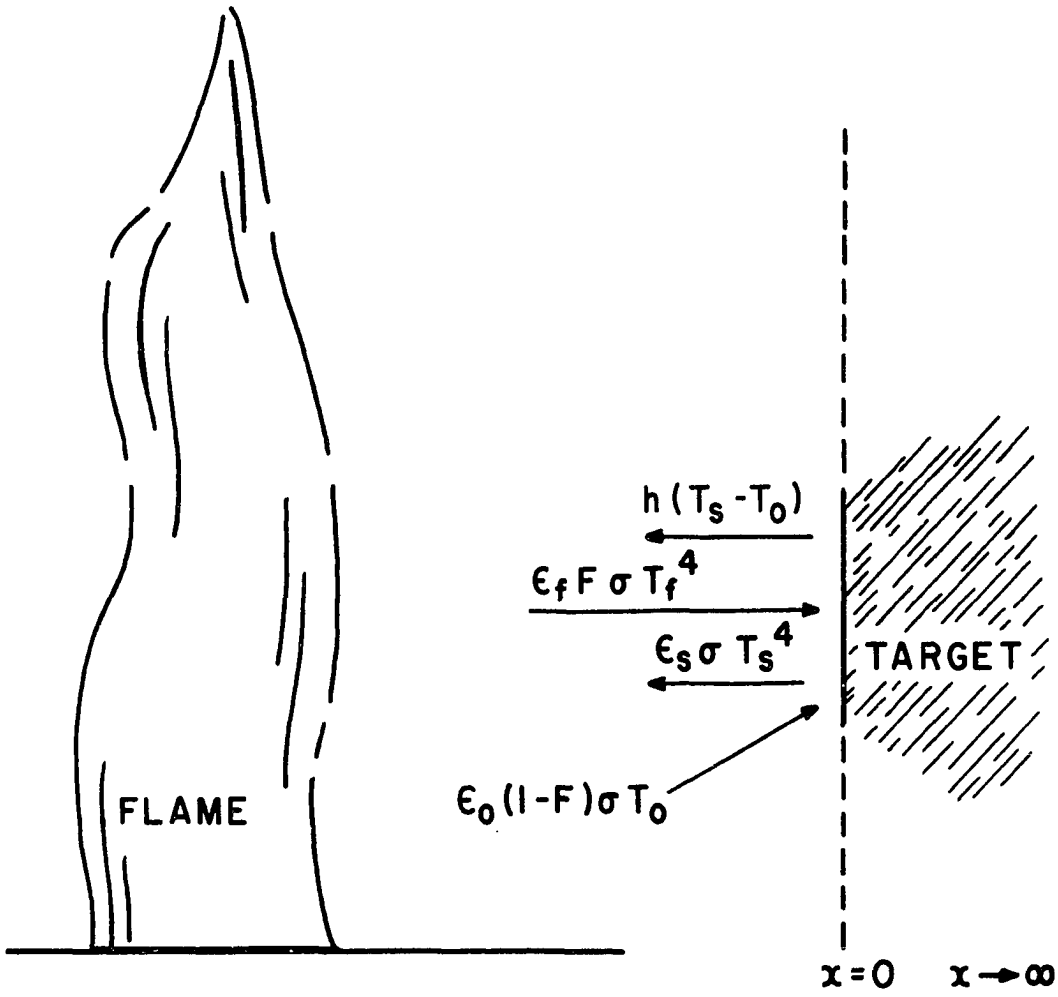

Figure C-1. Flame-Target Configuration.

removed from the flame so that the direction of heat transfer by convection is always toward the surroundings at constant temperature T_o. For target interaction with wind-blown flames, this assumption is not justified in some cases. For example, a target downwind from a flame may at first take on the heat both by radiation from the flame and by convection from the flame wake-gases; then, at a later stage in the heating process, the target temperature may exceed the wake-gas temperature, at which time, the direction of heat transfer by convection, is reversed.

Equations C-2 (a thru d) are conveniently put into dimensionless form, with the reasonable assumptions that values of the emissivities ϵ_o and ϵ_s are near unity, and the introduction of the dimensionless variables

$$\tau \text{ (dimensionless time} = \frac{K}{\rho c}\frac{t}{\lambda^2}$$

$$\nu \text{ (dimensionless temperature)} = (T-T_o)/T_R$$

$$X \text{ (dimensionless length)} = x/\lambda$$

where

$$T_R = \frac{\lambda\sigma}{K}\left[\epsilon_f T_f^4 - T_o^4\right]$$

$$\lambda = \text{characteristic length}$$

$$q_R' = F\frac{K}{\lambda}T_R = F\left[(q_R)_{max} - \sigma T_o^4\right]$$

With these transformations, the problem stated in dimensionless form is

$$\frac{\partial^2 \nu}{\partial X^2} = \frac{\partial \nu}{\partial t} \qquad \text{(C-3a)}$$

$$-\frac{\partial \nu}{\partial X} = F - \nu\ \alpha(\nu);\ X = 0,\ \tau > 0 \qquad \text{(C-3b)}$$

$$-\frac{\partial \nu}{\partial X} = 0;\ X = \infty,\ \tau > 0 \qquad \text{(C-3c)}$$

where

$$\beta(T) \equiv \frac{\lambda}{K}\left\{\sigma\left(T_s^2 + T_o^2\right)\left(T_s + T_o\right) + h\right\}$$

is transformed to the function $\alpha(\nu)$ through the substitution

$$\nu = (T - T_o)/T_R$$

and $\nu\ \alpha(\nu) \equiv f(\nu)$ by definition.

To obtain an approximate solution to this nonlinear problem, one can represent $f(\nu)$ with the staircase function; i.e.,

$$f(\nu) \approx \sum_{i=1}^{n} \delta f_i\ H(\nu - \nu_i) \qquad \text{(C-4)}$$

in which

$$H(y) = 0;\ y \leq 0$$

$$= 1;\ y > 0$$

$$\delta f_i = f(\nu_i) - f(\nu_{i-1});\ 1 \leq i \leq n$$

Figure C-2 shows such a staircase function for an arbitrary function $f(\nu)$.

If τ_i is the time at which $\nu(0,\tau) = \nu_i$, then one can write

$$f(\nu) = \Sigma \delta f_i\, H(\tau - \tau_i) \qquad \text{(C-5)}$$

Then upon applying the principle of superposition, $\nu(X,\tau)$ can be expressed as

$$\nu(X,\tau) = \nu_o + FU(X,\tau) + \sum_{i=1}^{n} \delta f_i\, U(X,\tau - \tau_i) \qquad \text{(C-6)}$$

where $U(X,\tau)$ is the solution of the problem

$$\frac{\partial^2 U}{\partial X^2} = \frac{\partial U}{\partial \tau};\ 0 < X < \infty,\ \tau > 0 \qquad \text{(C-7a)}$$

$$-\frac{\partial U}{\partial X} = 1;\ X = 0,\ \tau > 0 \qquad \text{(C-7b)}$$

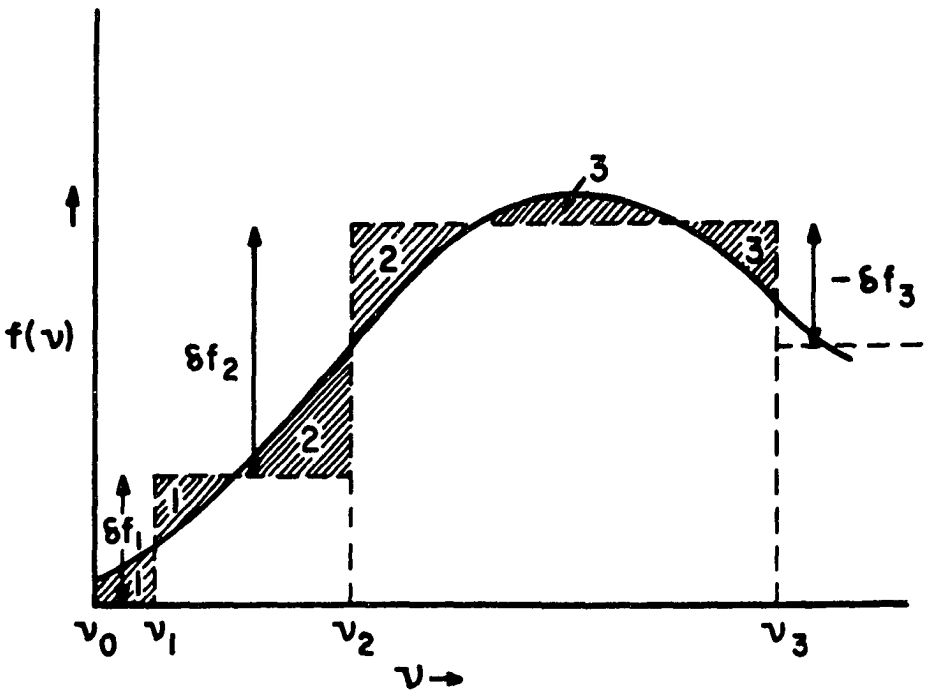

Figure C-2. Staircase Function Representation for the Function f(ν)

$$\frac{\partial U}{\partial X} = 0;\ X = \infty,\ \tau > 0 \qquad \text{(C-7c)}$$

$$U(X,0) = 0 \qquad \text{(C-7d)}$$

From the known solution $U(X,\tau)$, it is possible to find the unknown solution $\nu(X,\tau)$, by a graphical method described as follows:

For $\nu(X,\tau) \leq \nu_1$, $\nu - \nu_o = FU$

For $\nu_1 < \nu \leq \nu_2$, $(\nu - \nu_1) = (1 - \delta f_1/F)\ F(U - U_1)$,

and in general,

$$(\nu - \nu_i) = F\left(1 - \frac{1}{F}\sum_{j=1}^{i} \delta f_j\right)(U - U_i) \quad \text{for } \nu_{i+1} \geq \nu > \nu_i$$

where $U_i = U(X,\tau - \tau_i)$. In the graphical method, $(\nu - \nu_o)$ represents the ordinate and FU the abscissa. To start the procedure, a straight line of unit slope is drawn through the origin. Next, a line of slope $(1 - \delta f_1/F)$ is drawn to intersect the line $FU = (\nu - \nu_o)$ at the point $(\nu - \nu_o) = (\nu_1 - \nu_o)$. At point $(\nu - \nu_o) = (\nu_2 - \nu_o)$ on the second line a third line is passed with slope of $[1 - (\delta f_1 + \delta f_2)/F]$. This procedure is repeated until i = n. Figure C-3 shows the

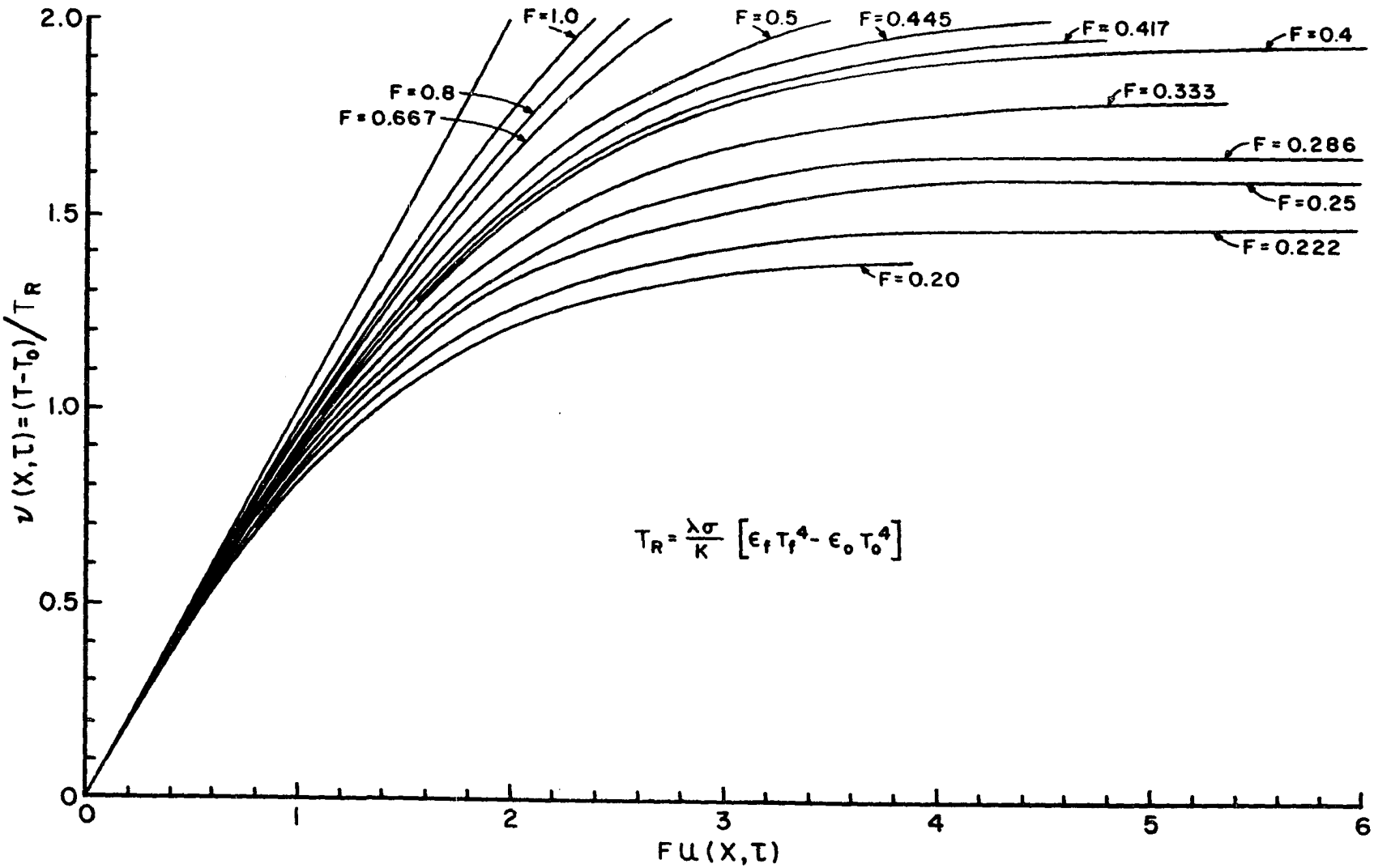

Figure C-3. Solution Curves for Equation C-3.

solutions obtained by this method for various values of F. The function $f(\nu)$ is plotted in Figure C-4. These curves relate the known boundary value problem solution for Equations C-7 to the unknown solution of Equation C-3.

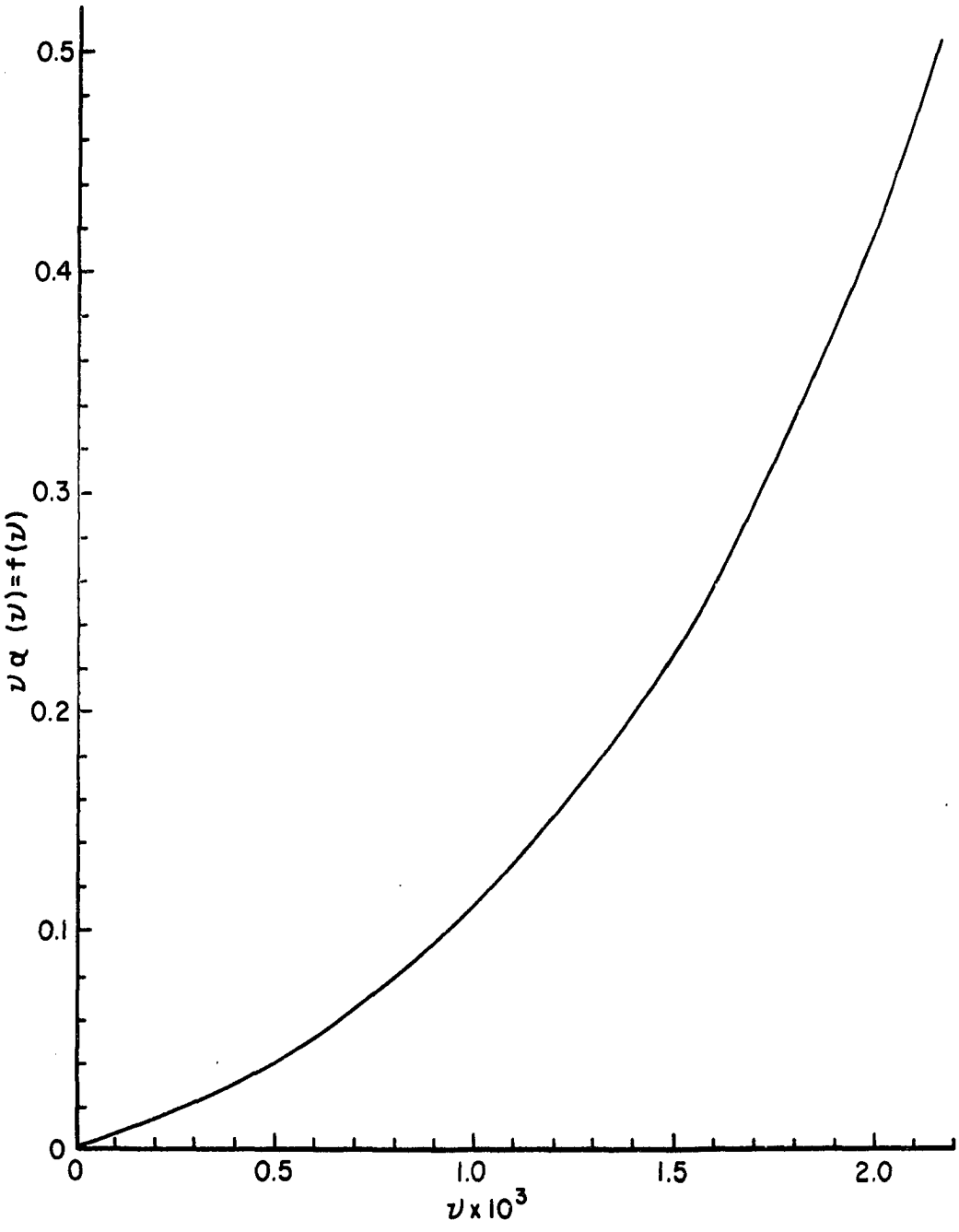

Figure C-4. Nonlinear Function $\nu\alpha(\nu)$ versus Dimensionless Temperature.

APPENDIX D

REFERENCES

1. Alvares, N. J., Private Communication to Dr. J. R. Welker, O.U.R.I. (May 1967).

2. Bamford, C. H., J. Crank, and D. H. Malan, "The Combustion of Wood, Part I," Proc. of Cambridge Philos. Soc., 42, 166 (1946).

3. Brown, C. R., "Determination of the Ignition Temperatures of Solid Materials," Fuel. 14, 14 (1935).

4. Browne, F. L., "Theories of the Combustion of Wood and its Control," USDA Forest Products Lab., Report No. 2136 (1958).

5. Buschman, A. J., Jr., "Ignition of Some Woods Exposed to Low Level Thermal Radiation," NBS Project No. 1002-11-10427, Tech. Rept. No. 1 (1961).

6. Butler, C. P., S. B. Martin and W. Lai, "Thermal Radiation Damage to Cellulosic Materials--Part II--Ignition of Alpha-Cellulose by Square Wave Exposure, "U.S. Naval Radiological Defense Lab; Tech. Rept. USNRDL-TR-135, NS-081-001, AFSWP-906 (1956).

7. Carslaw, H. S., and J. C. Jaeger, Conduction of Heat in Solids, Oxford at the Clarendon Press, Second Edition (1959).

8. Chung, P. K., and M. L. Jackson, "Thermal Diffusivity of Low Conductive Materials," Ind. and Eng. Chem., 46 (12), 2563-6 (1954).

9. deLhery, G. R., W. Derksen, and T. I. Monahan, "Research Report on the Spectral Reflectance and Transmittance

of Standard Fabrics for Thermal Radiation Effects Studies," Lab. Project 5046-3, Part 91, Final Report NS. 081-001, Technical Objective AW-9, AFSWP 957, Naval Material Laboratory, Brooklyn, N. Y. (1956).

10. Earing, D. G., and J. A. Smith, "Target Signatures Analysis Center: Data Compilation," Infrared and Optical Sensor Lab., Willow Run Laboratories, Institute of Science and Technology, The University of Michigan, Ann Arbor, Mich. (1966).

11. Fons, W. L., "Heating and Ignition of Small Wood Cylinders," Ind. & Eng. Chem., 4L, 2130 (1950).

12. Gaydon, A. G., and H. G. Wolfhard, Flames: Their Structure, Radiation and Temperature, Chapman & Hall LTD. (1960).

13. Havens, J. A., "Thermal Decomposition of Wood," Doctor of Philosophy Thesis, The University of Oklahoma (1969).

14. Koohyar, A. N., "Ignition of Wood by Flame Radiation," Doctor of Philosophy Thesis, The University of Oklahoma (1967).

15. Koohyar, A. N., J. R. Welker, and C. M. Sliepcevich, "An Experimental Technique for the Ignition of Solids by Flame Radiation," Fire Technology, 4, 221 (1968).

16. Koohyar, A. N., J. R. Welker, and C. M. Sliepcevich, "The Irradiation and Ignition of Wood by Flame," Fire Technology, 4, 284 (1968).

17. Lawrence, E. K., "Analytical Study of Flame Initiation," S. M. Thesis, Chem. Eng., MIT (1952).

18. Lawson, D. I., and D. L. Simms, "The Ignition of Wood by Radiation," Brit. J. of Appl. Phys., 3, 288-292 (1952).

19. Lee, B. T., Private Communication to Dr. J. R. Welker, O.U.R.I. (March 1968).

20. Lee, B. T., and J. J. Alvares, "The Effect of Irradiance on the Ignition and the Rate of Fire Spread

Along Composite Cellulosic Materials," Spring Meeting, Western States Section, The Combustion Institute, La Jolla, California (April 1967).

21. Lincoln, K. A., "Flash Pyrolysis of Solid-Fuel Materials by Thermal Radiation," Western States Section Meeting of the Combustion Inst., Stanford, California, April (1964).

22. Lipska, A. E., "The Pyrolysis of Cellulosic and Synthetic Materials in a Fire Environment," U.S. Naval Radiological Defense Laboratory, USNRDL-TR-1113 (1966).

23. Love, T. J., Radiative Heat Transfer, Charles E. Merrill Book Co., First Edition (1968).

24. MacLean, J. D., "Thermal Conductivity of Wood," Transactions American Society of Heating and Ventilating Engineers, 1941, 47, 1184 P. 323-354.

25. Martin, S. B., "Ignition-Ablation Responses at Cellulosic Materials to High Radiant Heat Loads," U.S. Naval Radiological Defense Laboratory, San Francisco, California, 1964 Spring Meeting, Western States Section, The Combustion Institute, Stanford University, Paper No. WSS/C1 64-8 (1964).

26. Martin, S. B., "The Mechanism of Ignition of Cellulosic Materials by Intense Thermal Radiation," U.S. Naval Radiological Defense Laboratory, Tech. Rept. USNRDL-TR-102NS 081-001, AFSWP-779 (1956).

27. Martin, S. B., and N. J. Alvares, "Critical Irradiance for Ignition of Cellulosic Fuels," U.S. Naval Radiological Defense Laboratory, San Francisco, California, Report No. WSC1-66-33 (1966).

28. Martin, S. B., and R. W. Ramstad, "Temperature Profile in Thermally Irradiated Cellulose Accompanying its Spontaneous Ignition," U.S. Naval Rad. Def. Lab., Tech. Rept. USNRDL-TR-810 (1965).

29. McAdams, W. H., Heat Transmission, McGraw Hill Book Co., Inc., Third Ed. (1954).

30. Monahan, T. I., W. L. Derksen, J. M. McGreevy, and J. J. Bates, "The Effects of Thermal Radiation on Materials," Annals of the New York Academy of Sciences, Vol. 82, ART. 3, p. 667, (October 1959).

31. Moysey, E. B., and W. E. Muir, "Pilot Ignition of Building Materials by Radiation," Fire Technology, Vol. 4, No. 1, p. 46 February (1968).

32. Muir, W. E., "Studies of Fire Spread Between Buildings," Ph.D. Thesis, Agricultural Eng. University of Saskatchewan (1967).

33. Palmer, J. D., O. A. Pipkin, and C. M. Sliepcevich, "New Concepts for Flame Weapons, Quarterly Progress Report (Part I)," OURI Report No. 1454-QRP-6(I), June (1966).

34. Ryan, L. R., G. J. Penzias, and R. H. Tourin, "An Atlas of Infrared Spectra of Flames. Part I. Infrared Spectra of Hydrocarbon Flames in the 1-5 μ Region," Scientific Report No. 1, Contract AF19 (604)-6106, Air Force Cambridge Research Laboratories, Bedford, Massachusetts (July 1961).

35. Sauer, F. M., "The Charring of Wood during Exposure to Thermal Radiation: Correlation Analysis for Semi-infinite Solids," USDA Forest Service California Forest and Range Experiment Station, Berkeley, California Interior Tech. Rept. AFSWP-838, August (1956).

36. Schaffer, E. L., "Effect of Panel Thickness and Non-Combustible Inserts on Surface Flammability of Plywood," U.S. Forest Service Research Note, FPL-0252, January 1967.

37. Schaffer, E. L., "Review of Information Related to the Charring Rate of Wood," U.S. Forest Service Research Note FPL-0145, November (1966).

38. Simms, D. L., "The Correlation of Ignition Time with the Physical Properties of Material, Part I, Spontaneous Ignition of Cellulosic Materials," Fire Research Note No. 319, Joint Fire Research Organization, England (1958).

39. Simms, D. L., "Ignition of Cellulosic Materials by Radiation," Combustion and Flame, 4 (4), 293-300 (1960).

40. Simms, D. L., "Experiments on the Ignition of Cellulosic Materials by Thermal Radiation," Combustion and Flame, 5, 369-375 (1961).

41. Simms, D. L., "Damage to Cellulosic Solids by Thermal Radiation," Combustion and Flame, 6 (4), 303-318 (1962).

42. Simms, D. L., "On the Pilot Ignition of Wood by Radiation," Combustion and Flame, 7, 253-261 (1963).

43. Simms, D. L., and J. E. Coiley, "Some Radiation Characteristics of a Gas Fired Panel," British Journal of Applied Physics, Vol. 14, 292-294 (1963).

44. Simms, D. L., and M. Law, "The Ignition of Wet and Dry Wood by Radiation," Combustion and Flame, 11, 377-388 (1967).

45. Smith, W. K., "Ignition of Materials by Radiant Heat," Naval Weapons Center Tech. Note 40604-8 (1968).

46. Sparrow, E. M., and R. D. Cess, "Radiation Heat Transfer," Brooks/Cole Publishing Co. (1967).

47. Thomas, P. H., D. L. Simms, and M. Law, "The Effects of Moisture Content on the Spontaneous Ignition of Wood by Radiation," Fire Research Note No. 280, Joint Fire Research Organization, England (1956).

48. Weatherford, W. D., Jr., D. M. Sheppard, and M. L. Valtierra, "An Experimental and Mathematical Study of the Mechanism of Wood Ignition," Southwest Research Inst., San Antonio, Texas, NBS Contract CST-1102 Final Report, November (1965).

49. Welker, J. R., H. R. Wesson, and C. M. Sliepcevich, "Ignition of Alpha-Cellulose and Cotton Fabric by Flame Radiation," Fire Technology, 5, 59 (1969).

50. Williams, C. C., "Damage Iniation in Organic Materials Exposed to High-Intensity Thermal Radiation," Sc.D. Thesis, Chem Eng., MIT (1953).

APPENDIX E

NOMENCLATURE

A	= area	cm^2
c	= heat capacity	cal/gm°C
C_σ	= average heat content of volatile products	cal/gm°C
d	= depth of char	cm
E	= activation energy	$cal/cm^2/sec$
e	= emissive power of radiating source	
H	= radiant energy	cal/cm^2sec
H_λ	= monochromatic emissive power	cal/cm^2sec
f	= function of	
F	= Fourier modulus, $\alpha t/L^2$	dimensionless
f	= frequency factor	sec^{-1}
H, H_i	= incident irradiance	cal/cm^2sec
H_o	= critical irradiance	cal/cm^2sec
H_p, H_s	= critical irradiance for pilot ignition	cal/cm^2sec
h	= overall surface heat transfer coefficients	$cal/cm^2sec°C$

h	= Plank's constant	
	= 6.6236×10	erg/sec
h_c	= heat transfer coefficient due to convection	$cal/cm^2 sec°C$
K	= thermal conductivity	$cal/cm^2 sec°C/cm$
k	= Boltzmann constant	
	= 1.3802×10^{-16}	erg/°K
L	= sample thickness	cm
l	= vertical height of sample	cm
m	= the rate of mass flow of decomposition gas per unit area	gm/cm^2-sec
n	= constant depending on wood species	
Q	= overall heat of decomposition reaction per unit volume	$cal/cm^2 sec/cm^3$
g_c	= heat loss due to surface	$cal/cm^2 sec$
g_r	= heat loss due to radiation from surface to surroundings	$cal/cm^2 sec$
g_ρ	= heat loss due to surface reflection	$cal/cm^2 sec$
g''	= heat supplied as a plane source	$cal/cm^2 sec$
r	= radial distance from cylinder axis	cm

R	= gas constant	cm/gm mole°K
R	= radius of cylinder	cm
T	= temperature	°K, °C
T_a	= ambient temperature	°K, °C
T_f	= flame temperature	°K, °C
T_o	= initial temperature	°K, °C
T_s	= surface temperature	°K, °C
ΔT	= temperature rise, $T - T_o$	°C
ΔT_m	= mean temperature rise, $T_m - T_o$	°C
ΔT_s	= surface temperature rise, $T_s - T_o$	°C
t	= time	
t_p	= time to reach the peak of a pulse	sec
x,y,z	= spatial distance	cm
V	= free stream air velocity	cm/sec
v	= velocity	cm/sec

Greek

α	= thermal diffusivity, $K/\rho c$	cm^2/sec
$\bar{\alpha}$	= surface absorptance, average	dimensionless
$\bar{\bar{\alpha}}$	= surface absorptance averaged over exposure time	dimensionless
α_λ	= monochromatic surface absorptance	dimensionless

$\bar{\alpha}_\lambda$	= average monochromatic surface absorptance	dimensionless
β	= cooling modulus, $h\sqrt{t}/\sqrt{K\rho c}$	dimensionless
γ	= Lambert's law absorption coefficient	cm^{-1}
ϵ	= emittance	dimensionless
ϵ_d	= directional emittance	dimensionless
ζ	= constant	sec^{-1}
λ	= wavelength	cm
λ	= shape factor	dimensionless
μ	= viscosity	gm/cm sec
ζ	= x/L	dimensionless
ρ	= density	gm/cm^3
ρ	= reflectance	dimensionless
ρ_d	= directional reflectance	dimensionless
σ	= Stefan-Boltzmann constant $= 1.356 \times 10^{-12}$	$cal/cm^2 sec°K^4$
τ	= ft, dimensionless time	dimensionless
Φ	= RT/E	dimensionless
Φ_o	= RT_o/E	dimensionless
ω	= weight of volatile products of pyrolysis	gm
ω_o	= initial weight of volatiles present in sample	gm

θ = temperature rise of sample surface °C

ψ = rate of loss of heat per degree temperature rise cal/sec°C